



**HAL**  
open science

# Biogaz en vue de son utilisation en production d'énergie : séparation des siloxanes et du sulfure d'hydrogène

Carolina Rojas Devia

## ► To cite this version:

Carolina Rojas Devia. Biogaz en vue de son utilisation en production d'énergie : séparation des siloxanes et du sulfure d'hydrogène. Génie des procédés. Ecole des Mines de Nantes, 2013. Français. NNT : 2013EMNA0074 . tel-00824324

**HAL Id: tel-00824324**

**<https://theses.hal.science/tel-00824324>**

Submitted on 21 May 2013

**HAL** is a multi-disciplinary open access archive for the deposit and dissemination of scientific research documents, whether they are published or not. The documents may come from teaching and research institutions in France or abroad, or from public or private research centers.

L'archive ouverte pluridisciplinaire **HAL**, est destinée au dépôt et à la diffusion de documents scientifiques de niveau recherche, publiés ou non, émanant des établissements d'enseignement et de recherche français ou étrangers, des laboratoires publics ou privés.

# Thèse de Doctorat

## Carolina Rojas Devia

*Mémoire présenté en vue de l'obtention*

**du grade de Docteur de l'Ecole Nationale Supérieure des Mines de Nantes**

*Sous le label de l'Université Nantes Angers Le Mans*

**Discipline** : Sciences pour l'ingénieur

**Spécialité** : Génie des Procédés

**Laboratoire** : Génie des Procédés Environnement Agro-alimentaire (GEPEA)

**École doctorale** : Science Pour l'Ingénieur, Géosciences, Architecture (SPIGA)

**Soutenu le 11 février 2013**

**Thèse N°2013EMNA0074**

## **Biogaz en vue de son utilisation en production d'énergie : séparation des siloxanes et du sulfure d'hydrogène.**

### JURY

Rapporteurs :

**M. Jean-Louis FANLO**, Professeur, Ecole des Mines d'Alès, France

**Mme. Michelle HEITZ**, Professeure, Université de Sherbrooke, Canada

Examineurs :

**M. Jean-Christophe Batsale**, Professeur, ENSAM, Bordeaux, France

**M. Michel BAUDU**, Professeur, Université de Limoges, France

**Mme. Laurence LE COQ**, Professeure, Ecole de Mines de Nantes, France

**M. Patrick GERMAIN**, Professeur, Insa de Lyon, France

Directeur de Thèse :

**M. Albert SUBRENAT**, Maître Assistent- HDR, Ecole des Mines de Nantes



# Acknowledgments

Au cours de ces trois années de recherche au sein du Département Systèmes Energétiques et Environnement, j'ai eu la possibilité d'accroître mes connaissances sur le génie chimique, un des principaux objectifs de ma carrière, et aujourd'hui cette expérience enrichissante est arrivée à sa fin.

Avant tout, je tiens à remercier Monsieur Albert Subrenat, mon directeur de thèse, pour m'avoir donné la possibilité de réaliser ce doctorat; pour son accueil et la confiance qu'il m'a accordée dès mon arrivée à l'école ainsi que la motivation pour travailler sur ce sujet passionnant.

Je remercie également Monsieur Patrick Germain, professeur à l'Insa de Lyon pour avoir accepté la présidence de cette thèse.

Je suis particulièrement sensible à l'intérêt que Madame Michelle Heitz, professeure à l'Université de Sherbrooke et Monsieur Jean-Louis Fanlo, professeur à l'Ecole des Mines d'Ales, ont porté à ce travail en tant que rapporteurs. Je remercie également Madame Laurence Le Coq, professeure et directrice du département DSEE, pour sa disponibilité et la confiance qu'elle a su m'accorder au sein du département ainsi que pour avoir participé à l'examen de cette thèse. Mes remerciements s'adressent également à Monsieur Michel Baudu, professeur à l'Université de Limoges, et Monsieur Jean-Christophe Batsale, professeur à l'ENSAM de Bordeaux, pour m'avoir fait l'honneur d'évaluer cette thèse.

Je remercie aussi François-Xavier Blanchet, Yvan Gouriou et Jérôme Martin pour la construction des pilotes ainsi que Thomas Bergantz pour sa disponibilité et ses conseils au cours des manips. Je remercie également Marie Laure, Dominique et Eric ainsi que l'ensemble du personnel du département pour leur accueil sympathique et leur coopération professionnelle tout au long de ces trois années.

Je remercie amicalement Lomig Hamon, enseignant chercheur à l'Ecole de Mines de Nantes, pour ses conseils dans le domaine des transferts de masse et son aide désintéressée dans mon travail.

Je remercie Monsieur David Bossan pour m'avoir donné son regard d'industriel de la production du biogaz ainsi que l'opportunité de travailler avec lui.

Je tiens à remercier spécialement Adrien Aubert, pour le soutien au cours de ces trois années ; pour les intéressantes discussions pendant les pauses, ainsi que pour tout le temps qu'il a consacré aux corrections de ce manuscrit.

Je tiens également à remercier mes collègues de bureau Younes Matar et Laura Sarperi pour le temps que nous avons passé ensemble, ainsi qu'à tous mes collègues, Andrea Romero, Laura Ayala, Jonathan Torres, David Garcia, Luisa F Gonzalez, Olivier Debono, Audrey Forthome, Vanessa Maroga, Espérance Kinata, Séverine, Shivaji Ramalingan, Mario Hernandez, Cristian Barca et Stéphane Prigent pour le bon temps pendant cette période.

J'adresse un remerciement spécial à mon amie, Deyanira Ricaurte, pour avoir pensé à moi pour réaliser cette thèse, m'avoir accueilli à Nantes et partagé avec moi ses connaissances. Egalement, je tiens à remercier Patricia Nonmartin pour le temps que nous avons passé ensemble à améliorer l'anglais de ce manuscrit.

Je donne mes sincères remerciements à ma famille, pour les enseignements que m'ont donnés mon père, ma mère, ma sœur et mon frère, qui ont toujours cru en moi et qui m'ont apportés un grand soutien à chaque étape et décision de ma vie.

Pour mes collègues de Givaudan, en particulier Yolanda Segura, pour la confiance et le grand soutien qu'elle m'a donné à ce changement de vie. Je remercie également ma famille colombienne en Nantes : Lili, Andrea, Paula, Michael, Diana, Carlos, Victor et Adriana.

Enfin, je voudrais adresser un salut spécial à Jean-Claude, Martine, Viviane, Nicole, Aicha, et mes deux super supports Olivier de la Brosse et Mathieu de la Soudière, merci pour les encouragements et la confiance partagés avec moi les derniers mois de la thèse.

*« Une fois que tu as décidé de faire quelque chose, assume et va jusqu'au bout »  
Daisaku Ikeda*

# Summary

ACKNOWLEDGMENTS.....	3
SUMMARY .....	5
TABLES LIST .....	11
FIGURES LIST.....	15
CHAPTER 1 BIBLIOGRAPHICAL STUDY .....	23
1 BIOGAS CONTEXT .....	23
1.1 Biogas in Europe.....	23
1.2 Biogas origin.....	26
1.3 Biogas production .....	27
1.4 Biogas composition.....	28
1.4.1 Siloxanes .....	28
1.4.2 H <sub>2</sub> S .....	29
1.4.3 Other compounds .....	30
1.5 Biogas uses.....	31
1.5.1 Siloxanes in biogas.....	33
1.5.2 Hydrogen sulfide in biogas .....	34
1.6 Conclusion about biogas .....	34
2 SILOXANES.....	35
2.1 Characteristics of siloxanes.....	35
2.2 Technologies to remove siloxanes .....	36

2.2.1	Adsorption.....	36
2.2.2	Absorption.....	38
2.2.3	Biological degradation .....	39
2.3	Conclusions about siloxanes treatment .....	39
3	HYDROGEN SULFIDE .....	41
3.1	Hydrogen sulfide characteristics .....	41
3.2	Technologies to remove H <sub>2</sub> S.....	41
3.2.1	Removal in the digester.....	41
3.2.2	Absorption.....	42
3.2.3	Biological treatment .....	43
3.2.4	Adsorption into materials impregnated with iron oxides.....	43
3.2.5	Adsorption into activated carbon .....	44
3.3	Conclusions about H <sub>2</sub> S treatment .....	46
4	CONCLUSION .....	48
CHAPTER 2 STUDY OF DYNAMIC TREATMENT OF SILOXANES BY ABSORPTION AND ADSORPTION PROCESSES .....		50
1	REMOVAL OF SILOXANES BY ABSORPTION .....	50
1.1	Absorption approach .....	50
1.2	Materials and methods .....	51
1.2.1	Materials : siloxanes and absorbents used .....	51
1.2.2	Laboratory unit.....	53
1.2.3	Operational conditions: Siloxane L2 absorption into (motor oil, cutting oil and water-cutting oil mixture) .....	59
1.2.4	Operational conditions: Siloxane D4 absorption into (motor oil, cutting oil and water-cutting oil mixture) .....	61
1.3	Results and discussion .....	62
1.3.1	Siloxane L2 .....	62
1.3.2	Siloxane D4.....	74

1.4	Conclusions .....	83
2	REMOVAL OF SILOXANES BY ADSORPTION .....	87
2.1	Adsorption approach .....	87
2.1.1	Activated carbon .....	88
2.1.2	Adsorption in static .....	89
2.1.3	Adsorption process in dynamic system .....	92
2.2	Materials and methods .....	93
2.2.1	Materials .....	93
2.2.2	Laboratory unit .....	94
2.2.3	Operational conditions .....	95
2.3	Results and discussion .....	96
2.3.1	Breakthrough curves .....	96
2.3.2	Adsorption Capacity .....	97
2.4	Conclusions .....	98
CHAPTER 3 H <sub>2</sub> S TREATMENT BY ADSORPTION INTO ACTIVATED CARBONS – REGENERATION MATERIAL .....		99
1	H <sub>2</sub> S ADSORPTION INTO ACTIVATED CARBONS .....	100
1.1	H <sub>2</sub> S transfer and reaction into activated carbons .....	100
1.1.1	Mechanisms in a dry atmosphere .....	100
1.1.2	Mechanisms in a humid atmosphere .....	101
1.1.3	Modifying the surface .....	103
1.1.4	The origins and manufacturing conditions of activated carbon fibers .....	104
1.2	Regeneration of activated carbon .....	105
1.2.1	Regeneration of activated carbon : H <sub>2</sub> S .....	106
2	MATERIALS AND METHODS .....	107
2.1	Materials : adsorbents characteristics .....	108
2.1.1	pH of carbon surface .....	108



2.1.2	BET Porous structure .....	109
2.1.3	Surface acid function.....	109
2.1.4	Adsorption Isotherms .....	110
2.2	Laboratory unit.....	112
2.2.1	Desorption system.....	114
2.2.2	Characterization of filter with the Joule effect.....	114
2.2.3	Operating conditions .....	121
2.3	Results and discussion .....	122
2.3.1	Temperature effect: .....	123
2.3.2	Pressure effect .....	124
2.3.3	Influence of the delay and the duration.....	128
2.3.4	Adsorption – Desorption sustainability.....	129
2.3.5	General conclusion regarding the regeneration system at dry conditions.....	130
2.3.6	Humidity effect into adsorption- regeneration.....	131
2.3.7	Sustainability of regeneration under wet conditions.....	134
3	CONCLUSIONS.....	136
	CONCLUSIONS AND PERSPECTIVES.....	138
1	CONCLUSIONS.....	138
2	PERSPECTIVES.....	142
	APPENDIX A.RESUME DE LA THESE.....	144
	INTRODUCTION.....	144
1	LE CONTEXTE DU BIOGAZ .....	146
1.1	Le biogaz en Europe.....	146
1.2	L’origine du biogaz .....	146
1.3	Les applications du biogaz.....	147

1.4	La composition du biogaz .....	147
1.5	Les siloxanes .....	148
1.5.1	Les siloxanes dans le biogaz .....	148
1.5.2	Les technologies pour éliminer les siloxanes.....	149
1.6	H <sub>2</sub> S .....	151
1.6.1	Le sulfure d'hydrogène dans le biogaz .....	151
1.6.2	Les technologies pour le traitement du H <sub>2</sub> S.....	151
1.7	Conclusion .....	153
2	ÉTUDE SUR LE TRAITEMENT DES SILOXANES PAR ABSORPTION. PROCEDE EN DYNAMIQUE.....	154
2.1	Matériels et méthodes .....	154
2.1.1	Les absorbants.....	155
2.1.2	Le dispositif expérimental.....	156
2.1.3	Les conditions expérimentales .....	158
2.2	Résultats et discussion .....	161
2.2.1	Absorption du siloxane L2 dans l'huile de moteur.....	161
2.2.2	Absorption du siloxane L2 dans l'huile de coupe .....	166
2.2.3	Absorption du siloxane L2 dans le mélange eau-huile de coupe.....	168
2.2.4	Absorption du siloxane D4 dans l'huile de moteur .....	169
2.2.5	Absorption du siloxane D4 dans l'huile de coupe .....	171
2.2.6	Absorption du siloxane D4 dans le mélange eau-huile de coupe.....	173
2.3	Conclusions.....	174
3	ETUDE DE L'ADSORPTION ET DESORPTION DE L'H <sub>2</sub> S SUR DES CHARBONS ACTIFS .....	178
3.1	Adsorption de l'H <sub>2</sub> S sur des charbons actifs.....	178
3.1.1	La régénération du charbon actif : H <sub>2</sub> S .....	179
3.2	Matériels et Méthodes .....	180
3.2.1	Le dispositif expérimental.....	181
3.2.2	Le système de désorption .....	181

3.2.3	Les conditions de fonctionnement .....	182
3.3	Résultats et discussion .....	183
3.3.1	Effet de la température .....	183
3.3.2	Effet de la pression.....	185
3.3.3	Influence du temps entre les cycles et de la durée des cycles .....	188
3.3.4	Pérennité de cycles adsorption/désorption .....	189
3.3.5	Conclusion générale sur le système de régénération dans des conditions sèches....	190
3.3.6	Effet de l'humidité sur l'adsorption-régénération .....	191
3.3.7	Pérennité des cycles d'adsorption/désorption dans les conditions humides .....	193
3.4	Conclusions .....	194
4	CONCLUSIONS ET PERSPECTIVES .....	195
4.1	Conclusions .....	195
4.2	Perspectives.....	197
	REFERENCES.....	198

# Tables List

Table 1. Primary production of Biogas in the European Union 2009 – 2010. (EurObserv'ER 2011) .....	24
Table 2. Biogas composition (Deublein and Steinhauser 2008; Rasi et al. 2007; Ryckeboosch et al. 2011). .....	28
Table 3. Siloxanes concentration in Biogas, Landfill and Anaerobic digester gas (Papadias et al. 2012). .....	29
Table 4. Sulfur compounds in Biogas, Landfill and Anaerobic digester gas, (Papadias et al. 2012) .....	29
Table 5. VOC compounds in Biogas, Landfill and Anaerobic digester gas. (Papadias et al. 2012). .....	30
Table 6. Halogen compounds in Biogas, Landfill and Anaerobic digester gas, WWTP (Papadias et al. 2012). .....	31
Table 7. Biomethane in France. Specification SPEC GrDF .....	32
Table 8. Siloxanes maximal values(Accettola et al. 2008) (Wheless and Pierce 2004). .....	34
Table 9. H <sub>2</sub> S specification (Deublein, Steinhauser 2008). .....	34
Table 10. Physical chemical properties of siloxanes. (Schweigkofler, Niessner 1999). .....	36
Table 11. Adsorption capacity for different activated carbons in Air 0%RH. (Ricaurte, Subrenat 2009). .....	37
Table 12 Adsorption capacity for activated carbon fiber FM30K (Air – HR = 70% - Temperature = 60°C – [Toluene] = 10 g.m <sup>-3</sup> ). (Ricaurte, Subrenat 2009). .....	37
Table 13. Removal of siloxanes .....	40
Table 14. H <sub>2</sub> S adsorption capacity of GAC (Granular Activated Carbons). .....	45
Table 15. Techniques for H <sub>2</sub> S treatment .....	47
Table 16. Physical properties of motor oil and cutting oil .....	52
Table 17. Chemical properties of motor oil and cutting oil .....	52
Table 18. Gas bubble diameter and interfacial area calculated for the experimental conditions. Motor oil, cutting oil and Water-cutting oil. Temperature 25°C. Correlations (Treybal, 1980). .....	57

Table 19. Operating conditions corresponding to the absorption of Hexamethylsiloxane (L2) into water, motor oil, cutting oil and water-cutting oil. ....	60
Table 20. Operating conditions corresponding to the absorption of Octamethyltetracyclosiloxane (D4) into water, motor oil, cutting oil and water-cutting oil. ....	61
Table 21. Concentration effect. Absorption of siloxane L2 into motor oil. ....	65
Table 22. Effect of the residence time on the absorption capacity of siloxane L2 into motor oil. ....	66
Table 23. Effect of the temperature on the absorption capacity of siloxane L2 into motor oil. ....	67
Table 24. Effect of the concentration on the absorption capacity of siloxane L2 into cutting oil. ....	70
Table 25. Effect of the residence time on the absorption capacity of siloxane L2 into cutting oil. ....	70
Table 26. Hexamethyldisiloxane (L2) absorption capacity of water-cutting oil. ....	71
Table 27. Comparison of the absorption capacity of water-cutting oil and the 5% wt of the cutting oil. Hexamethyldisiloxane (L2) absorption into water-cutting oil. ....	73
Table 28. Octamethyltetracyclosiloxane (D4) absorption into motor oil. Absorption capacity $q_{D4}$ ( $\text{mg.L}^{-1}$ ). ....	74
Table 29. Octamethyltetracyclosiloxane (D4) absorption into cutting oil. Absorption capacity $q_{D4}$ ( $\text{mg.L}^{-1}$ ). ....	77
Table 30. Octamethyltetracyclosiloxane (D4) absorption into water-cutting oil. Absorption capacity $q_{D4}$ ( $\text{mg.L}^{-1}$ ). ....	80
Table 31. Summary of absorption capacity of siloxane L2 into: water, motor oil, cutting oil and water-cutting oil. ....	84
Table 32. Summary of absorption capacity of siloxane D4 into: water, motor oil, cutting oil and water-cutting oil. ....	85
Table 33. Physical properties of activated carbons. ....	94
Table 34. pH of adsorbent surface. ....	103
Table 35. Activated carbon fiber cloths characteristics. ....	110
Table 36. Values of the parameters of the Freundlich Model of activated carbon cloth ACF6 (FM30K) previously adsorbed with $\text{H}_2\text{S}$ . ....	111

Table 37. Studied parameters influencing the regeneration quality (a) dry atmosphere (b) wet atmosphere. ....	122
Table 38. Summary of adsorption capacity (q) of the first and second adsorption. Regeneration conditions: Temperature 20 and 110°C and Pressure: 700 and 1000 mbar. Breaktrought point: 5 ppmv. ....	128
Table 39. Adsorption capacity of the first and second adsorption. Regeneration conditions: regeneration time: 30, 60, 180 min. Time delay after first adsorption 4 and 24 h.....	128



# Figures List

Figure 1. Comparison of biogas electricity trend against the NREAP, EurObserv'ER 2011..	23
Figure 2. Primary production of Biogas in the European Union 2007. (EurObserv'ER 2011).	
.....	25
Figure 3. Biogas yield ( $\text{m}^3/\text{t}$ fresh mass) and methane content (%) in function of biomass ...	27
Figure 4. Siloxanes deposits in an engine .....	33
Figure 5. Linear and cyclic structure of siloxanes .....	35
Figure 6. Flow diagram of a possible biogas treatment for the upgrading of biogas.....	49
Figure 7. Diagram and photography of the perforated plate. ....	53
Figure 8. Diagram of the laboratory unit. Generation of siloxanes loaded in siloxanes and absorption column.....	54
Figure 9. Photography of the laboratory unit. Generation of air loaded in siloxanes and absorption column.....	55
Figure 10. Residence time (s) and interfacial area ( $\text{m}^2 \cdot \text{m}^{-3}$ ) in function of flow rate ( $\text{L} \cdot \text{min}^{-1}$ ). Calculated based on the geometry of the absorption column for motor oil T: 25°C. Correlations (Treybal, 1980).....	57
Figure 11. Experiments diagram corresponding the absorption of Hexamethylsiloxane (L2) into (a) Motor oil (b) Cutting oil.....	61
Figure 12. Experiments diagram corresponding the absorption of Octamethyltetracyclosiloxane (D4) into (a) Motor oil and Cutting oil. ....	62
Figure 13. Hexamethylsiloxane (L2) absorption into motor oil. Breakthrough curves in function of time (s). Experimental conditions: flow rate $8.03 \text{ L} \cdot \text{min}^{-1}$ ; siloxane concentration ( $800 - 1200 \text{ mg} \cdot \text{m}^{-3}$ ). Temperature (25; 50 °C).....	63
Figure 14. Hexamethylsiloxane (L2) absorption into motor oil. Absorption capacity $q_{\text{L2}}$ ( $\text{mg} \cdot \text{L}^{-1}$ ) in function of time (s). Experimental conditions: flow rate $8.03 \text{ L} \cdot \text{min}^{-1}$ ; siloxane concentration ( $800 - 1200 \text{ mg} \cdot \text{m}^{-3}$ ). Temperature (25; 50 °C).....	64
Figure 15 . Temperature effect (25; 50; 90 °C). Absorption of siloxane L2 into motor oil. $C_{\text{in}}$ : $1200 \text{ mg} \cdot \text{m}^{-3}$ ; Flow rate: $8.03 \text{ L} \cdot \text{min}^{-1}$ , Mass: 300 g. ....	67



Figure 16. Hexamethyldisiloxane (L2) absorption into cutting oil. Breakthrough curves in function of time (s).Experimental conditions: flow rate(1.0- 8.03 L.min <sup>-1</sup> ); siloxane concentration (1200 -4800 mg.m <sup>-3</sup> ). Temperature (25°C).....	68
Figure 17. Hexamethyldisiloxane (L2) absorption into cutting oil. Absorption capacity q <sub>L2</sub> (mg.L <sup>-1</sup> ) in function of time (s).Experimental conditions: flow rate(1.0- 8.03 L.min <sup>-1</sup> ); siloxane concentration (1200 -4800 mg.m <sup>-3</sup> ). Temperature (25°C).....	69
Figure 18. Hexamethyldisiloxane (L2) absorption into water-cutting oil. Breakthrough curves in function of time (s).Experimental conditions: flow rate(8.03-8.2 L.min <sup>-1</sup> ); siloxane concentration (1000 -1800 mg.m <sup>-3</sup> ). Temperature (25°C).....	72
Figure 19. Hexamethyldisiloxane (L2) absorption into water-cutting oil. Absorption capacity q <sub>L2</sub> (mg.L <sup>-1</sup> ) in function of time (s).Experimental conditions: flow rate (8.03 – 8.2 L.min <sup>-1</sup> ); siloxane concentration (1000 - 1800 mg.m <sup>-3</sup> ). Temperature (25°C).....	73
Figure 20. Octamethyltetracyclosiloxane (D4) absorption into motor oil. Breakthrough curves in function of time (s).Experimental conditions: flow rate (3.2 L.min <sup>-1</sup> ); siloxane concentration (800 mg.m <sup>-3</sup> ). Temperature (25°C). ....	75
Figure 21. Octamethyltetracyclosiloxane (D4) absorption into motor oil. Absorption capacity q <sub>D4</sub> (mg.L <sup>-1</sup> ) in function of time (min).Experimental conditions: flow rate (3.2 L.min <sup>-1</sup> ); siloxane concentration (800 mg.m <sup>-3</sup> ). Temperature (25°C).....	76
Figure 22. Octamethyltetracyclosiloxane (D4) absorption into cutting oil. Breakthrough curves in function of time (s).Experimental conditions: flow rate (3.2 L.min <sup>-1</sup> ); siloxane concentration (800 mg.m <sup>-3</sup> ). Temperature (25°C). ....	77
Figure 23. Octamethyltetracyclosiloxane (D4) absorption into cutting oil. Absorption capacity q <sub>D4</sub> (mg.L <sup>-1</sup> ) in function of time (min).Experimental conditions: flow rate (3.2 L.min <sup>-1</sup> ); siloxane concentration (800 mg.m <sup>-3</sup> ). Temperature (25°C).....	78
Figure 24. Octamethyltetracyclosiloxane (D4) absorption into water-cutting oil. Breakthrough curves in function of time (s).Experimental conditions: flow rate (3.2 L.min <sup>-1</sup> ); siloxane concentration (800 mg.m <sup>-3</sup> ). Temperature (25°C). ....	79
Figure 25. Comparision of octamethyltetracyclosiloxane (D4) absorption into cutting oil and water-cutting oil. Breakthrough curves in function of time (s).Experimental conditions: flow rate (3.2 L.min <sup>-1</sup> ); siloxane concentration (800 mg.m <sup>-3</sup> ). Temperature (25°C).....	81

Figure 26. Octamethyltetracyclosiloxane (D4) absorption into water-cutting oil. Absorption capacity $q_{D4}$ ( $\text{mg.L}^{-1}$ ) in function of time (min). Experimental conditions: flow rate ( $3.2 \text{ L.min}^{-1}$ ); siloxane concentration ( $800 \text{ mg.m}^{-3}$ ). Temperature ( $25^\circ\text{C}$ ).....	82
Figure 27. Diffusion from the bulk of the gas phase to the surface of the adsorbent .....	87
Figure 28. Activated carbon presentations. (a) Granular activated carbon (b) Extruded activated carbon (c) Activated carbon cloth .....	89
Figure 29. Classification of gas adsorption isotherms by IUPAC .....	90
Figure 30. Breakthrough curve, outlet profile.....	92
Figure 31. Diagram of adsorption process .....	95
Figure 32. Hexamethyldisiloxane (L2) adsorption into granular activated carbon (TE 60; NC 60) and activated carbon cloth in cloth (FM30 K). Breakthrough curves in function of time (s). .....	96
Figure 33. Hexamethyldisiloxane (L2) adsorption into granular activated carbon (TE 60; NC 60) and activated carbon cloth in cloth (FM30 K). time (s). Adsorption capacity of activated carbon as a function of time (s). Experimental conditions: $C_{in} L2 = 1200 \text{ mg.m}^{-3}$ ; $T: 25^\circ\text{C}$ . .....	98
Figure 34. Adsorption Static system .....	111
Figure 35. Adsorption Isotherm of ACF6 (FM30 K). Temperature $20^\circ\text{C}$ . $\text{H}_2\text{S}$ under a dry atmosphere of air.....	112
Figure 36. Flow diagram and photography of adsorption / desorption process of an activated carbon filter heated by Joule effect and under vacuum pressure. Adsorption of $\text{H}_2\text{S}$ . ...	113
Figure 37. Schematic representation of the adsorption-desorption process. Temperature and pressure variation. Regeneration conditions: $T = 110^\circ\text{C}$ , $P = 700 \text{ mbar}$ during 60 min. ....	114
Figure 38. Schematic representation of the characterization of filter AFC6 (FM30K) with electrical current.....	115
Figure 39. Electric characterization of the filter (FM30 K). Power (W) in function of the temperature (K). Experimental conditions at the air at the environmental conditions. ..	116
Figure 40. Electric characterization of the filter (FM30 K). Resistance ( $\Omega$ ) in function of the temperature (K). Experimental conditions at the air at the environmental conditions. ..	116
Figure 41. Schema of the Filter holder with electrical contact. ....	117

Figure 42. Electric characterization of the filter (FM30 K). Experimental conditions: (a) without flow through the filter and no humidification. (b) air flow through the filter and no humidification. (c) air flow through the filter and pre-humidification. Power (W) in function of temperature (K). .....	118
Figure 43. Layers of activated carbon in a parallel configuration .....	118
Figure 44. Resistance ( $\Omega$ ) in function of the temperature (K). Electric characterization of the filter (FM30 K). Experimental conditions: (a) without flow through the filter and no humidification. ....	120
Figure 45. Resistance ( $\Omega$ ) in function of the temperature (K). Electric characterization of the filter (FM30 K). Experimental conditions: (b) air flow through the filter and no humidification. ....	120
Figure 46. Resistance ( $\Omega$ ) in function of the temperature (K). Electric characterization of the filter (FM30 K). Experimental conditions: (c) air flow through the filter and pre-humidification. ....	121
Figure 47. Adsorption of $H_2S$ into activated carbon cloth ACF6 (FM30 K). concentration profile ( $mg.m^{-3}$ ) in function of time (min). Curve 1st and 2 <sup>nd</sup> adsorption /regeneration. Regeneration conditions: T: 20°C and P:1 bar. ....	123
Figure 48. Adsorption of $H_2S$ into activated carbon cloth FM30 K. Concentration profile ( $mg.m^{-3}$ ) in function of time (min). Curve (1) first adsorption with a new filter. Curve (2) second adsorption after regeneration. Regeneration conditions: Temperature: 110°C and Pressure: 1 bar.....	124
Figure 49. Adsorption of $H_2S$ into activated carbon cloth ACF6 (FM30 K). Concentration profile ( $mg.m^{-3}$ ) in function of time (min). Curve (1) first adsorption with a new filter. Curve (2) second adsorption after regeneration. Regeneration conditions: Temperature: 20°C and Pressure: 700 mbar.....	125
Figure 50. Adsorption of $H_2S$ into activated carbon cloth ACF6 (FM30 K). Concentration profile ( $mg.m^{-3}$ ) in function of time (min). Curve (1) first adsorption with a new filter. Curve (2) second adsorption after regeneration. Regeneration conditions: Temperature: 110°C and Pressure: 700 mbar.....	126
Figure 51. Yield adsorption capacity ( $q_2/q_1$ ) in function of time (min). Activated carbon cloth ACF6 (FM30 K). Regeneration conditions (A) T :110° and P: 700 mbar, (B) T :110° and P: 1000 bar, (C) T :20° and P: 700 mbar, (D) T :20° and P: 1000 mbar. ....	127

Figure 52. Adsorption of H <sub>2</sub> S into activated carbon ACF6 (FM30 K). Delay time between the first adsorption and the second adsorption.(a) 0 h ; (b) 4 h; (c) 24 h. Regeneration conditions: temperature: 110°C and pressure: 700 mbar. ....	129
Figure 53. Adsorption of H <sub>2</sub> S into activated carbon ACF6 (FM30 K). Sustainability of the process: adsorption– desorption cycles carried out in sequence. Regeneration conditions: temperature: 110°C and pressure: 700 mbar. ....	130
Figure 54. Equipement for the generation of Air humidify. ....	131
Figure 55. TG Pre-humidified activated carbon cloth ACF6. ....	132
Figure 56. Adsorption of H <sub>2</sub> S into activated carbon cloth ACF6 (FM30 K). Breakthrough curves in function of time. Comparison of dry and a pre-humidified adsorbent. Summary of the cycles adsorption-regeneration. Regeneration conditions T:110°C ; P:0.7 bar....	133
Figure 57. Histogram of the adsorption rate capacity at the saturation point. Relative humidity (a) 0 % wt (b) 20 % wt (c) 44 % wt. Regeneration conditions: 110°C and 700 mbar. Heating by Joule effect. ....	134
Figure 58. Adsorption/Regeneration cycles of ACF6 Breakthrough curves for different number of cycles. Regeneration conditions: 110°C; 700 mbar; RH 44% wt. Heating by Joule effect. ....	135
Figure 59. Adsorption/Regeneration cycles of ACF6. H <sub>2</sub> S treatment capacity for the ten first cycles. Regeneration conditions: 110°C; 700 mbar; RH 44% wt. Heating by Joule effect. ....	136
Figure 60. Diagram of biogas up-grading process. H <sub>2</sub> S and siloxanes treatment by adsorption and absorption as a finishing process. ....	140
Figure 61. Diagram of biogas up-grading process. H <sub>2</sub> S and siloxanes treatment by adsorption and absorption as a finishing process. ....	142



# Introduction

Nowadays, the development of renewables sources of energy is an important aspect to the society. On one hand, the reserves of fossil fuels are decreasing and the problems associated with the use of them are more evident, opening big questions such as: How long these resources will last? What strategies are developed to face this situation? How can we solve the problem of climate change? In response of it, environmental policies in search of finding solutions have been established. With this new awareness, a line of research have been focusing on the development of new energy sources. The eolian, solar radiation, hydroelectric and biogas are some of the emerging solutions.

These solutions are related in some way to the ambient conditions of the countries as well as the seasons. For instance, the eolian depends on the power of wind; the solar radiation is more effective in the countries where the radiation is higher; the hydroelectric depends on the physical geography. One solution could be biogas. It can be easily applied. Home waste recycling is simple and economical comparing with other technologies. Additionally, biogas implies a change in mentality and compromise the society, to create recycling strategies and to set up an organization to plan the waste control in countries where it has not been considered. One alternative who contributes solve the problematic of the world could be biogas. This thesis focuses on study biogas as a new source of energy.

One of the most important characteristics of biogas is that it is composed by a high percentage of methane. It opens the possibility of use in the same way that the natural gas. However, as a result of biological process, its composition depends on the organic material and on the operational and environmental conditions. During biodegradation some non methane compounds are also produced. Among those, we can find: carbon dioxide, hydrogen sulfide, sulfur compounds, volatile organic compounds, siloxanes, ammonia and water vapor. These compounds decrease biogas potential and in some ways avoid its use as a renewable energy.

The first chapter of this thesis is therefore focused on the different aspects of biogas. Starting with biogas potential in Europe and the policies established by the governments and how it contributes to those strategies. There are many sources of biogas presented for the production and composition. Depending on the organic material the final composition varies. We focused here on two types of biogas, first of all, where the industries and domestic waste are being disposed. And secondly, farm waste. They are characterized by different compounds. Before being used, the separation of non methane components is needed. The siloxanes and the hydrogen sulfide is one of the most harmful components in biogas.

Therefore, they will be the drive of this thesis. To accomplish this research a revision of existing removal technologies are being described to show the major constraints and opportunities in terms of the separation process. A proposal of a finishing process to achieve the required values for a further biogas application is presented and developed in the second and third chapter.

The second chapter is dedicated to siloxanes removal. These components have been identified as critical for the application of biogas. In fact, they are responsible for the formation of silicon dioxide in the engines as well as being harmful to other biogas applications. This study is focused on the experimental design and evaluation of the separation processes. Firstly, the siloxanes are treated by an absorption process and secondly an approach of adsorption removal is carried out. This experimental phase is to take in account the possibility of coupling technologies and the development of new alternatives for the siloxanes removal. For that, two siloxanes that are usually found in biogas were selected: hexamethyldisiloxane (L2) and octamethylcyclotetrasiloxane (D4). In the absorption process three different solvents were studied: motor oil, cutting oil and water-cutting oil mixture. To evaluate the interactions between the pollutant and the absorbent a bubble column was designed. A set of experiments were carried out in a dynamic semi-batch reactor varying some parameters as inlet concentration, residence time and temperature. A second removal process important to VMS was also studied to compare with the latter under the same behavior. For that the adsorption was carried out into three different activated carbons in a dynamic semi-batch reactor. Finally, the results presented show the comparison of the advantages of the absorption and adsorption capacities.

In the Chapter 3, the hydrogen sulfide removal process is considered. Hydrogen sulfide is almost present in all kinds of biogas as a result of the biodegradation of the organic material. Hydrogen sulfide is a harmful compound for human being and contributes to the acid rain formation. Therefore, the environmental importance to be removed from biogas. Different technologies have been developed. However, the regeneration of the activated carbon presents a great challenge. This chapter aim is to treat the hydrogen sulfide by an adsorption – regeneration process. Different activated carbons were studied. As a result, activated carbon cloth were chosen. The regeneration system is then analyzed and different operational parameters were studied such as temperature, regeneration time, pressure and relative humidity. The experiments were carried out in a dynamic system. As a result, a novel method to regenerate the material has been proposed.

# Chapter 1

## Bibliographical study

---

### 1 Biogas Context

#### 1.1 Biogas in Europe

The EU-Climate Change and Energy commission established that in 2020, 20% of the European energy must come from renewable sources. Technologies such as eolian, solar radiation, hydroelectric and biogas are some of the emerging solutions. Among them, biogas in addition to be an alternative source of energy, also offers the possibility of transforming organic waste materials into energy. Moreover, its valorization is an effective way to decrease greenhouse emissions to the atmosphere. As global warming potential of methane is 23 times stronger than carbon dioxide, consequently, biogas states a promising solution for sustainable growth for the world.

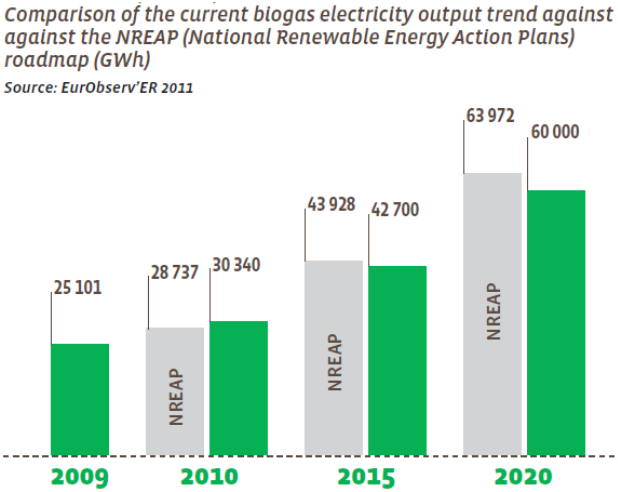


Figure 1. Comparison of biogas electricity trend against the NREAP, EurObserv'ER 2011.



Within the framework of the new policies, the NREAP (National Renewable Energy Action Plans) biogas forecast for the European Union is of 64 TWh for 2020. The comparison of biogas electricity trend according to the plan is very positive as shown in Figure 1. However, this growth is in majority accomplished by Germany. As shown in Table 1 it represents the 60% of the total primary production of biogases. The 90 % of the production were coming from sources different from landfill and sewage sludge. Moreover, its policy is mainly focused in the energy crops. The main purpose is the use of high quality biogases, such as the gas grid injection. On the other hand, the other European countries follow a contrary trend. In the case of France, 526.2 ktoe of biogas were produced in 2009 from where 84 % is coming from landfill, 8.5% is coming from sewage sludge gas and only 7.5% is obtained from other sources (EurObserv'ER 2011). In Figure 2, a scope of 2007 EU is shown. As observed, the majority of the countries follows the latter behavior.

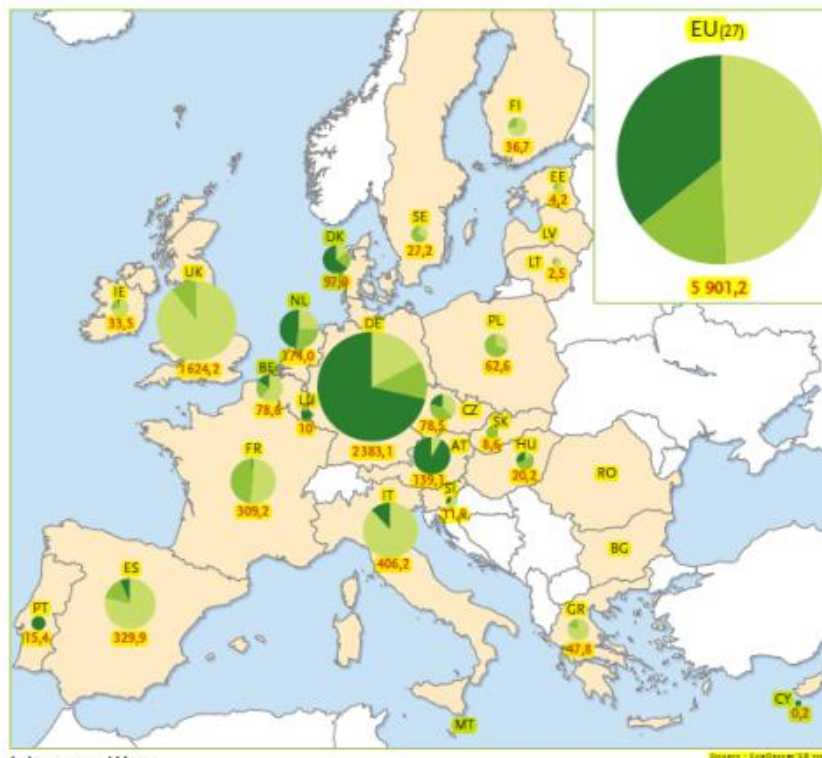
Table 1. Primary production of Biogas in the European Union 2009 – 2010.  
(EurObserv'ER 2011)

Primary production of biogas in the European Union in 2009 and 2010\* (ktoe)

	2009				2010*			
	Décharges Landfill gas	Stations d'épuration <sup>2</sup> Sewage sludge gas <sup>2</sup>	Autres biogaz <sup>2</sup> Other biogas <sup>2</sup>	Total	Décharges Landfill gas	Stations d'épuration <sup>2</sup> Sewage sludge gas <sup>2</sup>	Autres biogaz <sup>2</sup> Other biogas <sup>2</sup>	Total
Germany	265,5	386,7	3 561,2	4 213,4	232,5	402,6	6 034,5	6 669,6
UK	1 474,4	222,6	0,0	1 697,0	1 499,4	272,8	0,0	1 772,2
Italy	361,8	5,0	77,5	444,3	383,8	7,0	87,7	478,5
France**	442,3	45,2	38,7	526,2	323,7	41,6	48,0	413,3
Netherlands	39,2	48,9	179,8	267,9	36,7	50,2	206,5	293,4
Spain	140,9	10,0	32,9	183,7	119,6	12,4	66,7	198,7
Czech Rep.	29,2	33,7	67,0	129,9	29,5	35,9	111,3	176,7
Austria	4,9	19,0	135,9	159,8	5,1	22,5	143,9	171,5
Belgium	42,7	2,1	80,5	125,3	41,9	14,6	70,9	127,4
Poland	35,7	58,0	4,5	98,0	43,3	63,3	8,0	114,6
Sweden	34,5	60,0	14,7	109,2	35,7	60,7	14,8	111,2
Denmark	6,2	20,0	73,4	99,6	8,1	20,1	74,0	102,2
Greece	46,3	9,5	0,2	56,0	51,7	15,0	1,0	67,7
Ireland	42,2	8,1	4,1	54,4	44,2	8,6	4,5	57,3
Finland	26,0	12,6	2,8	41,4	22,7	13,2	4,5	40,4
Hungary	2,8	10,5	17,5	30,9	2,6	12,3	19,3	34,2
Portugal	21,3	1,5	1,0	23,8	28,2	1,7	0,8	30,7
Slovenia	8,3	7,7	11,0	27,1	7,7	2,8	19,9	30,4
Latvia	6,8	2,7	0,2	9,7	7,9	3,3	2,2	13,3
Luxembourg	0,0	1,4	11,0	12,4	0,1	1,2	11,7	13,0
Slovakia	0,8	14,8	0,7	16,3	0,8	9,5	1,8	12,2
Lithuania	1,3	2,1	1,2	4,7	2,0	3,0	5,0	10,0
Estonia	1,6	1,0	0,0	2,5	2,7	1,1	0,0	3,7
Romania	0,0	0,0	1,1	1,1	0,0	0,0	1,1	1,1
Cyprus	0,0	0,0	0,2	0,2	0,0	0,0	0,2	0,2
<b>Total EU</b>	<b>3 034,6</b>	<b>982,9</b>	<b>4 317,1</b>	<b>8 334,7</b>	<b>2 929,8</b>	<b>1 075,2</b>	<b>6 938,3</b>	<b>10 943,3</b>

\* Estimation. Estimate. \*\* DOM non inclus. Overseas departments not included. 1- Urbaines et industrielles. Urban and industrial.  
2- Unités décentralisées de biogaz agricole, unités de méthanisation des déchets municipaux solides, unités centralisées de codigestion et multiproduit. Decentralised agricultural plants, municipal solid waste, methanation plants, centralised codigestion and multi-product plants. - Les décimales sont séparées par une virgule. Decimals are written with a comma. Source: EurObserv'ER 2011

PRIMARY ENERGY PRODUCTION OF BIOGAS IN EUROPE IN 2007\*



LÉGENDE/KEY

Production d'énergie primaire de biogaz de l'Union européenne en 2007 (en ktoe)/  
Primary energy production of biogas of the European Union in 2007 (in ktoe)

- Biogaz de décharges/Landfill gas
- Biogaz de stations d'épuration/Sewage sludge gas
- Autres biogaz (unités décentralisées de biogaz agricole, etc.)/Other biogases (decentralised agricultural plant, etc.)

**5 901,2** Les chiffres en rouge indiquent la production totale en ktoe/Red figures show total production in ktoe

\* Estimation/Estimate.

Figure 2. Primary production of Biogas in the European Union 2007. (EurObserv'ER 2011).

Biogas is a valuable renewable energy source, however besides the methane, other components are part of it. Biogas is considered a carbon dioxide neutral biofuel, it represents a solution to increase the renewable energy sources.

## 1.2 Biogas origin

Renewable waste materials from industries and domestic sources are converted to useful energy forms like biogas. It is produced by anaerobic digestion and is mainly composed of methane CH<sub>4</sub> (45-70%), carbon dioxide CO<sub>2</sub> (15-45 %), hydrogen sulfide H<sub>2</sub>S (0.005% - 2%) and other contaminants like halogenated compounds and siloxanes (Ryckebosch et al. 2011). The methane bacterias responsible for the biogas formation are naturally present in the environment. Four major phases including hydrolysis, acidogenesis, acetogenesis and methanogenesis are involved and described below (Deublein, Steinhauser 2008):

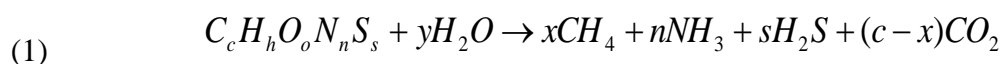
**Hydrolysis:** is the first phase of the biodegradation, biopolymers of high-molecular weight (carbohydrates, proteins, cellulose and fats) are cracked by the enzyme hydrolase into monomers (amino acids, fatty acids, monosaccharide) and water.

**Acidogenesis:** the monomers that results from the hydrolysis are degraded into short-chain organic acids (butyric acid, propionic acid, acetate, acetic alcohol), alcohol (methanol, ethanol, propanol, butanol, glycerin and acetone) and gases (carbon dioxide, hydrogen sulfide and ammonia).

**Acetogenesis:** in this step the acetogenic bacteria form the acetate by oxidation of a long chain of fatty acids.

**Methanogenesis:** is the last step in which the formation of methane, carbon dioxide and water takes place. The 27-30% of methane is produced by the reduction of CO<sub>2</sub> + H<sub>2</sub> and 70% by the oxidation of acetic acid.

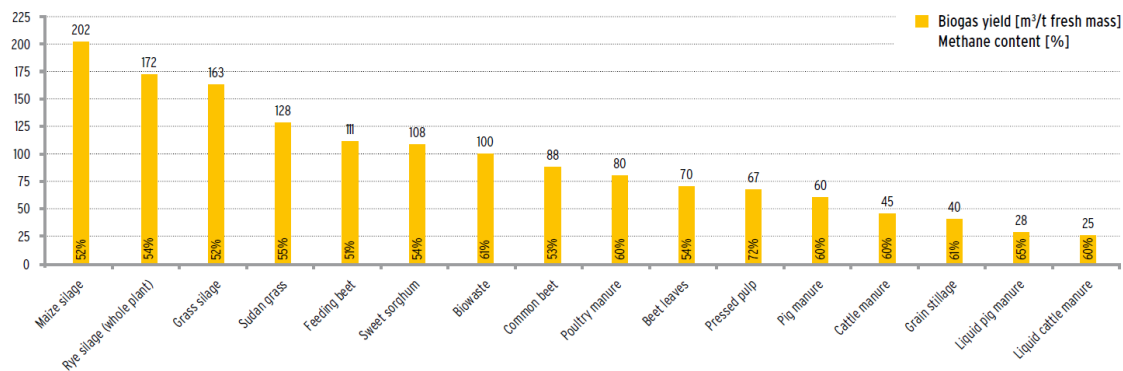
According to Buswell equation (1930), the formation of methane follows the next equation, however depending on substrate the biogas yields and methane content varies as illustrated in Figure 3. Other factors that may affect the biogas yield include pH and temperature (Yusuf, Ify 2011).



$$x = \frac{1}{8}(4c + h - 20 - 3n - 2s)$$

$$y = \frac{1}{4}(4c - h - 20 + 3n + 3s)$$

Biogas yields<sup>4</sup>



Handreichung Biogas, Fachagentur Nachwachsende Rohstoffe, 2006; Energiepflanzen, KTBL, 2006

Figure 3. Biogas yield ( m<sup>3</sup>/t fresh mass) and methane content (%) in function of biomass

## 1.3 Biogas production

The production of biogas may include a small scale domestic digester or large scale waste water treatment plants or landfill where the organic materials are collected and converted into biogas. The technology used is linked to the environmental conditions. For instance in India, the technology is very simple resulting in a big development of domestic digesters. The environmental conditions such as temperature and humidity facilitate the biogas formation. The residues from household and farm activity are transformed into biogases and finally used for cooking and electric energy. Below are listed the main ways of biogases production:

- Domestic (household) digesters
- Farms
- Centralized co-digestion
- Waste water treatment plants( WWTP)
- Industrial biogas plants (food and beverages)
- Landfill

Landfill is one of the most singular way of production. Organic material degradation is carried out in a discontinuous process. Parameters such as the landfill age and the kind of residues disposed differ significantly from the other types of productions. It represents in

general an environmental risk due to the gas emissions which can include toxic gases, thus the importance of biogas recovery.

## 1.4 Biogas composition

Depending on the sources, the technology and the operational conditions, the composition of such biogases differs. Furthermore biogases contents vary during the daily production. Thus measurements are taken regularly to indicate the fermentation process and biogases quality. It is very important to know the characteristics in order to design the separation process. A content overview of three different biogases production: landfill, sewage digester and farm, are shown in Table 2. (Deublein and Steinhauser 2008; Rasi et al. 2007; Ryckebosch et al. 2011).

Table 2. Biogas composition (Deublein and Steinhauser 2008; Rasi et al. 2007; Ryckebosch et al. 2011).

	Landfill	Sewage digester	Farm plant
CH <sub>4</sub> (%) vol	47-67,9	57,8-65	55-70
CO <sub>2</sub> (%) vol	37-41	33-39	37-38
O <sub>2</sub> (%) vol	<1	<1	<1
N <sub>2</sub> (%) vol	<17	<3,7	<1-2
H <sub>2</sub> S (ppmv)	<8000	<8000	10-20000
NH <sub>3</sub> (mg. Nm <sup>-3</sup> )	Traces	Traces	<2000
Siloxanes (mg. Nm <sup>-3</sup> )	1-400	-	-
Relative humidity (%)	100	100	100

### 1.4.1 Siloxanes

There are several industrial applications of siloxanes. They are added to consumer products such as cosmetics, shampoos, detergents, paper coatings and textiles. Its explain their existence in the environment (Dewil, Appels & Baeyens 2006). During anaerobic digestion, siloxanes volatilized from the sludge and reaches biogas. Additionally, polydimethylsiloxanes (PDMS) hydrolysis has been identified as another source of siloxanes in biogas (Soreanu et al. 2011, Piechota, Hagmann & Buczkowski 2012). Among the different kind of siloxanes the principal are D4, followed by L2, D5 and L3 (Wheless, Pierce 2004). VMS (Volatyl Methyl siloxanes) have a relative low molecular weight and high vapor pressure. However, another kind of siloxanes as trimethylsilanol presents a vapor pressure and

water solubility much higher. The pathway of this component is therefore found mostly in the liquid wastes. Eventhought, trimethylsilanol is comonly present in biogas. By contrast, VMS are found mostly in the gas phase. This study is primarily focused on highly volatile siloxanes with a low solubility in water. Their content fluctuates highly. In biogas coming from landfill and sewage treatment (with industrial residues) the siloxanes content is higher than those coming from other sources (Dewil, Appels & Baeyens 2006, Accettola, Guebitz & Schoeftner 2008). Siloxanes content in biogas can be found between 0 and 140 mg. m<sup>-3</sup> (Wheless, Pierce 2004) while recent values ranging between 1 and 400 mg. m<sup>-3</sup> have been reported (Ryckebosch, Drouillon & Vervaeren 2011). In Table 3 is shown an example of a biogas from a landfill site (Papadias et al. 2012).

Table 3. Siloxanes concentration in Biogas, Landfill and Anaerobic digester gas (Papadias et al. 2012).

Siloxane Compound		Concentration in Landfill Gas and Anaerobic digester gas (ppb)
C <sub>6</sub> H <sub>18</sub> O <sub>3</sub> Si <sub>3</sub>	(D3)	297
C <sub>8</sub> H <sub>24</sub> O <sub>4</sub> Si <sub>4</sub>	(D4)	825
C <sub>10</sub> H <sub>30</sub> O <sub>5</sub> Si <sub>5</sub>	(D5)	1698
C <sub>12</sub> H <sub>36</sub> O <sub>6</sub> Si <sub>6</sub>	(D6)	88
C <sub>6</sub> H <sub>18</sub> OSi <sub>2</sub>	(L2)	122
C <sub>8</sub> H <sub>24</sub> O <sub>2</sub> Si <sub>3</sub>	(L3)	61
C <sub>10</sub> H <sub>30</sub> O <sub>3</sub> Si <sub>4</sub>	(L4)	35
C <sub>3</sub> H <sub>10</sub> OSi	(TMS)	559

## 1.4.2 H<sub>2</sub>S

H<sub>2</sub>S is in general present in all types of biogases as a result of natural degradation of organic material. In biogas coming from farms (with animal residues) the H<sub>2</sub>S content is higher as shown in Table 2. Other sulfur compounds are described in the Table 4.

Table 4. Sulfur compounds in Biogas, Landfill and Anaerobic digester gas, (Papadias et al. 2012)

Sulfur Compound	Concentration in Landfill Gas (ppm)
H <sub>2</sub> S	5400
Methyl Mercaptan	3.91
Carbonyl sulfide	0.27
Carbon Disulfide	0.34
Dimethyl sulfide (DMS)	14.3
Ethyl Mercaptan	0.83
Dimethyl Disulfide (DMDS)	0.42

## 1.4.3 Other compounds

### 1.4.3.1 Volatile organic compounds VOC

Among the different volatile organic compounds found in biogases are benzene, toluene and xylene. They are usually present in Landfill biogas on high concentration. The next table presents the maximal values reported in Landfill and Anaerobic digester gas WWTP (Papadias et al. 2012).

Table 5. VOC compounds in Biogas, Landfill and Anaerobic digester gas. (Papadias et al. 2012).

Compound		WWTP (ppb) max values
C <sub>6</sub> H <sub>6</sub>	Benzene	850
C <sub>7</sub> H <sub>8</sub>	Toluene (Methylbenzene)	430000
C <sub>8</sub> H <sub>10</sub>	Ethylbenzene	3135
C <sub>8</sub> H <sub>10</sub>	Xylenes (o-, m-, p-, mixtures)	5724
C <sub>9</sub> H <sub>12</sub>	Propylbenzene	1600
C <sub>9</sub> H <sub>12</sub>	1,2,3-Trimethylbenzene	167
C <sub>9</sub> H <sub>12</sub>	1,2,4-Trimethylbenzene	530
C <sub>9</sub> H <sub>12</sub>	1-Ethyl-2-methylbenzene (o-Ethyltoluene)	8100

### 1.4.3.2 Halogenated compounds

Halogenated compounds are mainly present in Landfill biogas. They are used as components in industrial production which explain their prevalence. Halogen compounds reported in biogas coming from Landfill and WWTP are listed in Table 6. The most common is chlorine. Fluorine and bromine are in general at lower levels. In the presence of water, the halogen compounds react to form an acid solution causing corrosion in the engines. Biomethane maximal values have been established of 1 mg.m<sup>-3</sup> for chlore and 10 mg.m<sup>-3</sup> fluor.

Table 6. Halogen compounds in Biogas, Landfill and Anaerobic digester gas, WWTP (Papadias et al. 2012).

	Halogen Compound	Concentration in Landfill Gas (ppm)	Concentration in WWTP Biogas (ppb)
CH <sub>2</sub> Cl <sub>2</sub>	Dichloromethane	40.1 ppm	
C <sub>2</sub> H <sub>3</sub> Cl	Chloroethene (Vinyl Chloride)	15.6 ppm	
C <sub>2</sub> H <sub>4</sub> Cl <sub>2</sub>	1,2-Dichloroethane	15.4 ppm	
C <sub>2</sub> HCl <sub>3</sub>	Trichloroethylene	3.1 ppm	
C <sub>2</sub> H <sub>3</sub> Cl <sub>3</sub>	1,1,1-Trichloroethane	0.8 ppm	
C <sub>2</sub> Cl <sub>4</sub>	Tetrachloroethylene	8.1 ppm	
C <sub>6</sub> H <sub>5</sub> Cl	Chlorobenzene	6.8 ppm	
C <sub>6</sub> H <sub>4</sub> Cl <sub>2</sub>	Dichlorobenzene	5.5 ppm	
C <sub>7</sub> H <sub>7</sub> Cl	Benzyl Chloride (Chloromethyl Benzene)		234 ppb
HF	Hydrogen Fluoride		16 ppb

### 1.4.3.3 Ammonia

A high content of ammonia is obtained from biogas produced within animal manure and food waste compared with the other biogas sources. The ammonia content can be up to 2000 ppm ((Jack) Guo et al. 2009).

### 1.4.3.4 Water

Raw biogas is saturated with water. The content vary between 1 to 5 % in volume. Water must be removed to avoid its reaction with acid gases like H<sub>2</sub>S, NH<sub>3</sub> and CO<sub>2</sub> to avoid corrosion in the equipments and ustencils. Usually, when the water is removed other components like dust are also eliminated.

## 1.5 Biogas uses

Biogas has many applications such as alternative renewable energy. Depending on the biogas production it can be directly transformed into heat by combustion. It is generally used for the small domestic biogas production. However, as seen in the last section, there are many components frequently found in biogases therefore it is necessary to remove them.

Among the potential applications of biogas we found also:



**Combined heat and power generation (CHP)** is a very common way to transform the methane in heat. It consists in a combustion engine coupled with a generator. The energy produced can be used, stocked, and in many countries sold to the national electricity grid.

**Micro gas turbine** the mixture of air and biogas is burned and forwarded to hot gas. It is released to the turbine which is connected to the electricity generator. In the same way, the electricity can be stocked and sold.

**Fuel cells** are electrochemical devices characterized by high efficiency. The biogas is fed to the anode and the oxygen to the cathode. An electrochemical reaction is developed and an electric current is produced. Different kind of fuel cells can be used. There are different kind of classification based on the temperature of reaction in low PEM (80°C), medium and high (MCFM 600 – 700 °C and SOCF (750 to 1000°C). Here biogas must be exempted from H<sub>2</sub>S, siloxanes and sulfur compounds.

**Vehicle fuel** the use of biogas in the vehicles is another final application which has increased in the last years; it can be used in the same way as natural gas. Thus biogas must be up-graded and compressed.

**Gas grid injection** after treatment, biogas quality is usually measured by the content of CH<sub>4</sub> (95%) and the Wobbe index and called biomethane. Specification to the injection into the gas grid in France is listed in Table 7 ("Cahier Des Charges Fonctionnel Du Contrôle Des Caractéristiques Du Biogaz Injecté (Éléments Génériques." 2010).

Table 7. Biomethane in France. Specification SPEC GrDF

Sulfur total	under 30 mgS/m <sup>3</sup> (n)
Sulfur mercaptans	under 6 mgS/m <sup>3</sup> (n)
Sulfur (H <sub>2</sub> S + COS)	under 5 mgS/m <sup>3</sup> (n)
CO <sub>2</sub>	under 2,5 % (molar)
O <sub>2</sub>	under 100 ppmv
Hg	under 1 mg/m <sup>3</sup> (n)
Cl	under 1 mg/m <sup>3</sup> (n)
F	under 10 mg/m <sup>3</sup> (n)
H <sub>2</sub>	under 6 %
NH <sub>3</sub>	under 3 mg/m <sup>3</sup> (n)
CO	under 2 %

Among the non methane components, the most dangerous to the final uses are the H<sub>2</sub>S, the halogenated components and the siloxanes. They can lead to great damage in the

production lines and also in the engine parts of the energy conversion process. Thus to obtain a high quality of biogas most of them must be treated. In this study we are primarily interested in the siloxanes and in the hydrogen sulfide. The principal constraints of those trace compounds in biogas applications are being presented.

### 1.5.1 Siloxanes in biogas

Biogas use as an alternative source of energy is limited by siloxanes presence. At high temperature, they react during the combustion process to be converted into silicon dioxide and micro-crystalline quartz, as shown in the equation (2) and Figure 4. These particles thus contribute to the abrasion of the engine's inner surface (Schweigkofler and Niessner 2001) causing from one side an increasing in the maintenance of the equipments and also lowering power generator capacity (Tower 2004).

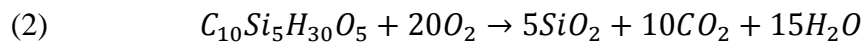


Figure 4. Siloxanes deposits in an engine

In addition, solid oxide fuel cells (SOFC) are poisoned by siloxanes (Haga et al. 2008; Sasaki et al. 2011). SOFC degradation was observed with a biogas containing 10 ppm of siloxane D5 (Haga et al. 2008).

Consequently, siloxanes treatment has become very important for biogas use as renewable energy. Depending upon further use, several thresholds of siloxanes in biogas have already been established by engines manufactures as detailed in Table 8 (Accettola et al. 2008) (Wheless and Pierce 2004). For the injection in the natural gas grid in France the specification does not consider the siloxanes level as detailed in the SPEC from GrDF.

Table 8. Siloxanes maximal values(Accettola et al. 2008) (Wheless and Pierce 2004).

Equipment	Siloxanes (mg. Nm <sup>-3</sup> )
Microturbines	0.03-0.06
Internal combustion engines	5-28
Turbines	0.1
Fuel cells	100ppmv

## 1.5.2 Hydrogen sulfide in biogas

The H<sub>2</sub>S is one of the most pollutant components in biogas. H<sub>2</sub>S content fluctuates highly. In general, it is present between 0.005% and 2% (Ryckebosch, Drouillon & Vervaeren 2011). Hydrogen sulfide is a toxic gas to nature. In the presence of water forms sulfuric acid which is highly corrosive causing damage to e.g. tanks, pipelines and process equipment. The SO<sub>2</sub> and SO<sub>3</sub> formation (upon combustion) is more toxic than H<sub>2</sub>S and contribute to the acid rain formation. Consequently, the H<sub>2</sub>S removal from biogas is necessary before using it. The final content in biogas depends upon the further use. Some specification values are shown in Table 9 (Deublein, Steinhauser 2008).

Table 9. H<sub>2</sub>S specification (Deublein, Steinhauser 2008).

Application	Hydrogen sulfide (mg. Nm <sup>-3</sup> )
Fuel cell MCFC	<0.1
Injection into the gas grid	<5
Gas Motor	<200

## 1.6 Conclusion about biogas

This review showed the several components that can be found in biogases. As explained earlier, the production process such as landfill, sewage sludge, farm plants are the origin of the trace compounds in the complex gas matrix. Moreover, as a result of biodegradation process it exists many parameters that contribute in the variability of the final

composition. From the final applications of biogas, some trace components establish a constraint for its valorization. Siloxanes and hydrogen sulfide are part of them. Evidence such as decreases in power generation given siloxanes reaction and corrosion in pipelines and motor by the reaction of H<sub>2</sub>S with water are one of them. That is why the interest of removing those compounds from the biogas are essentials.

## 2 Siloxanes

### 2.1 Characteristics of siloxanes

Volatile methyl siloxanes (VMS) compounds have a significantly low solubility in water and are highly volatile. Their structural units consisting of  $-(\text{CH}_3)_2\text{SiO}-$  and can be cyclic or linear as shown in the Figure 5 (Dewil et al. 2006; Allen et al. 1997). Physicochemical properties of representative siloxanes are listed in the Table 10 (Schweigkofler, Niessner 1999). As can be seen, VMS has a relative low molecular weight and high vapor pressure. However, another kind of siloxanes as trimethylsilanol presents a vapor pressure and water solubility much higher. The pathway of this component is therefore found mostly in the liquid wastes. Eventhought, trimethylsilanol is comonly present in biogas. By contrast, VMS are found mostly in the gas phase. This study is primarily focused on highly volatile siloxanes with a low solubility in water. This physicochemical condition established a limitation in the VMS treatment in water presence. Moreover, raw biogas is saturated in water, as a consequence the non solubility in water is a key factor to design a separation process.

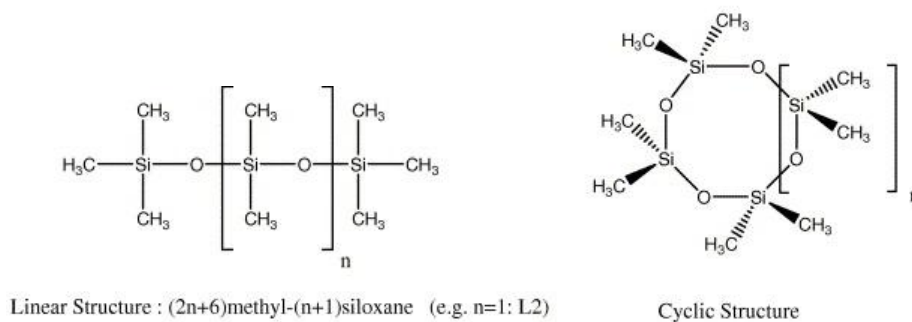


Figure 5. Linear and cyclic structure of siloxanes

Table 10. Physical chemical properties of siloxanes. (Schweigkofler, Niessner 1999).

Siloxane Compound	Abbreviation	Molecular Weight (g.mol <sup>-1</sup> )	Boiling Point (°F)	Solubility in water (mg.L <sup>-1</sup> )	Vapor Pressure (kPa) 25 °C
Hexamethylcyclotrisiloxane C <sub>12</sub> H <sub>18</sub> O <sub>3</sub> Si <sub>3</sub>	D3	222.46	273	1.56	1.14
Octamethylcyclotetrasiloxane C <sub>8</sub> H <sub>24</sub> O <sub>4</sub> Si <sub>4</sub>	D4	296.61	347	0.056	0.13
Decamethylcyclopentasiloxane C <sub>10</sub> H <sub>30</sub> O <sub>5</sub> Si <sub>5</sub>	D5	370.77	410	0.017	0.05
Dodecamethylcyclohexasiloxane C <sub>10</sub> H <sub>36</sub> O <sub>6</sub> Si <sub>6</sub>	D6	445.00	473	0.005	0.003
Hexamethyldisiloxane C <sub>6</sub> H <sub>18</sub> Si <sub>2</sub> O	L2	162.4	212	0.93	4.12
Decamethyltetrasiloxane C <sub>10</sub> H <sub>30</sub> Si <sub>4</sub> O <sub>3</sub>	L4	310.7	381	0.00674	0.073
Trimethylsilanol C <sub>3</sub> H <sub>10</sub> OSi (Schweigkofler and Niessner 2001)	TMS	90.2	210	35000	2.13

## 2.2 Technologies to remove siloxanes

Different technologies are used to remove siloxanes from biogas such as adsorption into porous materials, physical and chemical absorption, deep chilling, treatment by membranes, catalytic processes and biodegradation (Ajhar et al. 2010). Below some of them are described.

### 2.2.1 Adsorption

Among those techniques, the use of activated carbon to siloxanes abatement has been applied (Ryckebosch et al. 2011). Materials such as Granular Activated Carbon (GAC), Activated Carbon Cloths (ACC), silica gel, and molecular sieves has been used showing that activated carbon is a good alternative for siloxanes treatment (Matsui and Imamura 2010; Ricourte and Subrenat 2009).

Previous studies in adsorption were done in a static reactor and results are shown in Table 11 (Ricourte, Subrenat 2009). They had proposed a model according to the isotherm results which allows to calculate the adsorption capacity of the material in function of the concentration in the gas phase. Freundlich model proposed is described in equation (3).

$$(3) \quad q_e = K C_e^{1/n}$$

With  $q_e$  the equilibrium adsorption capacity ( $\text{mg.g}^{-1}$ ) and  $C_e$  the equilibrium concentration ( $\text{g.m}^{-3}$ ). From the materials tested the activated carbon cloth FM 30K presents a good performance.

Table 11. Adsorption capacity for different activated carbons in Air 0%RH. (Ricaurte, Subrenat 2009).

Adsorbent	K	1/n	R <sup>2</sup>	q <sub>e</sub> (mg.g <sup>-1</sup> )		
				C <sub>e</sub> 50 mg.m <sup>-3</sup>	C <sub>e</sub> 100 mg.m <sup>-3</sup>	C <sub>e</sub> 200 mg.m <sup>-3</sup>
Silice gel	145,04	0,374	0,99	47	61	79
Zeolite day 40	134,63	0,186	0,97	77	88	100
BC 120	468,71	0,236	0,99	231	272	321
NC 60	341,14	0,115	0,94	242	262	283
FM 10	275,34	0,065	0,97	227	237	248
FM 100	244,32	0,029	0,89	224	229	233
FM 30K	311,68	0,076	0,94	248	262	276

Table 12 (Ricaurte, Subrenat 2009) lists the Freundlich model parameters corresponding to a model biogas with the following characteristics: high relative humidity (70%), temperature (60°C) and concentration of toluene of 10 g.m<sup>-3</sup>.

Table 12 Adsorption capacity for activated carbon fiber FM30K (Air – HR = 70% - Temperature = 60°C – [Toluene] = 10 g.m<sup>-3</sup>). (Ricaurte, Subrenat 2009).

Compound	K	1/n	R <sup>2</sup>	C <sub>e</sub> :	C <sub>e</sub> :	C <sub>e</sub>
				50 mg.m <sup>-3</sup>	100 mg. Nm <sup>-3</sup>	200 mg.m <sup>-3</sup>
				q <sub>e</sub> (mg.g <sup>-1</sup> )	q <sub>e</sub> (mg.g <sup>-1</sup> )	q <sub>e</sub> (mg.g <sup>-1</sup> )
L2	222,3	0,04	0,97	197	203	208
D4	350,3	0,04	0,98	311	319	328

Other studies have shown similar results. The material that presents the highest adsorption capacity is activated carbon followed by molecular sieves and silica gel. (Matsui and Imamura 2010) studied D4 adsorption (one of the most common siloxanes present in biogas) in lab scale with N<sub>2</sub> as gas carrier. At an inlet concentration of 4500 mg.m<sup>-3</sup> the adsorption capacity observed was of 150-200 g.kg<sup>-1</sup> for activated carbon; 80 -100 g.kg<sup>-1</sup> for molecular sieves, and 100 g.kg<sup>-1</sup> for silica gel. Forward, a test with the best activated carbon

was carried out in a sewage gas with D5  $15 \text{ mg.m}^{-3}$  and D4  $3 \text{ mg.m}^{-3}$ , showing an adsorption capacity of 1.25 % wt for D4 and 6.5%wt for D5 for  $(C/C_0)= 10\%$ .

## 2.2.2 Absorption

Among the other techniques that present a high efficiency to remove siloxanes is chemical absorption by acid solutions (Schweigkofler and Niessner 2001; Wheless and Pierce 2004). Schweigkofler and Niessner used sulphuric, nitric and phosphoric acid for removal of D5 and L2. They obtained a siloxane elimination efficiency up to 95% with sulphuric acid (48 wt%) and nitric acid (65 wt%) at  $60^\circ\text{C}$ . However, the use of strong acids like sulfuric or nitric present many disadvantages as corrosion in the equipments, by- and co-product generation, and a negative impact on health and on the environment.

Absorption by organic solvents has shown good efficiencies. However, in general, the associated cost is relatively high for biogas production and process information is limited. Selexol®, removed up to 99% of siloxanes (Wheless and Pierce 2004). It has been patented.

In the case of absorption by mineral oils (Stoddart et al. 1999) studied the removal with hydrocarbon oil using a scrubbing system. Results show the possibility to remove chlorinated compounds and siloxanes. The efficiency of siloxanes removal was of 60 %. However, operational parameters such as gas flow rate, oil absorption capacity were not presented. Oil regeneration was done by a combination of thermal desorption at  $120^\circ\text{C}$ , under vacuum and passing a flow through the oil with efficiencies of 40-60%.

Recent studies on VOC (volatile organic compounds) absorption had shown good elimination capacities using different kind of oils (Lalanne et al. 2008, Ozturk, Yilmaz 2006, Heymes et al. 2006) . (Heymes et al. 2006) studied toluene absorption in silicon oil wich resulted in a good absorption capacity of  $5.31 \text{ g.L}^{-1}$  at an inlet concentration of  $3.7 \text{ g.m}^{-3}$ . (Lalanne et al. 2008) studied the use of mixture of water and cutting oil in order to increase the mass transfer from hydrophobic pollutants to the liquid phase showing than the higher cutting oil percentage in the solution the better the absorption capacities ( $110\text{mg.L}^{-1}$  at an inlet concentration of  $100 \text{ mg.m}^{-3}$ ). Nevertheless, it is not possible to compare different absorbents with other pollutants given that the absorption process depends strongly on the physico-chemical interactions between the present's compounds. It is important to emphasize that information as absorption capacity of siloxanes in mineral oils is insufficient, or not readily available in the literature.

### 2.2.3 Biological degradation

Preliminary studies suggest the possibility of removing siloxanes by biodegradation, however removal efficiency is low (20-43%) (Accettola et al. 2008; Grümping et al. 1999; Popat and Deshusses 2008) and long time of process are required. The biological treatment implies in the first place the transfer of pollutants from the gas phase to an aqueous phase. The studies with siloxanes are not easy to perform given that VMS are often scarcely soluble in water. (Popat, Deshusses 2008) studied the addition of an organic solvent (oleyl alcohol) to the liquid phase. As a result a higher siloxane removal was attained mostly due to siloxane D4 absorption into the organic phase than by the biodegradation process. It suggests that mass transfer limitations play an important role in the low biodegradation of D4.

## 2.3 Conclusions about siloxanes treatment

During the past few years the release of silicon compounds in the environment have highly increased. This point leads us to think that in the future there will be an increase of the siloxanes content in the sewage treatment and landfill sites. Thus, the necessity of processes to decrease the content and treat high volumes of gas. On one hand, absorption processes are generally applied to treat high volumes and high concentration; however because of VMS physic-chemical properties, a limitation in separation process has been shown impossible. For instance, the separation by absorption in water, which is a very simple and current technology can be applied in the case of the high solubility of the components. However, siloxanes requires another kind of solvents to be treated.

The main points of the different technologies described previously are summarized in Table 13. From these technologies, it seems that adsorption is today the most interesting way to treat siloxanes in biogas in terms of efficiency (by using for example activated carbon), however the adsorption capacity is low (1-5% wt) and disposal of material must be considered. The requirement of new technologies to treat high volumes as well as high concentrations of siloxanes is evident. Moreover, the study of alternatives to enhance the life cycle of activated carbons is also an important point in the development of sustainable technologies. The consequences are the new separation processes: absorption with a vision of a new separation system and secondly adsorption as a finishing process.

Both subject will be studied in the second chapter.



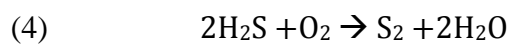
Table 13. Removal of siloxanes

Process	Description	Advantages	Disadvantages
Chemical absorption	Acid sulfuric and nitric	95% efficiency	By-products, environmental and hazard problems
Physical Absorption	Selexol®(dimethylether of polyethylene glycol)	99 % efficiency	High cost of solvent
	Motor oil	60% efficiency	By-products
Condensation	-5°C	88% efficiency	High cost
Biodegradation	D4	Low cost, environmental	Low efficiency (20-43%)
Adsorption	Activated Carbon	High efficiency	Final disposal
	Silica gel	High efficiency	Final disposal
	Molecular sieve	High efficiency	Final disposal

# 3 Hydrogen sulfide

## 3.1 Hydrogen sulfide characteristics

Hydrogen sulfide, H<sub>2</sub>S, is a toxic gas specially known by its rotten egg odor. It is colorless and heavier than the air. It is relatively easy oxidized in the presence of radicals when dissolved in water and dissociated. In the presence of air, oxidation of H<sub>2</sub>S can be developed as described in equation (4):

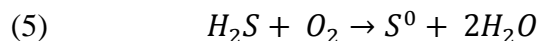


## 3.2 Technologies to remove H<sub>2</sub>S

Different techniques have been used to remove H<sub>2</sub>S from biogas such as adsorption onto porous materials, reactive adsorption, water absorption or mix water-solvents (applies in general to large scales) and biodegradation. Following, the principal processes are described.

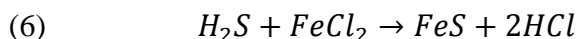
### 3.2.1 Removal in the digester

Hydrogen sulfide can be partially treated by dosing air directly to the digester. A small amount (2-6%) of O<sub>2</sub> is required for the oxidation of H<sub>2</sub>S (Ryckebosch, Drouillon & Vervaeren 2011, Kapdi et al. 2005). As a result, the concentration of H<sub>2</sub>S is decreased and elemental sulfur is formed as described in equation (5).



This process is normally used in the farms; it is simple and low cost. However, disadvantages as air overdosing (6-12%) makes biogas explosive. Additionally, the anaerobic bacteria might be inhibited, stopping the biomass digestion and decreasing biogas production.

Another technique of H<sub>2</sub>S removal in the digester, is based on the reaction of iron chloride plus H<sub>2</sub>S, as result iron sulfur is formed and level of H<sub>2</sub>S is decreased as shown equation(6).

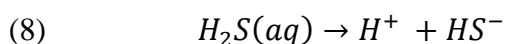
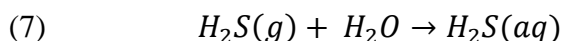


Thus the remaining concentration of H<sub>2</sub>S is still high (100 ppmv) (Ryckebosch, Drouillon & Vervaeren 2011), other processes must be implemented to attain the required level.

## 3.2.2 Absorption

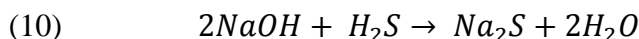
### 3.2.2.1 Physical absorption

In Physical absorption, H<sub>2</sub>S is removed from the gas phase by the absorption into the solvent. In most cases, the solvent used is water. The H<sub>2</sub>S gas is absorbed to the liquid phase as described in equations (7) (8) and (9). This process requires a high consumption of water. To reduce the water volume and increase the absorption capacity, the addition of some chemicals is applied.

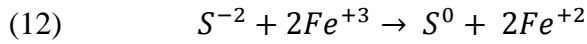


### 3.2.2.2 Chemical absorption

The most used are: NaOH, iron chloride and iron-chelate. NaOH forms sodium sulfide or sodium hydrosulfide, as shown in equations (10) and (11). (Kapdi et al. 2005). It is not regenerated and disposal has to be considered.



The addition of iron chloride to water is very effective. It consists in the formation of FeS insoluble as described in equation (6). As mentioned before, it can be added directly to the digester. Then, removal of precipitates is required. Another type of chemical absorption is the use of iron-chelate (Horikawa et al. 2004). The reaction is described in equation (12). In this test a solution containing 0.2 mol.L<sup>-1</sup> of Fe-EDTA (ethylenediaminetetraacetate) was used. Elemental sulfur is produced, forward a separation is needed. The major advantage of this process is the feasible regeneration of the solution by oxygenation.



### 3.2.3 Biological treatment

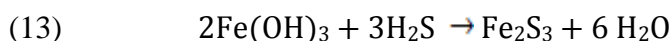
Different methods have been developed to treat H<sub>2</sub>S by biological processes like e.g biofilter, biotricling, bioscrubbing (Syed et al. 2006). In general, the use of aerobic bacteria is not recommended due to risk of biogas explosion in the presence of air. To avoid this condition, the process can be separated into two phases. In the first one, H<sub>2</sub>S is usually absorbed into the water, and then the biological treatment is achieved (Nishimura, Yoda 1997). Moreover, the use of anaerobic microorganisms have been developed showing high removal efficiencies.

In general, biotreatment efficiency depends strongly on the operational parameters like e.g H<sub>2</sub>S concentration, biogas flow rate, temperature, among other (Soreanu et al. 2010). Given that those parameters vary commonly in biogas plants, the remaining H<sub>2</sub>S present in the gas is about (50 -100 ppm). Consecutively, other process must be used at the end of biotreatment in order to decrease the content.

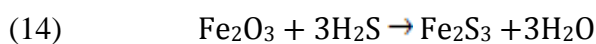
### 3.2.4 Adsorption into materials impregnated with iron oxides

Iron sponge is based on the reaction of H<sub>2</sub>S in presence of iron oxide or iron hydroxide, the support material is usually wood chips or wood pellets that are previously impregnated with the iron oxide. This technology is highly efficient, it works at inlet concentrations between 100 to 10000 ppm and treated biogas between of 1.5 to 150 mg. m<sup>-3</sup>. (Deublein and Steinhauser 2008; Truong and Abatzoglou 2005). Adsorption capacity at the saturation is between of 200-500 g. kg<sup>-1</sup>. Reactions are described in the following equations:

Iron ore: H<sub>2</sub>S is adsorbed into iron (III) hydroxide Fe(OH)<sub>3</sub> or iron (III) oxide Fe<sub>2</sub>O<sub>3</sub>



Iron sponge, SULFATREAT: H<sub>2</sub>S is converted into iron (III) sulfide

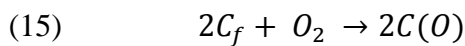


### 3.2.5 Adsorption into activated carbon

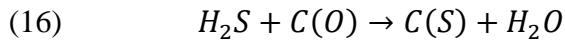
The use of activated carbon to H<sub>2</sub>S abatement has been extensively applied (Bagreev et al. 2005; Monteleone et al. 2011). It is effective and simple. Modified carbons are used to increase selectivity and adsorption capacity.

In the H<sub>2</sub>S adsorption three phenomena have been identified: physisorption, chemisorptions and oxidation. In the physisorption phenomena, the adsorption is controlled by the intermolecular forces of the van der Waals type and equilibrium is established between the activated carbon and the gas phase. In the chemisorption, the adsorption is caused by stronger valence forces on the active sites of the carbon surface (Rodríguez-Reinoso 2001) and the surface can be modified chemically. A mechanism of chemisorption proposed by (Cariaso and Walker Jr. 1975) is described in the eq (15) and (16). Hydrogen sulfide reacts forming elemental sulfur. Chemisorption is no reversible.

Chemisorption dissociative of oxygen:



Chemical reaction between the oxygen chemisorbed and the H<sub>2</sub>S gas:

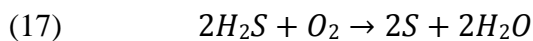


C<sub>f</sub> : active site

C(O) : site where chemisorption is achieved

C(S) : elemental sulfur chemisorbed

Also the oxidation phenomena can occur. Biogas coming from landfill and sewage treatment plants usually contains air (Rasi et al. 2007). Oxidation is described in equation (17). Table 11 summarizes some examples of different performance for activated carbon (with or without impregnation) for the H<sub>2</sub>S.



The activated carbon is highly efficient. It removes H<sub>2</sub>S content according to specified requirements. Additionally, other advantages like simple operation and maintenance, compact technology, low operation temperature make of adsorption an adequate technology. One of the main characteristic of the adsorption process is the life cycle of the adsorbent involved. Generally, activated carbon is used a limited number of times and forward disposal must be

done. It represents an increase in the operating costs, mainly caused by the replacement of the material. Regeneration of material is forward an important key to optimize operating cost and decrease environmental impact.

Table 14. H<sub>2</sub>S adsorption capacity of GAC (Granular Activated Carbons).

Type of activated carbon	Pathway	Operational Conditions	Performances
Granular activated carbons (GAC)	Chemisorption/oxydation	8000 ppm(v) 140 mL.min <sup>-1</sup> T = 20°C / P = 1 atm / Air	q <sub>e</sub> =4,21 mg.g <sup>-1</sup>
GAC -KOH	Chemisorption/oxydation	8000 ppm(v) 140 mL.min <sup>-1</sup> T = 20°C / P = 1 atm / Air	q <sub>e</sub> =23,2 mg.g <sup>-1</sup>
GAC -Na <sub>2</sub> CO <sub>3</sub>			q <sub>e</sub> =17,4 mg.g <sup>-1</sup>
GAC -K <sub>2</sub> CO <sub>3</sub>			q <sub>e</sub> =29,5 mg.g <sup>-1</sup>
GAC -NaOH			q <sub>e</sub> =23,7 mg.g <sup>-1</sup>
GAC-ZnFe <sub>3</sub> O <sub>4</sub>		10000 ppm(v) 5 mL.min <sup>-1</sup> T = 400°C / P = 1 atm / Ar	Capacité (%)
GAC-CuFe <sub>3</sub> O <sub>4</sub>			63,8
			60,3
GAC	Chemisorption/oxydation	2000 ppm(v) 200 mL.min <sup>-1</sup> T = 550°C / P = 1 atm / N <sub>2</sub> /CO <sub>2</sub>	b <sub>t</sub> = 280 min
GAC-Cu (1 %)			b <sub>t</sub> = 340 min
GAC-Zn (3 %)			b <sub>t</sub> = 380 min

(q<sub>e</sub>: amount eliminated saturation, b<sub>t</sub> breakthrough time)

### 3.2.5.1 Activated carbon regeneration

Previous studies have been done to test the regeneration of exhausted activated carbons. Generally, desorption is based on thermal treatment during a period of time. The temperature ranged between 200 °C and 500°C. Among those, (Monteleone et al. 2011) tested the regeneration at 300 °C for 4h in nitrogen stream and air stream. Results show that after N<sub>2</sub> regeneration the adsorption capacity decrease (1.71g /g to 0.17g/g). On the other hand, the use of air stream has shown better results (1.45 g/g), which seems to play an important role in the H<sub>2</sub>S removal. The test was carried out at 50 ppm and adsorption capacity was measured at 5ppm. Also, (Bagreev et al. 2002) studied the regeneration of activated carbons used as H<sub>2</sub>S adsorbents in water treatment plants. Adsorption was carried out at 3000 ppm and stopped at 700 ppm in air humid at 80%. Regeneration was carried out by heating the sample at 300 °C for 120 min in the air atmosphere. After heating regeneration no adsorption capacity was observed. Indeed, at high regeneration temperature, alteration in the surface chemistry is developed and the adsorption capacity of the material is decreased (Bagreev et al. 2002). The high temperature and low adsorption capacity after regeneration make that in most cases, activated carbon is replaced rather than regenerated (Bagreev et al. 2002; Monteleone et al. 2011; Ryckebosch et al. 2011). Consecutively, the regeneration of activated carbons previously adsorbed by H<sub>2</sub>S represents an important area of study.

The energy necessary to regenerate the material is linked to the previous phenomena developed during the adsorption. Thermal desorption at high temperature is needed due to products formed during chemisorptions and oxidation phase. To test the ability of the adsorbents to be thermally regenerated TGA analysis has been used. Peaks between 200 °C and 450°C were associated with the removal of SO<sub>2</sub> and a peak at 700 °C was associated with the desorption of elemental sulfur (Elsayed et al. 2009; Monteleone et al.2011 ).

To regenerate the activated carbon high temperature is needed. Values between 200°C and 450°C have been tested (Ryckebosch, Drouillon & Vervaeren 2011, Bagreev, Rahman & Bandosz 2002, Monteleone et al. 2011). It makes regeneration an expensive process. In most cases activated carbon is replaced rather than regenerated.

### 3.3 Conclusions about H<sub>2</sub>S treatment

Many processes have been developed to the abatement of H<sub>2</sub>S in the biogas. The choice of the process is related to several facts as efficiency, flow rate, concentration, final use, economic constraints and environmental impact. Table 15 listed the main points of the different technologies described previously. In general, when biogas contains high level of H<sub>2</sub>S and the flow rate is high, the optimal solution to treat it is the absorption process. This absorption process can be done in water or in water solutions to decrease the water volume and finally be combined with other technologies as biodegradation. However, the H<sub>2</sub>S content is still high for the final applications. The use of adsorption by activated carbon is one of the most efficient processes to remove H<sub>2</sub>S resulting in low levels according with the different requirements. However, one of the main disadvantages of the adsorption process is the low adsorption capacity in volume. As a consequence, the study of the separation of H<sub>2</sub>S by adsorption into activated carbon and the possibility of it regeneration is a main subject and will be studied in the third chapter.

Table 15. Techniques for H<sub>2</sub>S treatment

Process	Description	Advantages	Disadvantages
<b>Air Addition / oxygen into the biogas</b>	Oxygen quantity (2-6%) $2\text{H}_2\text{S} + \text{O}_2 \rightarrow 2\text{H}_2\text{O} + 2\text{S}$	Concentration under 50ppm Simple, Low cost	Risk of explosion
<b>Physical Absorption</b>	Multiple Tray airtight contact tower	H <sub>2</sub> S under detection limit	High volume of water
		Removal of CO <sub>2</sub>	High pressure (10-30bar)
<b>Chemical Absorption</b>	NaOH	Decrease in water volume	No regeneration
	FeCl <sub>3</sub>		Partially regenerate
<b>Membranes</b>		98% efficiency 250 ppm	High cost
		Abatement of CO <sub>2</sub>	
<b>Biodegradation</b>	Microorganisms supported in plastic fibers <i>Thiobacillus denitrificans</i>	Removal > 98% Low cost	
<b>Adsorption</b>	Iron sponge	Adsorption capacity= gH <sub>2</sub> S/g of wood 0.2g/g	Risk of fire during regeneration
	Grains of wood impregnated in oxide $\text{Fe}_2\text{O}_3 + \text{H}_2\text{S} \rightarrow \text{FeS}_3 + \text{H}_2\text{O}$		
	Sulfatreat 410 HP®		High cost regeneration
	$\text{Fe}_3\text{O}_4 + \text{H}_2\text{S} \rightarrow \text{FeS} + \text{S} + 4\text{H}_2\text{O}$		
	Iron Oxides	MgO, Al <sub>2</sub> O <sub>3</sub> , SiO <sub>2</sub> et ZrO <sub>2</sub>	High cost regeneration
<b>Adsorption</b>	Grain Activated carbon / Cloth Activated carbon	High H <sub>2</sub> S removal efficiency 100%	High cost regeneration, thermal regeneration at 450°C



## 4 Conclusion

As shown in the Bibliographic study, VMS (Volatile Methyl Siloxanes) are in general highly volatile and hydrophobic. This fact implies a technology limitation to remove them from the gas phase. Among the recent studies developed, adsorption into porous materials had shown high removal efficiencies. Materials such as activated carbon, silica gel, and molecular sieves were used. They showed that the polarity of the material is a key characteristic to obtain a good adsorption capacity. Furthermore, non polar activated carbons had shown a high removal capacity. However, only a small percentage of the adsorbent is used (1-5% wt) and after exhausted it is important to consider its final disposal.

Other techniques such as chemical absorption of VMSs into acid solutions were studied (Schweigkofler, Niessner 2001, Wheless, Pierce 2004). Schweigkofler and Niessner used sulphuric, nitric and phosphoric acid for removal of D5 and L2. However, the use of strong acids presents many disadvantages. Corrosion in the equipments, by- and co-product generation and a negative impact on health and on the environment, are one of them. The use of absorption by organic solvents has shown good efficiencies. Selexol® removed up to 99% of siloxanes (Wheless, Pierce 2004). However, its costs seems very high.

In that sense, the alternative to treat them by absorption into hydrophobic solvents, which is the purpose of this study, states an interesting field of research. In the same way, recent studies on Volatile Organic Compounds (VOC) are being focus on absorption into oil. As a result, they have shown good elimination (Lalanne et al. 2008, Ozturk, Yilmaz 2006, Heymes et al. 2006) opening the possibility of treating siloxanes in the same manner. Nevertheless, as absorption is strongly controlled by the physic-chemical interactions between the compounds in the liquid and gas phases, it is impossible to compare these previous studies with VMS.

Concerning the H<sub>2</sub>S, many technologies have been developed for its removal from the biogas. Among them, the present work focuses on the adsorption into activated carbons given its high efficiency to achieve low concentration. About this technology, many studies have shown the influence of different parameters in the adsorption phase (H<sub>2</sub>S gas to the adsorbent). However, the desorption process remains in the laboratory study due basically to the high temperature required. The non regeneration of material implies an increase of the costs by: 1) replacement of fresh activated carbon, 2) stopping the treatment process and 3) the disposal of the exhausted material.

The H<sub>2</sub>S research focuses on the development of a sustainable finishing process by adsorption into activated carbons. To attempt this objective a regeneration system of soft conditions has been studied in order to enhance the life cycle of the material as well as to minimize the frequency of the operating maintenance of the adsorption filters.

Some perspectives as the possibility of coupling technologies are considered. For instance, to enlarge the life cycle of activated carbon materials, one alternative is to treat the siloxanes or the H<sub>2</sub>S concentration by previous processes where by a decrease could offer an integral solution. A proposal of this process is shown in Figure 6.

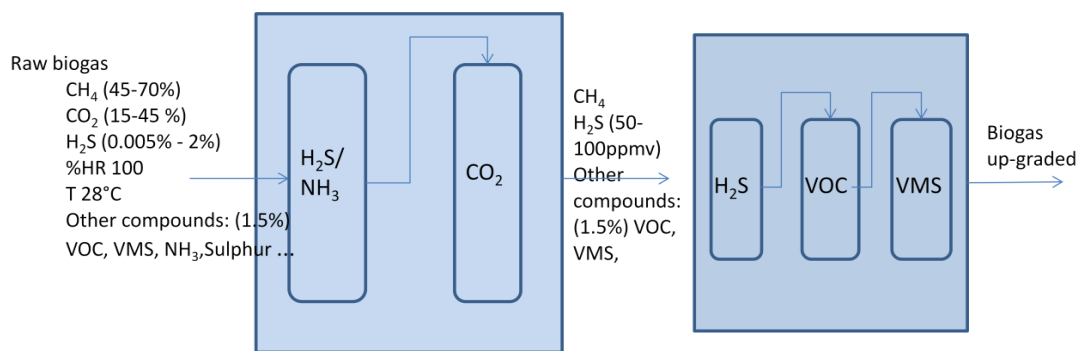


Figure 6. Flow diagram of a possible biogas treatment for the upgrading of biogas

The present work is organized as follows: the treatment of siloxanes is studied in the second chapter, firstly the absorption experimental process is exposed, secondly an approach of an adsorption process. The goal is to establish a comparison of both processes. Followed by, a proposal of a removal treatment which will be evaluated. Different scenarios have been considered facing nowadays requirements and possible increase of siloxanes content. Finally, the third chapter concerns the treatment of H<sub>2</sub>S by adsorption process. It will focus on the finishing process. The conditions to regenerate the filter will show a new use.

# Chapter 2

## Study of dynamic treatment of Siloxanes by absorption and adsorption processes

---

### 1 Removal of siloxanes by Absorption

#### 1.1 Absorption approach

This section enlighten the siloxanes removal by absorption process. Among those, a linear siloxane: L2 (hexamethylsiloxane) and a cyclic siloxane: D4 (octamethylcyclotetrasiloxane), which are currently presents in biogas (Wheless, Pierce 2004) are chosen to carry out the experiments. Oil selection based on several characteristics and previous studies. Motor oil is studied as a reference material, with the purpose of using waste oil deriving from the industry and vehicles. Cutting oil has been used previously for the VOC absorption and our approach is to analyze if the solution is good for the siloxanes removal. Additionally, in the industries cutting oil is mixed with water. So far water cutting oil mixture has been evaluated. Consequently, motor oil, cutting oil and water- cutting oil have been studied in more depht.

Thus a column was designed to carry out absorption of siloxanes. Different operating conditions were tested to determine the influence of, for instance, inlet concentration, flow rate, mass of absorbent and temperature. Its performance is measured primarily by the liquid absorption capacity of the solvent. Followed by a study of adsorption into activated carbons was carried out with L2. This allows us to compare the limitations and advantages of the two processes.

It is important to emphasize that information as absorption capacity of siloxanes in oils is insufficient, or not shown in the studies. Moreover, consideirng VMS absorption into cutting oil or water-cutting oil no studies have been found. This preliminary study will

therefore be provided for information about siloxane absorption into oil, which will be useful for subsequent research in this field.

## 1.2 Materials and methods

### 1.2.1 Materials : siloxanes and absorbents used

#### 1.2.1.1 *Siloxanes:*

Hexamethylsiloxane (L2) and octamethylcyclotetrasiloxane (D4) from Sigma Aldrich are used to generate the different concentrations. Their purity is of 98%. Siloxanes are normally present in a fluid form in the industry, where they are used in many applications. Then the pathway to arrive in a gas form is accomplished by its volatilization during the anaerobic digestion. Here the fluid siloxanes are volatilized by a gas generation system which is explained later.

#### 1.2.1.2 *Absorbents:*

Motor oil 5W40 is commercial motor oil frequently used in the vehicles; it is produced from different companies. Here we used motor oil 5W40 from Elf.

Cutting oil is currently used in the industries for the refrigeration of the machines. Here we used cutting oil produced in Germany: Hochleistungs-Schneidöl Alpha 93, Jokish® GmbH.

Water - cutting oil: cutting oil is normally diluted with water with the following proportions: 95 % wt of tap water and 5% wt of cutting oil.

### Characterization of oils: Viscosity

The viscosity was measured using an SV10-A&D sine-wave vibro viscometer. The motor oil (5W40) and cutting oil (Alpha 93) samples were heated with stirring. They were then put into the sampling box and values were read at the desired temperature. For both kinds of oil, the viscosity decreased significantly when the temperature was raised. The absorption phenomenon was thus studied at two different temperatures, 25°C and 50°C. Viscosity values are shown in Table 16.

Table 16. Physical properties of motor oil and cutting oil

	Motor oil	Cutting oil
Viscosity (mPa.s) 25°C	161	142
Viscosity (mPa.s) 50°C	41,7	59,4
Density (g.cm <sup>-3</sup> ) 25°C	0,86	0,90

## Characterization of oils: Chemical elementary

In Table 17 the chemical elementary of both oils is presented. As we can observe, they differ strongly. Motor oil is majorly composed of carbon and hydrogen, characteristic of the mineral oils. In contrast, cutting oil has a low content of carbon and about 50 % of the composition is not read by the elementary analyses. This is characteristic of synthetic oils where a lot of additives are part of the formulation.

Table 17. Chemical properties of motor oil and cutting oil

	Motor oil	Cutting oil
C (%)	84,54	38,49
H (%)	13,83	6,24
O (%)	1,78	28,17
N (%)	0,14	1,19
S (%)	n.d	n.d

n.d: non detected

## 1.2.2 Laboratory unit

The laboratory unit used to carry out the absorption processes is shown in Figure 9. As can be seen, it consists of the gas generation system and the absorption column. Each part is described below:

### 1.2.2.1 Column

A column in stainless steel was designed to carry out the experiments. Its characteristics are: height (0.4 m) and the inner diameter (0.05 m). It is equipped with a heating resistance in the external surface and a thermocouple located inside of the column which allows the temperature control by a software.

Inside the column, a perforated plate was arranged at the bottom to generate the gas dispersion. In a bubbling column, the use of an apparatus with several orifices enhances the contact between the phases (Treybal 1980). Thus a circular plate (3.9 cm in diameter) with numerous orifices (0.5 mm) was designed as shown in Figure 7.

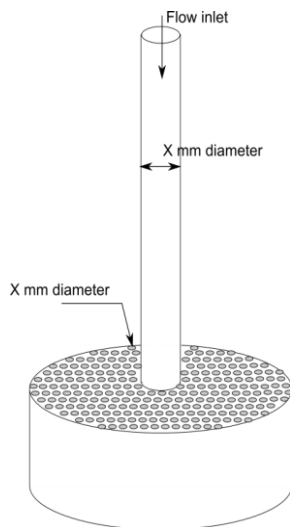


Figure 7. Diagram and photography of the perforated plate.

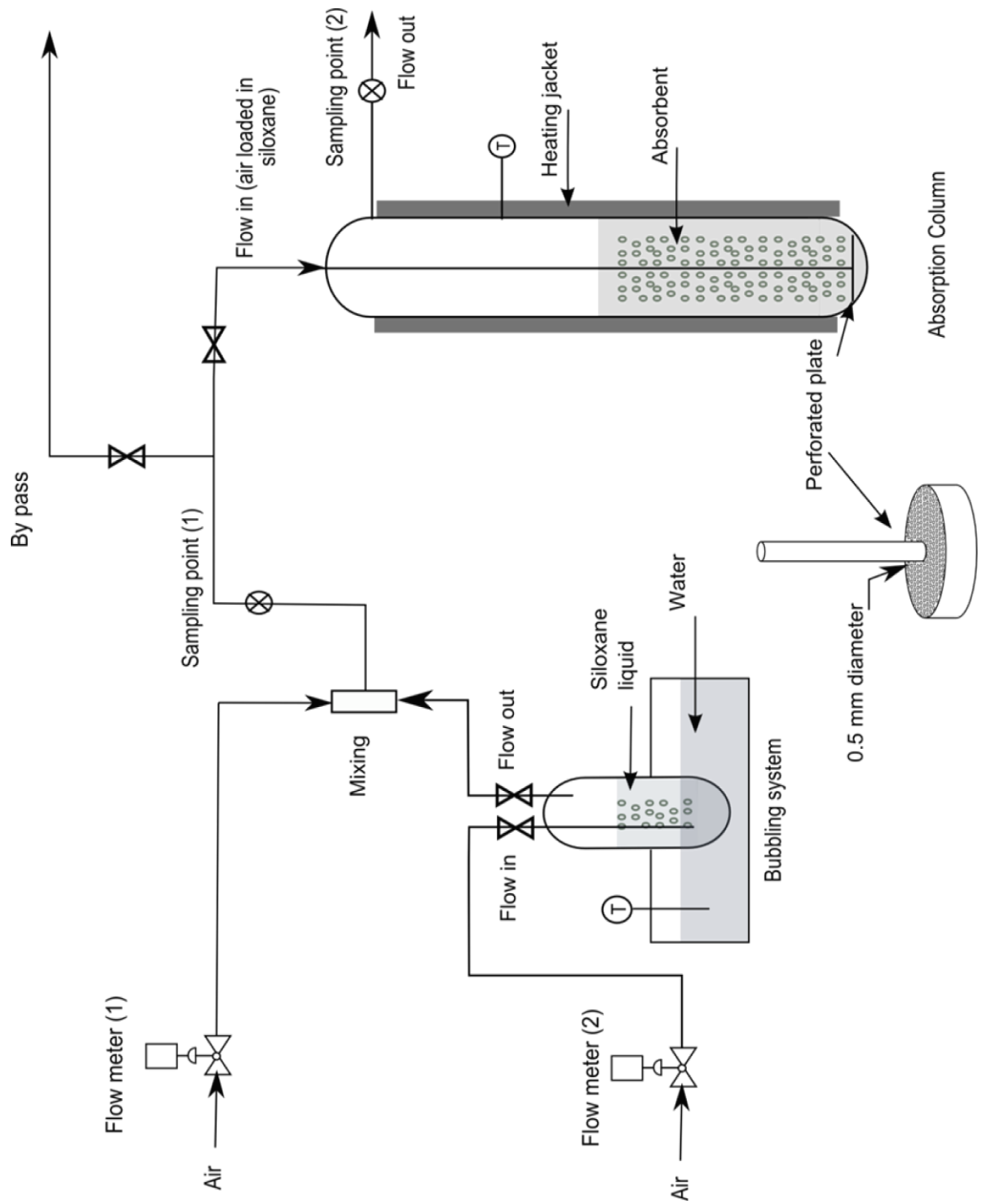


Figure 8. Diagram of the laboratory unit. Generation of siloxanes loaded in siloxanes and absorption column.

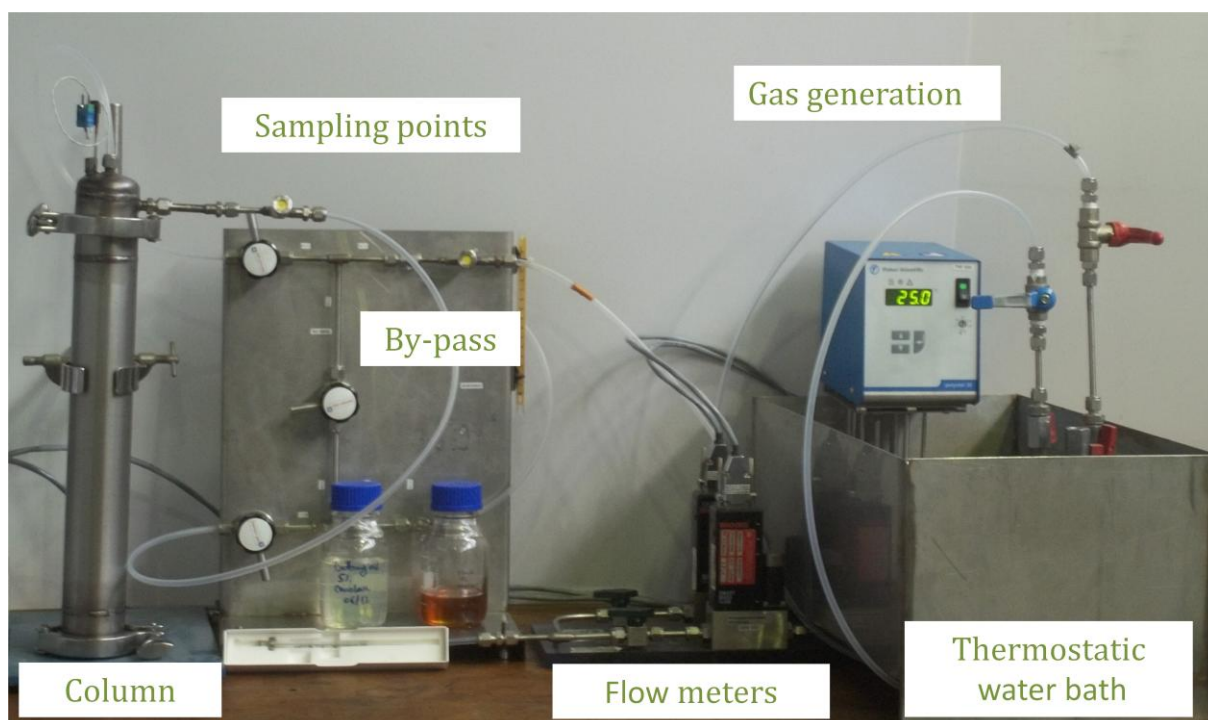


Figure 9. Photography of the laboratory unit. Generation of air loaded in siloxanes and absorption column.

### 1.2.2.2 *Gas generation process*

Gas saturated in siloxane is produced as described: a flow of air passes through a tank filled with liquid siloxane. The tank temperature is controlled by a thermostatic water bath set at 25°C provided with an agitation system. Forward, the outgoing gas (saturated in siloxane) is mixed with an air flow to decrease the concentration.

### 1.2.2.3 *Siloxanes analyses*

Siloxanes concentrations are analyzed by a gas chromatography with flame ionization detector (GC/FID, Agilent Technologies 7820A GC system). The principal parameters of the GC–FID are: oven temperature 70°C, injector temperature 100°C and detector temperature 130°C. The column specifications are: packing material 5%-Phenyl-methylpolysiloxane, column length of 30 m, diameter of 0.32 mm and film thickness of 0.25 μm. The gas flow rate is 0.5 ml.min<sup>-1</sup> of helium with a split injection of 1/20.

### 1.2.2.4 *Column characterization*

Gas dispersion is used to diffuse compounds into the liquid phase. In this study a column described previously was used for this purpose.



## Gas-bubble diameter

Different parameters such as flow rate, fluid properties and the geometry of the sparger influence the gas bubble diameter. In the case of small flow rate, the next equation based on force balance on the bubble, allows to calculate the gas-bubble diameter (Treybal 1980). We observe that for a small flow rate the diameter of the bubble is independent of the flow rate, and it is mainly controlled by the superficial tension

$$(18) \quad d_p = \left( \frac{6d_o \sigma g_c}{g \Delta \rho} \right)^{1/3}$$

Where  $d_p$  is the average bubble diameter,  $d_o$  is the orifice diameter,  $\sigma$  superficial tension,  $g_c$  conversion factor,  $g$  acceleration of gravity,  $\Delta \rho$  difference in density.

For an intermediate flow rate the diameter can be calculated by the equation (19) and we observe that a difference of at low flow rate, the volumetric gas flow rate per orifice ( $Q_{Go}$ ) is taken into account:

$$(19) \quad d_p = \left( \frac{72 \rho_L}{\pi^2 g \Delta \rho} \right)^{1/5} Q_{Go}^{0.4}$$

Where  $\rho_L$  is the liquid density.

### 1.2.2.5 Interfacial area

Interfacial area is calculated by the equation (20). It is based on the velocity of the liquid and the slip velocity on sparged vessels. Thus based on the properties of the absorbents and the geometry of the column and the sparger, we calculate the bubble diameter and the interfacial area for a given range of flow rates. Values for the different absorbents and the corresponding operational conditions studied are listed in Table 18:

$$(20) \quad a = \frac{6 \varphi_G}{d_p}$$

Here we observe that the higher is the flow rate, the higher is the interfacial area. However, once the flow rate overpass a value, around 27 L.min<sup>-1</sup>, equation (19) is applied. As a result, the bubble diameter increases and consecutively the area decreases. Thus the selection of a high flow rate to enhance the interfacial area must be considered taking into account this limit value. Also, at high flow rates the residence time of the gas into the liquid is smaller. Thus, in order to study the absorption we selected an operational range where the two conditions are optimized and named “working area”. An example of residence time and interfacial area in function of flow rate for motor oil is illustrated in Figure 10.

Table 18. Gas bubble diameter and interfacial area calculated for the experimental conditions. Motor oil, cutting oil and Water-cutting oil. Temperature 25°C. Correlations (Treybal, 1980).

Absorbent	Flow rate (L.min <sup>-1</sup> )	d <sub>p</sub> (m) x 10 <sup>-3</sup>	a (m <sup>2</sup> .m <sup>-3</sup> )
Motor oil	3.20	2.20	190.7
	8.03	2.20	408.6
	43.6	52.40	40.1
Cutting oil	1.01	2.95	38.6
	2.51	2.95	50.8
	3.20	2.95	111.8
	3.31	2.95	101.6
	8.03	2.95	223.5
Water-cutting oil	3.20	2.86	147.0
	8.03	2.86	210.0
	8.20	2.86	252.0

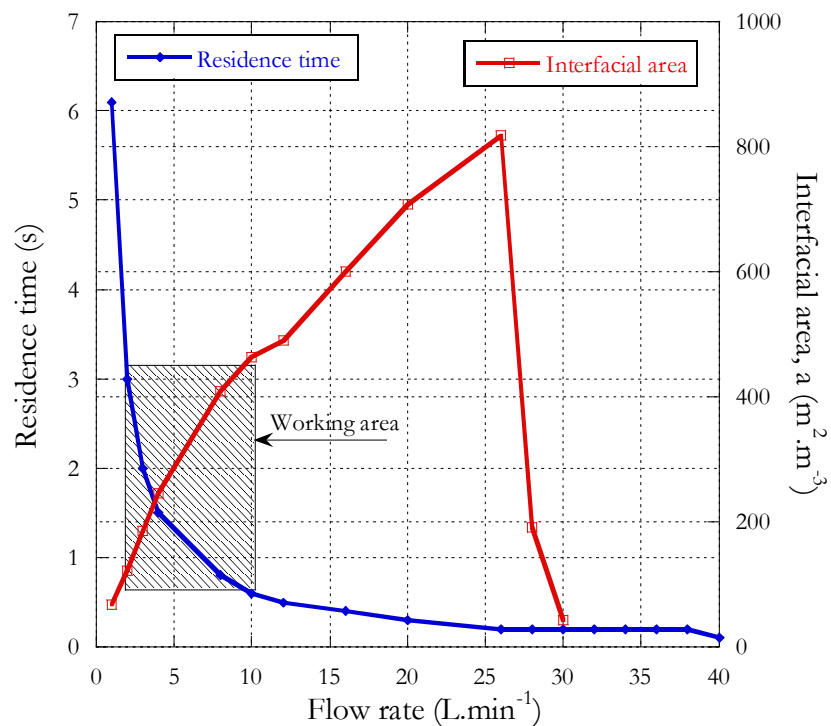


Figure 10. Residence time (s) and interfacial area (m<sup>2</sup>.m<sup>-3</sup>) in function of flow rate (L.min<sup>-1</sup>). Calculated based on the geometry of the absorption column for motor oil T: 25°C. Correlations (Treybal, 1980)

### 1.2.2.6 Absorption procedure

Each experiment is performed with the following procedure: the column is filled with liquid, the temperature is regulated and the gas generation is set up. Once the system reaches a stable steady state the absorption experiments are carried out until the outlet and inlet concentrations are the same. Gas samples are taken regularly at the sampling points located at the inlet and outlet of the column and analyzed by a gas chromatograph coupled with a flame ionization detector (GC/FID) described previously. Similar methods for VOCs absorption were previously used (Lalanne et al. 2008, Allen et al. 1997).

### Liquid absorption capacity

Absorbents performance is analyzed by the liquid absorption capacity. For a semi-batch reactor with a continuous flow of gas and a fixed quantity of liquid, the mass balance is written as shown in equation (21):

$$(21) \quad Q_g C_{in,g} = Q_g C_{out,g}(t) + V_L \frac{dC_L}{dt}$$

Where  $Q_g$  is the gas flow rate ( $m^3 \cdot s^{-1}$ ),  $V_L$  the solvent volume (L) and  $C_{in,g}$  and  $C_{out,g}$  are respectively inlet and outlet siloxanes concentration in the gas flow ( $mg \cdot m^{-3}$ ). The absorption capacity of the solvent ( $q_L$ ) can thus be calculated as described in equation (22). It is expressed in ( $mg \cdot L^{-1}$ ).

$$(22) \quad q_L = \frac{Q_g}{V_L} \int_{t=0}^{t^{sat}} (C_{in,g}(t) - C_{out,g}(t)) dt$$

Henry's law

The relation between two phases (i and j) at the equilibrium can be expressed by the generic partition coefficient  $K_{ij}$  as described in the equation (23). In this equation, the  $C_i^*$  and  $C_j^*$  are the saturation concentrations in the same unity. When one of the phases is a gas, the dimensionless constant is named Henry's law. Experimental design to obtain this value can be performed in static or dynamic (Allen et al. 1997). Here, dynamic test was carried out.

$$(23) \quad K_{ij} = \frac{C_i^*}{C_j^*}$$

### 1.2.2.7 Experimental conditions

The experimental study was performed in two parts. First, L2 was absorbed into different solvents such as water, motor oil, cutting oil, water-cutting oil. The influence of different parameters was studied such as siloxanes inlet concentration, residence time and

temperature. In the second phase of the study, D4 was absorbed into water, motor oil, cutting oil, water-cutting oil and as well as with the siloxanes L2, the influence of different parameters was studied such as inlet concentration and residence time. Hence, measurements of siloxanes treatment were performed while varying: material weight, siloxane concentration, gas flow rate, and temperature.

In order to facilitate the presentation of the experiments, the next abbreviation is used as a reference of each experiment:

[Absorbent]-[Number of experiment]-[Siloxane] [Concentration]-[Mass of absorbent]-[Flow rate]-[Temperature]

- Motor oil: M
- Cutting oil: C
- Water cutting oil: WC
- Water : W
- Number of experiments: i
- Siloxane : L2 or D4
- Concentration initial: mg.Nm<sup>-3</sup>
- Mass of absorbent: g
- Flow rate : L.min<sup>-1</sup>
- Temperature : °C

The experimental results are divided into two parts according to the pollutant treated. First the results of siloxane L2 absorption into each absorbent: motor oil, cutting oil and water cutting oil are presented. The second part describes the results of siloxane D4 absorption into the same absorbents. The breakthrough curves, absorption capacity and influence of parameters are thus discussed.

### 1.2.3 Operational conditions: Siloxane L2 absorption into (motor oil, cutting oil and water-cutting oil mixture)

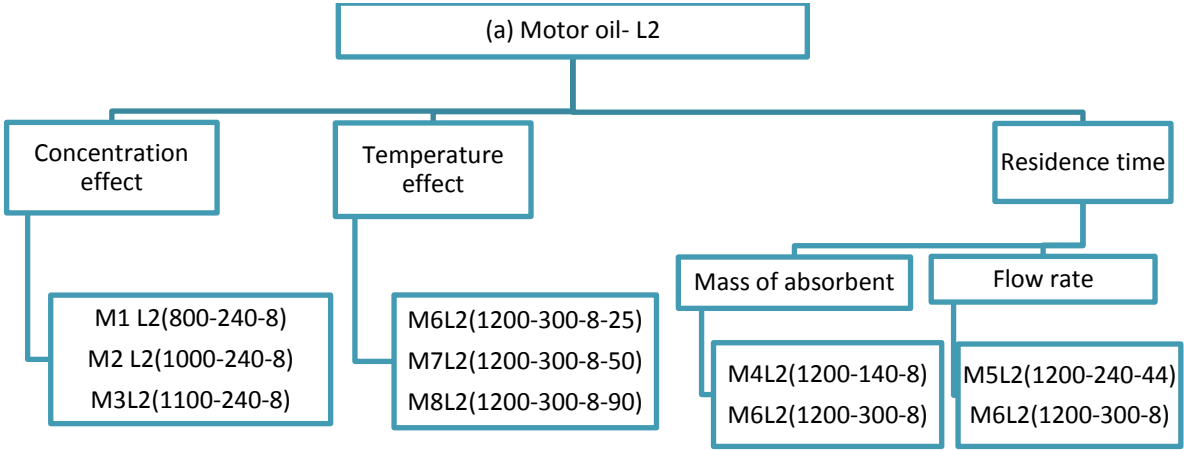
The corresponding operational conditions studied of siloxanes L2 absorption into motor oil, cutting oil and water cutting oil are presented in Table 19. Additionally, to facilitate the comprehension of the present work

Figure 11 synthesises the experimental conditions and purpose. It is important to highlight that the measure of siloxanes is a difficult method and many experiments were

carried out to arrive the following results. As well, before the experimental in dynamic, a calibration curve was carried out and repeated several times.

Table 19. Operating conditions corresponding to the absorption of Hexamethylsilixane (L2) into water, motor oil, cutting oil and water-cutting oil.

Absorbent	Concentration (mg.Nm <sup>-3</sup> )	Mass of absorbent (g)	Flow rate (L.min <sup>-1</sup> )	Temperature (°C)	Abbreviation
Water	1200	240	8.03	25	W1L2 (1200-240-8)
Motor oil	800	240	8.03	25	M1L2 (800-240-8)
	1000				M2L2 (1000-240-8)
	1100				M3L2 (1100-240-8)
	1200				M4L2 (1200-140-8)
	1200	140	8.03	25	M5L2 (1200-240-44)
		240	43.6	25	M6L2 (1200-300-8)
		300	8.03	25	M7L2 (1200-300-8-50)
				90	M8L2 (1200-300-8-90)
Cutting Oil	1200	240	8.03	25	C5L2 (1200-240-8)
	1200	350	3.31	25	C1L2 (1200-350-3.3)
	1200		8.03	25	C2L2 (1200-350-8)
	1800		2.51	25	C3L2 (1800-350-2.5)
	4800	300	1.01	25	C4L2 (4800-300-1)
Water-cutting oil	1000	300	8.03	25	WC1L2(1000-300-8)
	1800		8.2	25	WC2L2(1800-300-8)



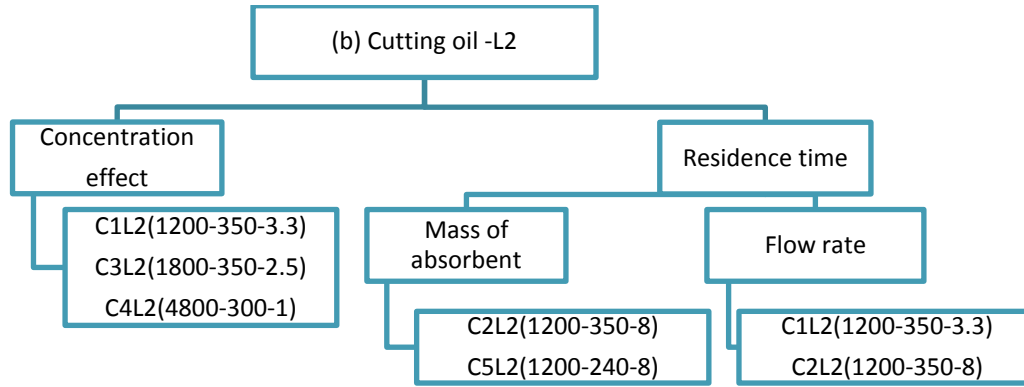


Figure 11. Experiments diagram corresponding the absorption of Hexamethylsiloxane (L2) into (a) Motor oil (b) Cutting oil.

## 1.2.4 Operational conditions: Siloxane D4 absorption into (motor oil, cutting oil and water-cutting oil mixture)

In this section the absorption of siloxane D4 is present. The operational conditions are listed in Table 20. As well, in Figure 12 the diagram of the experimental study is presented.

Table 20. Operating conditions corresponding to the absorption of Octamethyltetracyclosiloxane (D4) into water, motor oil, cutting oil and water-cutting oil.

Absorbent	Concentration (mg.m <sup>-3</sup> )	Mass of absorbent (g)	F low rate (L.min <sup>-1</sup> )	Tem perature (°C)	Abbreviation
Water	800	80	3.2	25	W1D4(800-80-3.2)
		300			W2D4(800-300-3.2)
Motor oil	800	80	3.2	25	M1D4(800-80-3.2)
		300			M2D4(800-300-3.2)
Cutting oil	800	80	3.2	25	C1D4(800-80-3.2)
		300			C2D4(800-300-3.2)
		350			C3D4(800-350-3.2)
Water cutting oil	800	80	3.2	25	WC1D4(800-80-3.2)
		300			WC2D4(800-300-3.2)

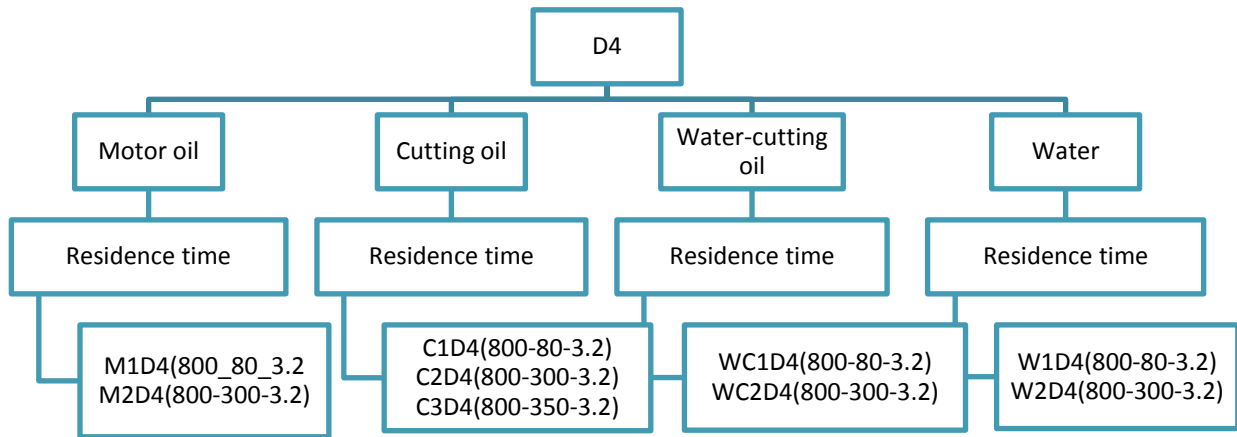


Figure 12. Experiments diagram corresponding the absorption of Octamethyltetracyclosiloxane (D4) into (a) Motor oil and Cutting oil.

## 1.3 Results and discussion

### 1.3.1 Siloxane L2

#### 1.3.1.1 Absorption into motor oil

Experimental data breakthrough of L2, defined as a normalized concentration ( $C_{out}/C_{in}$ ) for motor oil is shown in Figure 13. As can be seen, the experiments present a similar behavior. The concentration increases rapidly in the first seconds attaining a value of  $0.4 C/C_0$ , and forward the concentration increases slowly to finally reach equilibrium between the phases in about 1 h. For the condition 6 which was carried out at  $1200 \text{ mg.m}^{-3}$  and  $300 \text{ g}$  and  $8.03 \text{ L.min}^{-1}$ , the evolution concentration is slowly than the other ones. These curves are normally found in absorption process where a good absorption capacity of the pollutant in the liquid exists. In the first moments, the differences in concentrations in the liquid phase and in the gas phase are high, giving a high absorption capacity of the liquid. However, it is not observed a moment where all the pollutant is absorbed by the solvent. In fact the removal efficiency observed at the beginning of the process for those conditions is around 60%. For the conditions where the flow rate is high  $44 \text{ L.min}^{-1}$  or the mass of absorbent is low (140 g) or high temperature ( $90^\circ\text{C}$ ) no removal of L2 was observed in the gas. Other previous studies with motor oil were carried and have reported a removal efficiency of the siloxanes about 60% (Stoddart et al. 1999) suggesting that no highest removal efficiency can be obtained. However, not only the physical-chemical nature of the absorbents influence the absorption

process, parameters as interfacial area and residence time are extremely associated with the efficiency. Thus, we increased the absorbent mass in the experiment 300 g and a higher removal efficiency of 76% was obtained. The residence time effect is going to be discussed later for a better understanding. The overall responses of the outlet concentration showed a good performance for motor oil. To better understand this behavior the absorption capacity is calculated and showed in the Figure 14.

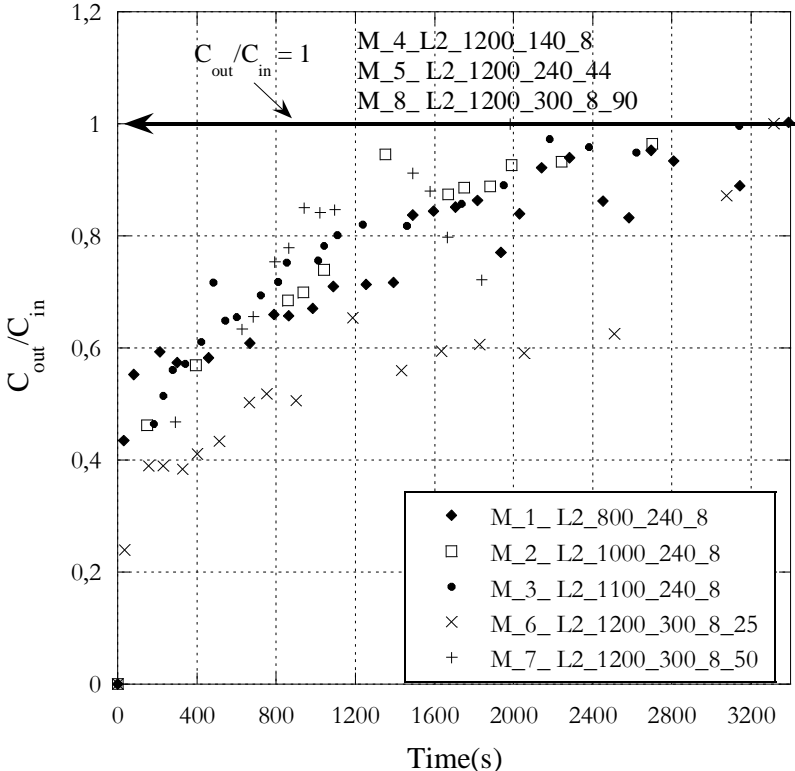


Figure 13. Hexamethyldisiloxane (L2) absorption into motor oil. Breakthrough curves in function of time (s). Experimental conditions: flow rate  $8.03 \text{ L}\cdot\text{min}^{-1}$ ; siloxane concentration ( $800 - 1200 \text{ mg}\cdot\text{m}^{-3}$ ). Temperature ( $25; 50 \text{ }^\circ\text{C}$ ).



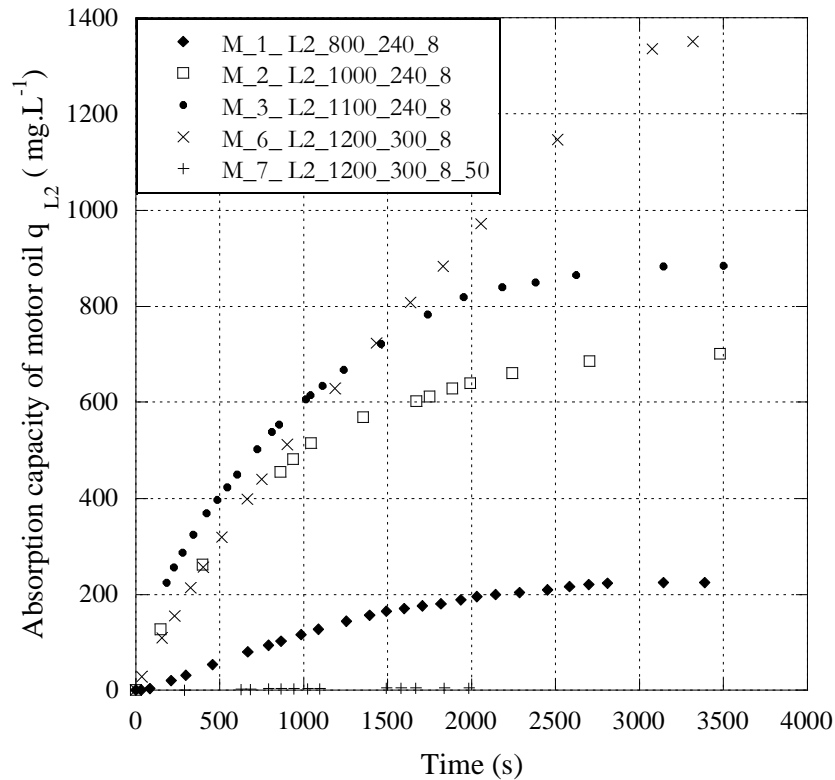


Figure 14. Hexamethyldisiloxane (L2) absorption into motor oil. Absorption capacity  $q_{L2}$  ( $\text{mg.L}^{-1}$ ) in function of time (s). Experimental conditions: flow rate  $8.03 \text{ L.min}^{-1}$ ; siloxane concentration (800 -1200  $\text{mg.m}^{-3}$ ). Temperature (25;50 °C).

Here we observe the absorption capacity of motor oil for all the conditions except the for the cases where no removal of L2 was observed ( flow rate =  $44 \text{ L.min}^{-1}$  or mass absorbent = 140 g or  $T= 90^\circ\text{C}$ ) and therefore there are not represented in the graphic. As observed, the values vary strongly for each operating condition. At the equilibrium, the highest value was about  $1350 \text{ mg.L}^{-1}$  which corresponds to the conditions of  $1200 \text{ mg. m}^{-3}$ , 300g of absorbent and a flow rate of  $8.03 \text{ L.min}^{-1}$ . Absorption capacities at the equilibrium for each experiment are presented later in Table 31 and they range between 0 and  $1350 \text{ mg.L}^{-1}$  depending on the operating parameters. To our knowledge, no other results of motor oil absorption capacity have been reported. In most cases, we observe that motor oil has a good trapping capacity of L2.

### Concentration effect: siloxane L2 into motor oil

Three different concentrations (800, 1000 and  $1100 \text{ mg.m}^{-3}$ ) were carried out as described in Table 21. For these experiments, the same behavior  $C_{in}/C_{out}$  was observed as shown in Figure 13. As a result, absorption capacity increases in function of the

concentration. The gradient of concentration between the phases is the driving force of the mass transfer, as higher gradient a higher pollutant is retained in the liquid phase.

Table 21. Concentration effect. Absorption of siloxane L2 into motor oil.

Absorbent	Concentration (mg.m <sup>-3</sup> )	Mass (g)	Flow rate (L.min <sup>-1</sup> )	T (°C)	q <sub>L2</sub> (mg.L <sup>-1</sup> )	Residence Time RT (s)	Reference
Motor oil	800	240	8.03	25	224	0.8	M1
	1000				701	0.8	M2
	1100				884	0.8	M3

As shown in the bibliography chapter, the concentration of siloxanes in biogas varies in function of the biogas production, and values for example of 400 mg.m<sup>-3</sup> have been reported (Schweigkofler, Niessner 1999). However, we know that this value is the average of the concentration and for example it does not take into account the dispersion of the VMSs by seasonal effects or material in the disposal, that can lead peaks of concentration. Therefore, some studies have been done for the characterization of odors in landfill sites focused in VOCs, H<sub>2</sub>S and NH<sub>3</sub> due their harmful effects when they are located close of to the population (Chiriac et al. 2011). Thus our interest in testing higher concentrations than those reported in biogas. From here we observe for example for a concentration of 1100 mg.m<sup>-3</sup> a motor oil absorption capacity of 884 mg.L<sup>-1</sup>. Resulting that for absorption process the increases in the siloxanes concentration is not a barrier in the process.

### Residence time effect: siloxane L2 into motor oil

Two parameters, flow rate and mass of the absorbent were changed to study residence time effect. Values are listed in Table 22. Results of the experiments carried out at 140 g and the one at 44 L.min<sup>-1</sup> has shown no absorption capacity of motor oil. These experiments correspond at a small residence time of (0.1 to 0.2s) as listed in Table 7. However, for longer contact time between the phases absorption capacity increases as a function of residence time, straighten out its relevance during the process. For motor oil, values between 0.8 s and 1.1 s shows good absorption capacities.

Table 22. Effect of the residence time on the absorption capacity of siloxane L2 into motor oil.

Absorbent	Mass (g)	Concentration (mg.m <sup>-3</sup> )	Flow rate (L.min <sup>-1</sup> )	T (°C)	q <sub>L2</sub> (mg.L <sup>-1</sup> )	Residence Time RT (s)	Abbreviation
Motor oil	140	1200	8.03	25	0	0.2	M4L2
	300				1350	1.1	M6L2
	240	880	8.03	25	224	0.8	M1L2
	240	1000	8.03	25	701	0.8	M2L2
	240	1100	8.03	25	884	0.8	M3L2
	240	1200	43.6	25	0	0.1	M5L2

Residence time–interfacial area: if we maintain the same interfacial area (408 m<sup>2</sup>.m<sup>-3</sup>) and we vary the residence time from 0.2 s to 1.1 s, as a result we observed no absorption for residence time of 0.2 s and in contrary, absorption of 1350 mg.L<sup>-1</sup> for 1.1 s. Also, we tested a high value of flow rate of 43.6 L.min<sup>-1</sup>, it gives a small residence time (0.1s) and as we cross the limit section the interfacial area drops at (40.1 m<sup>2</sup>.m<sup>-3</sup>). As a result, no absorption capacity was observed. These experiments show the importance of flow rate in a separation process. In a biogas plant, flow rate can vary, thus it is important to consider a buffer tank to collect the biogas before sending them to the absorption column and regulate it constantly during the process.

### Temperature effect: siloxane L2 into motor oil

Three temperatures were tested: 25, 50, and 90 °C to study its influence on the absorption. The experimental data are listed in Table 23. As a result, absorption capacity decreases as the temperature increases as shown in Figure 15. At 25°C absorption capacity was of 1350 mg.L<sup>-1</sup>, at 50°C absorption capacity was of 5.4 mg.L<sup>-1</sup> and at 90°C no absorption was observed. In such a way, high temperature is therefore not recommended for VMS absorption. At high temperature, viscosity decreases as listed in Table 6. This could lead a lower resistance from the liquid to the gas. As a consequence, the residence time of gas in the column is decreased explaining the lower trapping capacity of motor oil. Moreover, siloxanes are more volatile reducing significantly the diffusion from the gas phase to the liquid phase. Additionally, at highest temperature an undesirable pollution could be achieved by stripping of other compounds.

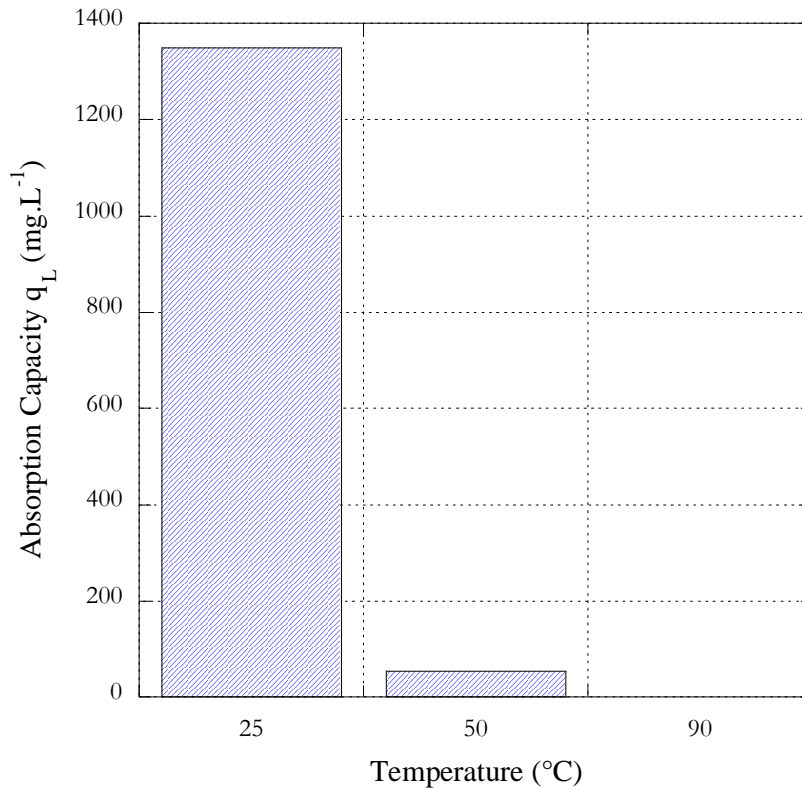


Figure 15. Temperature effect (25; 50; 90 °C). Absorption of siloxane L2 into motor oil.  $C_{in}$ : 1200 mg.m<sup>-3</sup>; Flow rate: 8.03 L.min<sup>-1</sup>, Mass: 300 g.

Table 23. Effect of the temperature on the absorption capacity of siloxane L2 into motor oil.

Absorbent	Concentration (mg.m <sup>-3</sup> )	Mass of absorbent (g)	Flow rate (L.min <sup>-1</sup> )	T °C	$q_{L2}$ (mg.L <sup>-1</sup> )	Residence Time RT (s)	Abbreviation
Motor oil	1200	300	8.03	25	1350	1.1	M6L2
				50	5.4	1.1	M7L2
				90	0	1.1	M8L2

### 1.3.1.2 Absorption of siloxane L2 into cutting oil

Experimental data of L2 gas concentration at the outlet of the absorption column with cutting oil is represented in figure 16. As illustrated, the concentration of L2 varies highly, at difference than with motor oil. For example, for the conditions 350 g and 8.03 L.min<sup>-1</sup>, the concentration increases rapidly at 0.8 C/Co and then it decreases at 0.6 C/Co. In general, the behavior is not optimal suggesting that cutting oil is not a good absorbent. Moreover, at the same operating conditions 8.03 L.min<sup>-1</sup> and 240 g which was tested previously with motor oil, no absorption of siloxane L2 was observed. Consequently, the gas flow rate was decreased

and the quantity of cutting oil was increased to allow absorption measurements. These experiments demonstrate again the importance of the nature of the absorbent and the impact of the residence time. Indeed, at the first 30 min of the process, the high variability between the outlet and inlet concentration reveals the interactions between the pollutant (siloxane L2) and the solvent. However, it is not enough to be trapped in the liquid phase. We can imagine that a stripping process is started resulting in a boost of the outlet concentration. This behavior suggests that L2 solubility in cutting oil is low. As a consequence, we increased the concentration strongly at 4800 mg.m<sup>-3</sup> to analyze if by a more important driving force the behavior is improved. Here we observe as well as in the other cases the oscillations between the outlet and inlet concentrations. This experiment was carried out also at low flow rate (1.01 L.min<sup>-1</sup>). Thus it is apparent that in most of the cases the cutting oil is not a good absorbent for siloxane L2.

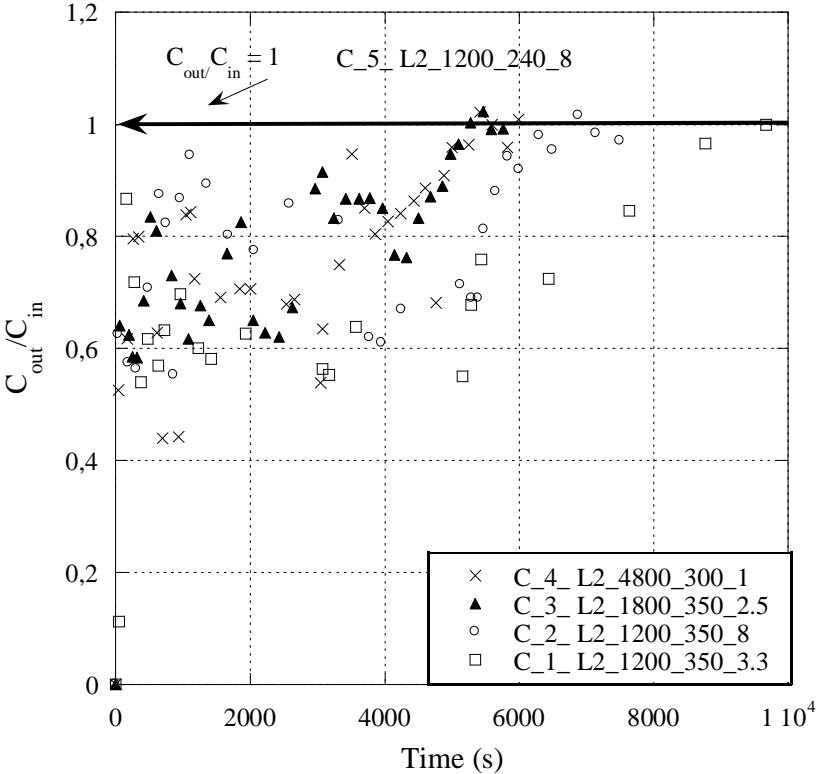


Figure 16. Hexamethyldisiloxane (L2) absorption into cutting oil. Breakthrough curves in function of time (s). Experimental conditions: flow rate(1.0- 8.03 L.min<sup>-1</sup>); siloxane concentration (1200 -4800 mg.m<sup>-3</sup>). Temperature (25°C).

In Figure 17 absorption capacity of cutting oil for different experimental conditions is presented. We observe an interesting absorption capacity for the experiments carried out at 300g and 350 g of absorbent with values which ranges around 200 to 700 mg.L<sup>-1</sup>. For those, the absorption capacity increases linearly the most of the time. The highest value obtained is

of  $684 \text{ mg. L}^{-1}$  which corresponds of the highest concentration ( $4800 \text{ mg.m}^{-3}$ ). Absorption capacities at the equilibrium are listed in Table 32, thus even if the concentration profile presents fluctuations it is important to highlight that cutting oil presents a potential to absorb siloxane L2.

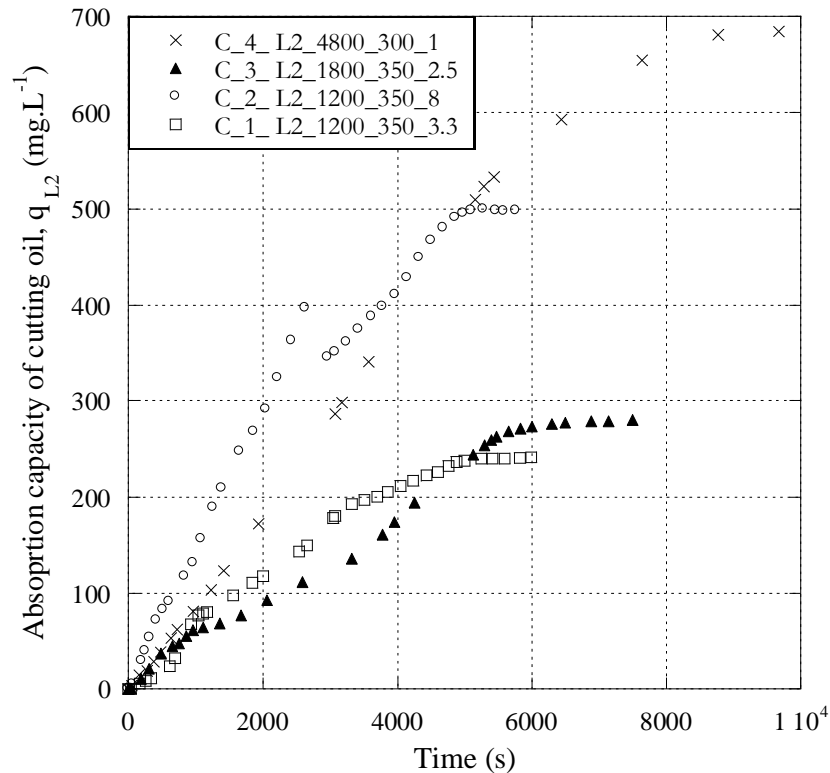


Figure 17. Hexamethyldisiloxane (L2) absorption into cutting oil. Absorption capacity  $q_{L2}$  ( $\text{mg.L}^{-1}$ ) in function of time (s). Experimental conditions: flow rate ( $1.0\text{--}8.03 \text{ L.min}^{-1}$ ); siloxane concentration ( $1200\text{--}4800 \text{ mg.m}^{-3}$ ). Temperature ( $25^\circ\text{C}$ ).

Comparing with motor oil at similar conditions (residence time of 1.1 s) the absorption capacity of cutting oil is of  $498 \text{ mg.L}^{-1}$ , 40% of the motor oil absorption capacity. Thus, experiments reveal that L2 affinity with cutting oil is lower than with motor oil.

### Concentration effect: siloxane L2 into cutting oil

Three concentrations were tested, 1200 1800 and  $4800 \text{ mg.m}^{-3}$ . For the three experiments, the same behavior  $C_{in}/C_{out}$  was observed as shown in Figure 16. For those, the absorption capacity increases. At high content of the pollutant in the gas flow, the gradient of concentration is higher, resulting in a higher absorption capacity. As explained before, the concentration was increased strongly to analyze if by a more important driving force the behavior is improved however the fluctuations in the gas at the outlet of the column were also observed.

Table 24. Effect of the concentration on the absorption capacity of siloxane L2 into cutting oil.

Absorbent	Concentration (mg.m <sup>-3</sup> )	Mass of absorbent (g)	Flow rate (L.min <sup>-1</sup> )	Residence Time RT (s)	q <sub>L2</sub> (mg.L <sup>-1</sup> )	Abbreviation
Cutting oil	1200	350	3.31	3.2	241	C1L2(1200-350-3.3)
	1800	350	2.51	4.3	280	C3L2(1800-350-2.5)
	4800	300	1.01	8.2	684	C4L2(4800-300-1.0)

### Residence time effect: siloxane L2 into cutting oil

The residence time effect was first studied by maintaining the mass of absorbent constant (350 g) and modifying the flow rate of 3.31 and 8.03 L.min<sup>-1</sup>, resulting in a residence time of 3.2 s and 1.3 s respectively. Here, we obtained a higher absorption capacity of 498 mg. L<sup>-1</sup> corresponding to the smallest residence time (1.3 s) and an absorption capacity of 241 mg. L<sup>-1</sup> for 3.2 s. It shows that increasing the flow rate improve significantly the absorption capacity. Moreover a higher flow rate the interfacial area is enhanced with values of (101.6 to 223.5 m<sup>2</sup>.m<sup>-3</sup>). Thus for the residence time ranges between 1 to 4 s, the absorption is improved by a higher interfacial area rather than the residence time.

Table 25. Effect of the residence time on the absorption capacity of siloxane L2 into cutting oil.

Absorbent	Concentration (mg.m <sup>-3</sup> )	Mass of absorbent (g)	Flow Rate (L.min <sup>-1</sup> )	q <sub>L2</sub> (mg.L <sup>-1</sup> )	Residence Time RT (s)	Abbreviation
Cutting oil	1200	240	8.03	0	0.7	C5L2(1200-240-8)
		350	3.31	241	3.2	C1L2(1200-350-3.3)
		350	8.03	498	1.3	C2L2(1200-350-8)

However, for the experiments were the flow rate is maintained constant (8.03 L.min<sup>-1</sup>) and the residence time is modified by changing the mass of absorbent from 350 to 240 g resulting in 1.3 to 0.7 s respectively, no absorption is observed at 0.7 s. Thus for the residence time ranges under 1 s, the absorption is improved by a higher residence.

According to the results it is evident that absorption processes depend strongly on the characteristics of the column and system of diffusion of gas. And the relevance of study parameters as interfacial area and residence time.

This study is focused on the availability of absorbents to treat siloxanes. Thus a simple system was used and it was not considered a study of optimal parameters. Nevertheless, it is apparent that the flow rate is a limiting factor as discussed previously with the motor oil. We remark that the effect of other parameters such as agitation, pressure and turbulent flow regime are known to have a huge impact in absorption process and must be considered on a scale-up study.

### 1.3.1.3 Absorption of siloxane L2 into water-cutting oil mixture

Experimental data of L2 gas concentration at the outlet of the absorption column with water-cutting oil is represented in Figure 18. The outlet concentration increases rapidly with values of 0.6 C/Co. However, these experiments shown a potential of water-cutting oil mixture to absorb L2. A simple addition of cutting oil fraction (5% wt) modifies strongly the water properties enhancing the adsorption capacity of the solution. Absorption capacity at the saturation is shown in Table 26. Moreover, comparing with cutting oil pure, its concentration profile is much more stable.

Table 26. Hexamethyldisiloxane (L2) absorption capacity of water-cutting oil.

Absorbent	Concentration (mg.m <sup>-3</sup> )	Mass of absorbent (g)	Flow rate (L.min <sup>-1</sup> )	Residence Time RT (s)	q <sub>L2</sub> (mg.L <sup>-1</sup> )	Abbreviation
Water	800	240	8.03	0.7	0	W1L2(1200-240-8)
Water - cutting oil	1000	300	8.03	1.0	57	WC1L2(1000-300-8)
	1800		8.2		95	WC2L2(1800-300-8)



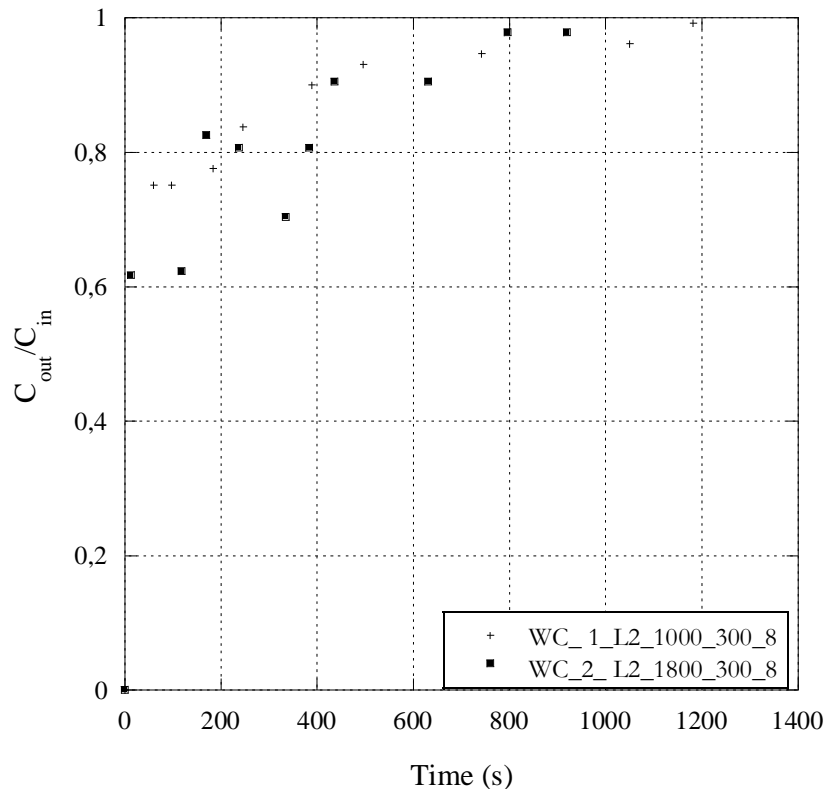


Figure18. Hexamethyldisiloxane (L2) absorption into water-cutting oil. Breakthrough curves in function of time (s). Experimental conditions: flow rate(8.03-8.2 L.min<sup>-1</sup>); siloxane concentration (1000 -1800 mg.m<sup>-3</sup>). Temperature (25°C).

Absorption capacity for water-cutting oil is presented in Figure 19, as can be seen, it increases with the concentration. The values are much lower than those obtained with pure cutting oil and motor oil. To compare with pure cutting oil, a calculus base on the 5% of cutting oil present in the mixture has been done and the results are presented in Table 27. It shows the enhancement in the contact surface between the phases, this can be explained by the theory of the second film which allows the enhancement of mass transfer from the gas phase of hydrophobic compounds in a water oil solution (Dumont, Delmas 2003).

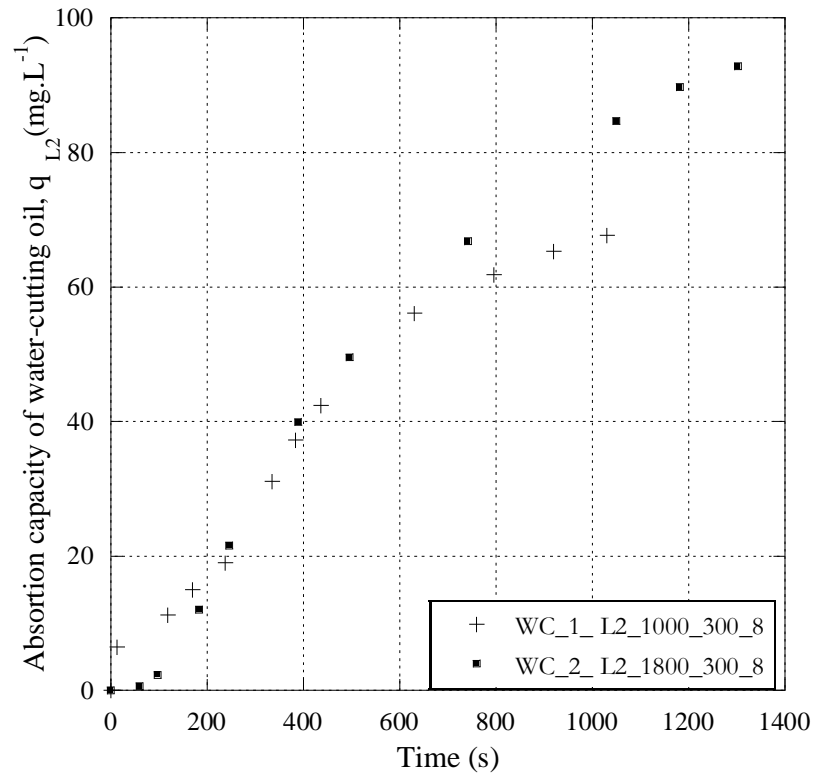


Figure 19. Hexamethyldisiloxane (L2) absorption into water-cutting oil. Absorption capacity  $q_{L2}$  ( $\text{mg.L}^{-1}$ ) in function of time (s). Experimental conditions: flow rate ( $8.03 - 8.2 \text{ L.min}^{-1}$ ); siloxane concentration ( $1000 - 1800 \text{ mg.m}^{-3}$ ). Temperature ( $25^\circ\text{C}$ ).

Table 27. Comparison of the absorption capacity of water-cutting oil and the 5% wt of the cutting oil. Hexamethyldisiloxane (L2) absorption into water-cutting oil.

Water-Cutting oil [Cin, Mass( g), flow rate( $\text{L.min}^{-1}$ ) ]	Water-cutting oil $q_{L2}$ ( $\text{mg.L}^{-1}$ )	$q_{L2}$ ( $\text{mg.L}^{-1}$ ) for the 5 % wt of cutting oil
WC1L2(1000;300;8)	56.8	1136.7
WC2L2(1800;300;8)	94.8	1856.6

## 1.3.2 Siloxane D4

### 1.3.2.1 Absorption of siloxane D4 into motor oil

In Figure 20 concentration profile for D4 into motor oil is illustrated. As we can see, the curve increases very slowly. This reveals a very good solubility of D4 in motor oil. Additionally, no picks of concentration are observed, which is an advantage in the process.

Regarding the removal efficiency we observe a value of 80%. It is much more important than the values reported previously where it was of 60% (Stoddart et al. 1999). However, as we know, this value depends on several parameters such as: bubble size, residence time, and solubility of the compounds. In (Stoddart et al. 1999) experiments, the conditions are not known so the comparison is difficult but it allows us to have a reference point of the process and highlight the importance of the parameters during the absorption process. This preliminary study reveals that motor oil has a huge potential to treat pollutants as D4.

Table 28. Octamethyltetracyclosiloxane (D4) absorption into motor oil. Absorption capacity  $q_{D4}$  ( $\text{mg.L}^{-1}$ ).

Siloxane	Absorbent	Concentration ( $\text{mg.m}^{-3}$ )	Mass of absorbent (g)	Flow rate ( $\text{L.min}^{-1}$ )	RT (s)	$q_{D4}$ ( $\text{mg.L}^{-1}$ )	Abbreviation
D4	Motor oil	800	80	3.2	1.6	8820.6	M1D4(800-80-3.2)
			300		5.5	Very long-stopped	M2D4(800-300-3.2)

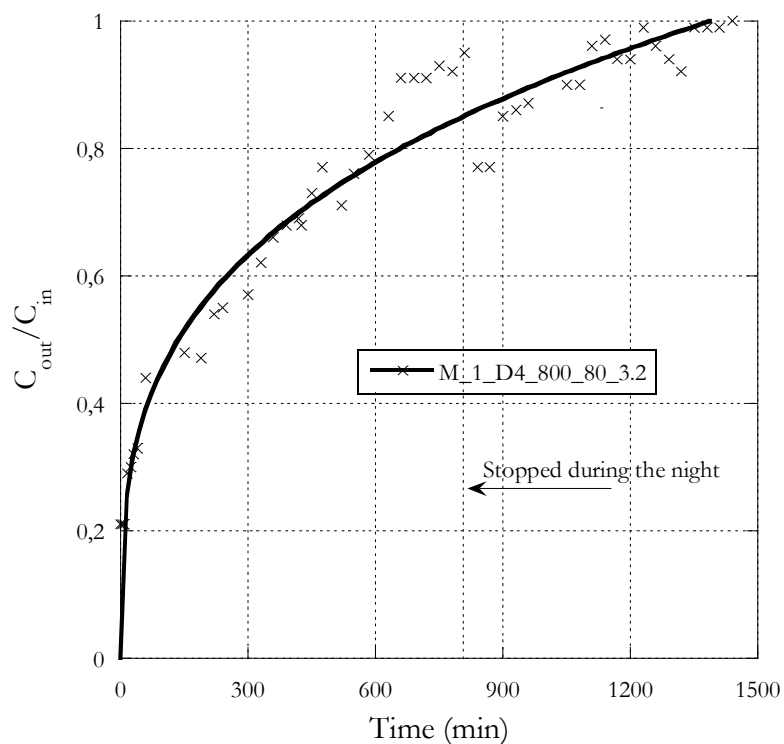


Figure 20. Octamethyltetracyclosiloxane (D4) absorption into motor oil. Breakthrough curves in function of time (s). Experimental conditions: flow rate ( $3.2 \text{ L}\cdot\text{min}^{-1}$ ); siloxane concentration ( $800 \text{ mg}\cdot\text{m}^{-3}$ ). Temperature ( $25^\circ\text{C}$ ).

Figure 21 represents the absorption capacity of motor oil with D4. As observed, motor oil presents the highest absorption capacity of the materials tested. These results show how the nature of the absorbent is one of the key characteristics of an absorption process, given that at the same conditions the other absorption capacities obtained are relatively small. As well, comparing with the results obtained with the L2 the highest absorption capacity obtained was that with motor oil. So for the two most relevant siloxanes present in biogases, D4 and L2, the use of motor oil can be an interesting solution. Absorption capacity at the saturation point is presented in Table 28.

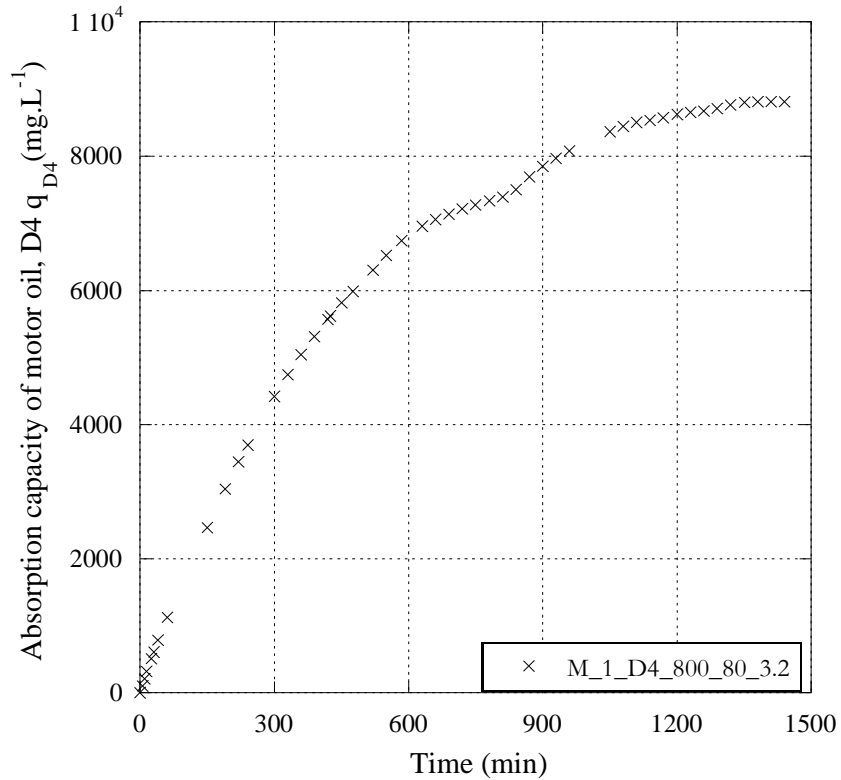


Figure 21. Octamethyltetracyclosiloxane (D4) absorption into motor oil. Absorption capacity  $q_{D4}$  ( $\text{mg.L}^{-1}$ ) in function of time (min). Experimental conditions: flow rate ( $3.2 \text{ L.min}^{-1}$ ); siloxane concentration ( $800 \text{ mg.m}^{-3}$ ). Temperature ( $25^\circ\text{C}$ ).

### 1.3.2.2 Absorption of siloxane D4 into Cutting oil

In Figure 22, the profile concentration of D4 into cutting oil is shown. As observed, at the lowest quantity of cutting oil (80 g) the outlet concentration increases rapidly, reaching the saturation value in the first 20 min. This result differs significantly from the concentration profile of D4 into motor oil, where the saturation point is observed at 1500 min. Forward, the experiments were performed increasing the quantity of cutting oil in order to enhance the absorption. Thus absorption was carried out at 300 g and 350 g. As a result, the concentration at the outlet increases more slowly and the saturation point is reached at 250 min. Additionally, removal efficiency was improved being for 80 g of 40%; for 300 g was of 56% and for 350 g was of 66%. Values are shown in Table 29.

Table 29. Octamethyltetracyclosiloxane (D4) absorption into cutting oil. Absorption capacity  $q_{D4}$  ( $\text{mg.L}^{-1}$ ).

Siloxane	Absorbent	Concentration ( $\text{mg.m}^{-3}$ )	Mass of absorbent (g)	Flow rate ( $\text{L.min}^{-1}$ )	RT (s)	$q_{D4}$ ( $\text{mg.L}^{-1}$ )	Abbreviation
D4	Cutting oil	800	80	3.2	1.3	2.83	C1D4(800-80-3.2)
			300		4.6	250.38	C2D4(800-300-3.2)
			350		5.3	449.67	C3D4(800-350-3.2)

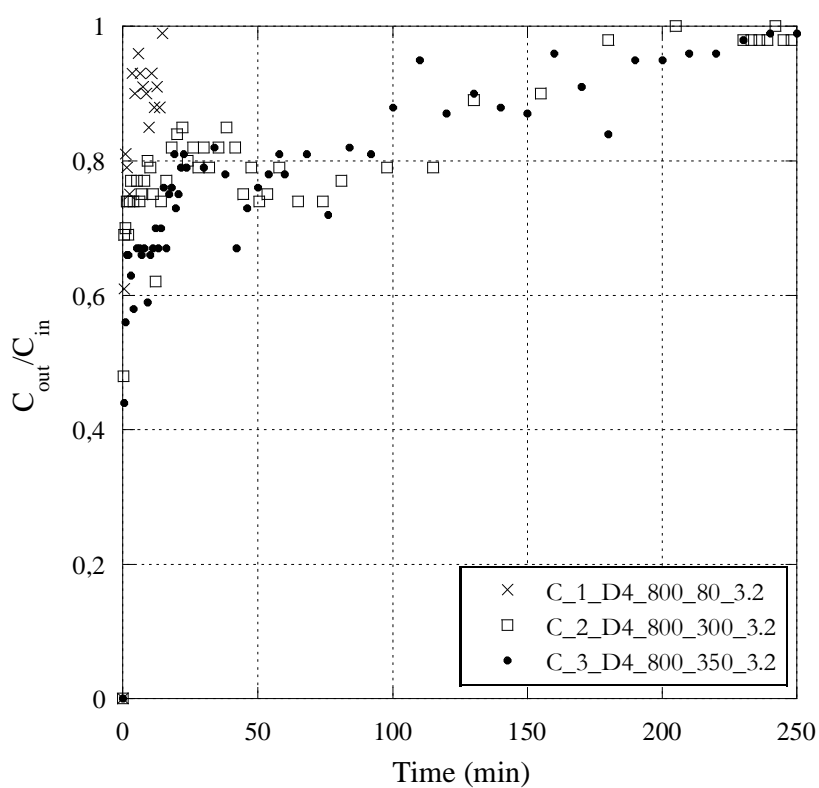


Figure 22. Octamethyltetracyclosiloxane (D4) absorption into cutting oil. Breakthrough curves in function of time (s). Experimental conditions: flow rate ( $3.2 \text{ L.min}^{-1}$ ); siloxane concentration ( $800 \text{ mg.m}^{-3}$ ). Temperature ( $25^\circ\text{C}$ ).

Absorption capacity of cutting oil is shown in Figure 23. As can be seen, at 300 g and 350 g the behavior is similar with an absorption capacity at the saturation point about 250  $\text{mg.L}^{-1}$ . However, at 80 g the absorption capacity is almost negligible. As a result, we observe that the mass transfer of siloxane D4 from the gas phase to the liquid phase (cutting oil) is determined by the mass of cutting oil and could be explained by the difference in residence time.

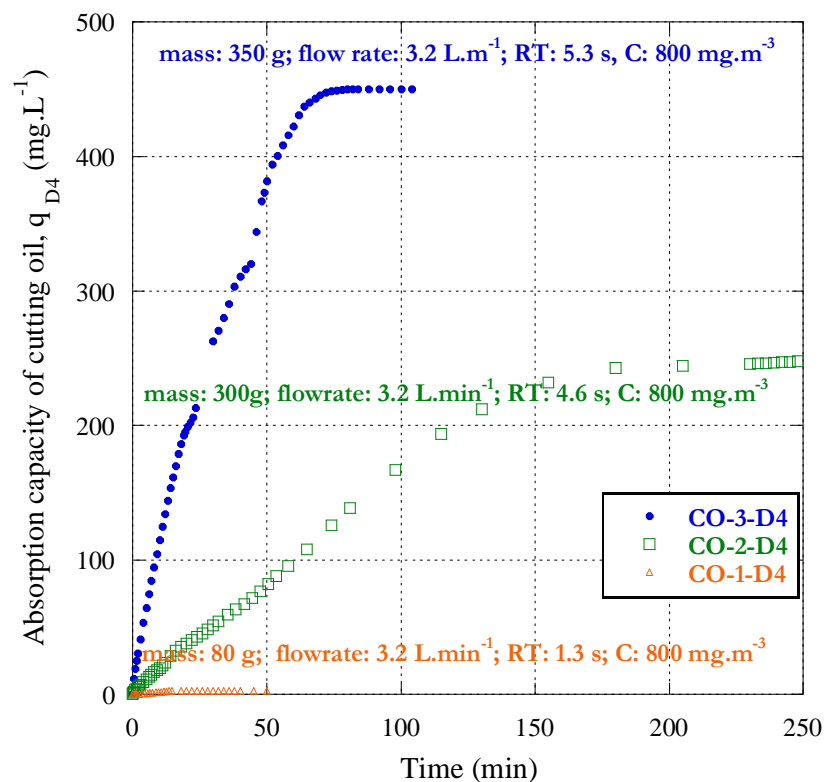


Figure 23. Octamethyltetracyclosiloxane (D4) absorption into cutting oil. Absorption capacity  $q_{D4}$  ( $\text{mg.L}^{-1}$ ) in function of time (min). Experimental conditions: flow rate ( $3.2 \text{ L.min}^{-1}$ ); siloxane concentration ( $800 \text{ mg.m}^{-3}$ ). Temperature ( $25^\circ\text{C}$ ).

### 1.3.2.3 Absorption of siloxane D4 into water-cutting oil

As we can observe in Figure 24, the concentration profile for water-cutting oil reveals strong variations. Indeed, for the conditions at 80 g, the concentration at the outlet reaches rapidly the saturation point, suggesting a low solubility of D4 in water-cutting oil. Nevertheless, in the second curve, which corresponds to 300 g we observe that passing 5 minutes, the concentration decreases strongly to reach a value of 0.31  $C_{in}/C_{out}$ . After that, the concentration profile increases slowly to finally reach the equilibrium. This experiment evidence the possibility of removal of siloxane D4 in a water-cutting oil mixture. However, it is important to obtain high removal efficiency since the beginning of the process. Values are shown in Table 30.

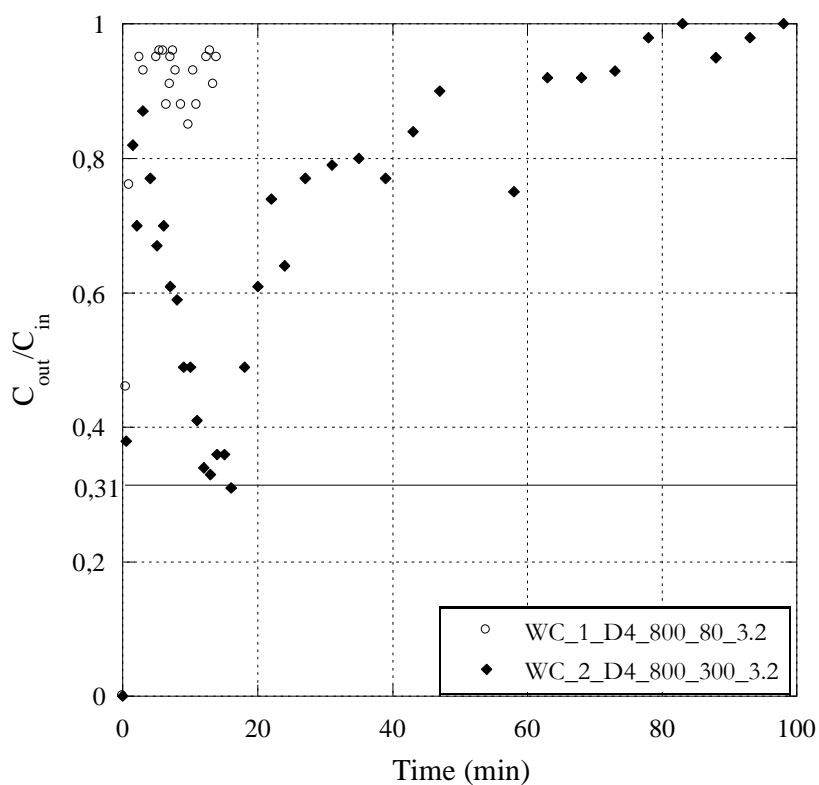


Figure 24. Octamethyltetracyclosiloxane (D4) absorption into water-cutting oil. Breakthrough curves in function of time (s). Experimental conditions: flow rate ( $3.2 \text{ L}\cdot\text{min}^{-1}$ ); siloxane concentration ( $800 \text{ mg}\cdot\text{m}^{-3}$ ). Temperature ( $25^\circ\text{C}$ ).



Table 30. Octamethyltetracyclosiloxane (D4) absorption into water-cutting oil.  
Absorption capacity  $q_{D4}$  ( $\text{mg.L}^{-1}$ ).

Siloxane	Absorbent	Concentration ( $\text{mg.m}^{-3}$ )	Mass of absorbent (g)	Flow rate ( $\text{L.min}^{-1}$ )	RT (s)	$q_{D4}$ ( $\text{mg.L}^{-1}$ )	Abbreviation
D4	Water-Cutting oil	800	80	3.2	1.3	51.00	WC1D4(800-80-3.2)
			300		4.6	170.05	WC2D4(800-300-3.2)

For that, one solution can be achieved passing a gas into the solution in order to create the bubbles and therefore increase the surface of contact since the beginning and forward send the gas loaded of the pollutant. This can improve the mass transfer from the gas phase to the liquid phase. As well, some studies have been done with micro emulsion, which has the same purpose to increase the surface area. In this study, as the focus was to see the absorption ability of the oils, the considerations of how optimize the process were not taken into account. However, we highlight the possibility to treat these pollutants by the use of water-cutting oil, which seems an interesting solution from the economic and environmental point of view.

In Figure 25, the breakthrough curves of cutting oil and water-cutting oil, at the same operating conditions are represented. As can be seen, the removal efficiency of the water-cutting oil is much more important than that of the cutting oil pure. This suggests that the water-cutting oil is a better absorbent than the cutting oil pure. Previous studies of VOCs into cutting oil–water mixtures have shown a good absorption capacity within a small oil fraction (2.5 -10%)(Lalanne et al. 2008). However, they don't study the comparison with cutting oil pure. In this study we can observe that only with a fraction of 5% the removal efficiency is enhanced. This can be explained by the changes in the surface tension at low contents or the organic phase (Dumont, Delmas 2003). Considering a biogas treatment, where the VOC and VMS are treated in general at the end of the process, it is interesting to notice that water-cutting oil absorb as well VOCs, so a global solution to treat these volatile compounds.

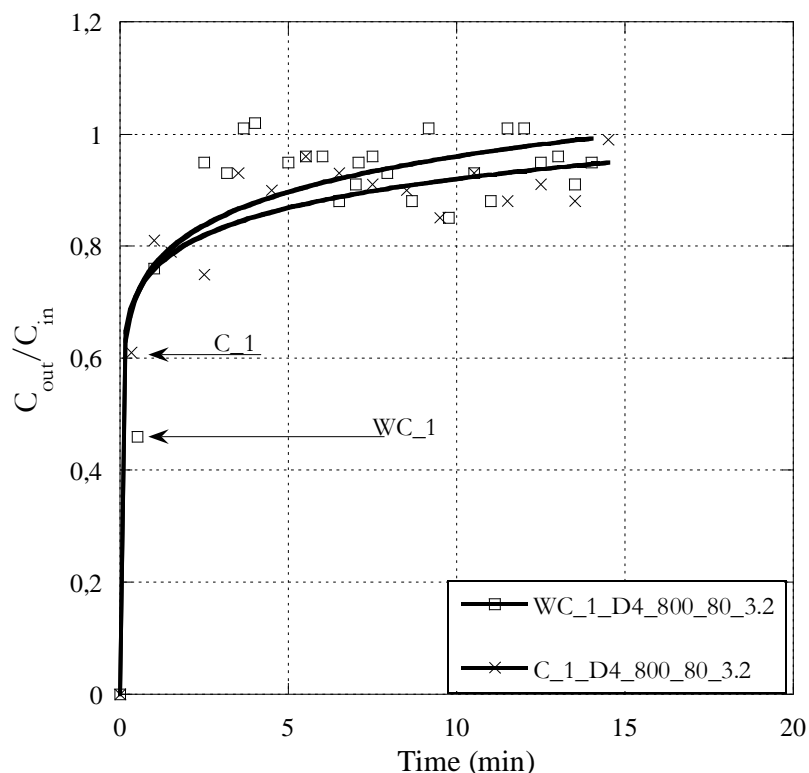


Figure 25. Comparison of octamethyltetracyclosiloxane (D4) absorption into cutting oil and water-cutting oil. Breakthrough curves in function of time (s). Experimental conditions: flow rate ( $3.2 \text{ L}\cdot\text{min}^{-1}$ ); siloxane concentration ( $800 \text{ mg}\cdot\text{m}^{-3}$ ). Temperature ( $25^\circ\text{C}$ ).

As detailed in figure 26, the absorption capacity of water-cutting oil for absorption carried out at 80 g is of  $50 \text{ mg}\cdot\text{L}^{-1}$  and it is enhanced for the absorption at 300 g achieving a value of  $170 \text{ mg}\cdot\text{L}^{-1}$ . As in the other cases, the influence of residence time in the absorption capacity was observed. Comparing the results with those of cutting oil pure, we found, in contrast with expected, that the absorption capacity is improved in the mixture with water at 80 g of solution. Showing, how the oil fraction enhances the mass transfer of water, giving a better performance than the cutting oil pure. However, this tendency was not observed in the absorption carried out at 300 g, where absorption capacity was higher for cutting oil pure.

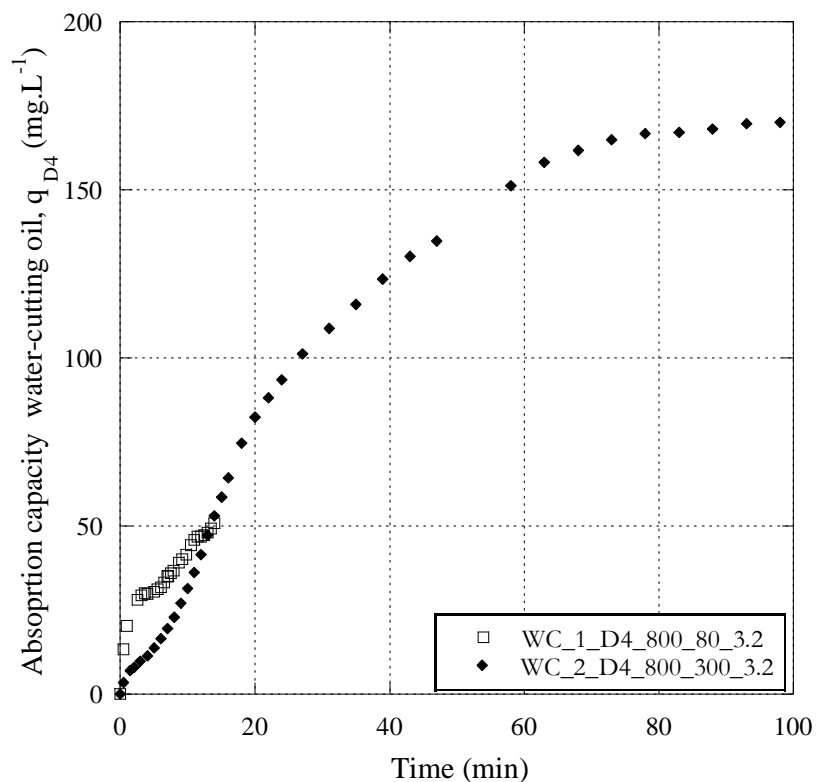


Figure 26. Octamethyltetracyclosiloxane (D4) absorption into water-cutting oil. Absorption capacity  $q_{D4}$  ( $\text{mg.L}^{-1}$ ) in function of time (min). Experimental conditions: flow rate ( $3.2 \text{ L.min}^{-1}$ ); siloxane concentration ( $800 \text{ mg.m}^{-3}$ ). Temperature ( $25^\circ\text{C}$ ).

Nevertheless, as we observed in the concentration profile in figure 24, during the first 15 min, when the concentration increases rapidly, the water-cutting oil was apparently not well mixed and this can influence negatively the result. As a conclusion, we consider that the cutting oil surface is optimized because of the water, creating a new film where bubbles are covered for the cutting oil and the enhancement of the mass transfer from the gas phase to the liquid phase is achieved. For that, the calculus of the interfacial area was done and we confirm that the area is enhanced from  $112 \text{ m}^2.\text{m}^{-3}$  for cutting oil pure to  $147 \text{ m}^2.\text{m}^{-3}$  for water-cutting oil.

Some previous studies of mixing water solutions with organic solvents to increase the solubility of D4 have been done. In this study they found an increase in the removal of D4 (Popat, Deshusses 2008). In the case of D4 or L2 into water-cutting oil no studies have been reported. However, other hydrophobic compounds as ethylbenzene were studied (Lalanne et al. 2008). Here they found an absorption capacity of water was enhanced by the addition of (5%) the cutting oil fraction. For a inlet concentration of  $100 \text{ mg.m}^{-3}$  the liquid concentration was around  $28 \text{ mg.L}^{-1}$ . The use of cutting oil in a diluted solution is a very economical solution. After the experiments performed, we observed that residence time is a

limiting factor in the absorption process. We evidence the potential of treating siloxanes with water-cutting oil. The summary of the results is presented in Table 32.

## 1.4 Conclusions

Results show that motor oil has a better absorption capacity than cutting oil and water-cutting oil. The summary of the results is listed in Table 31. Different parameters were studied: absorbent material, residence time, temperature, and siloxane concentration. The results show that the absorption process depends strongly on the material characteristics and operating conditions. An increase in the oil temperature results in a decrease in the treatment capacity, thus high temperature is therefore not recommended for VMS absorption.

Absorption capacity increases as a function of residence time for motor oil, cutting oil and cutting oil water. Once optimized the residence time, we can vary the flow rate to increase the interfacial area and thus the mass transfer between the phases. However, the effect is more important for motor oil than for the other solvents. In order to increase the mass transfer rate, further studies are required. Packed or tray columns are generally implemented for this purpose.

Table 31. Summary of absorption capacity of siloxane L2 into: water, motor oil, cutting oil and water-cutting oil.

Absorbent	Concentration (mg.m <sup>-3</sup> )	Mass of absorbent (g)	Flow rate (L.min <sup>-1</sup> )	T (°C)	Residence Time RT (s)	q <sub>L2</sub> (mg.L <sup>-1</sup> )	Abbreviation
Water	800	240	8.03	25	0.7	0	W1L2(1200-240-8)
Motor oil	880	240	8.03	25	0.8	224	M1 L2(800-240-8)
	1000					701	M2 L2(1000-240-8)
	1100					884	M3 L2(1100-240-8)
	1200	140	8.03	25	0.2	0	M4 L2(1200-140-8)
					240	43.6	25
		300	8.03	25	1.1	1350	M6 L2(1200-300-8)
					50	5.4	M7 L2(1200-300-8-50)
					90	0	M8 L2(1200-300-8-90)
Cutting oil	1200	240	8.03	25	0.7	0	C5 L2(1200-240-8)
		350	3.31	25	3.2	241	C1 L2(1200-350-3.3)
		350	8.03	25	1.3	498	C2L2(1200-350-8)
	1800	350	2.51	25	4.3	280	C3L2(1800-350-2.5)
	4800	300	1.01	25	8.2	684	C4L2(4800-300-1)
Cutting oil water	1000	300	8.03	25	1.0	57	WC1L2(1000-300-8)
	1800	300	8.2	25	1.0	95	WC2L2(1800-300-8)

Table 32. Summary of absorption capacity of siloxane D4 into: water, motor oil, cutting oil and water-cutting oil.

Siloxane	Absorbent	Concentration (mg.m <sup>-3</sup> )	Mass of absorbent (g)	Flow rate (L.min <sup>-1</sup> )	RT (s)	q <sub>D4</sub> (mg.L <sup>-1</sup> )	Abbreviation
D4	Water	800	80	3.2	-	0	W1D4(800-80-3.2)
			300		-	0	W2D4(800-300-3.2)
	Motor oil	800	80	3.2	1.6	8820.6	M1D4(800-80-3.2)
			300		5.5	Very long-stopped	M2D4(800-300-3.2)
	Cutting oil	800	80	3.2	1.3	2.83	C1D4(800-80-3.2)
			300		4.6	250.38	C2D4(800-300-3.2)
			350		5.3	449.67	C3D4(800-350-3.2)
	Cutting oil water	800	80	3.2	1.3	51.00	WC1D4(800-80-3.2)
			300		4.6	170.05	WC2D4(800-300-3.2)

The best performance for the removal of both siloxanes, in terms of absorption capacity, was observed for motor oil prevailing for D4 than for L2. Moreover, motor oil removal efficiency for D4 was of 80% whereas for L2 was of 60%, indicating that D4 is easier absorbed than L2. In the case of water-cutting oil, it showed a mass transfer enhancement from the gas phase to the liquid phase compared with water alone. Furthermore, a removal efficiency of 70% for D4 was observed, showing that the addition of oil fraction in a water system improves the absorption of VMS. Results show that VMSs absorption into oils is a promising way to achieve their abatement.

Results show that motor oil has a better absorption capacity than cutting oil and water-cutting oil for L2 and D4. Different parameters were studied: absorbent material, residence time, temperature, and siloxane concentration. The results show that the absorption process depends strongly on the nature of the absorbent and the operating conditions. An increase in the oil temperature results in a decrease in the treatment capacity, thus high temperature is therefore not recommended for VMS absorption.

Absorption capacity increases as a function of residence time for motor oil, cutting oil and cutting oil water. Once optimized the residence time, we can vary the flow rate to increase the interfacial area and thus the mass transfer between the phases. However, the effect is more important for motor oil than for the other solvents. The use of cutting oil in a diluted solution is a very economical solution. We evidence the potential of treat siloxanes with water-cutting oil mixture. Moreover, the use of packing material it is a promising way to

enhance residence time and surface of contact. In order to increase the mass transfer rate, further studies are required.

In Figure 20, the concentration profile for D4 into motor oil is illustrated. As we can see, as difference with cutting oil and water-cutting oil the curve increases very slowly. This reveals a very good solubility of D4 in motor oil. Additionally, no picks of concentration are observed, which is a process advantage.

Regarding the physical chemical properties of VMSs, vapor pressure of D4 is higher than L2, as well as we observe that D4 has a lower solubility in water than L2. Showing that D4 is less polar and less volatile than L2. Thus easier to be removed from the gas phase. Indeed, regarding the coefficient of partition octanol water  $K_{ow}$ , L2 is 4.76 and D4 5.09.

According to the results it is evident that absorption processes depend strongly on the characteristics of the column and system of diffusion of gas. And how once the solvent is choose the relevance of study parameters as interfacial area and residence time.

This study is focused on the availability of absorbents to treat siloxanes. Thus a simple system was used and it was not considered a study of optimal parameters. Nevertheless, it is apparent that the flow rate is a limiting factor as discussed previously with the motor oil. We remark that the effect of other parameters such as agitation, pressure and turbulent flow regime are known that have a huge impact in absorption process and must be considered in a scale-up study.

Finally the experiments carried out during this study showed that the concentration level could be decreased by the absorption of siloxanes into oils, achieving their partial abatement. As the outlet concentration is higher than the limit required for energy generation, the use of finishing process following absorption might be taken into consideration. Adsorption onto activated carbon has shown good results for this. For that we studied in the next section a dynamic adsorption into activated carbons.

## 2 Removal of siloxanes by Adsorption

In order to compare the absorption in oils with the adsorption in activated carbons, the next experiments were carried out in dynamic. Three different activated carbons: one activated carbon cloth (FM30K) and two activated carbons grain (TE60, NC60) were used. These were chosen based on the previous work from (Ortega, Subrenat 2009). In adsorption process the properties of material have a huge impact in the treatment as well as the compound properties. Depends on those interactions the adsorption capacity of the adsorbents changes. In the next section the adsorption approach is presented.

### 2.1 Adsorption approach

The adsorption process is characterized by the transfer of a substance from the gas phase to the solid phase. Different steps can be considered to describe the diffusion mechanism from the bulk of the gas phase to the surface of adsorbent as shown in Figure. Thus the following phases have been proposed (Perry's Handbook; Cloirec, Faur):

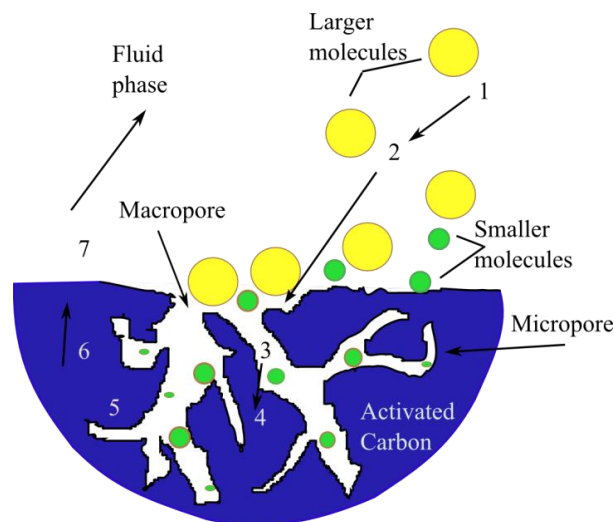


Figure 27. Diffusion from the bulk of the gas phase to the surface of the adsorbent

1. External mass transfer between the fluid phase and the external surface of the adsorbent.



2. Macropore diffusion: the driving force is approximated by the gradient of concentration of the pollutant in the fluid phase within the pore.
3. Solid diffusion in the adsorbent surface or micropore diffusion: internal transfer throughout the pores, the driving force can be approximated by the gradient in concentration in its adsorbent state.
4. Compound interactions within the surface.
5. Possible diffusion in the surface of the material
6. Heat released in the adsorbent given the exothermic of adsorption reaction
7. And heat diffusion to the fluid phase

Adsorption on the surface can be described by two principal mechanisms, physical adsorption or physisorption and chemical adsorption or chemisorptions.

In the physisorption phenomena, the adsorption is controlled by the intermolecular forces of Van der Waals type and equilibrium is established between the activated carbon and the gas phase. In the chemisorption, the adsorption is caused by stronger valence forces on the active sites of the carbon surface (Rodríguez-Reinoso 2001). Generally, in industrial applications, surface adsorbent is modified chemically to increase the adsorption capacity of such adsorbents.

## 2.1.1 Activated carbon

Activated carbon is produced from carbon materials such as coconut shells, wood, oil coke, among others. First, a carbonization step at high temperatures 400-500°C is carried out. After that, the activation step responsible for the development of the surface area and porosity of the material is followed. This activation process is carried out at higher temperatures about 800-1000 °C.

Activated carbons are frequently used in industrial applications for cleaning gas and liquid fluids. The efficiency as adsorbents will vary in function of pore surface, chemical structure and pH. Activated carbon can be found in different presentations. Among them we found GAC (granular activated carbon), ACC (activated carbon cloth) and EAC (extruded activated carbon). In general GAC is mostly used in industrial process. However, ACC presents many advantages in contrast of granular activated carbon. One of them is the possibility of regeneration by direct heating by Joule effect. This novel technology decreases

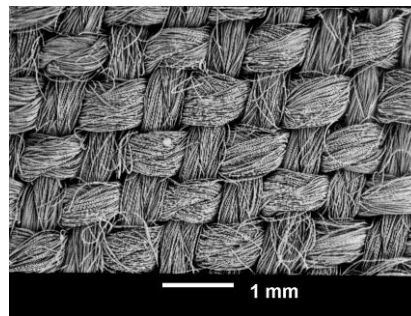
the cost of the regeneration process. Activated carbons in grain, extruded and cloth are shown in Figure.



(a) GAC



(b) EAC



(c) ACC

Figure 28. Activated carbon presentations. (a) Granular activated carbon (b) Extruded activated carbon (c) Activated carbon cloth

## 2.1.2 Adsorption in static

Isotherms adsorption is useful to characterize the interaction between a molecule and the adsorbent material. It consists of the mass transfer from the gas phase to the solid phase in a close system at a fixed temperature. To have a homogeneous atmosphere the reactor is continuously stirred under a constant temperature. The isotherms are classified from their shapes into 6 different types (IUPAC) as shown in Figure 29.

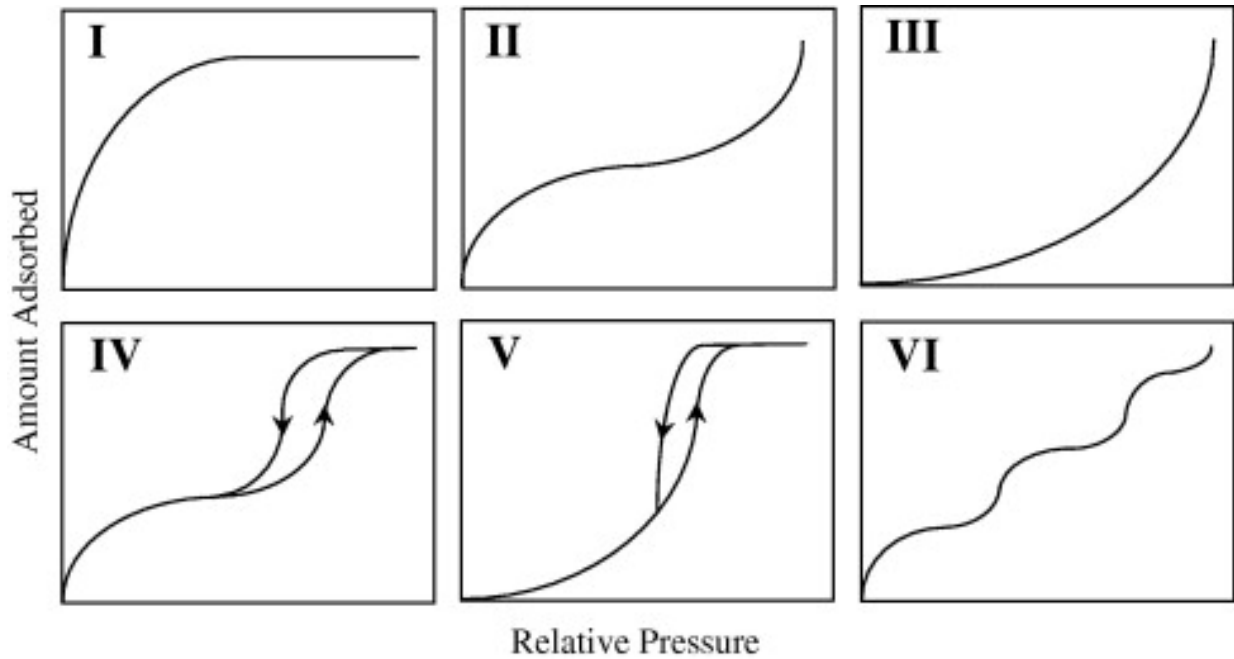


Figure 29. Classification of gas adsorption isotherms by IUPAC

Type I: these isotherms are found for microporous adsorbents where monolayer is a typical behavior. It is a physisorption phenomena.

Type II: these isotherms are conventionally observed for macroporous adsorbent where monolayer and multilayer adsorption is developed.

Type III: describe adsorption on macropore adsorbent with strong adsorbate–adsorbent interactions. The adsorption energy is equal or smaller than liquefaction energy. These isotherms are rarely encountered.

Type IV: represents adsorption isotherm with an adsorbent of large pore distribution. The interaction energy is supposed strong. The hysteresis is associated with capillary condensation in the mesopores.

Type V: these isotherms are rarely found. They are associated with mesopores adsorbents with weak interactions.

Type VI: multilayer adsorption. It is characteristic of materials that present a segmented distribution of pores. It is rarely observed.

From the previous shapes, isotherms type (I) and type (II) are the most found. Adsorption models and theories have been developed to represent the different types of isotherms. These models allow to calculate, based on the experimental data, the adsorption

capacity of an adsorbent for a specific concentration. Among them, we found the model of Freundlich, the model of Langmuir and the model of Langmuir-Freundlich.

The Freundlich model, proposed in 1906, is an empirical model. It's simple and describes isotherms at low concentration.

$$(24) \quad q_e = KC_e^{1/n}$$

Where:

$q_e$  : is the adsorption capacity at the equilibrium (mg.g<sup>-1</sup>)

$C_e$  : is the concentration in the gas phase at the equilibrium (mg.m<sup>-3</sup>)

$K$  : is a model constant (mg<sup>1-1/n</sup> .m<sup>3/n</sup> .g<sup>-1</sup>)

$1/n$  : is a model constant

The Langmuir model was developed in 1918. It assumes the dynamic equilibrium between the adsorption and desorption rate. This model is largely applied since it allows the description of the isotherms type (I) and (II). The next hypothesis are also considered:

- Molecules are adsorbed in defined sites.
- Each site adsorbs just one molecule.
- All the sites are the same energy.
- There are no interactions among the sites.

The Langmuir model is described by the next equation:

$$(25) \quad q_e = \frac{q_m b_L C_e}{1 + b_L C_e}$$

Where  $q_m$  = maximal adsorption capacity (mol.kg<sup>-1</sup>)

$b_L$  = the equilibrium constant of Langmuir (m<sup>3</sup> .mol<sup>-1</sup>)

The Langmuir–Freundlich model considers the two previous models and combined the expressions. It assumes that adsorption is developed not in one defined site but in a  $1/n_{LF}$  sites. The model expresses the adsorption capacity in the following form:

$$(26) \quad q_e = \frac{q_m b_{LF} C_e^{1/n_{LF}}}{1 + b_{LF} C_e^{1/n_{LF}}}$$

$b_{LF}$  = the equilibrium constant of Langmuir-Freundlich ( $m^{3n_{LF}} \cdot mol^{-1}$ )

$n_{LF}$  = the Langmuir-Freundlich parameter

The design of separation process by adsorption is usually based on: first the knowledge of adsorption equilibrium between the solute and the adsorbent. This experimental data and the understanding of the phenomena allows the selection of material which in general is used in fixed-bed processes from where the primary importance of the dynamic operations and study.

### 2.1.3 Adsorption process in dynamic system

After the characterization of the adsorbent and the pollutant by the static methods, it is essential to carry out the dynamic adsorptions. These studies consist in measuring the evolution of the concentration in response of a flow rate and specific operational conditions. The form of the curve and parameters such as time response are crucial to the forward design process. In function of the operational conditions the breakthrough front will change, thus the importance to define the optimal conditions to obtain a curve of the form presented in Figure:

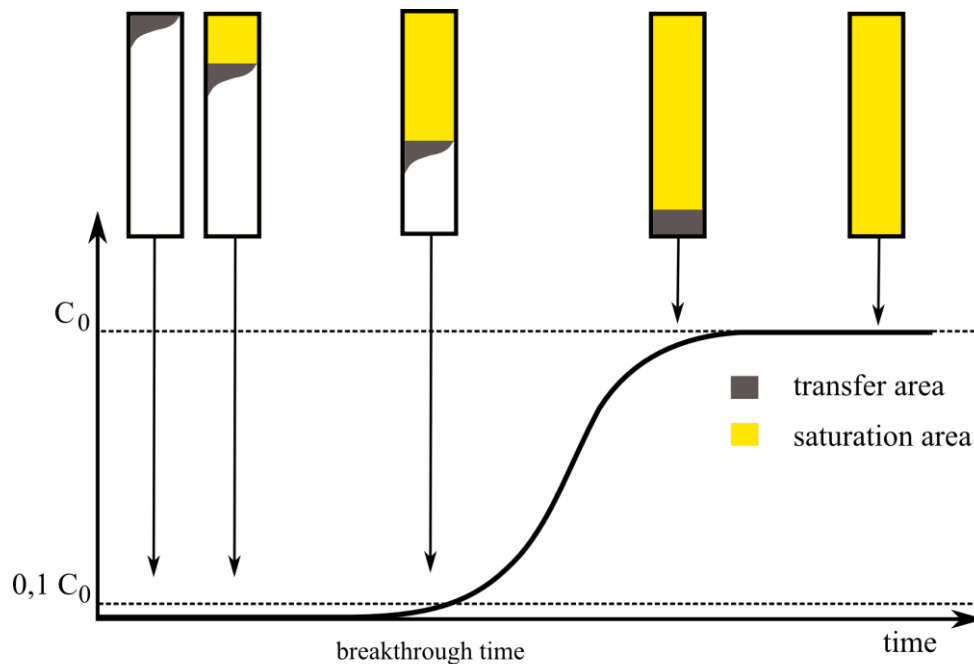


Figure 30. Breakthrough curve, outlet profile.

The adsorption and desorption cycles in the industrial applications are carried out without having the saturation point. Normally they are stopped at the breakthrough point, which can be defined in different forms. Sometimes its defined around the 10% to 5% of the

initial concentration. Also, it is determined based on the specific requirements of the separation process. An adsorption process in a dynamic system can be described by the next mass balance equation:

$$(27) \quad Q_g C_{in,g} = Q_g C_{out,g}(t) + m \frac{dq}{dt}$$

Where  $Q_g$  is the gas rate ( $m^3 \cdot s^{-1}$ ),  $m$  is the mass of adsorbent  $g$ ,  $C_{in,g}(t)$  is the concentration of the compound in the gas phase at the inlet of the reactor  $g \cdot m^{-3}$ ,  $C_{out,g}(t)$  is the concentration of the compound in the gas phase at the outlet of the reactor  $g \cdot m^{-3}$ , and  $q(t)$  is the adsorption capacity as a function of time

Adsorption capacity at the breakthrough point is therefore calculated with this equation. The integral is evaluated since  $t=0$  to  $t=$  breakthrough time. Also the mass balance is applied to the saturation point, defined as the result of the differences of the inlet and outlet concentration since  $t=0$  until arriving to the equilibrium between the phases. The mass balance follows the form:

$$(28) \quad q(t) = \frac{Q_g}{m} \int_{t=0}^t (C_{in,g} - C_{out,g}(t)) dt$$

## 2.2 Materials and methods

According to the previous discussion, the adsorption of hexamethylsiloxane into different activated carbons is carried out. First, the selection of the materials is based on the isotherms obtained in a previous work. Then, the physical properties characterization of materials is carried out. After that, the design of a dynamic system, with a stationary phase (adsorbent) is done in order to study the adsorption of siloxane.

### 2.2.1 Materials

Hexamethylsiloxane (L2) from Sigma Aldrich at 98% purity was used to carry out experiments. Three different activated carbons where one activated carbon cloth (FM30K) and two granular activated carbon (TE60 ; NC60), are used as adsorbents.

### 2.2.1.1 BET surface area

The BET surface area of the activated carbons is measured by the nitrogen adsorption at 77K. For this purpose the ASAP micrometrics analyzer was used. Prior to the measurements, the samples were dried in an oven at 100 °C and then placed in the sampling tube. After that, the sample is degassed for 2 days at 300°C. Then the sorption of nitrogen at 77K is carried out. The characteristics of materials are presented in Table 33.

Table 33. Physical properties of activated carbons

Material	TE60	NC60	FM30K
Texture	Grain	Grain	Cloth
BET surface ( $\text{m}^2 \text{g}^{-1}$ )	1024	1035	1087
% Volume Micropore	48	47	75

## 2.2.2 Laboratory unit

A laboratory unit has been designed to carry out the adsorption process with fixed bed and gas stream. The diagram is shown in Figure. The reactor was filled with different volumes of adsorbent material for each case. Samples of the output gas were taken regularly and analyzed by gas chromatography coupled with a flame ionization detector (GC/FID) until reach saturation value.

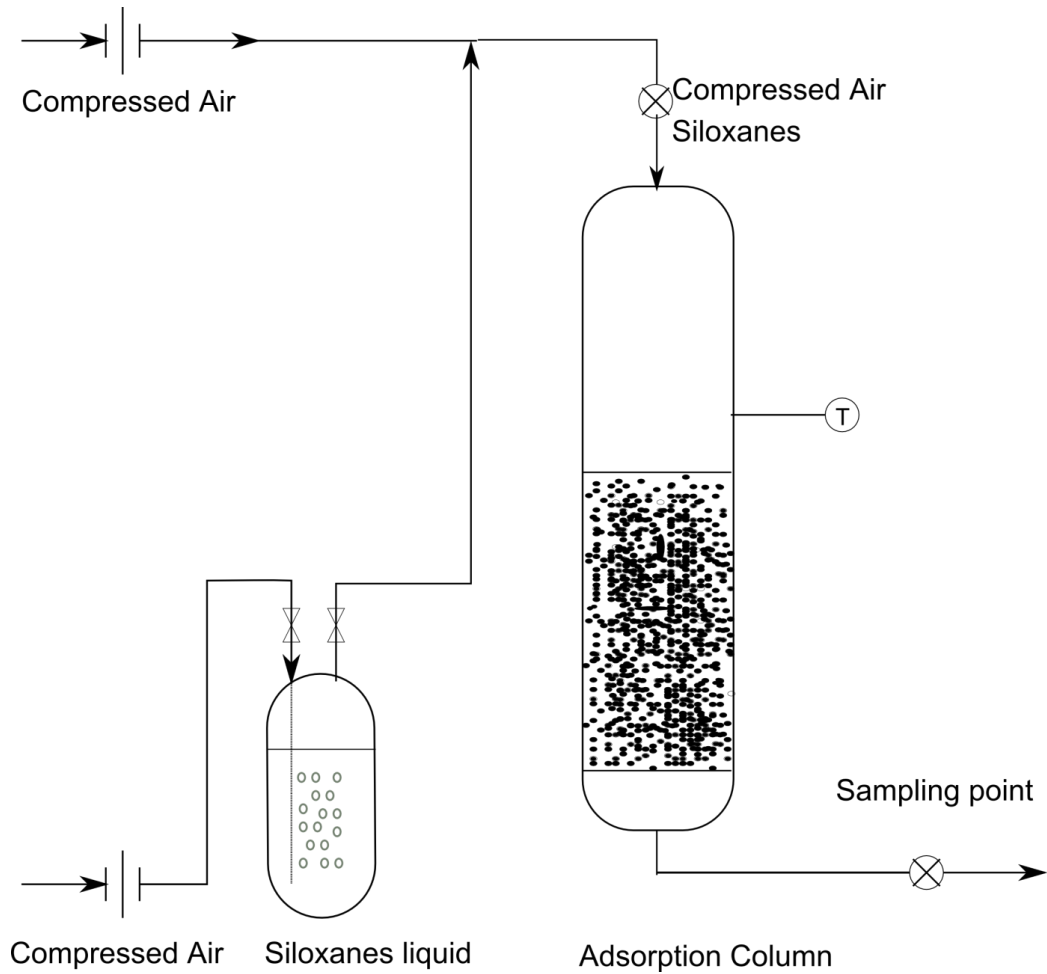


Figure 31. Diagram of adsorption process

### 2.2.3 Operational conditions

Material	TE60	NC60	FM30K
weight (g)	8	8	1,05
Superficial velocity (m/s)	0,443	0,443	0,123
Height (mm)	10	10	3
Residence Time (s)	0,023	0,023	0,023



## 2.3 Results and discussion

### 2.3.1 Breakthrough curves

The hexamethylsiloxane concentration profile can be observed in Figure 32. NC 60 profile, presents a first phase of 300s in which siloxanes concentration is zero. Then, a second phase in which siloxanes concentration increase rapidly during 1700 s, and a third phase in which siloxanes concentration increases slowly until it reaches a saturation point. For the second activated carbon in grain, TE 60, at the same conditions (flow rate and quantity of adsorbent), the first phase where the outlet concentration is zero is about 100 s. Then the breakthrough front has a good behavior and after 1800 s the saturation point is reached. Comparing with the activated carbon NC 60, the saturation point of TE 60 is observed before.

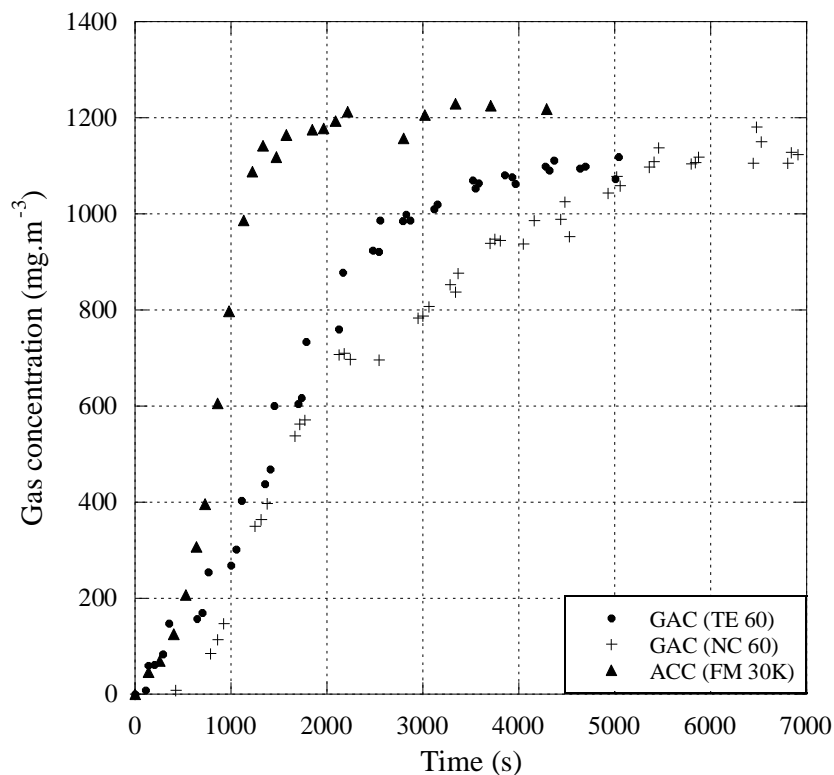


Figure 32. Hexamethylsiloxane (L2) adsorption into granular activated carbon (TE 60; NC 60) and activated carbon cloth in cloth (FM30 K). Breakthrough curves in function of time (s).

Concerning the activated carbon FM30K. The concentration increases rapidly, then the saturation point is reached at 3500 s. Globally, in the siloxanes concentration profile at the beginning of the process, there is a difference between the evolution of the adsorption kinetics of GAC and ACC, being the rate at which siloxanes are diffused in solid phase higher for ACC than for GAC.

### 2.3.2 Adsorption Capacity

Adsorption Capacity was determined applying equation (28). At the saturation point the adsorption capacity for FM 30K was  $520 \text{ mg.g}^{-1}$ ,  $253 \text{ mg.g}^{-1}$  for NC60 and  $177 \text{ mg.g}^{-1}$  for TE60, as shown in Figure 33, being ACC performance higher than GAC.

Breakthrough time is defined as  $C_{\text{outlet}}/C_{\text{in}} = 0.05$ . This condition is reached at 150 s for FM30K, at 220 s for TE 60, and at 600 s for NC 60. The breakthrough time difference shows that adsorption kinetic is faster for FM30K than for TE 60 and NC 60. Additionally, BET and pore volume is higher for FM30K than for TE60 and NC60. Values are presented in the Table 33. The adsorption capacity increases in function of BET and pore volume. The same relation had been reported by other authors (Matsui, Imamura 2010, Ortega, Subrenat 2009). This study confirms that these materials are suitable for siloxanes treatment in continuous processes. However, only 5 %wt of the activated carbon is really is used. In order to reduce costs and minimize environmental impacts, activated regeneration processes was studied (Ortega, Subrenat 2009) and a regeneration possibility at low temperature ( $90^{\circ}\text{C}$ ). This improves the feasibility of use adsorption onto activated carbon as a treatment process for siloxanes removal.

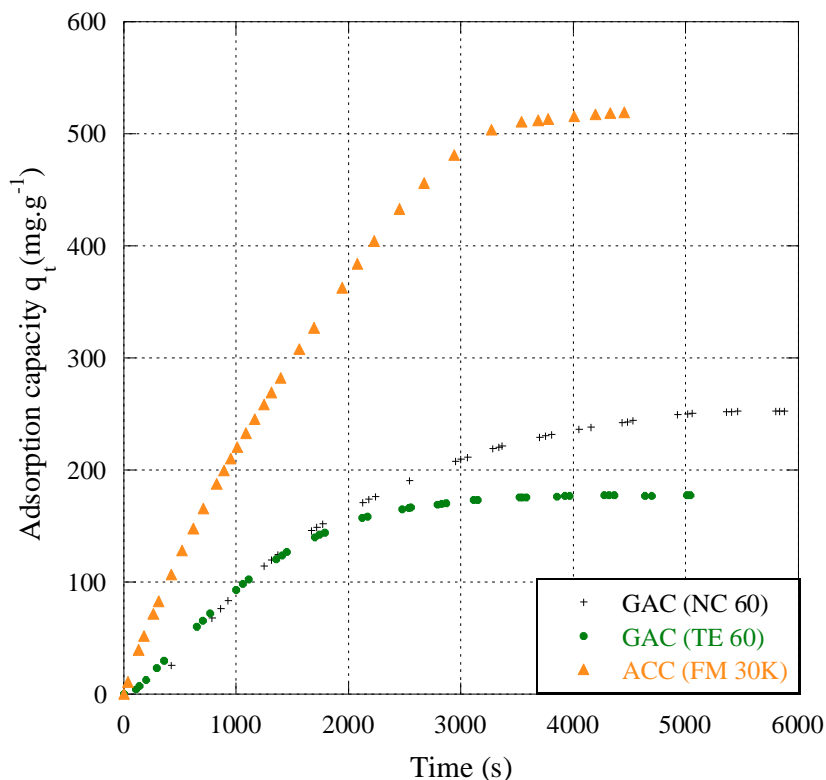


Figure 33. Hexamethyldisiloxane (L2) adsorption into granular activated carbon (TE 60; NC 60) and activated carbon cloth in cloth (FM30 K). time (s). Adsorption capacity of activated carbon as a function of time (s). Experimental conditions:  $C_{in}$  L2 =  $1200 \text{ mg.m}^{-3}$ ; T:  $25^\circ\text{C}$ .

## 2.4 Conclusions

This study shows the feasibility to use adsorption into porous materials and absorption into oils for siloxanes elimination. Comparing the two processes, for a  $1200 \text{ mg.m}^{-3}$  siloxanes concentration, liquid motor oil concentration was  $270 \text{ mg.L}^{-1}$ . At the same concentration, adsorption capacity for FM30K was  $520 \text{ mg.g}^{-1}$ . Confirming that activated carbons have a higher capacity than motor oil. Concerning the adsorption of siloxanes it was observed that kinetics adsorption with activated carbon cloth was faster than with granular activated carbon, given that intra porous diffusion is easier for ACC, revealing the importance of the material physical properties. This study presents that absorption and adsorption in continuous reactors are suitable processes for siloxanes treatment.

# Chapter 3

## H<sub>2</sub>S Treatment by adsorption into activated carbons – regeneration material

---

Among the technologies studied, adsorption into activated carbon is widely used in the industry for its easy operation and installation (Bagreev et al. 2005; Bandosz ; Monteleone et al.2011 ). Its major disadvantage concerns essentially the mass of material required and its regular renewal. Generally, activated carbons are modified chemically to enhance adsorption capacity. However, the activity of modified carbons is exhausted when the reaction is consumed. In most cases, the pores are blocked by reaction products like elemental sulfur. Depending on the impregnation, the material can be regenerated, but regeneration is expensive. Thus materials are replaced by fresh activated carbon after using it (Bagreev et al. 2002).

In this context, we were interested in the development of an H<sub>2</sub>S alternative separation technology by a regenerative adsorption process. The objective is to define operating conditions for an in situ regeneration of the adsorbent. To do it, activated carbon cloth has been chosen given its possibilities of direct electric heating as a novel regeneration method (Subrenat et al. 2001, Subrenat, Le Cloirec 2004). In the same way that granular activated carbons, the same mechanisms of transfer and reactions occur between the porous surface of activated carbon cloths and the H<sub>2</sub>S (Yang et al. 1999, Le Leuch, Subrenat & Le Cloirec 2003, Le Leuch, Subrenat & Le Cloirec 2005) . Moreover, to facilitate the regeneration of activated carbon, physisorption pathway is favored (Adib, Bagreev & Bandosz 2000). Consecutively, the study will focus on the impact of the conditions of adsorption on the efficiency of the regeneration as well as on the parameters of desorption (temperature, pressure, duration).

# 1 H<sub>2</sub>S adsorption into activated carbons

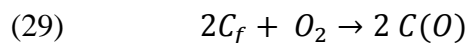
Numerous studies have focused on the physic-chemical mechanisms developed during the H<sub>2</sub>S adsorption. Porosity, surface chemistry, pH, and the products of surface reaction are some parameters involved in the complex reactions developed during adsorption (Bagreev et al. 1999). Three phenomena have been proposed: physisorption, chemisorption and oxidation. Also water plays an important role. Therefore, dry and wet pathways are described below.

## 1.1 H<sub>2</sub>S transfer and reaction into activated carbons

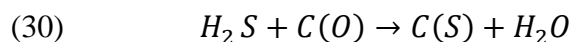
### 1.1.1 Mechanisms in a dry atmosphere

In a dry atmosphere, different mechanisms are proposed involving surface oxygenated groups and / or oxygen adsorbed in the oxidation of H<sub>2</sub>S (Furminsky, 1997). This oxidation is particularly favored by a large number of basic surface groups (Skokova and Radovic, 1996). At pH <4.5 only physical adsorption is taken into account. In this case, the processing capacity is low. The following catalytic reduction mechanism is proposed (Cariaso, Walker Jr. 1975).

Dissociative chemisorption of oxygen:



Chemical reaction between adsorbed oxygen and gaseous H<sub>2</sub>S:



Water desorption.

With

$C_f$ : reduced site (or free site)

$C(O)$ : oxygenated site or oxygenated surface group

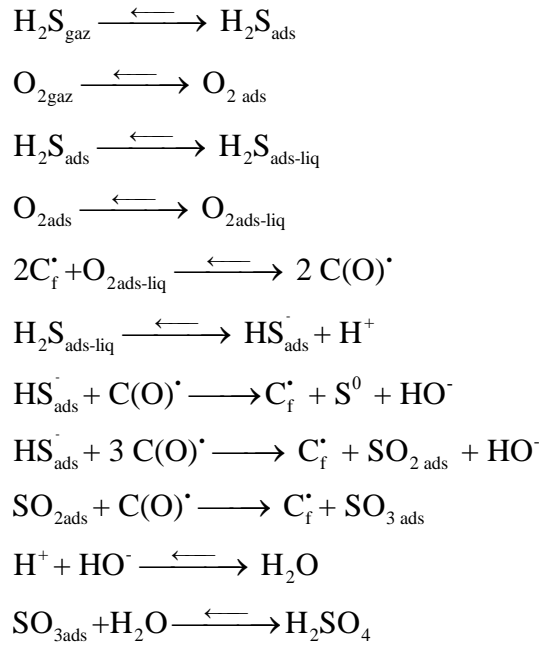
$C(S)$ : elemental sulfur chemisorbed

There is no reduction of the catalytic activity of carbon after the formation of sulfur. The authors suggest that it acts as a first layer for adsorption and this compensates the decrease of the specific surface area of the carbon. It should be noted that while the temperatures of adsorption is greater than 100 ° C, the desorption of the water formed during the reaction is involved.

At room temperature, the proposed mechanism follows 1st and 2nd steps. Water desorption is less considered. Thus, at 20 ° C, the presence of moisture will affect the result of the reaction and only the first two steps of the mechanism can then be observed (Kaliva and Smith, 1983-a).

## 1.1.2 Mechanisms in a humid atmosphere

In the case of a wet atmosphere, different approaches have been proposed. From one side, the mechanism involves a first dissolution of the  $H_2S$  molecules in a liquid film on the surface of activated carbon. In this film, the reagents  $O_2$  and  $H_2S$ , under normal conditions of temperature and pressure, are dissolved.  $O_2$  molecules adsorbed at the surface of the activated carbon are split into two radicals which are reactive.  $H_2S$  molecules are partially dissociated into protons and ions hydrosulfides. These radicals react with oxygen to form hydroxyl ions and sulfur deposited on activated carbon (Klein and Henning, 1984). This radical mechanism confirmed by different authors, would be the consequence of the dissolution of  $H_2S$  in a liquid film (Adib et al., 1999-b; Bandosz 1999; Bagreev et al., 2001). The balance of the dissociation reaction is:

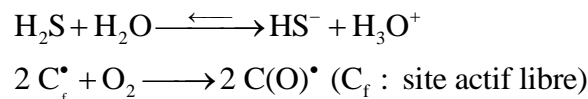


The effect of pH of the carbon surface must be taken into account in the previous reaction pathway. Indeed, the pKa of H<sub>2</sub>S at 20 ° C are 7.2 and 12 (Selleck et al., 1952). According to the pH of the adsorbent surface, the concentration of HS<sup>-</sup> in the liquid film will be very variable. The authors have proposed different reaction pathways.

In an acidic environment, hydrosulfides ions (HS<sup>-</sup>) will be low and will lead to oxidation of sulfur particles in the activated carbon. The sulfur may then be oxidized to SO<sub>2</sub> or SO<sub>3</sub> by adsorbed oxygen or by a close oxygenated functional group. SO<sub>3</sub> molecules react with water to give H<sup>+</sup> ions and SO<sub>4</sub><sup>2-</sup>.

In basic environment, the hydrosulfides ions formed will be numerous in the aqueous phase and islets sulfur will be the polysulfide (Steijns et al., 1976 (b)). Subsequently, these polysulfides could be rearranged to constitute more stable sulfur cycles (S<sub>8</sub>). There will be no further oxidation.

This reaction scheme can be summarized by:



The next table describes the pathways in function of the surface pH

Table 34. pH of adsorbent surface

pH of adsorbent surface		
Strongly acid (physisorption)	Moderately Basic	Strongly basic
$H_2S_{\text{gaz}} \longrightarrow H_2S_{\text{ads}}$	$HS^- + C(O)^* \rightarrow C(S^*) + HO^-$ $C(S^*) + O_2 \rightarrow SO_{2(\text{ads})} + C^*$ $SO_2 + O_2 \rightarrow SO_{3(\text{ads})}$ $SO_{3(\text{ads})} + H_2O_{(\text{ads})} \rightarrow 2 H^+ + 2 SO_4^{2-}$ $H^+ + HO^- \rightarrow H_2O$	$HS^- + C(O)^* \rightarrow C(S^*) + HO^-$ $C(S^*) + HS^- \rightarrow C(SSH)^*$ $C(SSH)^* + HS^- \rightarrow C(S_2SH)^* \rightarrow C(S_8)$ $H^+ + HO^- \rightarrow H_2O$

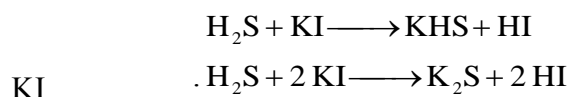
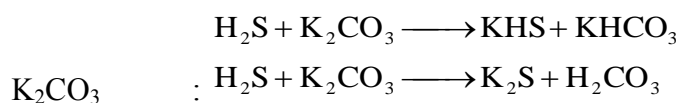
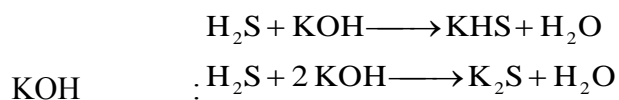
### 1.1.3 Modifying the surface

The capacity of activated carbon can be increased by modifying the physic-chemical surface. A first method is to chemically treat the surface with mineral compounds. Therefore, it is possible to change the composition of the surface by various chemical treatments during and after the manufacturing process of the carbon adsorbent to improve its capabilities to treat specific pollutants.

Chemical activation of the carbon fibers with ammonia gas is thus performed to include nitrogen groups at the surface. This increases the removal of acidic compounds such as  $H_2S$  due to the increased surface basic groups and dipole - dipole interactions (Mangun et al., 2001 (a and b), Li et al., 2001, Boudou et al, 2003). The authors, working with adsorption / thermal regeneration cycle noted an increase of the capacity of the materials impregnated with ammonia 10 times during the first cycle and 1.5 times in subsequent cycles. The impregnation of nitrogen groups in post-treatment was also studied (Adib et al, 2000; Bashkova et al, 2003; Raymundo-Pinero et al, 2003). The adsorbents are immersed in a solution of urea and then washed before being subjected to a heat treatment. At a temperature below  $450^\circ C$ , the nitrogen atoms are predominantly in the amides form, and decompose at higher temperatures to be incorporated into the carbon matrix forming functions pyridine. These changes will directly affect the surface chemistry by increasing the pH of surface favorable for the adsorption of acid gases. Different acid-base treatments can also be done in post-processing to modify the physic-chemical characteristics. The oxidation of the surface by various oxidizing agents such as nitric acid, sodium hypochlorite and hydrogen peroxide will influence the number and nature of the functional groups of the surface, increasing the acidic, basic and polar material (Pradhan and Sandle, 1999). These acid-base treatments can help to



eliminate acid gases by creating basic sites on the carbon surface. Many studies are thus interested in the use of activated carbon impregnated with a simple base such as KOH, KI, or  $K_2CO_3$  (Yan et al., 2002; Przepiorski et al., 1999). These authors noted an increase of the capacity of the treated activated carbon. The creation of active sites involves a substitution reaction mechanism, described below:



The formed products are elemental sulfur and the corresponding acid. The study conducted by Shin et al. (2001) also compared the efficiency of the materials according to the used bases (NaOH,  $Na_2CO_3$ , KI) and the concentration of the impregnate. The best results are obtained with materials impregnated with 9 wt% KI with a capacity of  $325 \text{ mg.g}^{-1}$  (for  $208 \text{ mg.g}^{-1}$  with the virgin activated carbon).

## 1.1.4 The origins and manufacturing conditions of activated carbon fibers

Among the precursors of activated carbon fibers, increased processing capacity of  $H_2S$  is obtained with PAN precursor materials (Polyacrylonitrile) compared to other types of fibers, for a similar specific surface and porous structure (Yang et al., 1999).

### 1.1.4.1 *The surface area and porous structure*

The micropores are favorable for physisorption of the molecule. However, in the immobilization process of this pollutant, the chemisorption plays an important role due to the creation of a water film on the surface of fibers, and more particularly within the mesopores

promoting oxidation of H<sub>2</sub>S. Contradictory results show the difficulties in establishing a relationship between the specific surface area and adsorption of H<sub>2</sub>S (Lee et al., 1999; Bandosz, 1999).

#### 1.1.4.2 *The activating agent*

The removal capacity of the fiber varies also depending on the activating agents used during the manufacturing process. The activated agent changes the chemical characteristics of the material surface. Activated fibers activated with basic agents and/or metal catalysts promote the adsorption of H<sub>2</sub>S. Thus, materials activated by KOH and H<sub>2</sub>O reveal an H<sub>2</sub>S elimination capacity 30% higher compared to activated fibers activated by H<sub>3</sub>PO<sub>4</sub> and H<sub>2</sub>O (Lee et al, 1999). Best results are obtained using other basic activation such as calcium carbonate (Przepiorski et al., 1999).

#### 1.1.4.3 *The surface chemistry*

The surface chemistry has an important role (Adib et al. 1999). A number of heteroatoms are included in the carbon structure. Among them, there are halogenated groups, nitrated, but complexes with oxygen are most often cited (Boehm, 1966). The surface oxides are formed by reaction of oxygen in the peripheral sites of graphite planes during the production steps of the material (Enoki et al. 1994). The presence of carboxylic groups has been reported to enhance the H<sub>2</sub>S adsorption (Bagreev et al. 2001a). The surface pH (related to surface chemistry) participates in the dissociation and oxidation of H<sub>2</sub>S. Thus, a basic pH activates the dissociation of H<sub>2</sub> in HS<sup>-</sup> ions, which are oxidized to elemental sulfur and sulfate ions. When the pH is low, there is a decrease in the amount of dissolved H<sub>2</sub>S and HS<sup>-</sup> ions and physical adsorption play a role. This means that when the pH of surface is acid the mechanisms of physisorption are favored rather than chemisorptions. In the last one the formation of SO<sub>2</sub> SO<sub>3</sub> and sulfur elemental are being identified as shown in Table 34. Thus, when stronger bonds are formed the energetic demand to break them is higher than in a physical sorption.

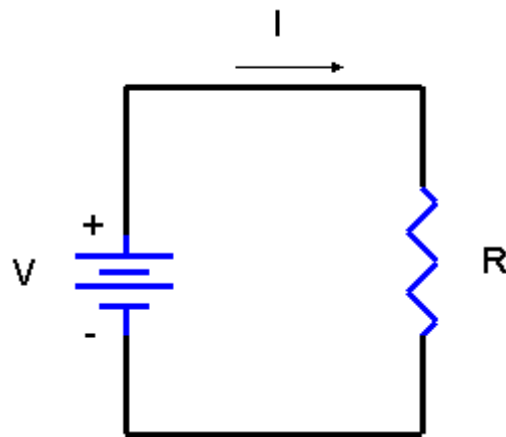
## 1.2 Regeneration of activated carbon

One of the main characteristic of the adsorption process is the life cycle of the adsorbent involved. Generally, activated carbon is used a limited number of times and forward disposal must be done. It represents an increase in the operating costs, mainly caused by the replacement of the material. Regeneration of material is forward an important key for

to optimize operating cost and decrease environmental impact. Among the techniques used in thermal regeneration, different methods are applied.

**Hot gas:** the material can be heated directly, using a hot stream through the adsorption column. The use of steam is the most common technique. Usually, for regeneration of volatile organic compounds, a flow between 105 °C and 140 °C is used (Cloirec, Faur ) and then the outgoing flow is condensate.

**Joule effect:** a recent development in activated carbon regeneration is a direct heating adsorbent by Joule effect, this is applied for activated carbon fibers and cloths ACC. It consists in the heat generated by a current flowing through a conductor (activated carbon). Then adsorbents are volatilized and eliminated by an inert stream through the filter. The major advantages are decrease in adsorption-desorption cycle time and in the energy needed.



The current is fed in continuing and is expressed in the form :

$$(31) \quad R = \frac{U}{I}$$

The power is expressed:

$$(32) \quad P = UI$$

When the electric current is stopped, the electric resistance can be measured with an ohmmeter.

## 1.2.1 Regeneration of activated carbon : H<sub>2</sub>S

In general, the regeneration of activated carbon previously used for the adsorption of H<sub>2</sub>S, is based on a thermal treatment during a period of time. The temperatures ranged

between 200°C and 500°C. Cal et al, 2000, study the desorption of sulfur compounds, previously adsorbed into activated carbons, and the temperature ranged between 400 and 600°C. Also, thermal desorption at 300°C was used during the regeneration cycles of granular activated carbons (Bagreev, Rahman & Bandosz 2001). However, the use of high temperature decreases the properties of the material. Numerous reaction products are formed during the regeneration at high temperature (Boulinguez, Le Cloirec 2010). Additionally, regeneration process takes place off-site (Bagreev, Rahman & Bandosz 2002), making the regeneration of activated carbons a process complex and expensive.

The use of thermal desorption at high temperature has been linked to the necessary energy required to remove the sulfur deposits formed in the surface material. TGA analysis detected peaks between 200 and 400°C. Those peaks were associated with SO<sub>2</sub> formation from sulfur species and intrinsically oxygen adsorbed on carbon. A peak at 700°C was associated with sulfur element located in the inner pores (Elsayed et al. 2009, Monteleone et al. 2011).

Therefore, this study focused on the regeneration of activated carbon previously used as H<sub>2</sub>S adsorbent. The study of regeneration by thermal desorption at lower temperature and the use of vacuum are considered. To attain this objective dynamic adsorption/desorption was used to evaluate the performance of the activated carbon for H<sub>2</sub>S adsorption. The tests were performed at 30 ppm and 2.3NL.min<sup>-1</sup>. The adsorption capacity (q) was then calculated using the mass balance according to equation (28). Where, C<sub>in</sub> is the inlet concentration (30 ppm), C<sub>out</sub> is the outlet concentration, m is the mass of carbon and Q<sub>g</sub> is the flow rate. According to the injection gas grid requirements we established the breakthrough point as the H<sub>2</sub>S limit value, which is 5 mg.Nm<sup>-3</sup>. This value corresponds to the 10 % of our initial concentration as shown in later section in Figure.

## 2 Materials and Methods

After reviewing the mechanisms of H<sub>2</sub>S adsorption in the activated carbon, we considered the next scenario for the study of the adsorption – desorption process. We took into account the principles of low cost, low environmental impact, and easy operation and maintenance. We defined the follow statements:

- Adsorption process as a finishing process
- Adsorption process at ambient conditions

- Adsorption process mostly governed by the physisorption instead of chemisorption
- Regeneration at low temperature

According to the second statement, at ambient conditions the adsorption process is much easier avoiding the use of other equipments that can increase the inversion cost and maintenance. Our interest is focused on the development of adsorption-regeneration process, for that we prefer to work at low temperatures to decrease the formation of sulfur compounds and the adsorbent degradation. The use of low temperature prevents in consequence the development of reactions.

According to the third statement, regeneration efficiency depends strongly on the previous phenomena developed during adsorption. Moreover, physisorption is controlled by the intermolecular forces of the Van der Waals thus the required energy to regenerate the material is lower than if the process is governed by chemisorption phenomena. Indeed, physisorption is a reversible process.

For the fourth statement, previous studies shown that the use of high temperature during the regeneration promotes the alteration in the surface chemistry and adsorption capacity is decreased (Bagreev, Rahman & Bandosz 2002). Thus, the purpose is to regenerate the material at low temperatures to avoid its degradation. Among the activated carbons, we have selected activated carbon cloth given the possible regeneration by Joule effect.

As consequence of the previous objectives the study of different ACC is carried out. Among the parameters involved in adsorption capacity the porosity, surface chemistry, pH, and the products of surface reaction are being highlighted (Bagreev et al. 1999). Thus six activated carbons were characterized.

## 2.1 Materials : adsorbents characteristics

### 2.1.1 pH of carbon surface

A sample of 0.4 g of dry carbon was added to 20ml of water and the suspension was stirred overnight to reach the equilibrium. Then, the sample was filtered and the pH of the solution was measured.

## 2.1.2 BET Porous structure

The determination of the porous distribution of activated charcoals is obtained by an analyzer ASAP 2010 by adsorption and desorption of nitrogen at 77 K. The specific surface is determined by the theory B.E.T. Applied to the isotherms of adsorption in the range of relative pressures  $P/P_0 = 0.04$  in  $0.2$ . The total pore volume (pores of lower size in  $2000 \text{ \AA}$ ) is obtained in the relative pressure  $P/P_0 = 0.1$ . The characteristics of micro porous distribution (for the diameters of pores lower than  $20 \text{ \AA}$  (Classification International Union of Pure and Applied Chemistry, on 1972) and average diameter of pores are determined by the theory of Howarth-Kawazoe, applied to the isotherm of adsorption in the range of relative pressures  $P/P_0 = 10^{-7}$  in  $0.1$ .

## 2.1.3 Surface acid function

The surface acid and basic functions are determined by the acid-basic Boehm method (Boehm, on 1966). It is based on an acid-basic depletion technique. So,  $1,0 \text{ g}$  of activated carbon is placed into  $50 \text{ cm}^3$  of the following solutions :  $\text{NaHCO}_3$ ,  $\text{Na}_2\text{CO}_3$ ,  $\text{NaOH}$ ,  $\text{NaOC}_2\text{H}_5$  at  $0,1 \text{ N}$ . The solutions are left during 48 hours under agitation. Then, after filtration,  $10 \text{ cm}^3$  of filtrate is collected and measured by titration with  $\text{HCl}$  ( $0,1 \text{ N}$ ) in the presence of helianthine for  $\text{NaHCO}_3$  and  $\text{Na}_2\text{CO}_3$  and of phenolphthalein for  $\text{NaOH}$  and  $\text{NaOC}_2\text{H}_5$ . The quantity of neutralizing base is given by the following relation:

$$[\text{C}]_{\text{neutral}} (\text{meq} \cdot \text{g}^{-1}) = \frac{(N_{\text{base}} - N_{\text{HCl}}) \cdot X(\text{cm}^3 \text{ de HCl}) \cdot 50}{10}$$

The concentrations in each of the groups are calculated as follows:

$$\text{GI} = [\text{NaHCO}_3]$$

$$\text{GII} = [\text{Na}_2\text{CO}_3] - [\text{NaHCO}_3]$$

$$\text{GIII} = [\text{NaOH}] - [\text{Na}_2\text{CO}_3]$$

$$\text{GIV} = [\text{NaOC}_2\text{H}_5] - [\text{NaOH}]$$

Table 35. Activated carbon fiber cloths characteristics

Reference	ACF 1	ACF 2	ACF 3	ACF 4	ACF 5	ACF 6
Weight (g/m <sup>2</sup> )	150	220	130	140	120	110
Thickness (mm)	0.61	0.6	0.47	0,4	0.5	0.4
S <sub>BET</sub> (m <sup>2</sup> .g <sup>-1</sup> )	1689	1461	873	790	1200	1100
Micropore volume < 20 Å (cm <sup>3</sup> .g <sup>-1</sup> )	0.665	0.506	0.435	0.31	0.306	0.300
Mesopore volume 20 Å < < 500 Å (cm <sup>3</sup> .g <sup>-1</sup> )	0.025	0.237	0.108	0.02	0.248	0.165
% Mesopore volume	3.6	31.9	19.9	6.1	44.8	35.5
G I	0.60	0.25	0.28	0.35	0.3	0.46
G II	0.10	0.15	0.00	0.00	0.65	0.48
G III	0.40	0.40	0.58	0.45	0	0
G IV	0.00	0.00	0.25	0.25	0.13	0
total	1.10	0.80	1.10	1.05	1.08	0.94
Basic function	0.45	0.5	0.9	0.5	0.6	0.9
Carbon surface pH	8	7	10	10	9	6

The choice of the material is based in an adsorbent partially mesopore, to favor the water adsorption and therefore mechanisms in the wet atmosphere (Bandosz 1999). This criterion excludes the activated carbons ACF 1 and ACF 4. According to the effect of surface pH, we prefer an adsorbent with acid pH to limit the acid-basic reactions with the H<sub>2</sub>S. It eliminates from the choice the activated carbon ACF 3 and ACF 5. Finally, between ACF 2 and ACF 6, the availability of the material drove us to choose the latter for the study of the cycles adsorption – regeneration. The adsorption - desorption study is carried out wet and dry atmosphere given the differences in the mechanisms.

## 2.1.4 Adsorption Isotherms

H<sub>2</sub>S adsorption was performed in 2 L batch reactors as shown in the Figure 15. A sample of 0.01 g was suspended in a metal support. Then, H<sub>2</sub>S pure was injected into each reactor and stirred for 6 hours. Forward, the samples were analyzed with the Spectroquant

method Merk<sup>®</sup> kit. A gas sample of H<sub>2</sub>S was taken from each reactor and injected in a basic solution pH (9-10). Then, with the addition of each reactant the Caro –Fisher reaction is done, and the concentration is measured by spectrophotometer at 665 nm.

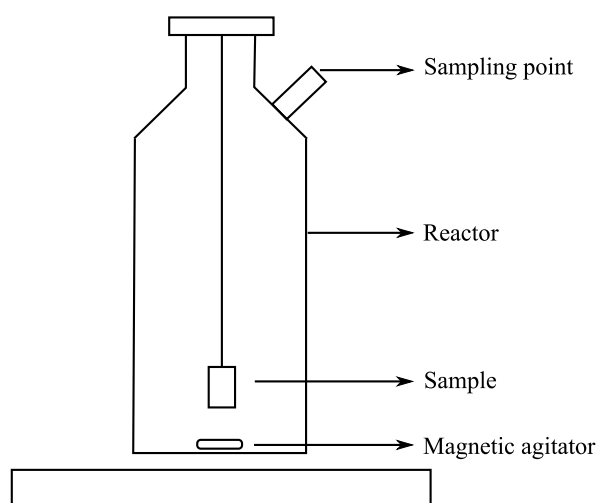


Figure 15. Adsorption Static system

Models such as Freundlich, Langmuir and Langmuir-Freundlich are generally used to describe the adsorption curves at the equilibrium. The three models were evaluated and the one that better describes the H<sub>2</sub>S adsorption curves is the Freundlich model (Eq 5). The isotherm adsorption is represented in Figure 35. The results of the parameters and the correlation coefficient are given in Table 36.

A big K value represents a good adsorption capacity at low concentrations. ACF6 presents a higher K value. It confirms a good performance for H<sub>2</sub>S adsorption. Other studies with fiber cloths ACC6 have shown also a good behavior during the sulfur compounds adsorption (Boulinguez and Le Cloirec 2010).

Table 36. Values of the parameters of the Freundlich Model of activated carbon cloth ACF6 (FM30K) previously adsorbed with H<sub>2</sub>S.

	K	n	1/n	R <sup>2</sup>
FM 30K	52.6	0.22	4.52	0.97



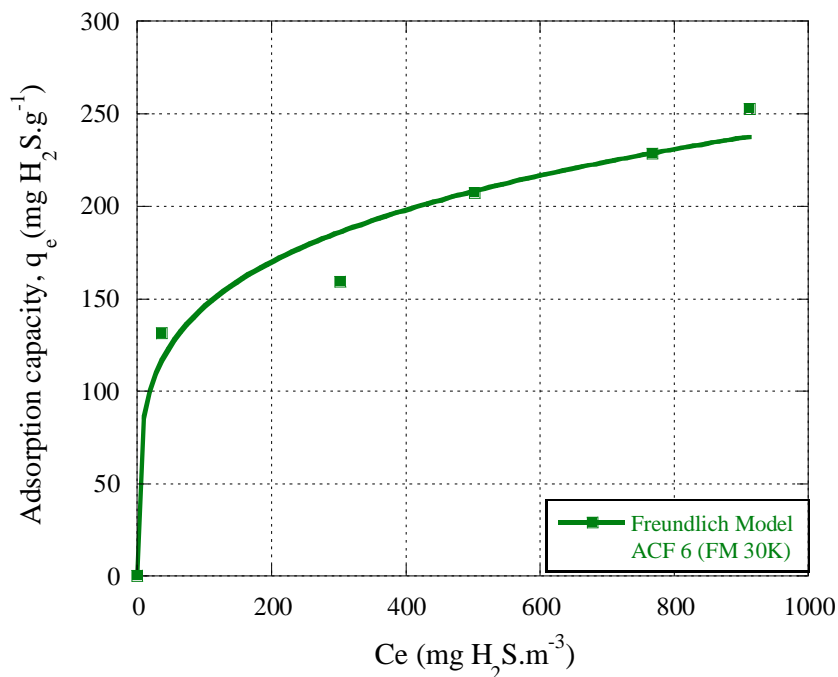


Figure 35. Adsorption Isotherm of ACF6 (FM30 K). Temperature 20 °C. H<sub>2</sub>S under a dry atmosphere of air.

## 2.2 Laboratory unit

The laboratory unit used in the adsorption / desorption process is shown in Figure. The adsorbent material was placed in a filter holder with a surface area of 7 cm<sup>2</sup> provided with a thermocouple. A standard bottle of H<sub>2</sub>S in N<sub>2</sub> at 400 ppmv was mixed with N<sub>2</sub>/O<sub>2</sub>. Two flow meters were used for this purpose. Output gas was analyzed by a SO<sub>2</sub> –H<sub>2</sub>S ONYX 5250 – COSMA detector.

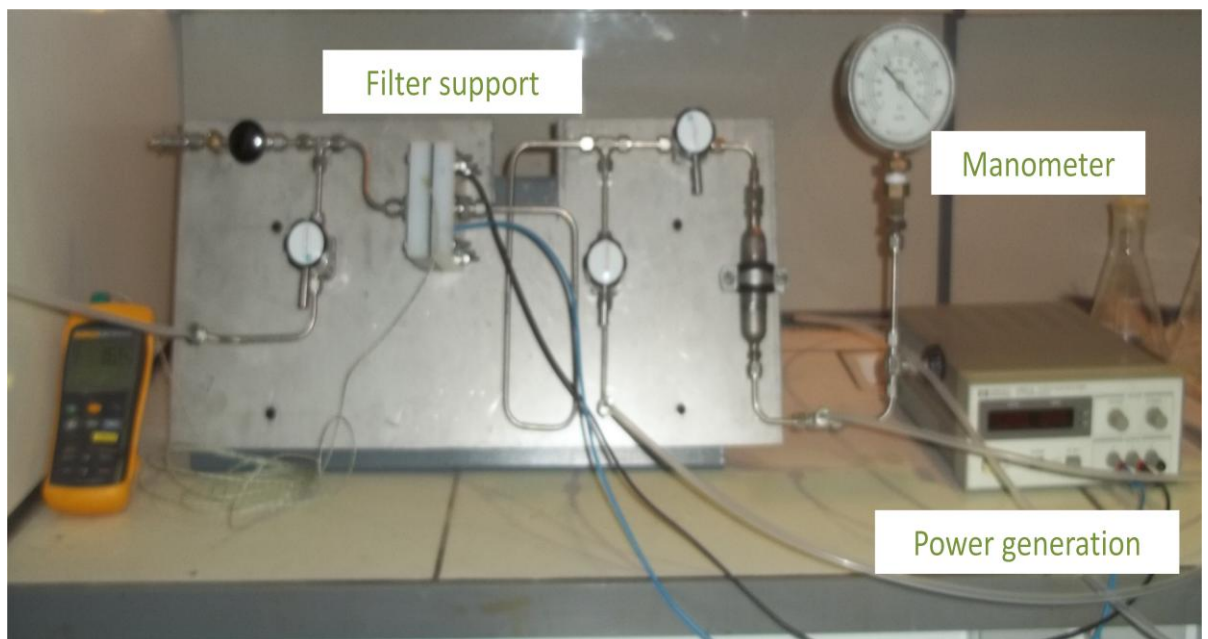
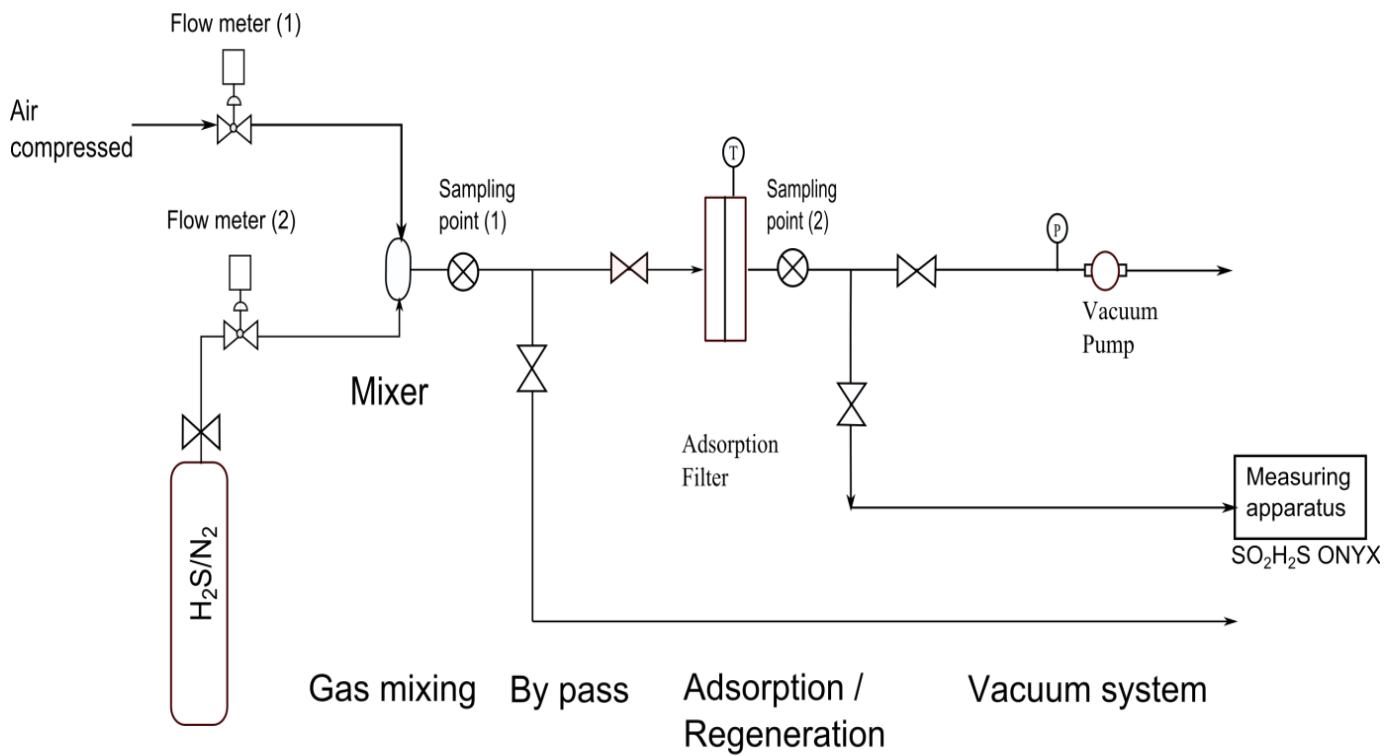


Figure 36. Flow diagram and photography of adsorption / desorption process of an activated carbon filter heated by Joule effect and under vacuum pressure. Adsorption of H<sub>2</sub>S.

## 2.2.1 Desorption system

A desorption system in situ was developed to regenerate the material. In this example two variables: temperature and pressure were analyzed. To increase the temperature, a heating system was installed provided with a thermocouple to control the process. To decrease the pressure, a vacuum pump was installed at the end of the line. The regeneration was carried out during 60 min. Forward, a second adsorption at the same operating conditions was done to test the material regeneration. An example of one of the conditions tested is presented in Figure.

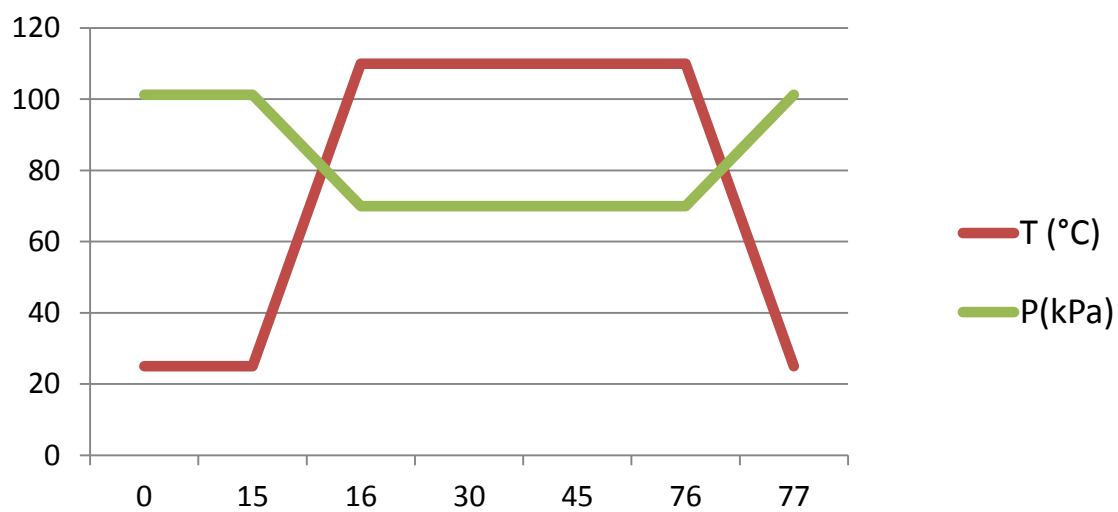


Figure 37. Schematic representation of the adsorption-desorption process. Temperature and pressure variation. Regeneration conditions:  $T = 110^{\circ}\text{C}$ ,  $P = 700 \text{ mbar}$  during 60 min.

## 2.2.2 Characterization of filter with the Joule effect

According to the different methods to regenerate the materials, we have selected the heating system by Joule effect. The material is previously characterized following the next procedure:

A layer of tissue with the next dimensions (23 mm x 30) mm are cut and dried during 48h in an oven at  $100^{\circ}\text{C}$ . These samples are then used to measure the current needed to increase the temperature since  $100^{\circ}\text{C}$  until  $350^{\circ}\text{C}$ . The samples are provided with a conductive material (copper tape) located at the both extremes of the tissue. A representation of the configuration is shown in Figure. Then the cloth piece is fed with an electric current.

For that a generator of power is connected to the system. The tension and the intensity are modified to arrive at different values of temperature. The temperature is measured with a thermocouple located in the center of the cloth. These values are registered and follow using the equation (32) the power is calculated. The Figure shows the thermal-electric response of the filter taken at ambient conditions.

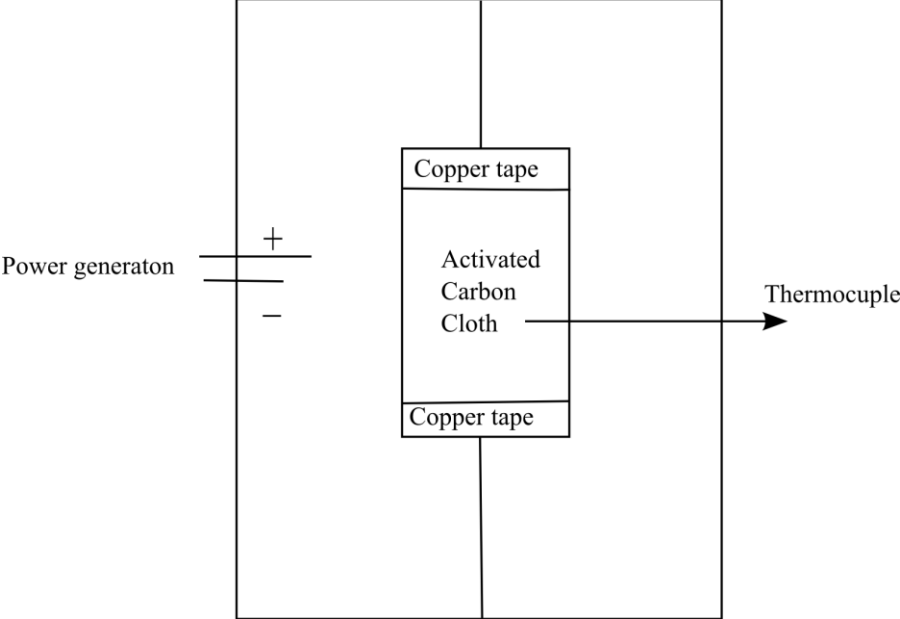


Figure 38. Schematic representation of the characterization of filter AFC6 (FM30K) with electrical current.

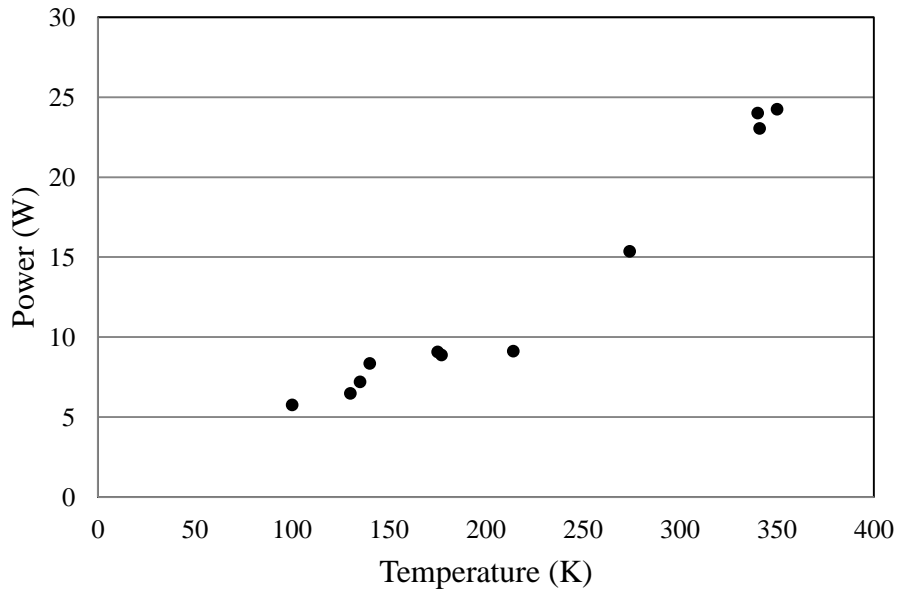


Figure 39. Electric characterization of the filter (FM30 K). Power (W) in function of the temperature (K). Experimental conditions at the air at the environmental conditions.

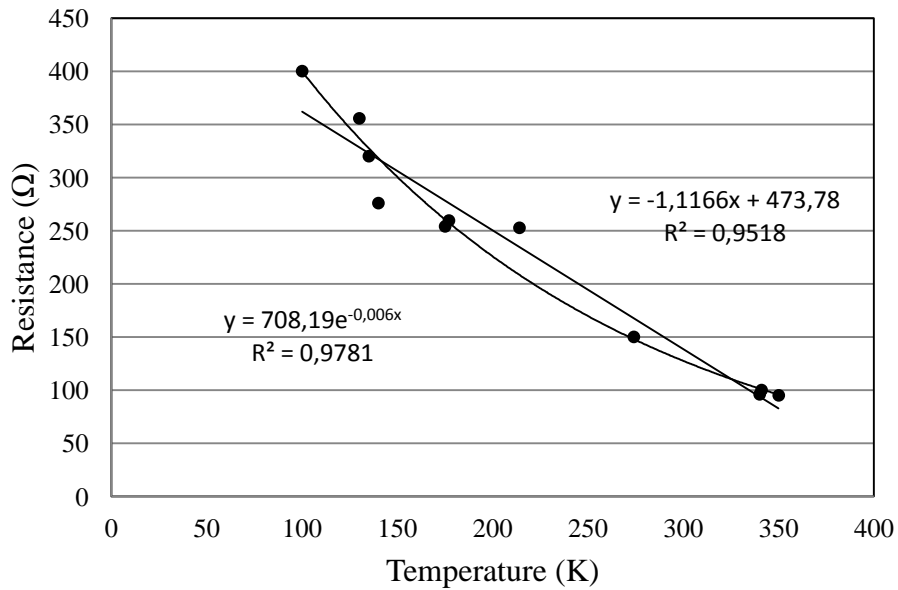


Figure 40. Electric characterization of the filter (FM30 K). Resistance ( $\Omega$ ) in function of the temperature (K). Experimental conditions at the air at the environmental conditions.

The activated carbon cloth is forward arranged in a teflon support allowing its power supply as shown in Figure 41. The layers of section 23 mm x 30 mm are settled to realize adsorptions in dynamics and the thermo-electric regenerations. The electrical response

characterization in function of the power was carried out at different conditions. As seen figure 41, the power needed to increase the temperature around 110°C ranged between 3 to 5 W. The power needed to increase the temperature is therefore in function of the dynamic conditions. The high demand of power (5 W ) corresponds to the dry filter with a flow air passing throughout it. The filter previously humidified shows a high point of 5 W around 60 °C. This point is associated with the energy required to evaporate the absorbed water, after that the power needed is decreased to finally arrive to 4 W at 110°C. This thermal-electric characterization is therefore used during the regeneration phase.

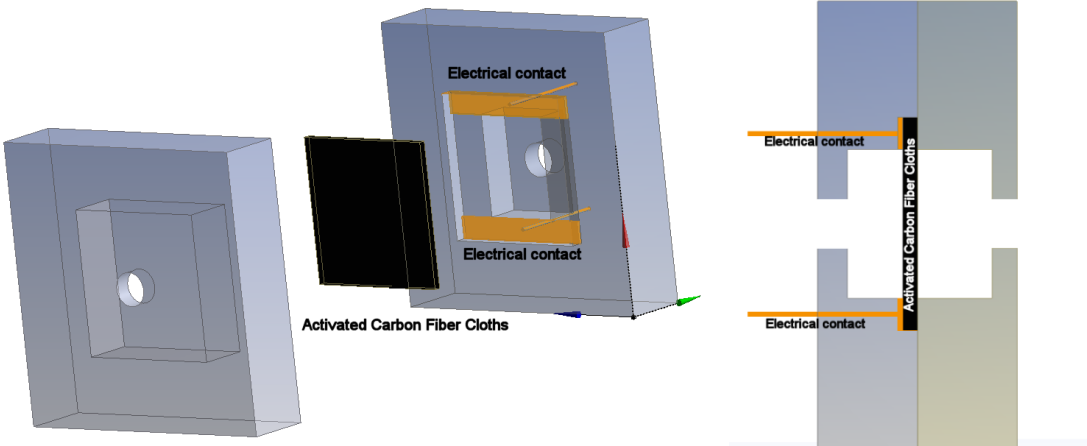


Figure 41. Schema of the Filter holder with electrical contact.

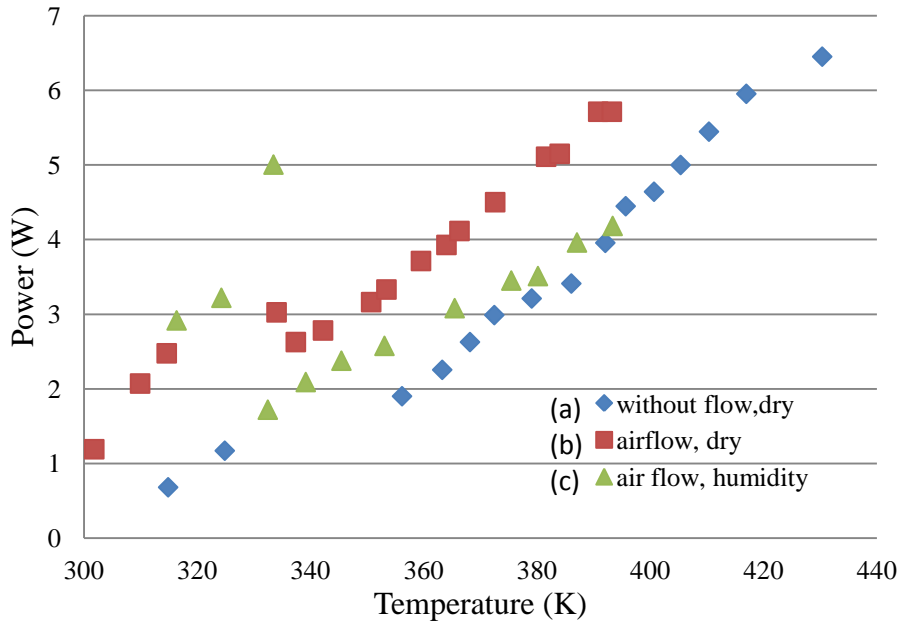


Figure 42. Electric characterization of the filter (FM30 K). Experimental conditions: (a) without flow through the filter and no humidification. (b) air flow through the filter and no humidification. (c) air flow through the filter and pre-humidification. Power (W) in function of temperature (K).

Several layers are used in the adsorption process in dynamic, all of them are joined by the tape copper. The electric current is therefore fed in the positive side and the current flow is divided into each layer throughout the negative side as shown in Figure 43. This configuration is therefore called in parallel. To calculate the equivalent resistance for a single layer the equation (33) is applied:

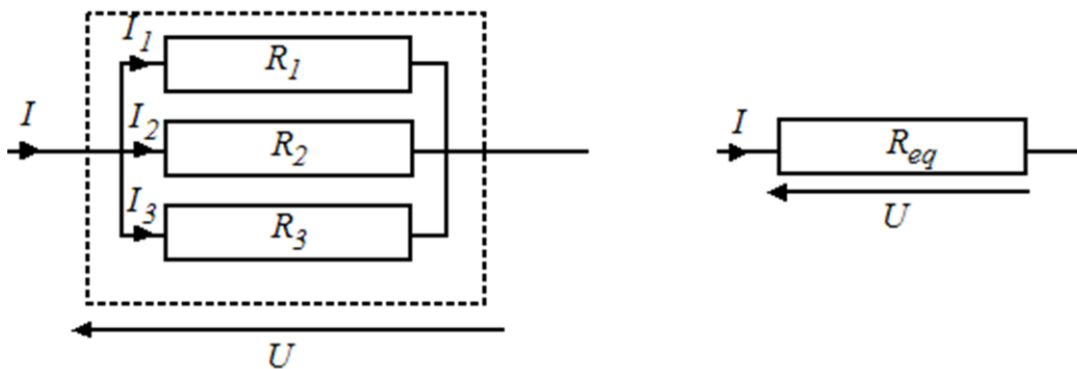


Figure 43. Layers of activated carbon in a parallel configuration

$$(33) \quad \frac{1}{R_{eq}} = \frac{1}{R_1} + \frac{1}{R_2} + \frac{1}{R_3}$$

In the next figures, the evolution of the resistance in function of the temperature is presented. According to previous studies (Subrenat et al. 2001), two models can be applied to

describe the behavior. The first one is a linear model proposed by (Nasar A.S., 1989). This model is shown in the equation (34).

$$(34) \quad R(T) = R(T_0)[1 + \alpha_0(T - T_0)]$$

Where,

R : electrical resistance at the temperature T

R<sub>0</sub> : electrical resistance at the temperature T<sub>0</sub>

α<sub>0</sub> : thermal coefficient at the temperature

T: material temperature (K)

T<sub>0</sub>: reference temperature (273 K)

However, according with the Figure, the linear form is not the best model, the electrical resistance is better described by an exponential curve. Previous studies have suggested the resistance modeling by exponential models (Steinhart, J.S & Hart, S.R. 1968) applied to semiconductor materials and to the thermistance with a negative coefficient thermic. In this study, the behavior of the electrical resistance is better described by an exponential model. In the next cases, when the filter is studied under dynamic conditions, the electrical resistance behavior changes in function of the system. In the first case, when there is not air flow passing through the filter, the electrical resistance is as well described by an exponential curve as shown in Figure 44. This means that at the beginning, the power consumption is bigger than some minutes latter, and the power demands decrease rapidly. However, in Figure 45 and Figure 46, which corresponds to the conditions under air flow passing through the filter, the electrical response is better described by a linear model. It is interesting to notice, that the pre-humidified filter shown in Figure 46, has a similar behavior after 60°C (353 K) that the filter without humidification. These results suggest that after 60°C a huge percentage of water has been removed.



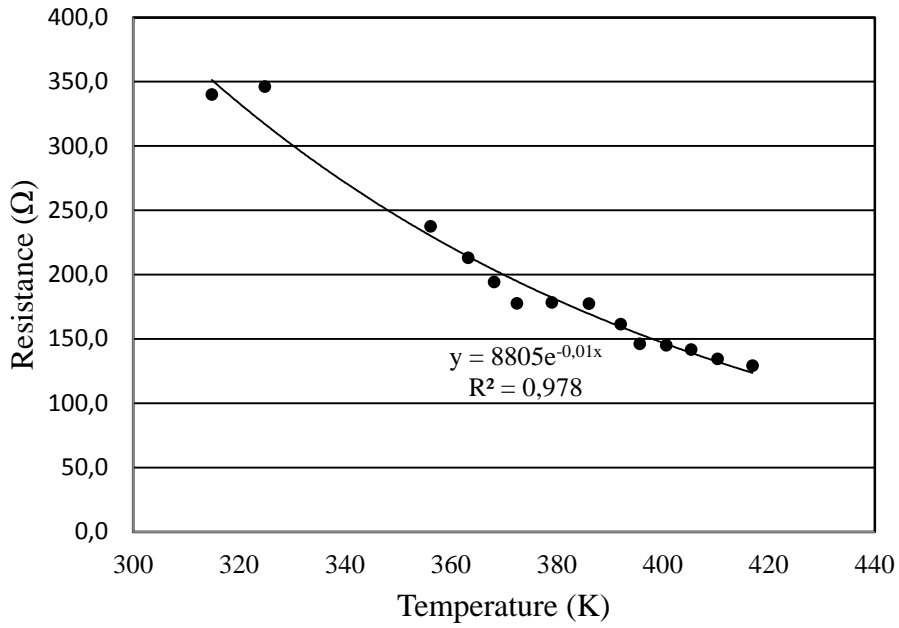


Figure 44. Resistance ( $\Omega$ ) in function of the temperature (K). Electric characterization of the filter (FM30 K). Experimental conditions: (a) without flow trough the filter and no humidification.

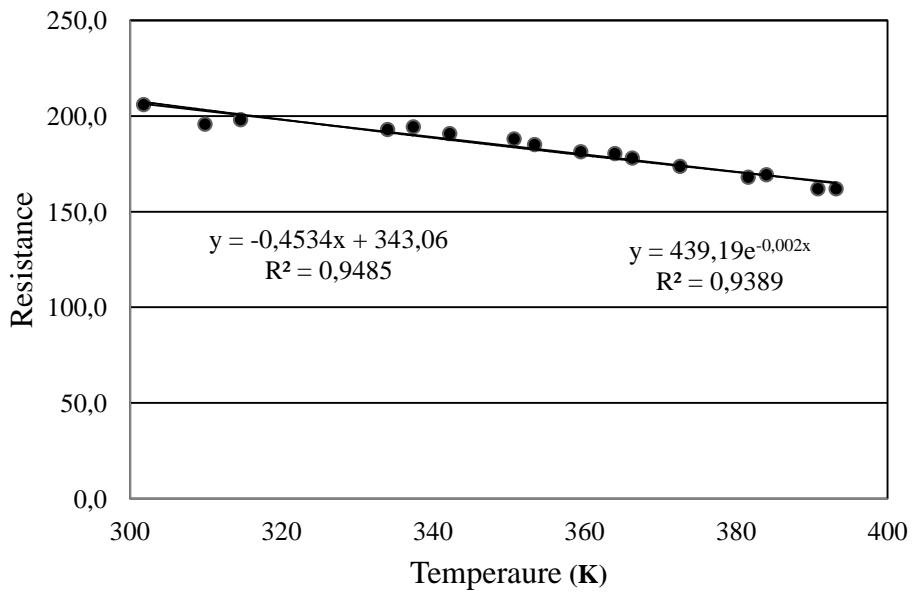


Figure 45. Resistance ( $\Omega$ ) in function of the temperature (K). Electric characterization of the filter (FM30 K). Experimental conditions: (b) air flow trough the filter and no humidification.

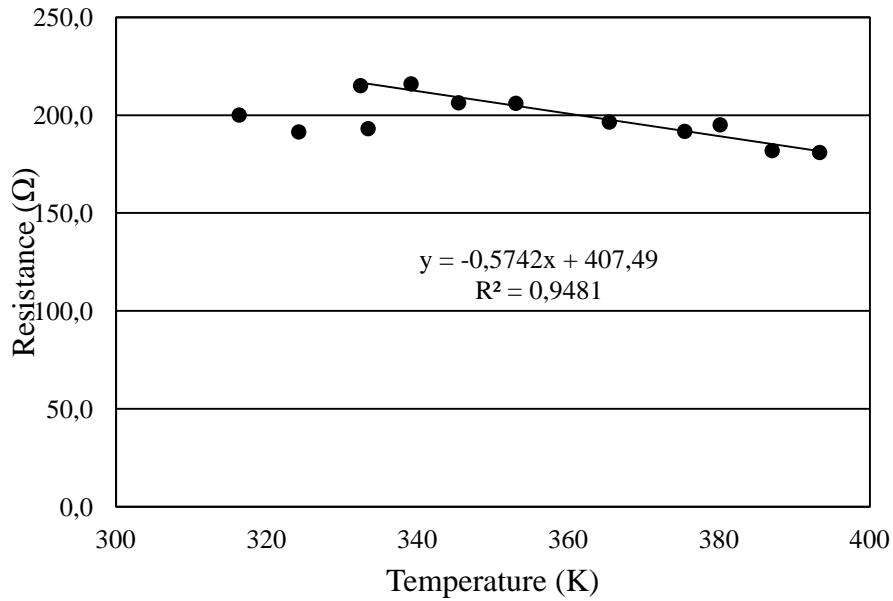


Figure 46. Resistance ( $\Omega$ ) in function of the temperature (K). Electric characterization of the filter (FM30 K). Experimental conditions: (c) air flow through the filter and pre-humidification.

### 2.2.3 Operating conditions

The studied parameters that can influence the quality and the efficiency of regenerations during the phase of adsorption are the relative humidity of the gas modifying the nature of the mechanisms of transfer and reactions and the level of load in  $H_2S$  of adsorption. The parameters influencing regeneration are clearly the duration, the temperature and the pressure in the reactor. Being in the presence of mechanisms of chemisorption, we can imagine that the time off between adsorption and regeneration can influence the performance of the latter.

A first trial series allowed to estimate the combined influence of the pressure (0,7 and 1 bar) and the temperature of regeneration (20 and 110°C). It is important to highlight that these operational conditions have been fixed during this thesis and no other authors has presented these conditions, and no combination of pressure and temperature during the desorption was founded, this point give a new approach of the regeneration process. The duration of the regeneration is fixed arbitrarily at 60 min and 0% of RH (relative humidity). An additional essay allowed estimating the influence of the humidity. In the same way, this aspect has been not studied previously. To create the wet atmosphere, the material is

humidified using an airflow saturated in water at 80-90 % HR. The humidification step is carried out for about 30 minutes.

The second trial series has for objective to estimate duration of sufficient regeneration (30, 60, and 180 minutes) as well as the influence of the waiting time between adsorption and regeneration (0, 4, 24 h). Finally a last series of cycle allows observing the influence of the level of load in H<sub>2</sub>S on the quality of desorption. Table 37 presents the values of the parameters studied.

Table 37. Studied parameters influencing the regeneration quality (a) dry atmosphere (b) wet atmosphere.

Parameters (a)	Values				
Desorption time (min)	60				
Pressure of regeneration (mbars)	700	700	1000	1000	
Temperature of regeneration (°C)	20	110	20	110	
Pressure of regeneration (mbars)	700				
Temperature of regeneration (°C)	110				
Desorption time (min)	30	60		180	
Time between adsorption and regeneration	0	0	4	24	0

Parameters (b)	Values				
Desorption time (min)	60				
Wet Air	90% RH				
Pressure of regeneration (mbars)	700				
Temperature of regeneration (°C)	110				
Outlet concentration (ppm)	5	15		30	

## 2.3 Results and discussion

In this section, the results obtained from the adsorption-regeneration experiments are presented. The regeneration efficiency was evaluated with a second adsorption test after regeneration. This methodology has already been used to evaluate regeneration process (Bagreev et al. 2001b; Monteleone et al. 2011) allowing the evaluation of the adsorbent at the same characteristics previously adsorbed (mass of adsorbent, sample, position in the filter, etc). It is important to highlight that here the regeneration process is carried out in situ, the filter is not opened and no manipulation of the material is done out of the system.

### 2.3.1 Temperature effect:

Two temperatures are tested, 20°C and 110°C. In the H<sub>2</sub>S adsorption, the combined mechanism of physisorption and chemisorption can be developed during the process. With the purpose of testing the strength of adsorption, we have tested the material after adsorption by simple purge with air. After that, a second adsorption is carried out and we obtain a fast saturation curve as shown in Figure 47. This indicates that the adsorption is stable and strong. This is important also in the process. A very weak adsorption might be a problem thus the desorption can be developed by a simple flow gas throughout the bed. Thus the temperature is increased at 110°C. In this case, the breakthrough profile is very interesting, as we can see in Figure, the second adsorption is very close to the first one. This suggests that at 110°C the energy to remove the previously H<sub>2</sub>S adsorbed is enough. Revealing that the temperature is a limiting factor to the regeneration.

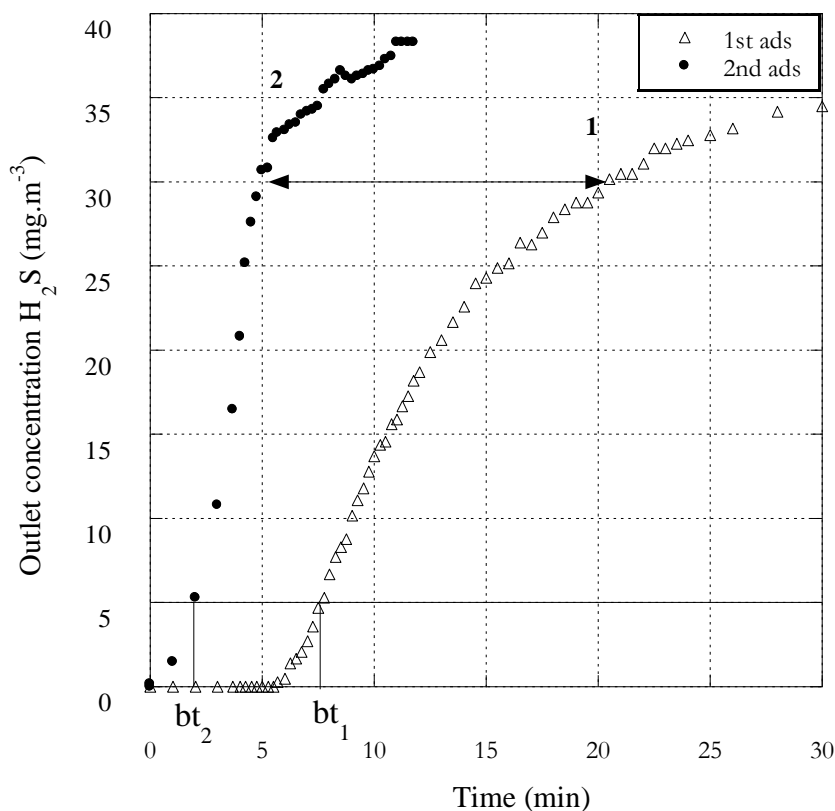


Figure 47. Adsorption of H<sub>2</sub>S into activated carbon cloth ACF6 (FM30 K). concentration profile (mg.m<sup>-3</sup>) in function of time (min). Curve 1st and 2<sup>nd</sup> adsorption /regeneration. Regeneration conditions: T: 20°C and P:1 bar.

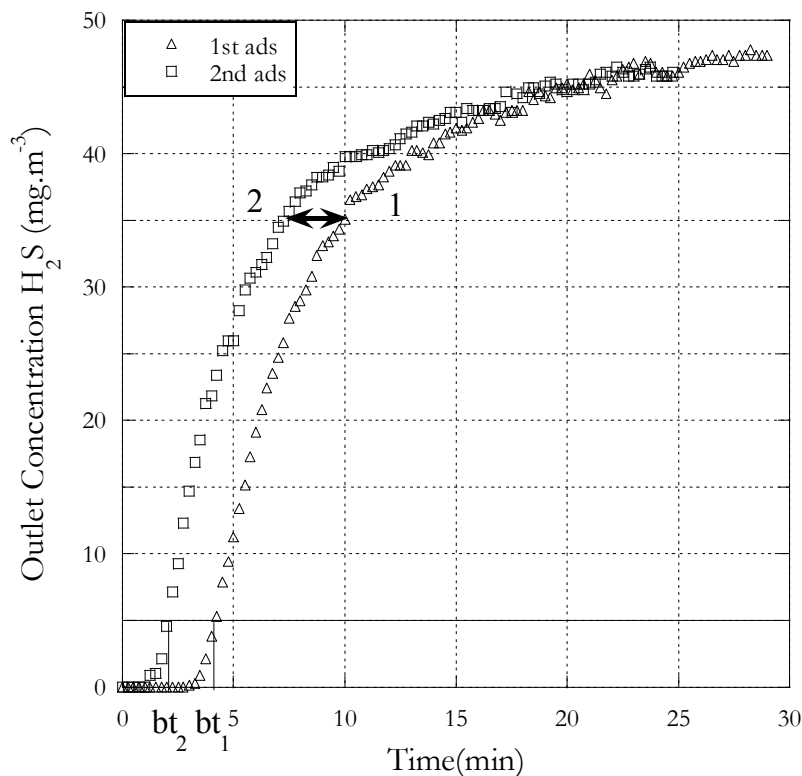


Figure 48. Adsorption of H<sub>2</sub>S into activated carbon cloth FM30 K. Concentration profile (mg.m<sup>-3</sup>) in function of time (min). Curve (1) first adsorption with a new filter. Curve (2) second adsorption after regeneration. Regeneration conditions: Temperature: 110°C and Pressure: 1 bar.

### 2.3.2 Pressure effect

The second parameter studied is the pressure during the regeneration; for that vacuum pump is used in the system and pressure is reduced at 0.7 bar. Here the purpose is to remove the compounds by a force different from the thermal effect. The decrease in pressure will allow to desorb the molecules from the adsorbent if the adsorption is mostly physical than chemical. In Figure 49, the concentration profile is presented. We notice that the gap between the two curves is smaller than at ambient conditions. This suggest from one side, that there is a fraction of the H<sub>2</sub>S that is physically adsorbed and removed because the vacuum force. From the other side, we confirm that stronger bonded are developed in the adsorbent and the flowing gas under vacuum is not enough to desorb completely the material. As a consequence, we have combined the two conditions, high temperature and vacuum pressure as shown in Figure 50. The latter shows a very good profile after regeneration. The gap between the first and the second curve is much smaller than only increasing the temperature. The desorbed compounds by thermic effect are removed from the activated carbon

simultaneously by the vacuum force applied in the filter. Thus material desorption is reached, avoiding the fixation of products in the surface. We can make the hypothesis that additionally of the desorption of  $H_2S$  physisorbed the sulfur compounds formed as sulfur elemental is also desorbed. Moreover, at vacuum pressure the sublimation temperature of the sulfur compounds is lower. In fact, the sublimation temperature of sulfur solid decreases with the downturn of the pressure. At 700 mbars, it is about  $90^\circ C$ . These results show that coupling thermal regeneration and vacuum effect a good regeneration is accomplished.

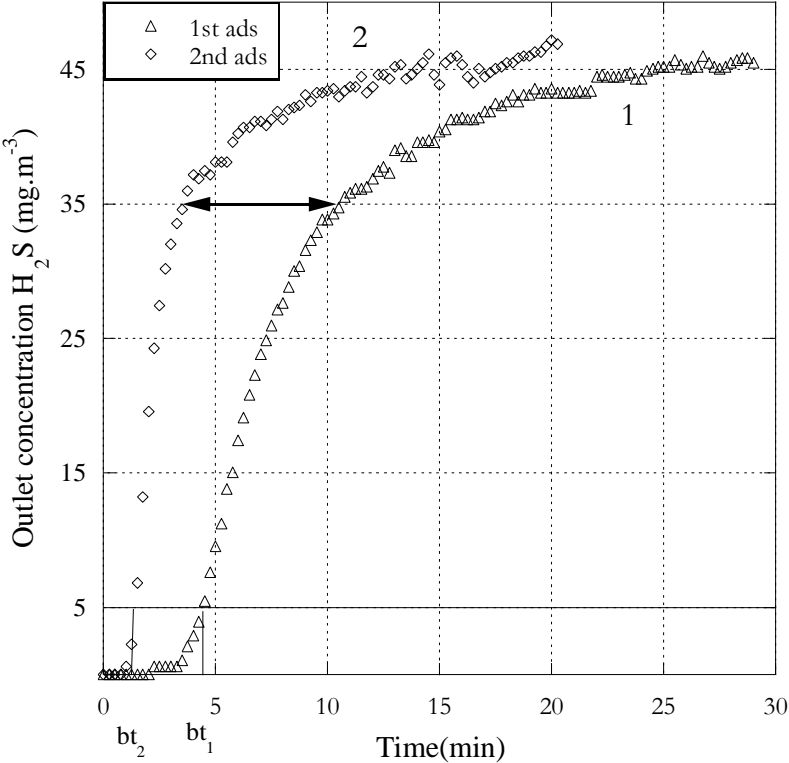


Figure 49. Adsorption of  $H_2S$  into activated carbon cloth ACF6 (FM30 K). Concentration profile ( $mg \cdot m^{-3}$ ) in function of time (min). Curve (1) first adsorption with a new filter. Curve (2) second adsorption after regeneration. Regeneration conditions: Temperature:  $20^\circ C$  and Pressure: 700 mbar.

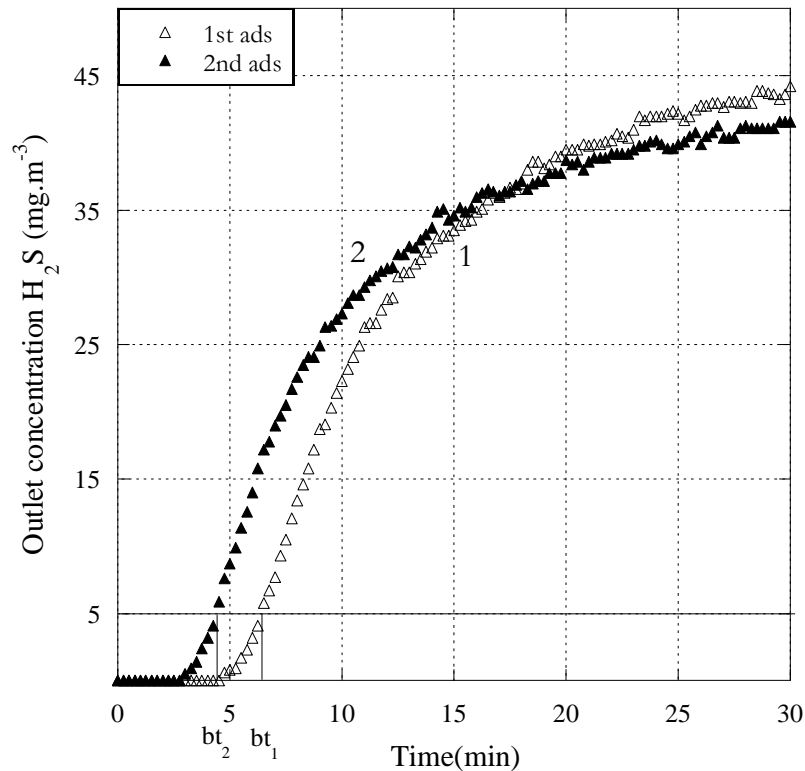


Figure 50. Adsorption of  $H_2S$  into activated carbon cloth ACF6 (FM30 K). Concentration profile ( $mg.m^{-3}$ ) in function of time (min). Curve (1) first adsorption with a new filter. Curve (2) second adsorption after regeneration. Regeneration conditions: Temperature:  $110^{\circ}C$  and Pressure: 700 mbar.

Adsorption capacity yield (adsorption capacity of the second adsorption under adsorption capacity of the first adsorption) is shown in Figure 51. Here we can observe more clearly which is the best combination of the operational parameters to regenerate the material. From the less effective to the more effective, we observe that at ambient conditions the adsorption capacity decrease quickly to attain an adsorption rate after regeneration around 35 %, followed by the conditions at  $20^{\circ}C$  and vacuum system with and adsorption rate at the saturation of 50%. Then, we observe the two curves at  $110^{\circ}C$ , here the two curves are close, at  $110^{\circ}C$  and pressure atmospheric, we obtain 75% and finally coupling the temperature  $110^{\circ}C$  and vacuum pressure we obtain 85% . Finally, the operational conditions that allow the best regeneration of the material correspond to parameters at  $110^{\circ}C$  and 700 mbar. Comparing with other authors, the regeneration temperature is much lower.

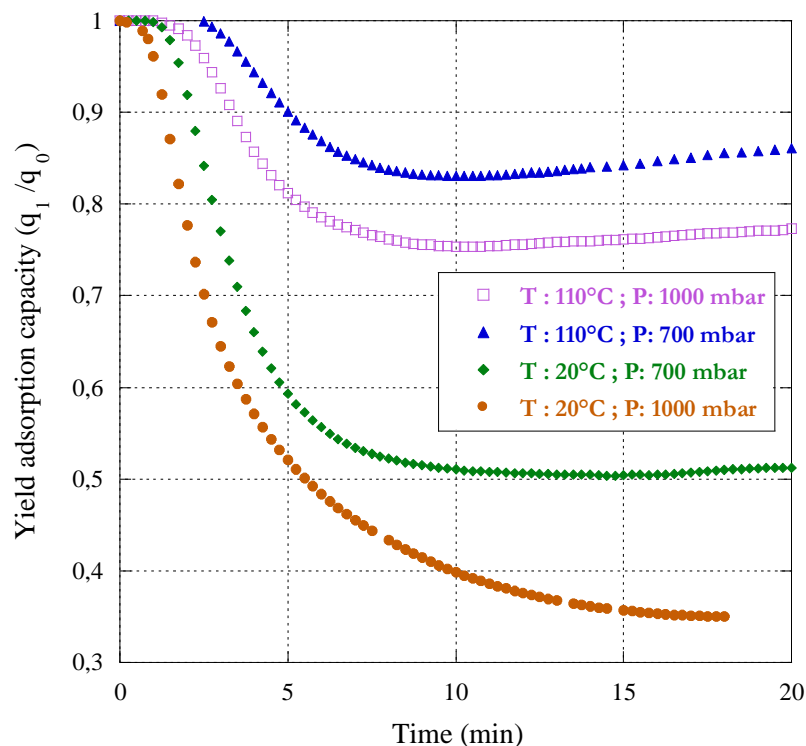


Figure 51. Yield adsorption capacity ( $q_2/q_1$ ) in function of time (min). Activated carbon cloth ACF6 (FM30 K). Regeneration conditions (A) T :110° and P: 700 mbar, (B) T :110° and P: 1000 bar, (C) T :20° and P: 700 mbar, (D) T :20° and P: 1000 mbar.

As we know, the adsorption process in the industry is not carried out to attain the saturation of the adsorbent, thus the yield capacity ( $q_2/q_1$ ) at the breakthrough point is listed in Table 38. Here, we observe that the adsorption rate varies following the same tendencies. Thus the best regeneration conditions at the breakthrough point are obtained at 110 °C and 0.7 bar, with an adsorption rate of 90%. Concerning the 10% of the material that is not regenerated, it can be done given a chemisorptions developed in the material which demands stronger temperatures or pressure to be removed from the material. Also, the development of products during the regeneration might be accomplished, blocking the pore structure for the next adsorption.

However, at the end of the curve, a better performance is observed. This behavior can be explained by the possible generation of new active sites of oxygen during the regeneration, promoting  $H_2S$  oxidation. Also, the enhancement in adsorption capacity has been suggested by the autocatalytic role of elemental sulfur. It is formed in the first steps of the process  $C(S)$  promoting the hydrogen sulfide oxidation until sulfur saturation.



Table 38. Summary of adsorption capacity (q) of the first and second adsorption. Regeneration conditions: Temperature 20 and 110°C and Pressure: 700 and 1000 mbar. Breakthrough point: 5 ppmv.

Pressure (mbar)	1000	1000	700	700
Temperature (°C)	20	110	20	110
$q_{bp}^0$ (mg.g-1)	1,2	1	1,1	1,2
$q_{bp}^1$ (mg.g-1)	0,2	0,47	0,4	1,1
$q_s^0$ (mg.g-1)	3	2,4	2,6	2,97
$q_s^1$ (mg.g-1)	1	1,8	1,2	2,96

bp : break point  
s : saturation

### 2.3.3 Influence of the delay and the duration

The influence of other parameters is also considered. Regeneration time is studied at three different times: 30 min, 60 min and 180 min. The adsorption capacity at the saturation and at the breakthrough point are shown in Table 39. As we can observe, the adsorption capacity at 30 min is lower than at 60 min. Then, we increased at 180 min. However, in this case it is not observed better performance. This confirms that 60 min is a suitable time.

Table 39. Adsorption capacity of the first and second adsorption. Regeneration conditions: regeneration time: 30, 60, 180 min. Time delay after first adsorption 4 and 24 h.

Delay (hour)	0	0	0	4	24
Regeneration duration (min)	30	60	180	60	60
$q_p^0$ (mg.g <sup>-1</sup> )	0.9	1.2	1.1	1.1	0.9
$q_p^1$ (mg.g <sup>-1</sup> )	0.6	1.1	1	0.5	0.3
$q_s^0$ (mg.g <sup>-1</sup> )	2.3	2.9	2.8	2.8	2.8
$q_s^1$ (mg.g <sup>-1</sup> )	2	2.9	2.7	1.6	1.4

Another aspect considered in the adsorption-regeneration cycles is the time off or delay time between the adsorption-desorption cycles, as shown in Figure 52. This time means, the time passed before carried out the regeneration. This scenario can be reproduced in an industrial biogas treatment, when for example the process line is stopped for a period of time. Thus we consider : 4 h, like a stop during the day, and 24 h that might be the case of a Sunday. Here we observe a decrease of the adsorption capacity rate after 4 h between the cycles. This decrease is more important after 24 h. This phenomena can be explained by the oxidation pathway of H<sub>2</sub>S and in consequence the formation of sulfur oxides which are more

difficult to desorb. To avoid this loss in the regeneration efficiency, the regeneration must be carried out as soon as the material is exhausted. A parallel filter is thus recommended for optimized adsorption-regeneration process.

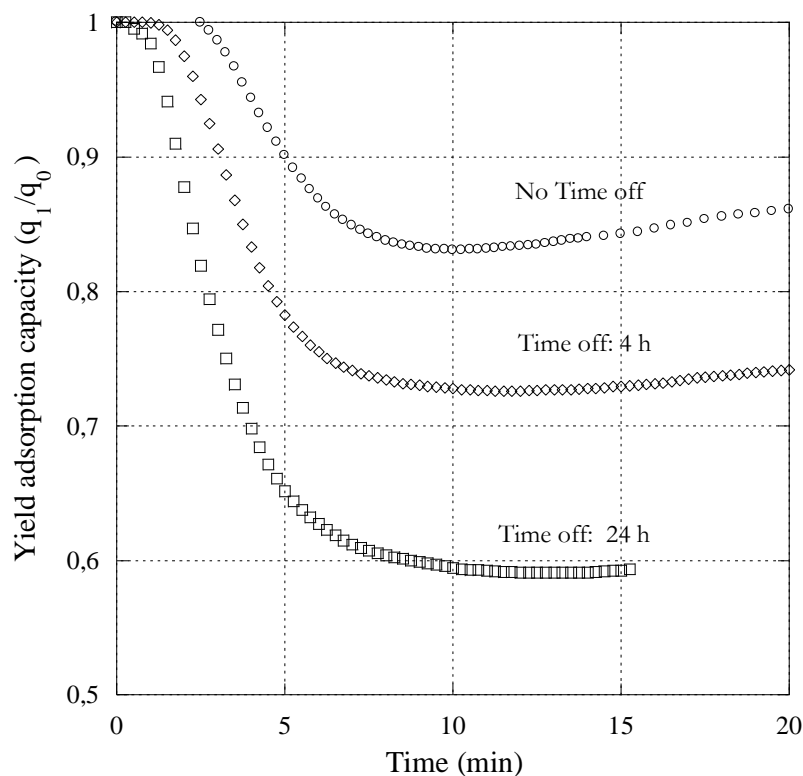


Figure 52. Adsorption of  $H_2S$  into activated carbon ACF6 (FM30 K). Delay time between the first adsorption and the second adsorption.(a) 0 h ; (b) 4 h ; (c) 24 h. Regeneration conditions: temperature:  $110^{\circ}C$  and pressure: 700 mbar.

### 2.3.4 Adsorption – Desorption sustainability

To analyze the sustainability of the process, adsorption – desorption cycles at the saturation point were carried out as shown in Figure 53. This graphic shows that after each regeneration adsorption changes significantly. Even if at the beginning adsorption capacity after regeneration is about 90%, after a sequence of adsorption-regeneration the adsorbent material is not regenerated. This can be explained by the formation of stronger compounds in the adsorbent. As a result the activated carbon is exhausted. As adsorption capacity decreases considerably after the fourth cycle, the process was stopped at this point. Thus, activated carbon was saturated and material was no longer useful as hydrogen sulfide adsorbent.

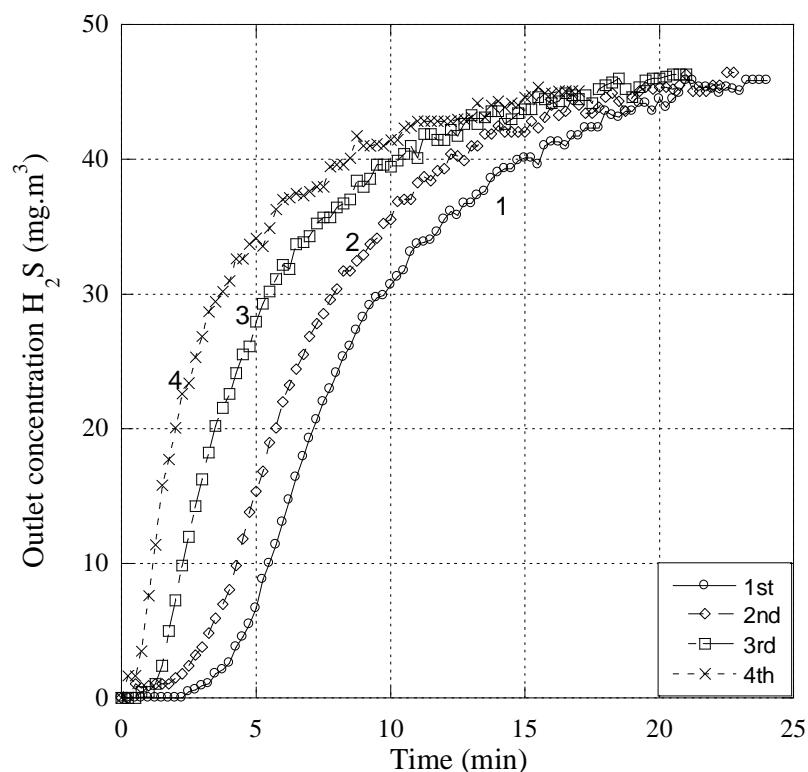


Figure 53. Adsorption of  $H_2S$  into activated carbon ACF6 (FM30 K). Sustainability of the process: adsorption–desorption cycles carried out in sequence. Regeneration conditions: temperature:  $110^\circ C$  and pressure: 700 mbar.

### 2.3.5 General conclusion regarding the regeneration system at dry conditions

The results presented in this study show that using low temperature  $110^\circ C$  and vacuum allow a good regeneration of exhausted activated carbon cloth. Indeed, the use of low temperature prevents the development of other reactions and further material degradation. These results open the possibility of regeneration of unmodified activated carbons by an efficient and economic way, increasing the life cycle of materials. However, adsorption–desorption cycles have shown that the adsorption capacity decreases after subsequently regenerations, showing that even in the first cycles regeneration is achieved, the process is not sustainable. This can be explained given that during the regeneration the formation of sulfur compounds is developed and in consequence the material is exhausted. To improve the regeneration process we have considered the film protection of the surface by the humidification system, where the adsorption of  $H_2S$  is going to be developed in the film, and

after that the increase in temperature desorb the compounds avoiding the reactions in the surface.

### 2.3.6 Humidity effect into adsorption- regeneration

The adsorption mechanisms in the dry and wet atmosphere have shown a different pathway. Thus we are focused on this part in the study of the influence of the humidity in the adsorption but especially in the regeneration process. The role of the humidity in the gas and the quantity adsorbed by the activated carbon is essential (Bagreev, Bandosz 2001, Huang, Chen & Chu 2006). They have shown the enhancement of the adsorption capacity by water presence.

In consequence 0%, 20% and 44% of water is adsorbed in the material. Pre-humidification process are thus carried out before the adsorption in the following way: an air flow rate saturated with water at 20°C is passed through the filter to create a wet atmosphere. The generator of wet air is shown in Figure 54. It is equipped of a column of water provided of a heating system. The airflow pass through the water column. A coupling of flowmeters allows to control the relative humidity in the flow.



Figure 54. Equipment for the generation of Air humidify.

Two methods were used to establish the water content in the filter. After the humidification process, a sample is analyzed by a thermal analyzer ATG SETSYS Evolution as shown in Figure 55. In parallel, a pre-humidified sample was weighted and dried in an

oven for 48h. Then, the quantity of water adsorbed was obtained by the mass difference. The two methods showed the same values.

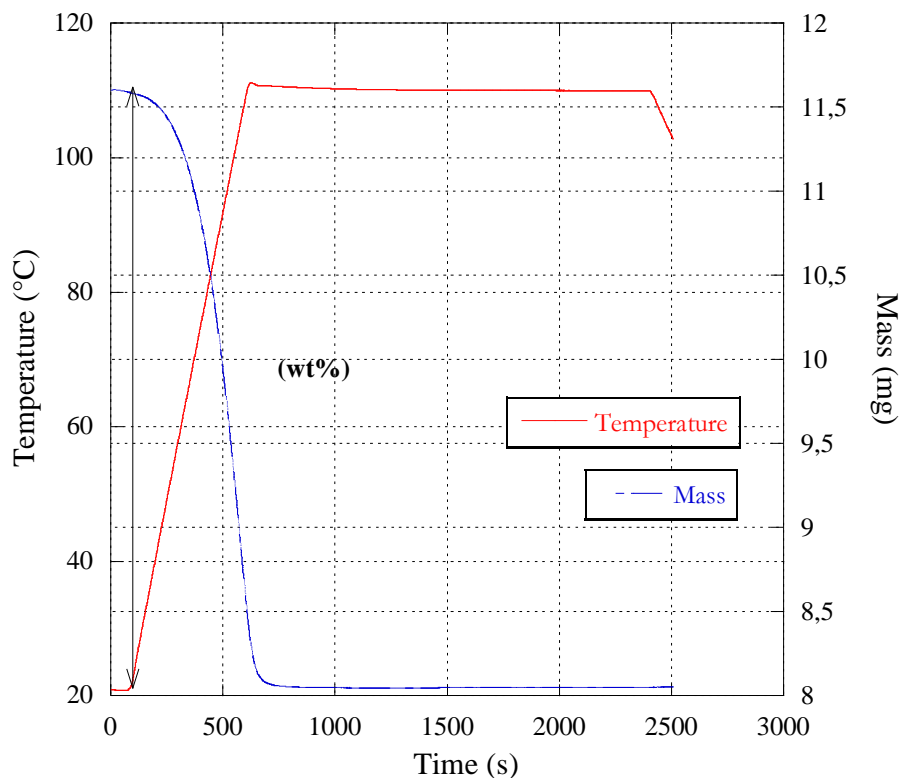


Figure 55. TG Pre-humidified activated carbon cloth ACF6

As discussed previously, under wet conditions  $H_2S$  adsorption mechanisms differ strongly from dried mechanisms. Thus the adsorption in dynamic conditions was carried out. An enhancing of 30% of the adsorption capacity is obtained. The same behavior was observed in the previous isotherms. Pore structure and surface chemistry of the material play a first role (Adib, Bagreev & Bandosz 1999). The presence of oxygenated functions in the surface favors the  $H_2S$  oxidation (Furimsky 1997). After water adsorption, thus the wet mechanism is developed. Water is a large molecule thus the importance of the macropore material to allow it adsorption. Consequently, the adsorption capacity is largely enhanced as shown in Figure 56. The first curve corresponds to dynamic adsorption without the pre-humidification step and the second with 30 min of pre-humidification at 80% RH.

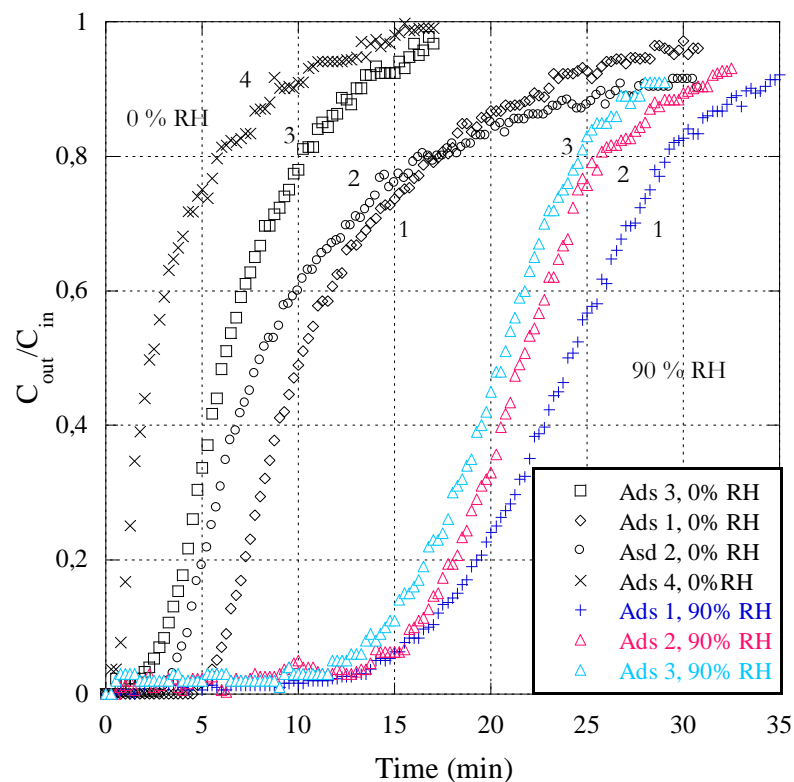


Figure 56. Adsorption of  $H_2S$  into activated carbon cloth ACF6 (FM30 K). Breakthrough curves in function of time. Comparison of dry and a pre-humidified adsorbent. Summary of the cycles adsorption-regeneration. Regeneration conditions  $T:110^{\circ}C$  ;  $P:0.7$  bar.

In Figure 57, the comparison in adsorption rate capacity at three conditions is presented. The correspondent concentration profile is shown in Figure 56. The rate was calculated at the saturation point. In dry conditions, the adsorption capacity decreases rapidly and attains 60% of the first adsorption capacity. At 20% wt of water adsorbed, the rate adsorption capacity decreases also, but this value is around 80% of the initial adsorption rate. Finally, for a condition at 44%wt of water adsorbed, the adsorption capacity is maintained at the same adsorption capacity after the regeneration. In wet conditions, the coupling of temperature and vacuum pressure allows to desorb the compounds where the  $H_2S$  has been previously dissolved. In that case, the quantity of sulfur elemental is lower than in dry conditions.

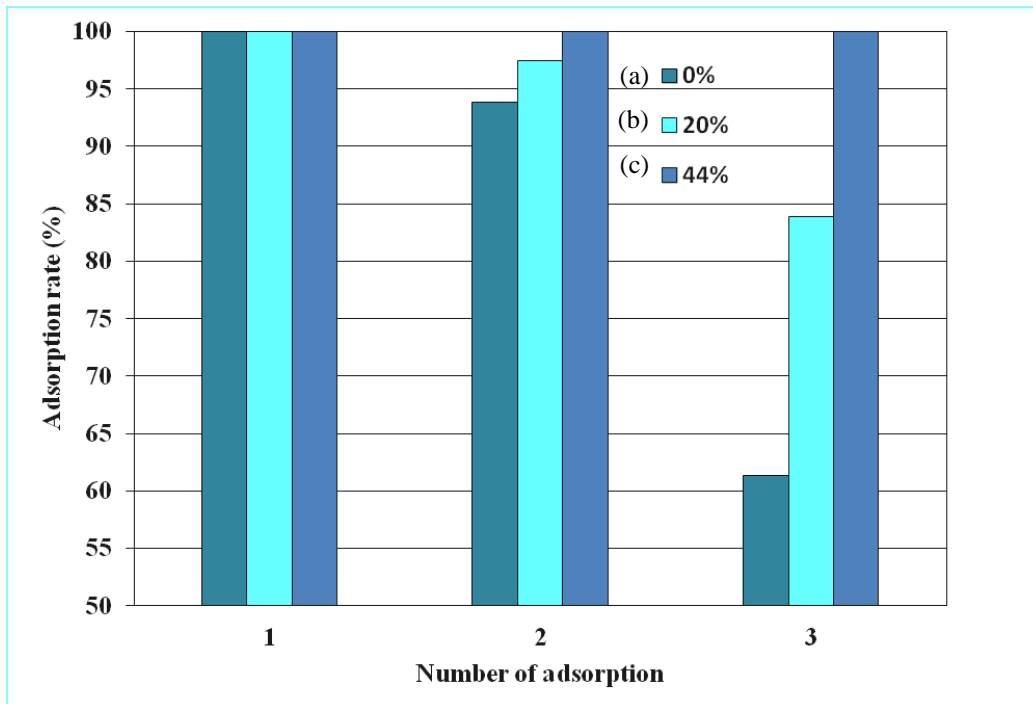


Figure 57. Histogram of the adsorption rate capacity at the saturation point. Relative humidity (a) 0 % wt (b) 20 % wt (c) 44 % wt. Regeneration conditions: 110°C and 700 mbar. Heating by Joule effect.

### 2.3.7 Sustainability of regeneration under wet conditions

The regeneration condition was fixed following the best results obtained. Pressure: 700mbar, temperature 110°C and pre-humidification with 40%wt of water. The adsorption was stopped at 15 ppmv. Ten cycles of regeneration adsorption were carried out. In Figure 58 are presented some of the curves.

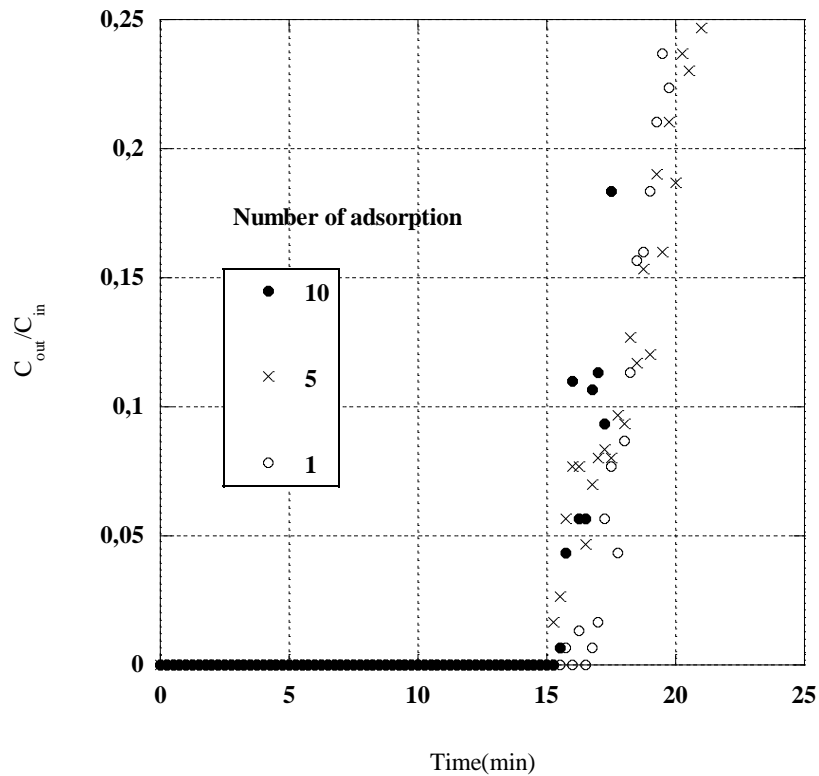


Figure 58. Adsorption/Regeneration cycles of ACF6 Breakthrough curves for different number of cycles. Regeneration conditions: 110°C; 700 mbar; RH 44% wt. Heating by Joule effect.

The adsorption capacity obtained from the previous curves is presented in Figure 59. We observe that the adsorption capacity maintains a value between 3.0 and 3.2 mg.g<sup>-1</sup>, cycle after cycle. As a result, the operating conditions as well as the pre-humidification of the material used, allow us to regenerate the activated carbon enhancing it's life cycle.



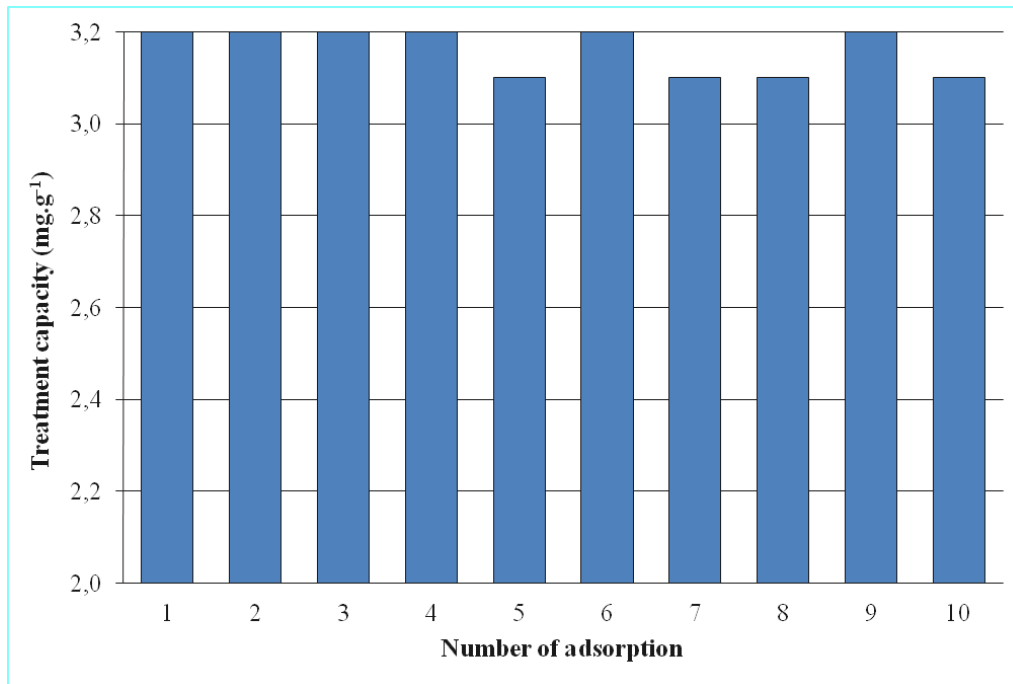


Figure 59. Adsorption/Regeneration cycles of ACF6. H<sub>2</sub>S treatment capacity for the ten first cycles. Regeneration conditions: 110°C; 700 mbar; RH 44% wt. Heating by Joule effect.

### 3 Conclusions

The regeneration method proposed is based on the theory that adsorption at low concentration is governed by the physisorption phenomena rather than chemisorption/oxidation, confirmed by the good performance after regeneration at low temperature. The regeneration proposed is based on two principles, thermal and vacuum regeneration. The desorbed compounds by thermal effect are removed from the activated carbon simultaneously by the vacuum force applied in the filter. Thus material desorption is accomplished reducing the development of the products of reaction, and therefore their fixation in the surface of the material. The use of low temperatures prevents the development of other reactions and the material degradation. These results suggest the possibility of regeneration of unmodified activated carbons. However, after the sustainability study under non pre-humidified conditions, it was observed that the performance decreases cycle after cycle. In response, it was considered the hypothesis of a water film to protect the material avoiding the fixation of strong bonds in the activated carbon. As a result, we observe a regeneration system of higher adsorption rate compared with non pre-humidified material.

Moreover, during the sustainability experiments, this adsorption rate is maintained after 10 cycles. In consequence, the regeneration material is achieved at a soft temperature (110°C), under vacuum and by an in-situ system. Additionally, it was observed that the adsorption capacity is enhanced in 30% compared with the material without pre-humidification phase. These results confirm the important role of water during the H<sub>2</sub>S treatment, allowing the enhancement of the life cycle of the material in at least 10 times.

# CONCLUSIONS AND PERSPECTIVES

---

## 1 Conclusions

Biogas is an important alternative source of energy. However, the presence of several components decreases its potential and limits its further applications. Among them, this thesis has been focused on two compounds of different nature, the siloxanes and the hydrogen sulfide. In the first case, the siloxanes studied are characterized by their low solubility in water, and high vapor pressure. Also, the content in biogas is low about  $400 \text{ mg.m}^{-3}$ . In contrast, the hydrogen sulfide is highly soluble in water and is found in higher concentrations in biogas. This state from the point of view of the design process a complexity in the process and the necessity treatment by a different separation process, beginning from the understanding of the physical-chemical behavior with the focus of reducing the content according with the requirements.

In the first chapter, the biogas sources and composition were reviewed with a focus on the separation process for siloxanes and hydrogen sulfide. In consequence, the selection of one main process for each of them was selected. Absorption in the case of siloxanes, studied in the second chapter and adsorption for hydrogen sulfide. The experimental results, as well as the scale lab reactors were designed with the purpose of carried out the processes under dynamic conditions.

Regarding a global treatment of biogas, the hydrogen sulfide is removed before the siloxanes as shown in Figure 60. According the flow diagram of the biogas treatment the conclusions about the experimental study are presented:

Once the abatement of  $\text{H}_2\text{S}$  is carried out by a separation process such as absorption, the remaining percentage was treated by adsorption onto activated carbon. This part of the process was the focus of the the third chapter. The methodology was divided into different aspects, in the first part the evaluation of different activated carbons was done obtaining the next results:

Concerning  $\text{H}_2\text{S}$  treatment, the use of adsorption by activated carbon was studied as a finishing process to remove  $\text{H}_2\text{S}$ .

- Activated carbon cloth ACF6 which corresponds to FM 30K was selected according to the criteria established to favor the mechanisms in wet atmosphere as well as the physisorption.
- It was confirmed that during the adsorption phase the wet atmosphere favored the H<sub>2</sub>S removal

Once the material was selected, the design of a dynamic process was done to study the experimental conditions in situ. Different conditions were tested during the adsorption-regeneration process with the next conclusions:

Dry atmosphere: The results presented in this study show that using a temperature about 110°C and vacuum pressure a good regeneration of exhausted activated carbon cloth was achieved. This temperature is much lower than the temperature reported in previous studies.

Indeed, the use of low temperature prevents the development of other reactions and further material degradation. These results open the possibility of regeneration of unmodified activated carbons by an efficient and economic way, increasing the life cycle of materials. However, adsorption–desorption cycles have shown that the adsorption capacity decreases after subsequently regenerations, showing that even in the first cycles regeneration is achieved the process is not sustainable. This can be explained given that during the regeneration the formation of sulfur compounds is developed and in consequence the material is exhausted.

- Wet atmosphere: To improve the regeneration process it has been considered a film protection of the surface by a pre-humidification system, where the adsorption of H<sub>2</sub>S is going to be developed in the film, and after that the increase in temperature desorb the compounds avoiding the reactions on the surface. As a result, it was observed a regeneration system of higher adsorption rate compared with non pre-humidified material. In consequence, the regeneration material is achieved at a temperature about 110°C, under vacuum pressure and with a pre-humidification of the filter. Also, the adsorption capacity is enhanced in 30% compared with the material without pre-humidification phase. These results show the important role of water during the H<sub>2</sub>S treatment, not only in the enhancement of the adsorption capacity but the role during the desorption phase. This process has shown an enhancement of the life cycle of the material in at least 10 times.

Considering a raw biogas with the following properties:

- Raw biogas
- Flow rate:  $100 \text{ m}^3 \cdot \text{h}^{-1}$
- $\text{H}_2\text{S}$ : 1000 ppm

The up-grading process can be considered in the next flow diagram:

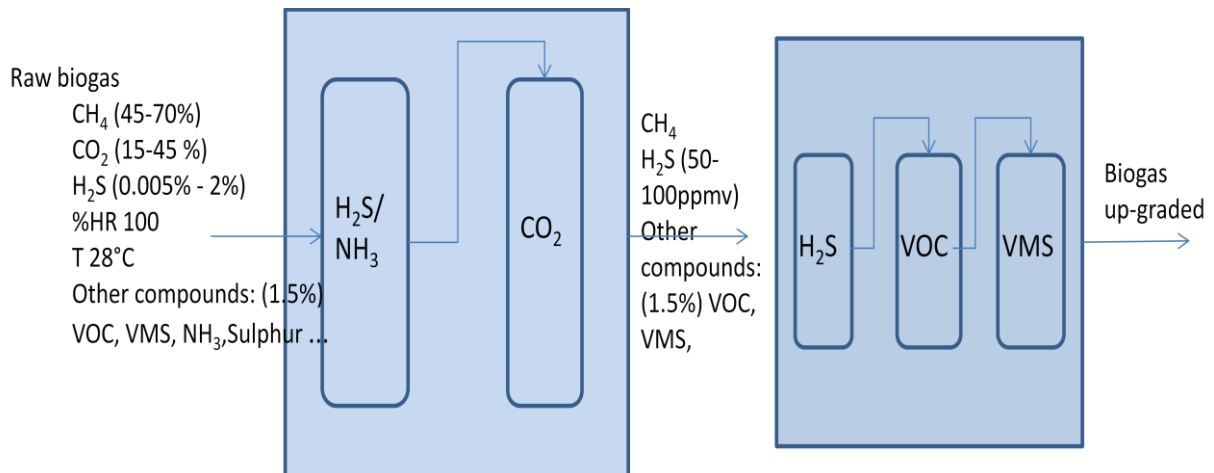


Figure 60. Diagram of biogas up-grading process.  $\text{H}_2\text{S}$  and siloxanes treatment by adsorption and absorption as a finishing process

Then, after the primary abatement of the  $\text{H}_2\text{S}$  concentration, the remaining concentration is about 50 ppm. According to results obtained from the experimental adsorption carried out, if we consider a flowrate of  $100 \text{ m}^3 \cdot \text{h}^{-1}$ , and  $C_{in} : 50 \text{ ppmv}$ ;  $C_{out} : 5 \text{ mg} \cdot \text{m}^{-3}$  with an adsorption capacity (q) of:  $4 \text{ mg} \cdot \text{g}^{-1}$ , the quantity of activated carbon filter required for a daily operation of 8h is of 16 kg of ACF 6.

The finishing process is proposed in a parallel configuration where the regeneration of the material is carried out in a filter while the adsorption is carried out in the second one. With a regeneration of the filter according to the results obtained in the laboratory (10 cycles of regeneration) the diminish in activated carbon consumption is about 90% of the material required in a month (20 days of operation). The decrease in the quantity of material is not only economically significant, moreover the decrease in the environmental impact is very important. Disposal of activated carbon is one of the major negative impact of this technology. The regeneration under soft conditions is thus an interesting solution to the process.

Once the separation of the hydrogen sulfide has been done, the treatment of siloxanes is the next operation in the finishing process as shown in Figure. In the second chapter, the next conclusions were obtained:

- Among the absorbents studied: motor oil, cutting oil and water-cutting oil mixture the best performance was obtained for motor oil.
- The parameters such as absorbent material, residence time, temperature, and siloxane concentration has shown that the absorption process depends strongly on the nature of the absorbent and the operating conditions.
- Motor oil removal efficiency for D4 was of 80% whereas for L2 was of 60%, indicating that D4 is easier absorbed than L2. In the case of water-cutting oil, it showed a mass transfer enhancement from the gas phase to the liquid phase compared with water alone. Furthermore, a removal efficiency of 70% for D4 was observed, showing that the addition of oil fraction in a water system improves the absorption of VMS.
- An increase in the oil temperature results in a decrease in the treatment capacity, thus high temperature is therefore not recommended for VMS absorption. Also, absorption capacity increases as a function of residence time.
- The importance of a good combination of parameters as flow rate and mass of absorbent in order to enhance the interfacial area, and therefore the mass transfer between the phases. Finally, the results using cutting oil in a diluted solution open the possibility of treat siloxanes by an economical and environmental solution.

During the siloxanes abatement motor oil has shown a better removal efficiency and the absorption capacity among the absorbents studied. Thus it is selected in order to calculate the required material in a finishing process. This is followed by an adsorption process that allows the decrease of the concentration to a low level according to the actual requirements.

In the same way, it was considered a raw biogas production of the next properties, a flow rate of  $100 \text{ m}^3 \cdot \text{h}^{-1}$ , an inlet concentration of siloxanes of  $C_{\text{in}} : 500 \text{ mg} \cdot \text{m}^{-3}$ , and a maximal concentration in the outlet of  $C_{\text{out}} : 0.1 \text{ mg} \cdot \text{m}^{-3}$ . If we consider the results obtained in this thesis, we know that the motor oil has an absorption capacity about  $100 \text{ mg} \cdot \text{L}$ , with a removal efficiency of about 60 %. Regarding the adsorption results, we have an activated carbon like FM30K with an adsorption capacity ( $q$ ) about  $40 \text{ mg} \cdot \text{g}^{-1}$ .

According with these characteristics, we have calculated the quantity required to treat the siloxanes. If we consider the coupling technologies, beginning with the partial abatement by the absorption, the estimated quantity of motor oil is of 500 L. After this step, the adsorption onto activated carbon is followed. The estimated quantity is of 4 kg. This study case, allow us to see in a more concret way, that, for example, the filter necessary for the treatment can be reduced at the half, comparing with a unique operation unit by adsorption. Thus following these principles, a diagram of a biogas up-grading process is described in Figure 61.

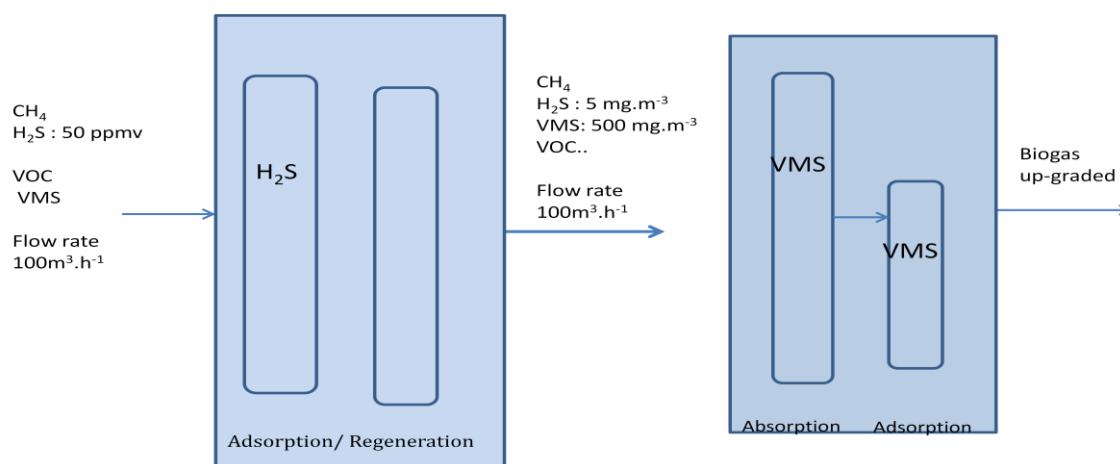


Figure 61. Diagram of biogas up-grading process. H<sub>2</sub>S and siloxanes treatment by adsorption and absorption as a finishing process.

## 2 Perspectives

Different aspects have been studied in this thesis. After that, the use of the adsorption as a finishing process were identified as a solution. Following this drive, two siloxanes a linear (L2) and a cyclic (D4) were studied. However, in the biogas there are many other siloxanes which might be taken in consideration in further studies. These compounds differ in their characteristics physic-chemical thus the importance of the consideration in future studies.

On the other way, since the point of view of the absorption, the possibility of decrease the concentration in the gas phase was observed. Results considering different absorbents such as cutting oil and the mixture of water cutting oil open the possibility of treating these compounds under different solutions. However, in order to increase the mass transfer rate, further studies are required. Some future studies considering the effects of other parameters such as agitation, pressure and the turbulent flow regime could be interesting to enhance the

absorption rates. Also, the study of an absorption process into packing columns might be appropriated. Moreover, the study of other kind of solvents, as well as the desorption process are subjects to continuing the research.

Concerning the treatment of siloxanes by adsorption, it was observed that it is highly efficient, specially using activated carbons. The opportunity to optimize the life of the materials was open, however, additional experiments are required to test the coupling of technologies analyzing, for example, the impact into the overall process.

Finally, considering the adsorption/regeneration of hydrogen sulfide, further studies are required. The perspective of increase the inlet concentration of hydrogen sulfide, could open the possibility of consider the adsorption/regeneration process as a major operation unit in the upgrading of biogas. In the same way, a parametric study of the operating conditions is necessary for the optimization of the process. Parameters such as, the regeneration time, the temperature, the vacuum pressure, between others might be taken into account. The examination of the interaction of other components presents in the biogas is an essential aspect. In consequence, the adsorption/regeneration experiments under real conditions, using a biogas, coming for example from the farm, is a point to study closer.



# APPENDIX A. RESUME DE LA THESE

## Introduction

Dans les dernières années, la consommation énergétique mondiale est devenue une thématique de recherche importante. D'une part, les réserves de combustibles fossiles diminuent et l'incertitude quant à ces ressources est évidente. D'autre part, l'utilisation de combustibles a des repercussions ces que le réchauffement climatique. Aujourd'hui, les conséquences de ces activités soulèvent d'immenses questions comme: Combien de temps ces ressources seront-elles disponibles? Quelles stratégies développer pour faire face à cette situation? Comment pouvons-nous résoudre le problème du réchauffement climatique? En réponse à celles-ci, des politiques environnementales en quête de solutions ont été établies. Avec cette nouvelle prise de conscience, une ligne de recherche a été axée vers le développement de nouvelles sources d'énergie. L'éolien, le rayonnement solaire, l'hydroélectricité et le biogaz sont quelques-unes des solutions émergentes.

Parmi celles-ci, le biogaz peut être facilement appliqué. Il permet le recyclage des déchets, il est simple et présente desavantages économiques par rapport à d'autres technologies. Il peut donc contribuer à résoudre la problématique énergétique. Cette thèse est en conséquence consacrée à l'étude du biogaz comme source d'énergie nouvelle. Une de ces caractéristiques les plus importantes est qu'il est composé d'une forte proportion de méthane. Toutefois, en raison de processus biologiques, sa composition dépend de la matière organique et des conditions de fonctionnement et d'environnement. Lors de la biodégradation, divers composés sont produits, parmi ceux-ci, on peut trouver: le dioxyde de carbone, le sulfure d'hydrogène, les composés soufrés, les composés organiques volatils, les siloxanes, de l'ammoniac et la vapeur d'eau. Ces composés diminuent le potentiel du biogaz et à certains égards empêchent son utilisation comme source d'énergie renouvelable.

Le premier chapitre de cette thèse est donc axé sur les différents aspects de la production de biogaz. Il débute avec le potentiel Européen et les politiques établies par les gouvernements. En conséquence de la variabilité de sa composition finale, le biogaz doit être traité avant son utilisation, pour cela la séparation des composants autres que le méthane est nécessaire. Les siloxanes et l'hydrogène sulfuré sont parmi les composantes les plus nuisibles, par conséquent, ils seront l'objectif de cette thèse. Pour réaliser cette étude une révision de technologies existantes est effectuée pour montrer les principales contraintes et opportunités

en termes de procédé de séparation. Une proposition d'un processus de finition pour atteindre les valeurs requises pour le biogaz est présentée.

Le deuxième chapitre est consacré à l'élimination des siloxanes. Ces composants ont été identifiés comme critiques pour l'utilisation du biogaz. En fait, ils sont responsables de la formation de dioxyde de silicium dans les moteurs et sont aussi préjudiciables à d'autres applications du biogaz. Cette étude se concentre sur la conception expérimentale et l'évaluation des procédés de séparation. Tout d'abord, les siloxanes sont traités par un procédé d'absorption et d'autre part une approche d'élimination par adsorption est mise en œuvre. Pour cela, deux siloxanes représentatifs présents dans le biogaz ont été sélectionnés: le hexaméthylsiloxane (L2) et l'octaméthylcyclotétrasiloxane (D4). Dans le processus d'absorption trois solvants différents ont été étudiés: l'huile de moteur, l'huile de coupe et un mélange eau-huile de coupe. Une colonne à bulles a été conçue pour évaluer les interactions entre le polluant et l'absorbant. Les expériences ont été réalisées en dynamique dans un réacteur semi-continu en faisant varier certains paramètres comme la concentration d'entrée, le temps de séjour et la température. Un deuxième point important dans le processus d'élimination des VMS a également été étudiés afin de pouvoir le comparer avec le résultats précédents. Ainsi l'adsorption a été réalisée avec trois charbons actifs différents dans un réacteur semi-continu. Enfin, les résultats présentés permettent de comparer les deux procédés et de mettre en évidence leurs avantages respectifs.

Dans le chapitre 3, le processus d'élimination du sulfure d'hydrogène est abordé. Le sulfure d'hydrogène est présent dans presque tous les types des biogaz, comme résultat de la biodégradation de la matière organique. Il est un composé nocif pour l'être humain, les animaux et la nature. Il contribue également à la formation des pluies acides et à la corrosion dans les moteurs et équipements. D'où, l'importance d'être retiré du biogaz. Pour cela, différentes technologies ont été développées. Parmi celles-ci, le traitement sur charbon actif est une des solutions efficace. Cependant, la régénération du charbon actif présente un grand défi. Ce chapitre a pour but de traiter le sulfure d'hydrogène par un procédé d'adsorption régénérative. Différents charbons actifs ont été étudiés. En conséquence, des tissus de charbon actif ont été choisis. Le système de régénération est ensuite analysé et différents paramètres de fonctionnement ont été étudiés tels que la température, le temps de régénération, la pression et l'humidité relative. Les expériences ont été effectuées dans un système dynamique in-situ. En conséquence, une nouvelle méthode pour régénérer le matériau est proposée.

# 1 Le contexte du biogaz

## 1.1 Le biogaz en Europe

La commission européenne de l'énergie a établi qu'en 2020, 20% de l'énergie européenne devra provenir de sources renouvelables. Les énergies telles que l'éolien, le rayonnement solaire, l'hydroélectricité et le biogaz sont quelques-unes des solutions émergentes. Parmi elles, le biogaz, en plus d'être une source d'énergie alternative, offre également la possibilité de transformer les déchets organiques en énergie. De plus, sa valorisation est un moyen efficace de réduire les émissions à effet de serre dans l'atmosphère. Le potentiel de réchauffement global du méthane est en effet 23 fois plus puissant que le dioxyde de carbone, le biogaz apparaît donc une solution prometteuse pour le développement durable. Toutefois, les applications finales telles que la cogénération ou l'injection dans le réseau du gaz imposent le développement de technologies efficaces pour apporter une solution durable. Le biogaz issu des centre d'enfouissement technique et des eaux usées représente notamment un grand défi et une opportunité pour créer de l'énergie. D'un côté, cela réduirait les émissions de méthane réels et de l'autre côté, il contribuerait à la demande énergétique de manière durable.

## 1.2 L'origine du biogaz

Il est produit par la digestion anaérobie et est principalement composé de méthane  $\text{CH}_4$  (45-70%), de dioxyde de carbone  $\text{CO}_2$  (15-45%), de sulfure d'hydrogène  $\text{H}_2\text{S}$  (0,005% - 2%) et d'autres contaminants tels que les composés halogénés et siloxanes (Ryckebosch et al. 2011). Les bactéries responsables de la formation de biogaz sont naturellement présentes dans l'environnement. La formation est composée de quatre grandes phases dont l'hydrolyse, l'acidogénèse, l'acétogénèse et la méthanogénèse (Deublein, Steinhauser 2008):

La production de biogaz peut se faire de l'échelle locale (petit digesteur) à la grande échelle: stations d'épuration ou centre d'enfouissement technique où les matières organiques sont rassemblées et transformées en biogaz. La technologie utilisée est liée aux conditions environnementales. Par exemple, en Inde, la technologie est très simple résultant en un grand développement de digesteurs domestiques. Les conditions environnementales telles que la

température et l'humidité favorisent la formation de biogaz. Les résidus provenant des ménages et les activités agricoles sont transformés en biogaz et finalement utilisés pour la cuisson et l'énergie électrique.

Le centre d'enfouissement technique est un des moyens les plus singuliers de la production. La dégradation de la matière organique est mise en oeuvre selon un processus discontinu. Des paramètres tels que l'âge et le genre de résidus éliminés diffèrent sensiblement des autres types de productions. Il représente en général un risque pour l'environnement en raison des émissions de gaz qui peuvent inclure des gaz toxiques, d'où l'importance du traitement du biogaz et sa valorisation.

## 1.3 Les applications du biogaz

Le biogaz a de nombreuses applications. En fonction de la production de biogaz il peut être directement transformé en chaleur par combustion. Cela est généralement utilisé pour les productions de biogaz domestique. Parmi les applications potentielles du biogaz on trouve: la production combinée de chaleur et d'électricité (CHP), les microturbines à gaz, les piles à combustible, le carburant des véhicules et l'injection dans le réseau de gaz.

## 1.4 La composition du biogaz

Selon les sources, la technologie et les conditions de fonctionnement, la composition du biogaz diffère. En outre, le contenu du biogaz varie au cours de la production quotidienne. Ainsi, des mesures sont prises régulièrement pour indiquer le processus de fermentation et donc la qualité des biogaz. Il est très important de connaître ses caractéristiques afin de concevoir le processus de séparation. Parmi les différents types de production, les plus importants sont : les centres d'enfouissement technique, la digestion des eaux usées et de la ferme. (Deublein et Steinhäuser 2008; Rasi et al 2007; Ryckebosch et al 2011). Parmi les composés qui se trouvent dans le biogaz, les plus dangereux pour les utilisations finales sont le H<sub>2</sub>S, et les siloxanes. Ils peuvent conduire à de grands dégâts dans les lignes de production ainsi que dans les pièces de moteur du processus de conversion d'énergie. Ainsi, pour obtenir une qualité élevée de biogaz la plupart d'entre eux doivent être traités. Dans cette étude, nous nous intéressons principalement aux siloxanes et au sulfure d'hydrogène.

## 1.5 Les siloxanes

Les siloxanes sont des composés qui ont une solubilité très faible dans l'eau et sont très volatils. Leurs unités structurales est constituée par  $-(\text{CH}_3)_2\text{SiO}-$  et ils peuvent être cyclique ou linéaire (Dewil et al, 2006; Allen et al 1997). Les Volatyl methyl siloxanes (VMS) ont une faible masse molaire et une haute pression de vapeur. Cependant, un autre type de siloxanes comme le triméthylsilanol présente une pression de vapeur et une solubilité dans l'eau beaucoup plus élevées. Cette composante se retrouve donc principalement dans les déchets liquides. Néanmoins, ils se retrouvent également dans le biogaz. Dans cette étude on s'intéresse principalement aux siloxanes avec une faible solubilité dans l'eau. Cette condition physico-chimique met en place une limitation dans le traitement des VMS en présence d'eau. En outre, le biogaz brut est saturé en eau, donc le non solubilité dans l'eau est un facteur clé pour la conception des procédés des séparations.

Il existe plusieurs applications industrielles des siloxanes. Ils sont ajoutés aux produits de consommation comme les cosmétiques, les shampooings, les détergents, les revêtements de papier et les textiles. Ce qui explique leur présence dans l'environnement (Dewil, Appels & Baeyens 2006). Lors de la digestion anaérobie, les siloxanes se volatilisent et atteignent le biogaz. En outre, l'hydrolyse de polydiméthylsiloxanes (PDMS) a été identifiée comme une autre source de siloxanes dans le biogaz (Soreanu et al. 2011, Piechota, Haggmann & Buczkowski 2012). Parmi les différents types de siloxanes le D4 est le principal, suivi de L2, L3 et D5 (Wheless, Pierce 2004). Pour ceux issues du traitement des eaux usées et des décharges (avec des résidus industriels) le contenu de siloxanes est plus élevé que ceux provenant d'autres sources (Dewil, Appels & Baeyens 2006, Accettola, Guebitz & Schoeftner 2008). Les siloxanes contenus dans le biogaz peuvent être trouvés entre 0 et  $140 \text{ mg.m}^{-3}$  (Wheless, Pierce 2004) tandis que des valeurs récentes comprise entre 1 et  $400 \text{ mg.m}^{-3}$  ont été rapportées (Ryckebosch, Drouillon & Vervaeren 2011).

### 1.5.1 Les siloxanes dans le biogaz

L'utilisation du biogaz comme une source alternative d'énergie est limité par la présence des siloxanes. En fait, ils réagissent pendant la combustion et se transforment en dioxyde de silicium. Ces particules contribuent à l'abrasion de la surface intérieure des moteurs (Schweigkofler et Niessner 2001) provoquant d'un côté une perte en puissance, et une augmentation de la maintenance des équipements (Tour 2004). Egalement, les piles à combustibles (SOFC) sont empoisonnées par les siloxanes (Haga et al 2008; Sasaki et al

2011). La dégradation d'une SOFC a été observée avec un biogaz contenant 10 ppm de siloxane D5 (Haga et al. 2008).

Par conséquent, le traitement des siloxanes est devenu très important pour l'utilisation du biogaz comme énergie renouvelable. Selon l'usage ultérieur, plusieurs seuils de siloxanes dans le biogaz ont déjà été mis en place par les fabricants des moteurs. Pour l'injection dans le réseau de gaz naturel en France, la spécification ne considère pas le niveau siloxanes comme détaillé dans le SPEC de GrDF.

## 1.5.2 Les technologies pour éliminer les siloxanes

Différentes technologies sont utilisées pour éliminer les siloxanes par exemple l'adsorption sur les matériaux poreux, l'absorption physique et chimique, le refroidissement, le traitement par membranes, les procédés catalytiques et la biodégradation (Ajhar et al. 2010). Parmi ces techniques, l'utilisation de charbon actif pour la réduction des siloxanes a été appliquée (Ryckebosch et al. 2011). Des matériaux tels que le charbon actif en grains (CAG), le charbon actif en tissu (ACC), le gel de silice, et le tamis moléculaire ont été utilisés montrant que le charbon actif est une bonne alternative pour le traitement des siloxanes.

Parmi les autres techniques qui présentent une grande efficacité pour éliminer les siloxanes se trouve l'absorption chimique par des solutions acides (Schweigkofler et Niessner 2001; Wheless et Pierce, 2004). Cependant, l'utilisation d'acides forts tels que l'acide sulfurique ou l'acide nitrique présente de nombreux inconvénients comme la corrosion dans les équipements, et un impact négatif sur la santé et sur l'environnement.

L'absorption par les solvants organiques a aussi montré de bons rendements. Cependant, en général, le coût associé est relativement élevé pour la production de biogaz, d'autre part l'information est limitée. Dans le cas de l'absorption par des huiles minérales (Stoddart et al. 1999) ont étudié l'élimination de l'huile d'hydrocarbures à l'aide d'un système d'épuration. Les résultats montrent la possibilité d'éliminer les composés chlorés et les siloxanes.

Concernant, la biodégradation, des études préliminaires suggèrent la possibilité d'éliminer les siloxanes, toutefois l'efficacité d'élimination est faible (20-43%) (Accettola et al 2008; Grumping et al, 1999; Popat et Deshusses 2008) et de long temps de processus sont nécessaires. Un résumé des technologies pour l'élimination des siloxanes est présenté dans le Tableau 13.

Tableau 13. Technologies pour l'élimination des siloxanes

<b>Processus</b>	<b>Description</b>	<b>Avantages</b>	<b>Inconvénients</b>
<b>Absorption chimique</b>	L'acide sulfurique et l'acide nitrique	Efficacité de 95%	Sous-produits, les problèmes environnementaux et les risques
<b>Absorption Physique</b>	Selexol ® (diméthyléther de polyéthylèneglycol)	Efficacité de 99%	Le coût élevé de solvant
	Huile moteur	Rendement de 60%	Sous-produits
<b>Condensation</b>	-5° C	Efficacité de 88%	Le coût élevé
<b>Biodégradation</b>	D4	Faible coût, l'environnement	Le manque d'efficacité (20-43%)
<b>Adsorption</b>	Charbon actif	À haut rendement	L'élimination finale
	Gel de silice	À haut rendement	L'élimination finale
	Tamis moléculaire	À haut rendement	L'élimination finale

## 1.6 H<sub>2</sub>S

H<sub>2</sub>S est en général présents dans tous les types de biogaz à la suite de la dégradation naturelle des matières organiques. Dans les biogaz provenant des résidus agricoles (avec des résidus d'origine animale) le teneur en H<sub>2</sub>S est plus élevée.

Le sulfure d'hydrogène, est un gaz toxique spécialement connu pour son odeur d'œuf pourri. Il est incolore et plus lourd que l'air. Il est relativement facilement oxydé en présence de radicaux lorsqu'il est dissous dans l'eau. En présence d'air, l'oxydation de H<sub>2</sub>S peut être réalisée.

### 1.6.1 Le sulfure d'hydrogène dans le biogaz

Le H<sub>2</sub>S est l'un des éléments les plus polluants du biogaz. Le teneur en H<sub>2</sub>S fluctue fortement. En général, il est présent entre 0,005% et 2% (Ryckebosch, Drouillon & Vervaeren 2011). Le sulfure d'hydrogène est un gaz toxique pour la nature. En présence d'eau il forme de l'acide sulfurique qui est très corrosif causant des dommages aux réservoirs, pipelines et installations de traitement. Le SO<sub>2</sub> et SO<sub>3</sub> formés lors de la combustion sont plus toxiques que H<sub>2</sub>S et contribuent à la formation de pluies acides. Par conséquent, l'élimination de l'H<sub>2</sub>S est nécessaire avant de l'utiliser. La teneur finale du biogaz dépend de l'utilisation ultérieure.

### 1.6.2 Les technologies pour le traitement du H<sub>2</sub>S

De nombreux procédés ont été développés pour l'élimination du H<sub>2</sub>S dans le biogaz. Le choix du procédé est lié à plusieurs conditions telles que l'efficacité, le débit, la concentration, l'utilisation finale, les contraintes économiques et l'impact environnemental. Le Tableau 15 récapitule les principaux points des différentes technologies. En général, lorsque le biogaz contient un niveau élevé de H<sub>2</sub>S et le débit est élevé, la solution optimale pour le traiter est le procédé d'absorption. Ce procédé peut être fait dans l'eau ou dans des solutions aqueuses pour diminuer le volume de l'eau et enfin être combinés avec d'autres technologies comment la biodégradation. Toutefois, la teneur en H<sub>2</sub>S peut être encore élevée pour les applications finales. L'utilisation d'adsorption sur des charbons actifs est l'un des procédés les plus efficaces pour éliminer H<sub>2</sub>S, il en résulte de faibles niveaux de concentration. Toutefois, l'un des principaux enjeux du processus d'adsorption est la faible capacité d'adsorption en volume.



Tableau 15. Technologies pour le traitement du H<sub>2</sub>S

Processus	Description	Avantages	Inconvénients
<b>Ajout d'air / oxygène dans le biogaz</b>	La quantité d'oxygène (2-6%) $2\text{H}_2\text{S} + \text{O}_2 \rightarrow 2\text{H}_2\text{O} + 2\text{S}$	Concentration sous 50ppm simple, à faible coût	Risque d'explosion
<b>L'absorption physique</b>		H <sub>2</sub> S dans la limite de détection	Grand volume d'eau
<b>Absorption chimique</b>	NaOH	Elimination de CO <sub>2</sub> Diminution du volume d'eau	Haute pression (10-30bar) Aucune régénération
	FeCl <sub>3</sub>		Régénération partielle
<b>Membranes</b>		98% d'efficacité 250 ppm	Coût élevé
		Réduction des émissions de CO <sub>2</sub>	
<b>Biodégradation</b>	Micro-organismes	Réduction > 98% Faible coût	
<b>Adsorption</b>	Éponge de fer	Capacité d'adsorption = gH <sub>2</sub> S/g de bois 0,2g /g	Risque d'incendie lors de la régénération
	Grains du bois imprégné à l'oxyde $\text{Fe}_2\text{O}_3 + \text{H}_2\text{S} \rightarrow \text{FeS}_3 + \text{H}_2\text{O}$		
	Sulfatreat 410 hPa ®		Coût élevé de régénération
	$\text{Fe}_3\text{O}_4 + \text{H}_2\text{S} \rightarrow \text{FeS} + \text{S} + 4\text{H}_2\text{O}$		
	Oxydes de fer	MgO, Al <sub>2</sub> O <sub>3</sub> , SiO <sub>2</sub> et ZrO <sub>2</sub>	Coût élevé de régénération
<b>Adsorption</b>	Charbon actif en grain/tissu	Rendement d'épuration élevé H <sub>2</sub> S à 100%	Le coût de la régénération élevé, régénération thermique à 450°C

## 1.7 Conclusion

Le travail présent est organisé comme suit: le traitement des siloxanes est étudié dans le deuxième chapitre. Les VMS (Volatile méthyl siloxanes) sont en général très volatils et hydrophobes. Ce fait implique une limitation de technologie pour les retirer de la phase gazeuse. Parmi les études récentes développées, l'adsorption dans les matériaux poreux a montré une efficacité élevée pour leur élimination. Des matériaux tels que le charbon actif, le gel de silice et des tamis moléculaires ont été utilisés. Ils ont montré que la polarité de la matière est une caractéristique clé pour obtenir une bonne capacité d'adsorption. Les charbons actifs non polaires ont montré une grande capacité d'élimination. Cependant, seul un faible pourcentage de l'adsorbant est utilisé (1-5% en masse) et après l'épuisement il est important de considérer son élimination et la gestion des déchets. En ce sens, la possibilité de les traiter par absorption dans des solvants hydrophobes, ce qui est l'objet de cette étude, indique un champ intéressant de la recherche. De la même manière, des études récentes sur les composés organiques volatils (COV) sont en cours mettant l'accent sur l'absorption dans l'huile. Ils ont montré une bonne capacité d'élimination (Lalanne et al. 2008, Ozturk, Yilmaz 2006, Heymes et al. 2006) ouvrant la possibilité de traiter des siloxanes de la même manière. Néanmoins, comme l'absorption est fortement contrôlée par les interactions physico-chimiques entre les composés dans les phases liquide et de gaz, il est impossible de comparer ces études antérieures avec le VMS.

En ce qui concerne l' $H_2S$ , de nombreuses technologies ont été développées pour l'élimination des biogaz. Parmi elles, le travail se concentre sur l'adsorption sur charbons actifs compte tenu de sa haute efficacité pour parvenir à une concentration faible. À propos de cette technologie, de nombreuses études ont montré l'influence de différents paramètres dans la phase d'adsorption. Cependant, le procédé de désorption reste à l'étude en laboratoire en raison essentiellement de la nécessité de température élevée. La non régénération du matériau implique une augmentation des coûts par: 1) le remplacement du charbon actif frais, 2) l'arrêt du procédé de traitement et 3) la gestion de déchets.

Donc, la recherche concernant l' $H_2S$  se concentre sur le développement d'un procédé durable de finition par adsorption sur charbon actif. Pour atteindre cet objectif un système de régénération dans des conditions douces a été étudié afin d'améliorer le cycle de vie du matériau ainsi que de réduire la fréquence de l'entretien de fonctionnement des filtres à adsorption.

## 2 Étude sur le traitement des siloxanes par absorption. Procédé en dynamique

Cette section est consacrée à l'étude de l'élimination des siloxanes par absorption. Un siloxane linéaire: L2 (hexaméthylsiloxane) et un siloxane cyclique: D4 (octaméthylcyclotétrasiloxane) ont été choisis parmi ceux que l'on rencontre dans le biogaz pour réaliser les expériences, (Wheless, Pierce 2004). Le choix de l'huile repose sur plusieurs caractéristiques et études antérieures. En premier instance, l'huile de moteur est étudiée comme matériau de référence, dans le but de valoriser les déchets provenant de l'industrie et des véhicules. L'huile de coupe a aussi été étudiée précédemment pour l'absorption des composés de type COV. D'où, l'intérêt d'analyser ces huiles pour trouver des nouvelles technologies pour l'élimination des siloxanes. Egalement, l'huile de coupe est utilisée dans l'industrie mélangée avec de l'eau. Jusqu'à présent, ce mélange n'a pas été évalué pour traiter les siloxanes. Par conséquent, trois solvants : l'huile de moteur, l'huile de coupe et le mélange eau-huile de coupe ont été étudiés.

Pour cet objectif une colonne d'absorption a été conçue. Différents paramètres d'opération ont été testés tels que la concentration, la masse d'absorbant et la température. La performance est mesurée principalement par la capacité d'absorption. Il est important de souligner que l'information concernant cette capacité, est insuffisante où ne figurent pas dans les études précédentes. Egalement, concernant l'absorption des VMS (Volatile Méthyle Siloxanes) dans l'huile de coupe ou dans le mélange eau-huile de coupe, aucune étude n'a été trouvée. En conséquence, cette recherche a pour objective fournir des informations sur l'absorption siloxane dans des huiles.

### 2.1 Matériels et méthodes

Le Hexaméthylsiloxane (L2) et le octaméthylcyclotétrasiloxane (D4) de Sigma Aldrich sont utilisés pour générer les différentes concentrations. Leur pureté est de 98%. Les siloxanes sont normalement présents sous une forme liquide dans l'industrie, où ils sont utilisés pour de nombreuses applications. Lors de la digestion anaérobie ils sont volatilisés

pour arriver dans la phase gaz. Ici, les siloxanes liquides sont volatilisés par un système de génération de gaz qui est décrit plus loin.

## 2.1.1 Les absorbants

Deux types d'huiles différentes sont étudiés pour l'absorption des siloxanes. Le premier est l'huile de moteur 5W40. C'est une huile moteur commerciale fréquemment utilisée dans les véhicules, elle est produite par différentes entreprises. Ici, nous avons utilisé l'huile moteur 5W40 de Elf. La deuxième est l'huile de coupe, qui est actuellement utilisée dans les industries pour la réfrigération des machines. Ici, nous avons utilisé une huile de coupe produite en Allemagne: Hochleistungs-Schneidl Alpha 93, Jokish® GmbH.

Egalement, un mélange eau-huile de coupe a été étudié. En effet, dans les industries l'huile de coupe est en générale utilisée diluée selon la proportion 95% en masse d'eau et 5% en masse d'huile de coupe.

### 2.1.1.1 *Caractérisation des huiles: Viscosité*

La viscosité a été mesurée à l'aide d'un vibro-viscosimètre SV10-A & D. Les échantillons d'huile de moteur (5W40) et d'huile de coupe (Alpha 93) ont été chauffés sous agitation. Ils ont ensuite été mis dans la boîte d'échantillonnage et les valeurs ont été lues à la température désirée. Pour les deux types d'huile, la viscosité diminue quand la température augmente. Le phénomène d'absorption a donc été étudié à deux températures différentes : 25 et 50 ° C.

### 2.1.1.2 *Caractérisation des huiles : analyse élémentaire*

Dans le tableau 17, la composition élémentaire chimique des deux huiles est présentée. Comme nous pouvons le constater, elles diffèrent fortement. L'huile de moteur est principalement composée de carbone et d'hydrogène, caractéristiques typique des huiles minérales. En revanche, l'huile de coupe a une faible teneur en carbone et environ 50% de la composition n'est pas détectée par les analyses élémentaires. Ceci est une caractéristique des huiles synthétiques où un grand nombre d'additifs font partie de la formulation.

Tableau 17. Propriétés chimiques de l'huile de moteur et l'huile de coupe

	Huile de moteur	Huile de coupe
C (%)	84,54	38,49
H (%)	13,83	6,24
O (%)	1,78	28,17
N (%)	0,14	1,19
S (%)	nd	Nd

nd: non détecté

## 2.1.2 Le dispositif expérimental

Le dispositif mis en place au laboratoire pour effectuer les mesures dans un processus d'absorption a été conçu. Il s'agit d'un système de production de gaz et d'une colonne d'absorption. Chaque pièce est décrite ci-dessous:

### 2.1.2.1 *La Colonne*

Une colonne en acier inoxydable a été conçue pour réaliser les expériences. Ses caractéristiques sont les suivantes : hauteur 0,4 m et diamètre intérieur 0,05 m. Elle est équipée d'une résistance chauffante autour de sa surface externe et d'un thermocouple placé à l'intérieur de la colonne, qui permet le contrôle de la température par un logiciel.

À l'intérieur de la colonne, une plaque perforée est disposée au fond afin de générer la dispersion du gaz. Dans une colonne à bulles, l'utilisation d'un appareil avec plusieurs orifices favorise le contact entre les phases (Treybal 1980). Ainsi, une plaque circulaire (3,9 cm de diamètre) avec de nombreux orifices (0,5 mm) a été conçue.

### 2.1.2.2 *Le processus de génération de gaz à différentes concentrations*

Le gaz saturé en siloxane est produit comme décrit ici : un flux d'air passe à travers un réservoir rempli siloxanes liquide. La température du réservoir est contrôlée par un bain-marie thermostatique réglé à 25°C et muni d'un système d'agitation. Le gaz sortant (saturé en siloxane) est mélangé avec un flux d'air pour ajuster sa concentration.

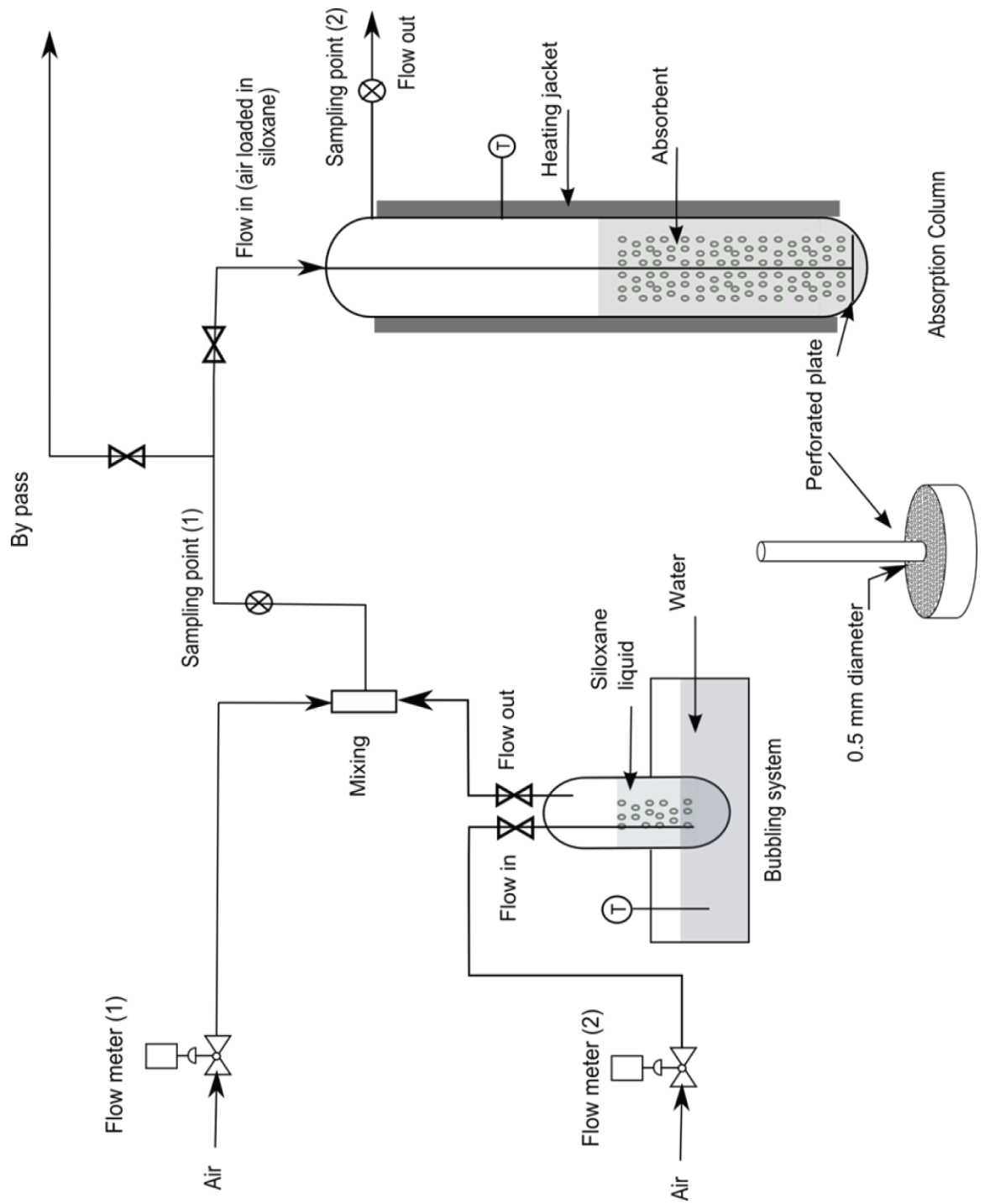


Figure 8. Diagram of the laboratory unit. Generation of siloxanes loaded in siloxanes and absorption column.

### 2.1.2.3 *Méthodologie de détection des siloxanes*

La concentration en siloxanes est analysée par chromatographie en phase gazeuse avec détecteur à ionisation de flamme (GC/FID, Agilent Technologies 7820A GC). Les principaux paramètres de la GC/FID sont les suivants : température du four 70 °C, température de l'injecteur 100 °C et température du détecteur 130° C. Les spécifications des colonnes sont: phényl-méthylpolysiloxane, longueur de la colonne 30 m, diamètre de 0,32 mm et une épaisseur de film de 0,25 µm. Le débit de gaz hélium est de 0,5 ml.min<sup>-1</sup>, avec une injection de 1/20.

### 2.1.2.4 *Procédure d'absorption*

Chaque expérience est réalisée avec la procédure suivante : la colonne est remplie de liquide, la température est réglée et la production de gaz est mise en place. Une fois que le système a atteint un état d'équilibre stable les expériences d'absorption sont effectuées jusqu'à ce que les concentrations de sortie et d'entrée soient les mêmes. Des échantillons de gaz sont prélevés régulièrement au niveau des points d'échantillonnage situés à l'entrée et à la sortie de la colonne et analysés par chromatographie en phase gazeuse couplée aux détecteur à ionisation de flamme (GC / FID) décrit précédemment. Des méthodes similaires pour l'absorption des COV ont été utilisées précédemment (Lalanne et al. 2008, Allen et al., 1997).

## 2.1.3 *Les conditions expérimentales*

L'étude expérimentale a été réalisée en deux parties. Tout d'abord, le siloxane L2 a été absorbé dans différents solvants tels que l'eau, l'huile de moteur, l'huile de coupe et le mélange eau-huile de coupe. L'influence de différents paramètres a été étudiée, tels que la concentration d'entrée en siloxanes, le temps de séjour et la température. Dans la deuxième phase de l'étude, le siloxane D4 a été absorbé dans l'eau, l'huile de moteur, l'huile de coupe et eau-huile de coupe et de la même manière, l'influence de différents paramètres a été étudiée tels que la concentration d'entrée et le temps de séjour. Par conséquent, les mesures de traitement des siloxanes ont été réalisées en faisant varier: la quantité d'absorbant, la concentration en siloxane, le débit de gaz, et la température.

Afin de faciliter la présentation des expériences, l'abréviation suivante est utilisée comme référence de chaque expérience:

[Absorbant] - [Numero de l'expérience] - [Siloxane] [Concentration] - [Masse d'absorbant] - [Débit] - [Température]

- Huile moteur: M
- Huile de coupe: C
- Eau - Huile de coupe: WC
- Eau: W
- Nombre d'expériences: i
- Siloxane: L2 ou D4
- Concentration initiale: mg.Nm-3
- Masse d'absorbant: g
- Débit: L.min-1
- Température: ° C

Les résultats expérimentaux sont scindés en deux parties selon le polluant traité. D'abord nous présentons les résultats concernant le siloxane L2 en absorption dans l'huile de moteur, l'huile de coupe et le mélange eau-huile de coupe. La deuxième partie décrit les résultats concernant le siloxane D4 en absorption dans les mêmes absorbants. Les courbes de percée, la capacité d'absorption et l'influence des paramètres sont ainsi abordés.

### *2.1.3.1 Conditions expérimentales pour l'absorption du Siloxane (L2) dans les huiles*

Les conditions opératoires correspondant au traitement du siloxane L2 par absorption dans l'huile de moteur, l'huile de coupe et de le mélange eau -huile de coupe sont présentés dans le tableau 19. En outre, afin de faciliter la compréhension de ce travail, la figure 11 synthétise les conditions expérimentales et le but visés par celles-ci. Il est important de souligner que la mesure des siloxanes est une méthode difficile et de nombreuses expériences ont été menées pour arriver aux résultats suivants. De même, avant l'expérimentation en dynamique, une courbe d'étalonnage a été réalisée et répétée plusieurs fois.



Tableau 19. Les conditions experimentales pour l'absorption du L2.

Absorbant	Concentration (mg.Nm <sup>-3</sup> )	Masse d'absorbant (g)	Débit (L.min <sup>-1</sup> )	Temperature (°C)	Abbréviation
Eau	1200	240	8.03	25	W1L2 (1200-240-8)
Huile de moteur	800	240	8.03	25	M1L2 (800-240-8)
	1000				M2L2 (1000-240-8)
	1100				M3L2 (1100-240-8)
	1200	140	8.03	25	M4L2 (1200-140-8)
			43.6		M5L2 (1200-240-44)
		300	8.03	25	M6L2 (1200-300-8)
				50	M7L2 (1200-300-8-50)
				90	M8L2 (1200-300-8-90)
Huile de coupe	1200	240	8.03	25	C5L2 (1200-240-8)
	1200	350	3.31	25	C1L2 (1200-350-3.3)
	1200		8.03	25	C2L2 (1200-350-8)
	1800		2.51	25	C3L2 (1800-350-2.5)
	4800	300	1.01	25	C4L2 (4800-300-1)
	Melange eau – huile de coupe	1000	300	8.03	25
1800		8.2		25	WC2L2(1800-300-8)

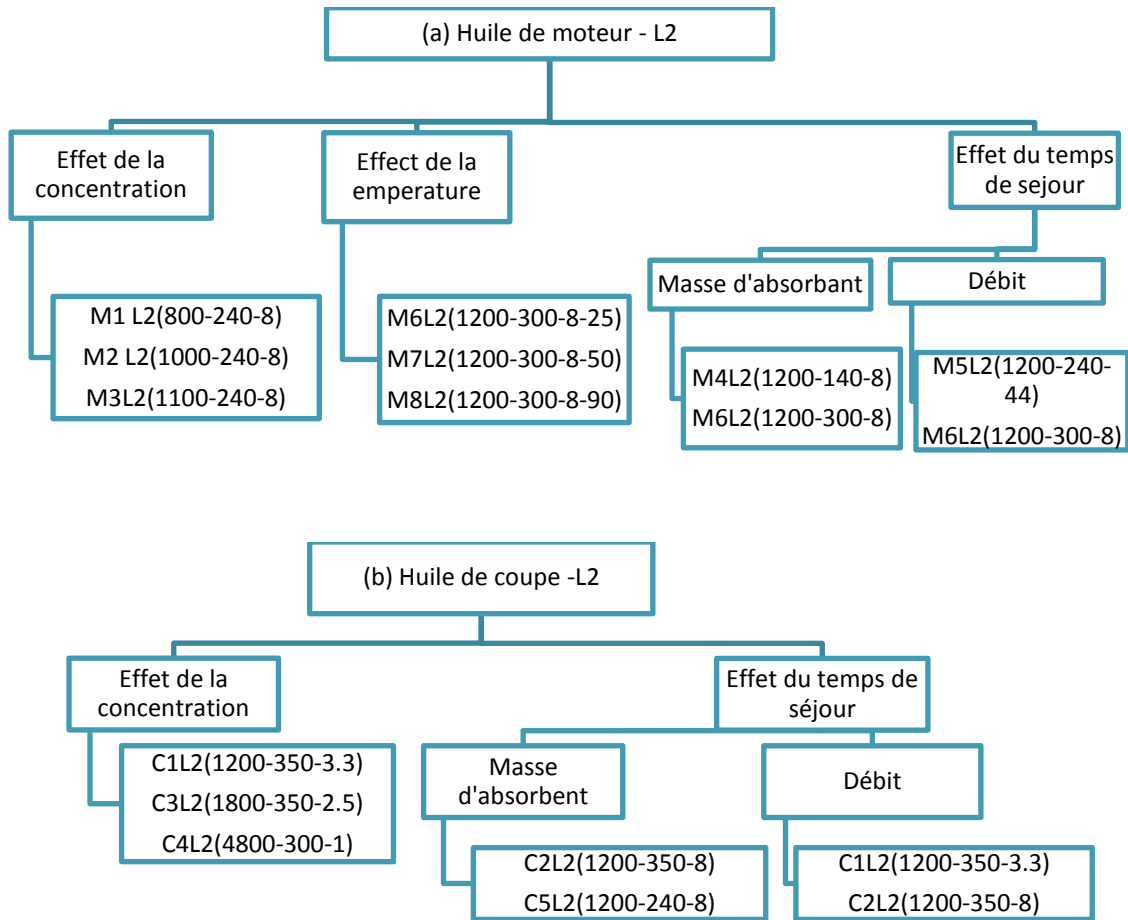


Figure 11. Experiments diagram corresponding to the absorption of Hexamethylsiloxane (L2) into (a) Motor oil (b) Cutting oil.

## 2.2 Résultats et discussion

### 2.2.1 Absorption du siloxane L2 dans l'huile de moteur

Les courbes de percée montrent que la concentration de sortie augmente rapidement dans les premières secondes atteignant une valeur de  $0,4 C/C_0$ , puis la concentration augmente lentement pour finalement atteindre l'équilibre entre les phases après environ 1 h. Pour la condition 6, qui a été réalisée à une concentration de L2 de  $1200 \text{ mg.m}^{-3}$ ,  $300 \text{ g d'}$  huile de moteur et un débit d'entrée dans la colonne de  $8,03 \text{ L.min}^{-1}$ , l'évolution de la concentration est plus lente que les autres. Ces courbes se rencontrent normalement dans les processus d'absorption où il existe une bonne capacité d'absorption du polluant dans le

liquide. Dans les premiers instants, les différences de concentrations en phase liquide et en phase gazeuse sont élevées, ce qui résulte d'une grande capacité d'absorption du liquide. Toutefois, il n'est pas observé de moment où tout le polluant est absorbé par le solvant. En fait, l'efficacité d'élimination observée au début du processus et dans ces conditions est d'environ 60%. Pour les conditions dans lesquelles le débit est important  $44 \text{ L}\cdot\text{min}^{-1}$  ou la masse d'absorbant est faible (140 g) ou quand la température est élevée ( $90^\circ\text{C}$ ), le matériau n'a pas montré d'absorption de L2. D'autres études antérieures avec l'huile de moteur ont été effectuées et ont rapportées une efficacité d'élimination des siloxanes d'environ 60% (Stoddart et al. 1999) suggérant qu'il n'est pas possible d'obtenir de meilleure efficacité d'élimination. Cependant, en plus de la nature physico-chimique des absorbants qui influence le processus d'absorption, des paramètres tels que la surface interfaciale et le temps de séjour sont extrêmement associés à l'efficacité. Ainsi, nous avons augmenté la masse d'absorbant dans l'expérience à 300 g et ainsi une plus grande efficacité d'élimination a été obtenue (76%). L'effet du temps de séjour va être discuté plus tard pour une meilleure compréhension. Les réponses globales de la concentration de sortie ont montrées une bonne performance pour l'absorption de l'huile de moteur. Pour mieux représenter ce comportement la capacité d'absorption est calculée et montrée dans la figure 14.

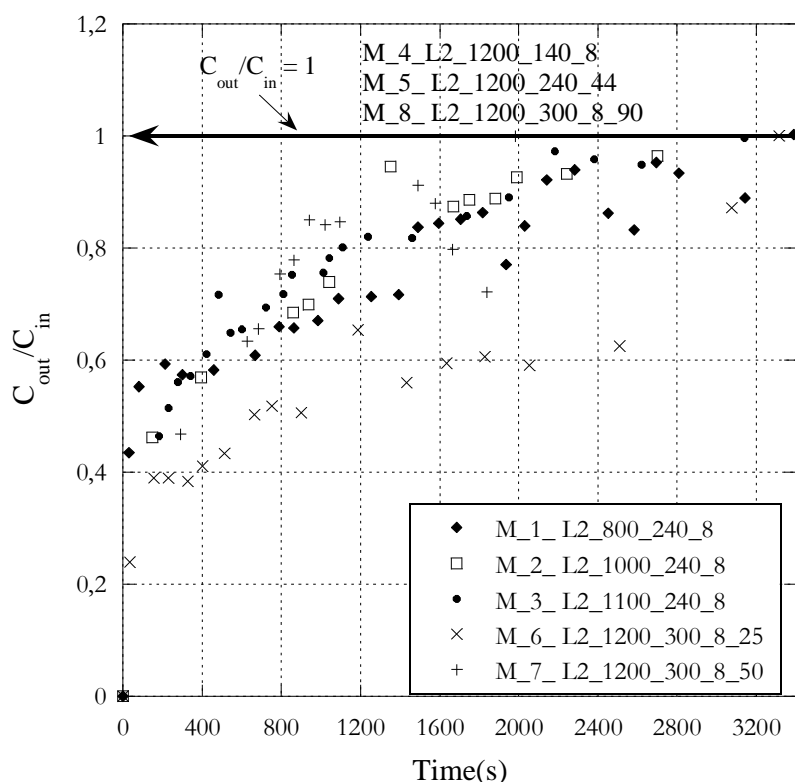


Figure 13. Absorption du siloxane L2 dans l'huile de moteur. Courbes de percée en fonction du temps (s).

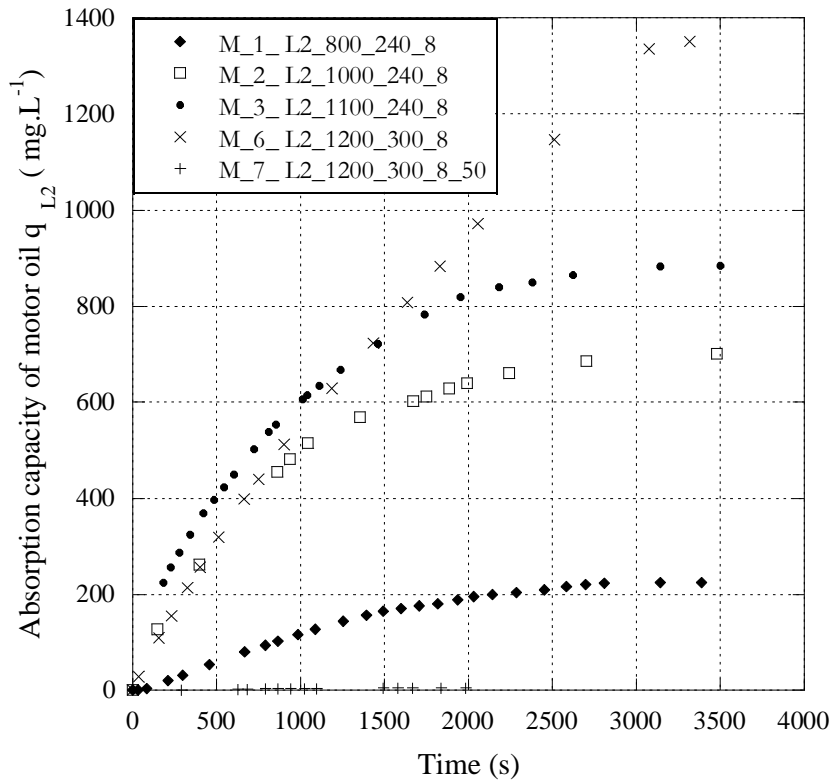


Figure 14. Absorption de siloxane L2 dans l'huile de moteur. Capacité d'absorption en fonction du temps (s).

Ici, nous observons la capacité d'absorption de l'huile de moteur pour toutes les conditions, sauf les cas où aucun enlèvement de L2 n'a été observé (débit = 44 L.min<sup>-1</sup> ou masse d'absorbant = 140 g ou T = 90 ° C). Comme on peut l'observer, les valeurs varient fortement pour chaque état de fonctionnement. A l'équilibre, la valeur la plus élevée est d'environ 1350 mg.L<sup>-1</sup> qui correspond à des conditions de 1200 mg.m<sup>-3</sup>, 300g d'absorbant et un débit de 8,03 L.min<sup>-1</sup>. Les capacités d'absorption à l'équilibre de chaque expérience sont présentées plus loin dans le tableau 31. Elles varient entre 0 et 1350 mg.L<sup>-1</sup> en fonction des paramètres de fonctionnement. Dans la plupart des cas, on observe que l'huile de moteur a une bonne capacité pour réduire la teneur L2.

Tableau 21. Effet de la concentration sur l'absorption du siloxane L2 dans l'huile de moteur

Absorbant	Concentration (mg.m <sup>-3</sup> )	Masse (g)	Débit (L.min <sup>-1</sup> )	T (° C)	q <sub>L2</sub> (mg.L <sup>-1</sup> )	Temps de séjour RT (s)	Référence
Huile de moteur	800	240	8,03	25	224	0,8	M1
	1000				701	0,8	M2
	1100				884	0,8	M3

Comme indiqué dans le chapitre bibliographie, la concentration en siloxanes dans le biogaz varie en fonction de la production. Des valeurs de  $400 \text{ mg.m}^{-3}$  ont par exemple été signalées (Schweigkofler, Niessner 1999). Cependant, nous savons que cette valeur est la moyenne de la concentration et par exemple, elle ne tient pas compte de la dispersion des VMS par des effets saisonniers ou des matières organiques à disposition, qui peuvent entraîner des pics de concentration (Chiriak et al. 2011). D'où notre intérêt pour tester des concentrations plus élevées que celles rapportées dans le biogaz. De là, nous observons par exemple pour une concentration de  $1100 \text{ mg.m}^{-3}$  une capacité d'absorption de l'huile moteur de  $884 \text{ mg.L}^{-1}$ . Ainsi il apparaît que l'augmentation de la concentration en siloxanes n'est pas un obstacle dans le procédé d'absorption.

### 2.2.1.1 Effet temps de séjour: siloxane L2 dans l'huile moteur

Deux paramètres, le débit et la masse de l'absorbant ont été modifiés pour étudier l'effet du temps de séjour. Les valeurs sont indiquées dans le tableau 22. Les résultats des expériences réalisées à  $140 \text{ g}$  et celle à  $44 \text{ L.min}^{-1}$  n'ont pas montré de capacité d'absorption de l'huile de moteur. Ces expériences correspondent à des temps de séjour court ( $0,1$  à  $0,2 \text{ s}$ ), comme indiqué dans le tableau 22. Cependant, pour les temps de contact plus long entre les phases, on observe une augmentation de la capacité d'absorption. Pour l'huile de moteur, des valeurs comprises entre  $0,8 \text{ s}$  et  $1,1 \text{ s}$  montrent de bonnes capacités d'absorption.

Tableau 22. Effet du temps de séjour sur l'absorption des siloxane L2 dans l'huile de moteur

Absorbant	Masse (g)	Concentration ( $\text{mg.m}^{-3}$ )	Débit ( $\text{L.min}^{-1}$ )	T ( $^{\circ}\text{C}$ )	$q_{L2}$ ( $\text{mg.L}^{-1}$ )	Temps de séjour RT (s)	Abréviation
Huile de moteur	140	1200	8,03	25	0	0,2	M4L2
	300				1350	1,1	M6L2
	240	880	8,03	25	224	0,8	M1L2
	240	1000	8,03	25	701	0,8	M2L2
	240	1100	8,03	25	884	0,8	M3L2
	240	1200	43,6	25	0	0,1	M5L2

### 2.2.1.2 Effet de la température: siloxane L2 dans l'huile de moteur

Trois températures ont été testées:  $25$ ,  $50$ , et  $90 \text{ }^{\circ}\text{C}$  pour étudier leurs influences sur l'absorption. Les données expérimentales sont énumérées dans le tableau 23. On observe que la capacité d'absorption diminue lorsque la température augmente comme le montre la Figure 15. À  $25 \text{ }^{\circ}\text{C}$  la capacité d'absorption est de  $1350 \text{ mg.L}^{-1}$ , à  $50 \text{ }^{\circ}\text{C}$  la capacité d'absorption est

de  $5,4 \text{ mg.L}^{-1}$  et à  $90 \text{ }^\circ\text{C}$  le matériau ne montre pas de capacité d'absorption. De cette façon, la température élevée n'est donc pas recommandée pour l'absorption des VMS. A haute température, la viscosité diminue comme indiqué dans le tableau 16. Il pourrait en résulter une diminution de la résistance du liquide au gaz. En conséquence, le temps de séjour du gaz dans la colonne est diminué expliquant la faible capacité de absorption de l'huile de moteur. En outre, les siloxanes sont plus volatils, et la diffusion de la phase gazeuse à la phase liquide est considérablement réduite.

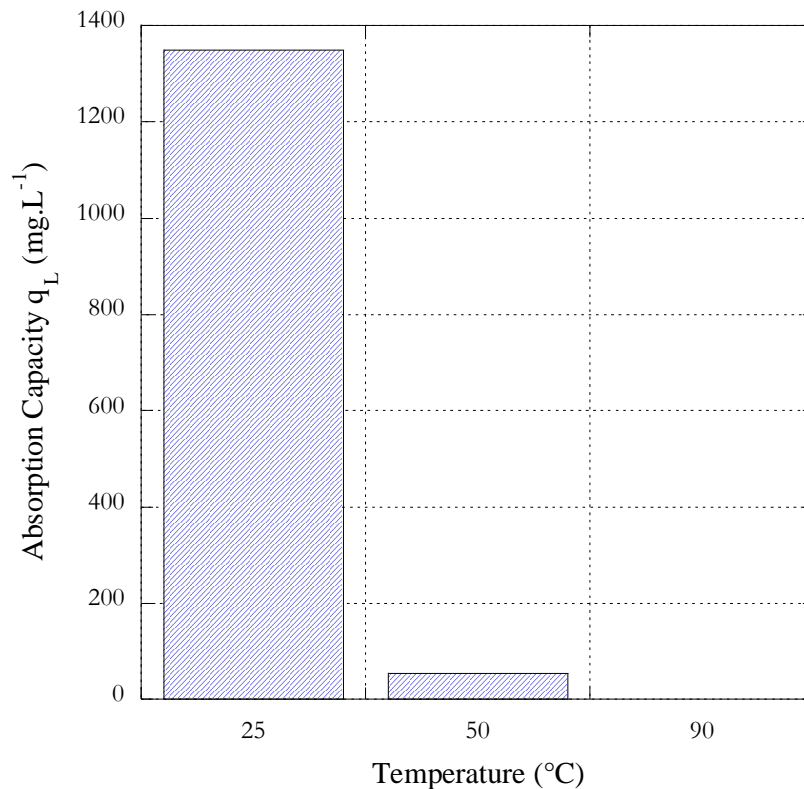


Figure 15. Effet de la température sur l'absorption du siloxane L2 dans l'huile de moteur.  
Débit :  $8,03 \text{ L.min}^{-1}$ , concentration :  $1200 \text{ mg.m}^{-3}$ , masse: 300 g.

Tableau 23. Effet de la température sur l'absorption du siloxane L2 dans l'huile de moteur

Absorbant	Concentration (mg.m <sup>-3</sup> )	Masse d'absorbant (g)	Débit (L.min <sup>-1</sup> )	T (°C)	$q_{L2}$ (mg.L <sup>-1</sup> )	Temps de séjour RT (s)	Abréviation
Huile de moteur	1200	300	8,03	25	1350	1,1	M6L2
				50	5,4	1,1	M7L2
				90	0	1,1	M8L2

## 2.2.2 Absorption du siloxane L2 dans l'huile de coupe

Sur la Figure 17, la capacité d'absorption de l'huile de coupe pour différentes conditions expérimentales est représentée. Nous observons une capacité d'absorption intéressante pour les expériences réalisées à 300g et 350 g d'absorbant avec des valeurs qui varient autour de 200 à 700 mg.L<sup>-1</sup>. Pour celles-ci, la capacité d'absorption augmente de façon linéaire la plupart de temps. La plus haute valeur obtenue est de 684 mg.L<sup>-1</sup>, ce qui correspond à la plus forte concentration (4800 mg.m<sup>-3</sup>). Les capacités d'absorption à l'équilibre sont reportées dans le tableau 32. Bien que le profil de concentration comporte des fluctuations, il est important de souligner que l'huile de coupe présente un potentiel pour absorber le siloxane L2. Par contre, le comportement général n'est pas optimal, ce qui suggère que l'huile de coupe n'est pas un bon absorbant. En outre, aux mêmes conditions de fonctionnement 8,03 L.min<sup>-1</sup> et 240 g, qui ont été testées précédemment avec l'huile de moteur, aucune absorption du siloxane L2 n'a été observée. Par conséquent, le débit de gaz a été diminué et la quantité d'huile de coupe augmentée pour permettre des mesures d'absorption. Ces expériences démontrent encore une fois l'importance de la nature de l'absorbant et l'impact du temps de séjour. En effet, aux premières 30 minutes du processus, la variabilité élevée entre la concentration de sortie et à l'entrée révèle les interactions entre le polluant (siloxane L2) et le solvant. Ce comportement suggère que la solubilité de L2 dans l'huile de coupe est faible. En conséquence, nous avons augmenté la concentration fortement (4800 mg.m<sup>-3</sup>) pour analyser si, par une force motrice plus importante le comportement serait amélioré. Ici, nous observons, comme dans les autres cas, des oscillations entre la sortie et les concentrations d'entrée. Cette expérience a été réalisée également à faible débit (1,01 L.min<sup>-1</sup>). Ainsi, il est évident que dans la plupart des cas, l'huile de coupe n'est pas un bon absorbant pour le siloxane L2.

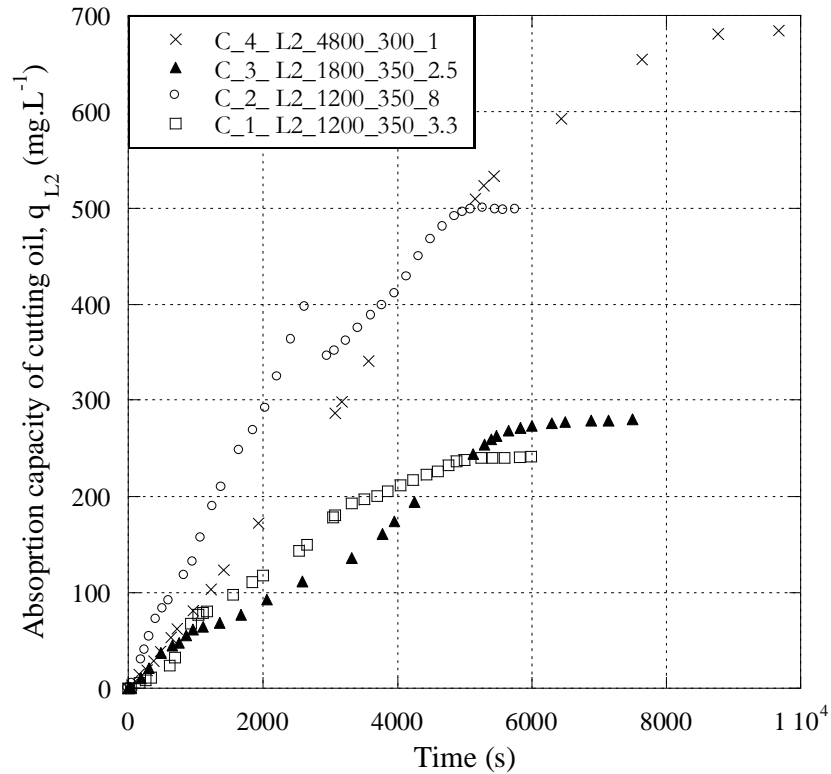


Figure 17. Absorption du siloxane L2 dans l'huile de coupe Capacité d'absorption en fonction du temps

### 2.2.2.1 Effet du temps de séjour: siloxane L2 dans l'huile de coupe

L'effet du temps de séjour a d'abord été étudié par le maintien de la masse d'absorbant (350 g) et la modification de la vitesse d'écoulement de 3,31 à 8,03 L.min<sup>-1</sup>, ce qui entraîne des temps de séjour de 3,2 et 1,3 s respectivement. Ici, nous avons obtenu une plus grande capacité d'absorption de 498 mg.L<sup>-1</sup> correspondant à la plus petite durée de séjour (1,3 s) et une capacité d'absorption de 241 mg.L<sup>-1</sup> pendant 3,2 s. Il apparaît que l'augmentation du débit a amélioré de façon significative la capacité d'absorption. Pour un débit plus élevé, la surface interfaciale est augmentée (avec des valeurs de 101,6 à 223,5 m<sup>2</sup>.m<sup>-3</sup>), ainsi, pour les intervalles de temps de séjour entre 1 à 4 s, l'absorption est améliorée par une plus grande aire interfaciale plutôt que par le temps de séjour. En comparaison avec l'huile de moteur dans des conditions similaires (temps de séjour de 1,1 s) la capacité d'absorption de l'huile de coupe est de 498 mg.L<sup>-1</sup>, soit 40% de la capacité d'absorption d'huile du moteur. Ainsi, les expériences montrent que le L2 a une affinité plus faible avec l'huile de coupe qu'avec l'huile de moteur.



Tableau 25. Effet du temps de séjour sur l'absorption du siloxane L2 dans l'huile de coupe

Absorbant	Concentration (mg.m <sup>-3</sup> )	Masse d'absorbant (g)	Débit (L.min <sup>-1</sup> )	q <sub>L2</sub> (mg.L <sup>-1</sup> )	Temps de séjour RT (s)	Abréviation
Huile de coupe	1200	240	8,03	0	0,7	C5L2 (1200-240-8)
		350	3,31	241	3,2	C1L2 (1200-350-3.3)
		350	8,03	498	1,3	C2L2 (1200-350-8)

### 2.2.3 Absorption du siloxane L2 dans le mélange eau-huile de coupe

La capacité d'absorption du mélange eau-huile de coupe est présentée sur la figure 19. Nous pouvons constater que cette dernière augmente avec la concentration. Les valeurs sont beaucoup plus faibles que celles obtenues avec de l'huile de coupe pure ou de l'huile de moteur. Cependant, ces expériences montrent un potentiel du mélange pour absorber le siloxane L2. En effet, une simple addition d'une fraction d'huile de coupe (5% en masse) modifie fortement les propriétés de l'eau améliorant ainsi la capacité d'adsorption de la solution. Les valeurs à la saturation sont indiquées dans le tableau 26. En outre, en comparaison avec l'huile de coupe pure, son profil de concentration est beaucoup plus stable.

Tableau 26. Capacité d'absorption du siloxane L2 dans le mélange eau-huile de coupe

Absorbant	Concentration (mg.m <sup>-3</sup> )	Masse d'absorbant (g)	Débit (L.min <sup>-1</sup> )	Temps de séjour RT (s)	q <sub>L2</sub> (mg.L <sup>-1</sup> )	Abréviation
Eau	800	240	8,03	0,7	0	W1L2 (1200-240-8)
Eau - huile de coupe	1000	300	8,03	1,0	57	WC1L2 (1000-300-8)
	1800		8,2		95	WC2L2 (1800-300-8)

Pour comparer les résultats avec l'huile de coupe pure, les capacités d'absorption ont été rapportées aux 5% d'huile de coupe présent dans le mélange. Les résultats sont présentés dans le tableau 27. On observe une amélioration de la capacité d'absorption, ce qui peut

s'expliquer par la théorie du second film qui permet l'amélioration du transfert de masse de la phase gazeuse des composés hydrophobes dans une solution d'huile dans l'eau (Dumont, Delmas 2003).

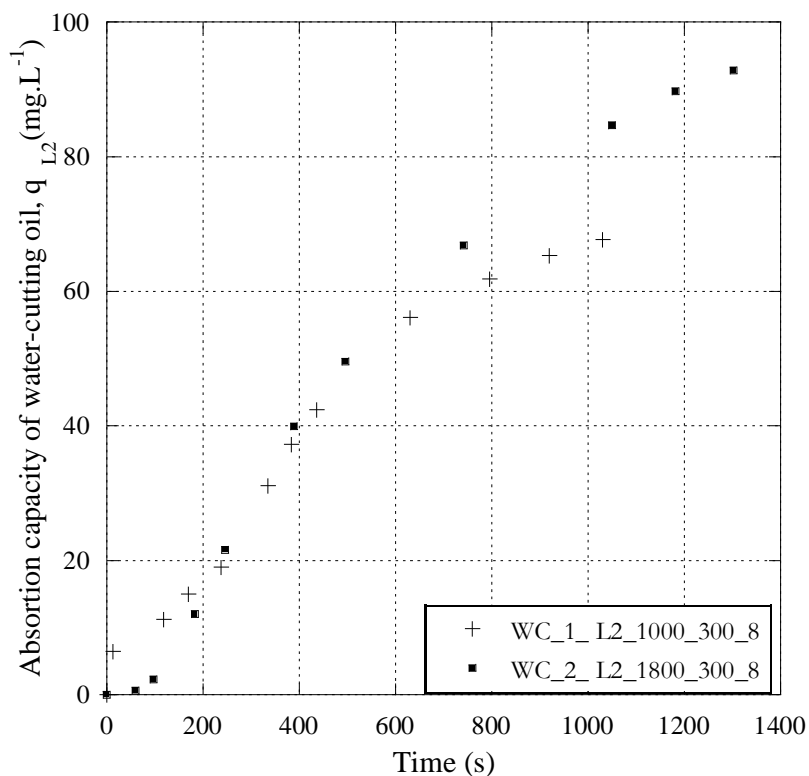


Figure 19. Absorption du siloxane L2 dans le melange eau-huile de coupe. Capacité d'absorption en fonction du temps

Tableau 27. Capacité d'absorption du siloxane L2 dans eau-huile de coupe

Eau- huile de coupe [Cin, Masse (g), Débit (L.min <sup>-1</sup> )]	q <sub>L2</sub> (mg.L <sup>-1</sup> ) eau-huile de coupe	q <sub>L2</sub> (mg.L <sup>-1</sup> ) rapportée au 5% wt de l'huile de coupe
WC1L2 (1000, 300, 8)	56,8	1136.7
WC2L2 (1800, 300, 8)	94,8	1856.6

## 2.2.4 Absorption du siloxane D4 dans l'huile de moteur

La figure 20 représente la capacité d'absorption de l'huile de moteur pour le siloxane D4. Comme nous pouvons le voir, la courbe augmente très lentement. Cela révèle une très

bonne solubilité du D4 dans l'huile de moteur. En ce qui concerne l'efficacité de l'élimination nous observons une valeur de 80%. Celle-ci est beaucoup plus importante que les valeurs indiquées précédemment où elle était de 60% (Stoddart et al. 1999). Cependant, comme nous le savons, cette valeur dépend de plusieurs paramètres tels que: la taille des bulles, le temps de séjour, et la solubilité des composés. Dans (Stoddart et al. 1999) les conditions expérimentales ne sont pas connues, la comparaison est alors difficile, mais cela nous permet d'avoir un point de référence pour le processus et de mettre en évidence l'importance des paramètres d'absorption. Cette étude préliminaire montre que l'huile de moteur a un énorme potentiel pour traiter les polluants comme le D4. Nous avons pu observer, à partir des expériences réalisées, que l'huile de moteur présente la plus grande capacité d'absorption des matériaux testés. Ces résultats montrent comment la nature de l'absorbant est l'une des caractéristiques clés d'un processus d'absorption, étant donné que pour des conditions expérimentales identiques, les capacités d'absorption obtenues pour d'autres matériaux sont relativement faibles. Donc, pour les deux siloxanes les plus pertinents présents dans les biogaz : D4 et L2, l'utilisation de l'huile de moteur peut être une solution intéressante. La capacité d'absorption au point de saturation est présentée dans le tableau 28.

Tableau 28. Capacité d'absorption du siloxane D4 dans l'huile de moteur

Absorbant	Concentration (mg.m <sup>-3</sup> )	Masse d'absorbant (g)	Débit (L.min <sup>-1</sup> )	RT (S)	q <sub>D4</sub> (mg.L <sup>-1</sup> )	Abréviation
Huile de moteur	800	80	3,2	1,6	8820.6	M1D4 (800-80-3.2)
		300		5,5	Très longue arrêté	M2D4 (800-300-3.2)

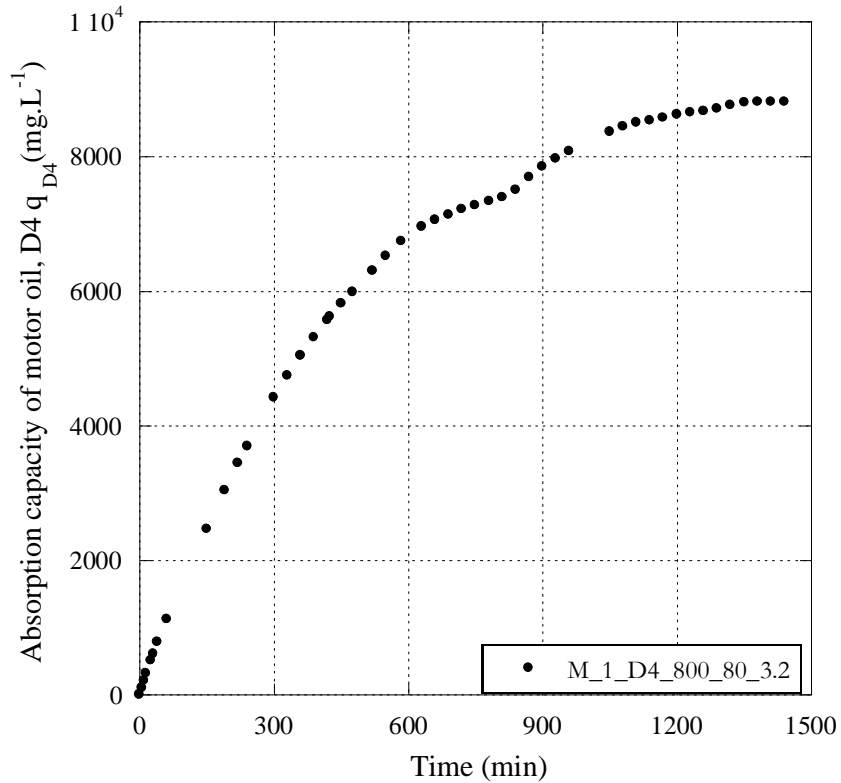


Figure 20. Absorption du siloxane D4 dans l’huile de moteur. Capacité d’absorption en fonction du temps

## 2.2.5 Absorption du siloxane D4 dans l’huile de coupe

La capacité d'absorption de l'huile de coupe pour le siloxane D4 est montrée dans la figure 22. Comme on peut l’observer, pour la plus petite quantité d'huile de coupe (80 g), la concentration de sortie augmente rapidement pour atteindre la valeur de saturation après seulement 20 minutes. Ce résultat diffère sensiblement du profil de concentration pour le D4 dans l'huile de moteur, où le point de saturation est observé après 1500 minutes. Ensuite, les expériences ont été réalisées en augmentant la quantité d'huile de coupe afin d'améliorer l'absorption. Les expériences d’absorption ont été effectuées avec 300 et 350 g d’huile de coupe. En conséquence, la concentration en sortie augmente plus lentement et le point de saturation est atteint après 250 minutes. En outre, l'efficacité du traitement a été améliorée passant de 40% pour 80 g à 56% pour 300 g et 66% pour 350 g. Les valeurs sont indiquées dans le tableau 29. En conséquence, on observe que le transfert de masse du siloxane D4 de la

phase gazeuse à la phase liquide (huile de coupe) est déterminé par la masse d'huile de coupe et pourrait être expliqué par la différence de temps de séjour.

Tableau 29. Capacité d'absorption du siloxane D4 dans l'huile de coupe

Absorbant	Concentration (mg.m <sup>-3</sup> )	Masse d'absorbant (g)	Débit (L.min <sup>-1</sup> )	RT (S)	q <sub>D4</sub> (mg.L <sup>-1</sup> )	Abréviation
Huile de coupe	800	80	3,2	1,3	2,83	C1D4 (800-80-3.2)
		300		4,6	250,38	C2D4 (800-300-3.2)
		350		5,3	449,67	C3D4 (800-350-3.2)

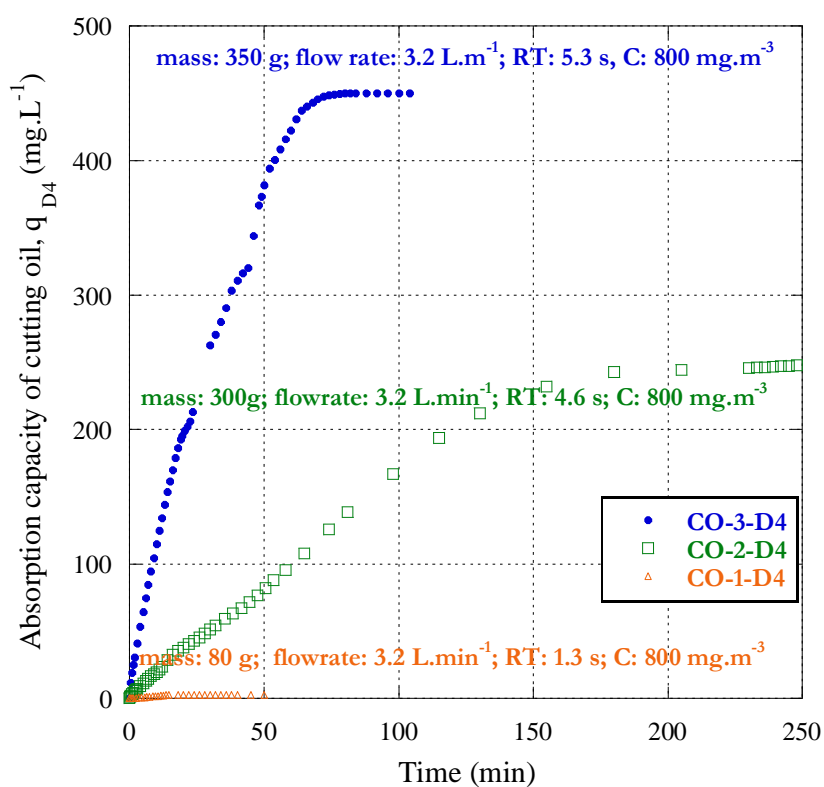


Figure 22. Absorption du siloxane D4 dans l'huile de coupe. Capacité d'absorption en fonction du temps

## 2.2.6 Absorption du siloxane D4 dans le mélange eau-huile de coupe

L'efficacité d'élimination du mélange eau-huile de coupe est beaucoup plus importante que celle de l'huile de coupe pure. Ceci suggère que le mélange est un meilleur absorbant que l'huile seule. Des études antérieures concernant des COV dans des mélanges similaires ont montrées une bonne capacité d'absorption pour des fractions d'huile faible (2,5 -10%) (Lalanne et al. 2008). Dans notre étude, nous pouvons observer qu'avec seulement une fraction de 5% l'efficacité d'élimination est nettement améliorée. Dans le traitement du biogaz, les COV et les VMS sont en général traités à la fin du processus, il est intéressant de noter que le mélange eau-huile de coupe permet de traiter les deux composés, cela pourrait donc être une solution globale pour traiter ces composés volatils.

Tableau 30. Capacité d'absorption du siloxane D4 dans le mélange eau-huile de coupe

Siloxane	Absorbant	Concentration (mg.m <sup>-3</sup> )	Masse d'absorbant (g)	Débit (L.min <sup>-1</sup> )	RT (S)	q <sub>D4</sub> (mg.L <sup>-1</sup> )	Abréviation
D4	Eau-huile de coupe	800	80	3,2	1,3	51,00	WC1D4 (800-80-3.2)
			300		4,6	170,05	WC2D4 (800-300-3.2)

Comme indiqué dans la figure 26, la capacité d'absorption du mélange eau-huile de coupe pour l'absorption effectuée avec 80 g est de 50 mg.L<sup>-1</sup> et il est améliorée pour une masse de 300 g et atteint ainsi une valeur de 170 mg.L<sup>-1</sup>. Comme dans les autres cas, l'influence du temps de séjour sur la capacité d'absorption a été observée. En comparant les résultats avec ceux de l'huile de coupe pure, nous avons trouvé, contrairement à nos attentes que, que la capacité d'absorption est améliorée dans le mélange pour 80 g de solution. Mettant en évidence comment la fraction d'huile améliore le transfert de masse dans l'eau, ce qui donne une meilleure performance que l'huile de coupe pure. Toutefois, cette tendance n'a pas été observée lorsque l'absorption a été réalisée avec 300 g.

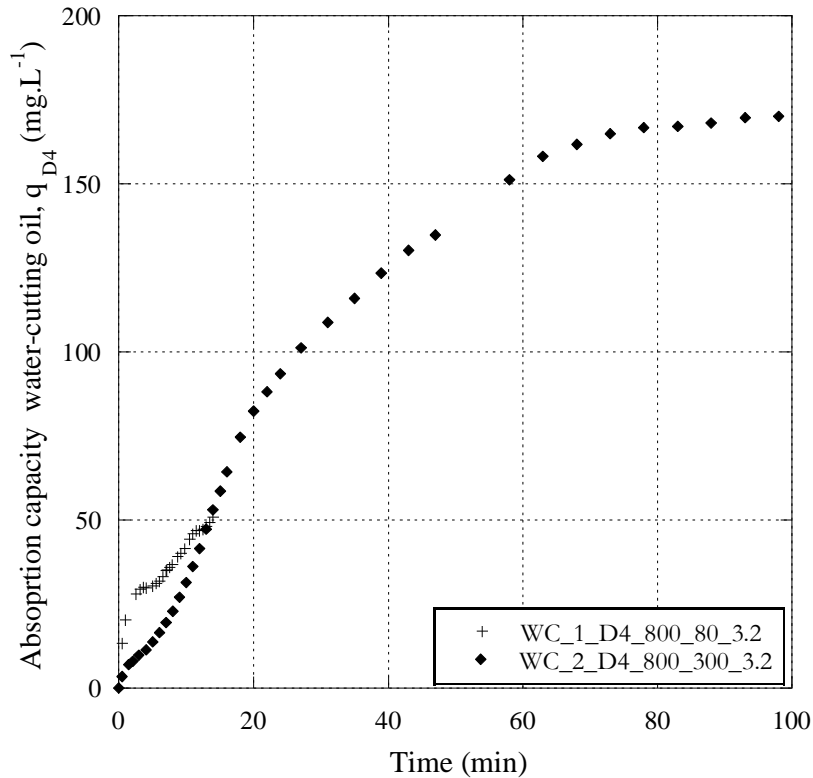


Figure 26. Capacité d'absorption du siloxane D4 dans le mélange eau-huile de coupe.

L'utilisation de l'huile de coupe dans une solution diluée est une solution très économique. Après les expériences réalisées, nous avons observé que le temps de séjour est un facteur limitant dans le processus d'absorption. Nous mettons en évidence le potentiel pour traiter les siloxanes avec un mélange de type eau-huile de coupe. Le résumé des résultats est présenté dans le tableau 32.

## 2.3 Conclusions

Les résultats montrent que l'huile de moteur a une meilleure capacité d'absorption que l'huile de coupe et que le mélange eau-huile de coupe pour les siloxanes L2 et D4. Différents paramètres ont été étudiés: matériau absorbant, temps de séjour, température et concentration en siloxane. Les résultats montrent que le processus d'absorption dépend fortement de la nature de l'absorbant et des conditions de fonctionnement. D'une augmentation de la température de l'huile résulte une diminution de la capacité de traitement, donc à haute température il n'est donc pas recommandé d'utiliser pour l'absorption pour les VMS.

La capacité d'absorption augmente en fonction du temps de séjour pour l'huile moteur, l'huile de coupe et le mélange eau-huile de coupe. Une fois le temps de séjour optimisé, on peut faire varier le débit d'écoulement pour augmenter la surface interfaciale et donc le transfert de masse entre les phases. Cependant, cet effet est plus marqué pour l'huile de moteur que pour les autres solvants. L'utilisation de l'huile de coupe dans une solution diluée est une solution très économique. Nous mettons en évidence le potentiel de traitement des siloxanes avec ce type de mélange. Afin d'augmenter le taux de transfert de masse, des études supplémentaires sont nécessaires.

En ce qui concerne les propriétés physico-chimiques des VMS, la pression de vapeur du D4 est supérieure à celle du L2, aussi nous observons que le D4 présente une faible solubilité dans l'eau par rapport au L2. Il apparaît aussi que le D4 est moins polaire et moins volatile que le L2. Donc plus facile à être absorbée. La meilleure performance pour l'enlèvement des deux siloxanes, en termes de capacité d'absorption, a été observée pour l'huile de moteur qui prévaut pour le D4 plutôt que pour le L2. Ainsi le rendement de l'huile de moteur en termes d'élimination du D4 était de 80% alors que pour le L2, elle était de 60%. Dans le cas du mélange eau-huile de coupe, on a observé une amélioration du transfert de masse de la phase gazeuse à la phase liquide par rapport à l'eau seule. Une efficacité d'élimination de 70% pour le D4 a été observée. Les résultats montrent que l'absorption des VMS dans des huiles est une voie prometteuse pour permettre leur traitement.

Selon les résultats, il est évident que les processus d'absorption dépendent fortement des caractéristiques de la colonne et du système de diffusion de gaz. Une fois le solvant choisi, il faut étudier la pertinence des paramètres de l'étude tels que la surface interfaciale et le temps de séjour. Cette étude met l'accent sur la capacité des absorbants à traiter les siloxanes. Ainsi, un système simple a été utilisé et il n'avait pas pour but de déterminer des paramètres optimaux. Néanmoins, il est évident que le débit est un facteur limitant tel que discuté au préalable pour l'huile de moteur. On remarque que l'effet d'autres paramètres tels que l'agitation, la pression et le régime d'écoulement sont connus pour avoir un impact énorme dans le processus d'absorption et doivent être considérés dans une étude à grande échelle. Enfin, les expériences réalisées au cours de cette étude ont montré que le niveau de concentration peut être réduit par l'absorption des siloxanes dans des huiles avec un abattement partiel. Néanmoins, la concentration de sortie est supérieure à la limite requise pour la production d'énergie, d'où l'importance de l'utilisation d'un autre procédé après l'absorption. Cela peut être pris en considération par un procédé d'adsorption. Le charbon actif a montré de bons résultats.



Tableau 31. Résumé de la capacité d'absorption du siloxane L2 dans l'huile de moteur, l'huile de coupe et le mélange eau-huile de coupe

Absorbant	Concentration (mg.m <sup>-3</sup> )	Masse d'absorbant (g)	Débit (L.min <sup>-1</sup> )	T (°C)	Temps de séjour RT (s)	q <sub>L2</sub> (mg.L <sup>-1</sup> )	Abréviation
Eau	800	240	8,03	25	0,7	0	W1L2 (1200-240-8)
Huile de moteur	880	240	8,03	25	0,8	224	M1 L2 (800-240-8)
	1000					701	M2 L2 (1000-240-8)
	1100					884	M3 L2 (1100-240-8)
	1200	140	8,03	25	0,2	0	M4 L2 (1200-140-8)
			43,6	25	0,1	0	M5 L2 (1200-240-44)
		300	8,03	25	1,1	1350	M6 L2 (1200-300-8)
				50		5,4	M7 L2 (1200-300-8-50)
				90		0	M8 L2 (1200-300-8-90)
Huile de coupe	1200	240	8,03	25	0,7	0	C5 L2 (1200-240-8)
		350	3,31	25	3,2	241	C1 L2 (1200-350-3.3)
		350	8,03	25	1,3	498	C2L2 (1200-350-8)
	1800	350	2,51	25	4,3	280	C3L2 (1800-350-2.5)
	4800	300	1,01	25	8,2	684	C4L2 (4800-300-1)
Eau-huile de coupe	1000	300	8,03	25	1,0	57	WC1L2 (1000-300-8)
	1800	300	8,2	25	1,0	95	WC2L2 (1800-300-8)

Tableau 32. Résumé de la capacité d'absorption du siloxane D4 dans l'huile moteur, l'huile de coupe et l'eau-huile de coupe.

Absorbant	Concentration (mg.m <sup>-3</sup> )	Masse d'absorbant (g)	Débit (L.min <sup>-1</sup> )	TS (S)	q <sub>D4</sub> (mg.L <sup>-1</sup> )	Abréviation
Eau	800	80	3,2	-	0	W1D4 (800-80-3.2)
		300		-	0	W2D4 (800-300-3.2)
Huile moteur	800	80	3,2	1,6	8820,6	M1D4 (800-80-3.2)
		300		5,5	Très longue arrêté	M2D4 (800-300-3.2)
Huile de coupe	800	80	3,2	1,3	2,83	C1D4 (800-80-3.2)
		300		4,6	250,38	C2D4 (800-300-3.2)
		350		5,3	449,67	C3D4 (800-350-3.2)
Eau-huile de coupe	800	80	3,2	1,3	51,00	WC1D4 (800-80-3.2)
		300		4,6	170,05	WC2D4 (800-300-3.2)

# 3 Etude de l'adsorption et désorption de l'H<sub>2</sub>S sur des charbons actifs

Parmi les technologies étudiées, l'adsorption sur charbon actif est largement utilisée dans l'industrie pour sa facilité d'utilisation et d'installation (Bagreev et al, 2005; Bandosz; Monteleone et al.2011). Son inconvénient majeur concerne essentiellement la masse de matériel nécessaire et son renouvellement régulier. Généralement, les charbons actifs sont modifiés chimiquement pour améliorer la capacité d'adsorption. Cependant, l'activité des charbons modifiés est épuisée. Dans la plupart des cas, les pores sont bloqués par des produits de réaction tels que le soufre élémentaire. En fonction de l'imprégnation, le matériau peut être régénéré, mais il s'agit d'un procédé coûteux. Ainsi, les matériaux sont remplacés par du charbon actif neuf après utilisation (Bagreev et al. 2002).

Dans ce contexte, nous nous sommes intéressés au développement de la technologie de séparation de l'H<sub>2</sub>S avec un processus d'adsorption régénératif efficace. L'objectif est de définir les conditions de fonctionnement d'une régénération in situ de l'adsorbant. Pour ce faire, le tissu de charbon actif a été choisi en raison de ses possibilités de chauffage électrique direct comme méthode de régénération (Subrenat et al. 2001, Subrenat, Le Cloirec 2004). Similairement aux charbons actifs en grains, les mécanismes de transfert et de réactions se produisent entre la surface poreuse des tissus de charbon actif et le H<sub>2</sub>S (Yang et al. 1999, Le Leuch, Subrenat & Le Cloirec 2003, Le Leuch, Subrenat & Le Cloirec 2005). En outre, afin de faciliter la régénération du charbon actif, la voie de physisorption est favorisée (Adib, Bagreev & Bandosz 2000). Consécutivement, l'étude portera sur l'impact des conditions d'adsorption sur l'efficacité de la régénération ainsi que sur les paramètres de désorption (température, pression, durée).

## 3.1 Adsorption de l'H<sub>2</sub>S sur des charbons actifs

De nombreuses études ont porté sur les mécanismes physico-chimiques développées au cours de l'adsorption du H<sub>2</sub>S. Porosité, chimie de surface, pH et produits de réaction de surface sont des paramètres qui interviennent dans les réactions complexes développées lors

de l'adsorption (al Bagreev et al. 1999). Trois mécanismes ont été proposés: physisorption, chimisorption et oxydation. Également l'eau apparaît jouer un rôle important.

### 3.1.1 La régénération du charbon actif : H<sub>2</sub>S

Une des principales caractéristiques du processus d'adsorption est le cycle de vie de l'adsorbant. En général, le charbon actif est utilisé un nombre de fois limité. Cela représente une augmentation des coûts, principalement causée par le remplacement du matériau. La régénération du matériau est une clé importante pour optimiser le procédé et réduire ainsi son impact environnemental. Parmi les techniques utilisées dans la régénération thermique, différentes méthodes sont appliquées.

Des études antérieures ont testé la régénération de charbons actifs épuisés. Généralement, la désorption est basée sur le traitement thermique pendant une période de temps. La température varie entre 200 °C et 500 °C (Cal et al. 2000). Une étude des températures de désorption de composés de soufre préalablement adsorbés sur charbon actif a montré que les températures nécessaires varient entre 400 et 600 °C. De plus, des cycles d'adsorption et de régénération des charbons actifs granulaires par désorption thermique ont été signalés à 300 °C (Bagreev, Rahman & Bandosz 2001). L'utilisation de hautes températures diminue cependant les propriétés du matériau. Également, pendant la régénération à 200 et 400 °C de nombreux sous-produits de réactions sont produits (Boulinguez, Le Cloirec 2010). La désorption thermique à une température élevée est nécessaire pour éliminer les dépôts de soufre de la surface du matériau. Des analyses TGA faites par d'autres auteurs ont détecté lors de la désorption des pics entre 200-400 °C. Ils sont associés à la formation de SO<sub>2</sub> et d'autres espèces de soufre et d'oxygène intrinsèquement adsorbés sur le charbon. Un pic à 700 °C a été associé à l'élément soufre localisé dans les pores internes (Elsayed et al. 2009, Monteleone et al. 2011). L'opération de régénération a généralement lieu hors du site rendant aussi le procédé plus complexe (Bagreev, Rahman & Bandosz 2002).

Par conséquent, l'objectif principal de cette étude est d'évaluer la possibilité de régénération du charbon actif à basse température. Pour atteindre cet objectif un système d'adsorption/désorption en dynamique a été utilisé pour évaluer les performances du charbon actif pour l'adsorption du H<sub>2</sub>S. Les tests ont été effectués à 30 ppm et 2.3 NL.min<sup>-1</sup>. La capacité d'adsorption (q) a ensuite été calculée en utilisant l'équation (29). Où, C<sub>in</sub> est la concentration d'entrée (30 ppm), C<sub>out</sub> est la concentration de sortie, m est la masse de charbon et Q<sub>g</sub> est le débit.

Selon les exigences pour l'injection du biométhane dans le réseau de Gaz Naturel, nous avons établi le point de percée en tant que valeur limite de l' $\text{H}_2\text{S}$ , qui est  $5 \text{ mg.Nm}^{-3}$ . Cette valeur correspond à 10% de notre concentration initiale.

## 3.2 Matériels et Méthodes

Après avoir examiné les mécanismes d'adsorption de  $\text{H}_2\text{S}$  dans le charbon actif, nous avons considéré le scénario suivant pour l'étude de l'adsorption/désorption. Nous avons pris en compte les principes de faible coût et de faible impact sur l'environnement et le fonctionnement et l'entretien. Nous avons choisi de nous placer dans les conditions suivantes :

- Processus d'adsorption comme un processus de finition
- Processus d'adsorption dans des conditions ambiantes
- Processus d'adsorption principalement régi par la physisorption au lieu de chimisorption
- Régénération à basse température

Nous placer dans les conditions ambiantes nous permet d'éviter l'utilisation d'autres équipements qui peuvent augmenter le coût d'investissement et d'entretien. Notre intérêt se portant sur le développement d'un procédé d'adsorption-régénération, nous préférons travailler à basse température pour diminuer la formation de composés soufrés et la dégradation d'adsorbant. L'utilisation d'une basse température empêche en conséquence le développement de réactions.

L'efficacité de la régénération dépend fortement des phénomènes développés lors de l'adsorption. La physisorption est contrôlée par les forces intermoléculaires de Van der Waals l'énergie nécessaire pour régénérer le matériau est ainsi plus faible que si le processus était régi par des phénomènes de chimisorption. La physisorption est un processus réversible.

Des études antérieures montrent que l'utilisation d'une température élevée au cours de la régénération favorise l'altération de la chimie de surface diminuant ainsi la capacité d'adsorption (Bagreev, Rahman et Bandosz 2002). Ainsi, le but est de régénérer le matériau à basse température pour éviter sa dégradation. Parmi les charbons actifs, nous avons sélectionné le tissu de charbon actif étant donné sa régénération possible par effet Joule.

### 3.2.1 Le dispositif expérimental

Le dispositif expérimental utilisé dans le procédé d'adsorption / désorption est représenté sur la figure 34. Le matériau adsorbant est placé dans un porte-filtre avec une surface spécifique de  $7 \text{ cm}^2$  et est équipé d'un thermocouple. Une bouteille standard de  $\text{H}_2\text{S}$  dans du  $\text{N}_2$  à 400 ppmv a été mélangée avec du  $\text{N}_2/\text{O}_2$ . Deux débitmètres ont été utilisés à cette fin. Le gaz de sortie a été analysé par un ONYX 5250  $\text{H}_2\text{S}/\text{SO}_2$ .

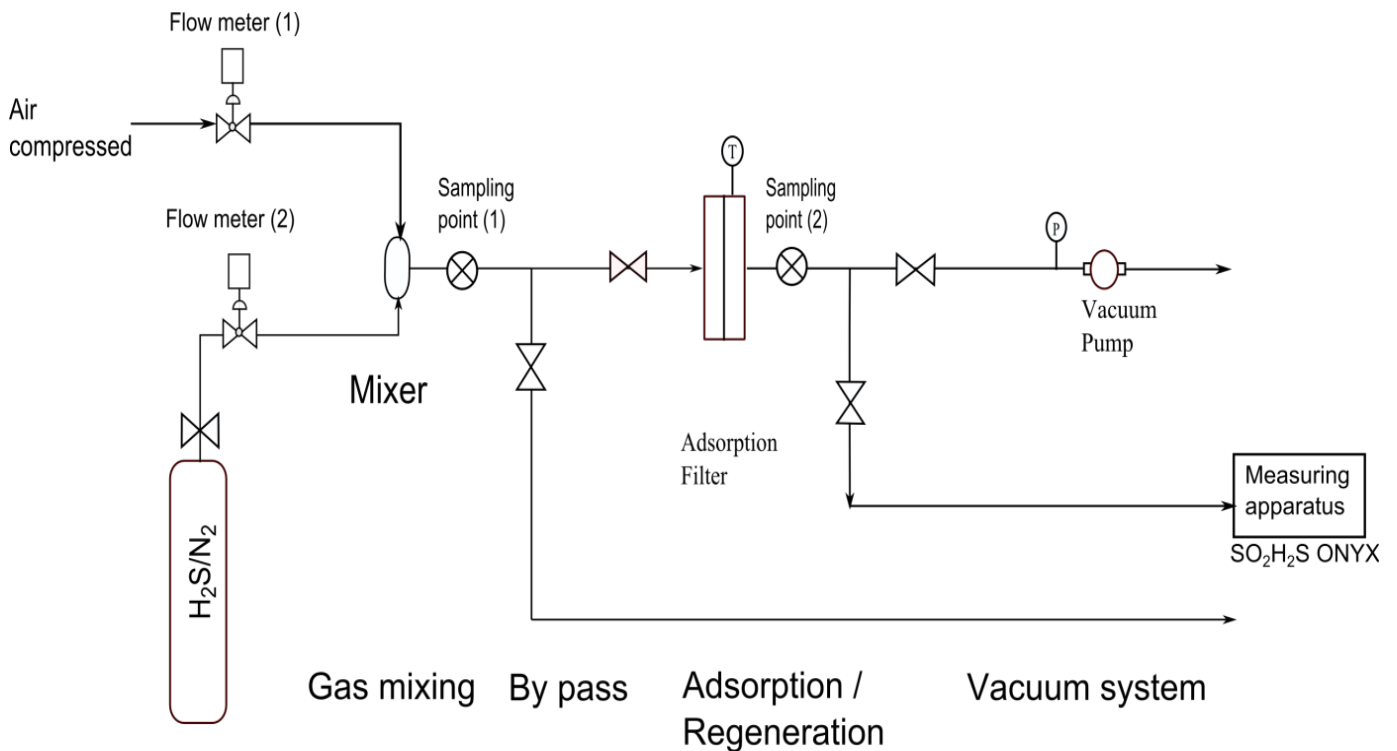


Figure 34. Schéma du procédé d'adsorption / désorption de  $\text{H}_2\text{S}$

### 3.2.2 Le système de désorption

Un système de désorption in-situ a été développé pour régénérer le matériau. Dans cet exemple, deux variables ont été analysées : la température et la pression. Pour augmenter la température, un système de chauffage a été installé. Il peut être contrôlé via la mesure effectuée par la thermocouple incorporé dans le filtre. Une pompe à vide a été installée à l'extrémité de la ligne pour permettre de diminuer la pression. La régénération a été réalisée

pendant une période de 60 minutes. Puis, une seconde adsorption dans les mêmes conditions opératoires a été effectuée pour tester la régénération du matériau.

### 3.2.3 Les conditions de fonctionnement

Les paramètres étudiés qui peuvent influencer sur la qualité et l'efficacité des régénérations pendant la phase d'adsorption sont le taux d'humidité relative du gaz en modifiant la nature des mécanismes de transfert et de réaction et le niveau de charge de H<sub>2</sub>S d'adsorption. Les paramètres influant dans la phase de régénération sont clairement la durée, la température et la pression dans le réacteur. En présence de mécanismes de chimisorption, on peut imaginer que le temps d'arrêt entre l'adsorption et la régénération peut influencer sur les performances de cette dernière.

Une série d'essais a dans un premier temps permis d'estimer l'influence combinée de la pression (0,7 et 1 bar) et de la température de régénération (20 et 110 ° C). La durée de la régénération est fixée arbitrairement à 60 min et 0% de HR (humidité relative). Un essai supplémentaire a permis l'estimation de l'influence de l'humidité. Dans ce cas, le matériau est chargé par circulation d'air dans 80% vol HR pendant 30 minutes.

La seconde série d'essais a pour objectif d'estimer la durée de la régénération nécessaire (30, 60, et 180 minutes), ainsi que l'influence du temps d'attente entre l'adsorption et la régénération (0, 4, 24 h). Enfin une dernière série de cycles permet d'observer l'influence de la concentration de H<sub>2</sub>S sur la qualité de désorption. Le tableau 37 présente les valeurs des paramètres étudiés.

Tableau 37 Les paramètres étudiés influençant la qualité de régénération

Paramètres	Valeurs				
Temps de désorption (min)	30				
Pression de régénération (mbar)	700	700	1000	1000	
Température de régénération (° C)	20	110	20	110	
Air humide	Non	Non	Oui	Non	Non
Pression de régénération (mbar)	700				
Température de régénération (° C)	110				
Air humide	Non				
Temps de désorption (min)	30	60		180	
Temps entre l'adsorption et de régénération	0	0	4	24	0

Pression de régénération (mbar)	700		
Température de régénération (° C)	110		
Air humide	Oui		
Temps de désorption (min)	60		
Temps entre l'adsorption et de régénération	0		
Concentration de sortie (ppm)	5	15	30

## 3.3 Résultats et discussion

Dans cette section, les résultats obtenus à partir des expériences d'adsorption-régénération sont présentés. L'efficacité de la régénération a été évaluée par un second test d'adsorption après la régénération. Cette méthode a déjà été utilisée pour évaluer le processus de régénération (Bagreev et al, 2001b; Monteleone et al 2011) permettant l'évaluation de l'adsorbant dans les mêmes caractéristiques que précédemment (masse d'adsorbant, l'échantillon, la position dans le filtre, etc.). Il est important de souligner qu'ici le procédé de régénération est mis en œuvre in-situ, le filtre n'est pas ouvert et aucune manipulation du matériau n'est effectuée sur le système.

### 3.3.1 Effet de la température

Deux températures sont testées, 20 et 110 °C. Dans l'adsorption de H<sub>2</sub>S, les mécanismes combinés de physisorption et chimisorption peuvent être développés au cours du processus. Dans le but de tester la résistance de l'adsorption, nous avons testé le matériel après adsorption par purge simple avec l'air. Après cela, une deuxième adsorption est effectuée et on obtient une courbe de saturation rapide comme le montre la figure 47. Ainsi, la température est augmentée à 110 °C. Dans ce cas, le profil de percée est très intéressant, comme on peut le voir sur la figure 48, la deuxième courbe d'adsorption est très proche de la première. Cela laisse à penser que, à 110 °C l'énergie pour enlever le H<sub>2</sub>S précédemment adsorbé est suffisante, révélant ainsi que la température est un facteur limitant pour la régénération.



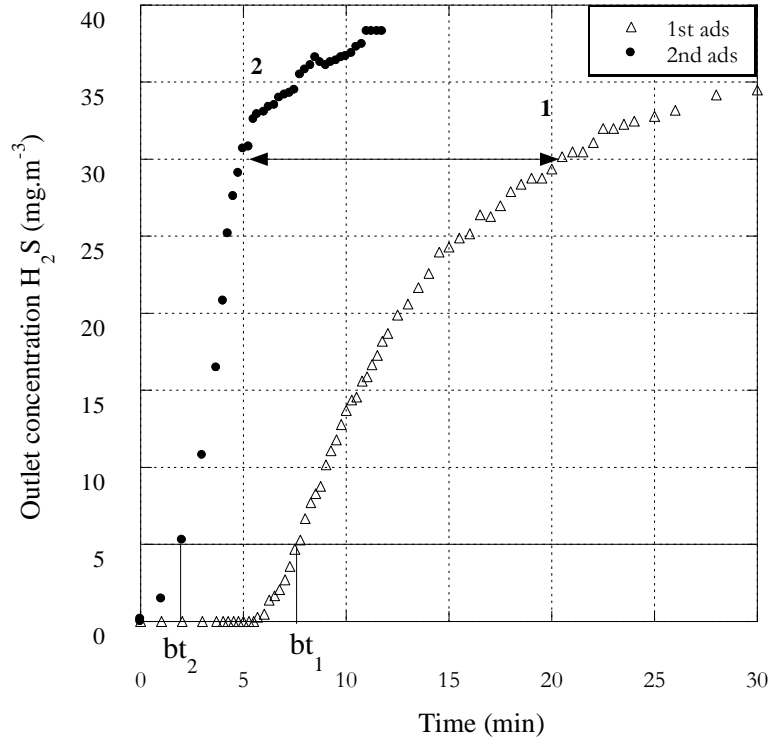


Figure 47. Courbe de percée de l' $H_2S$ , adsorption et régénération du cycle. Régénération dans les conditions ambiantes: T: 20 °C; P: 1 bar

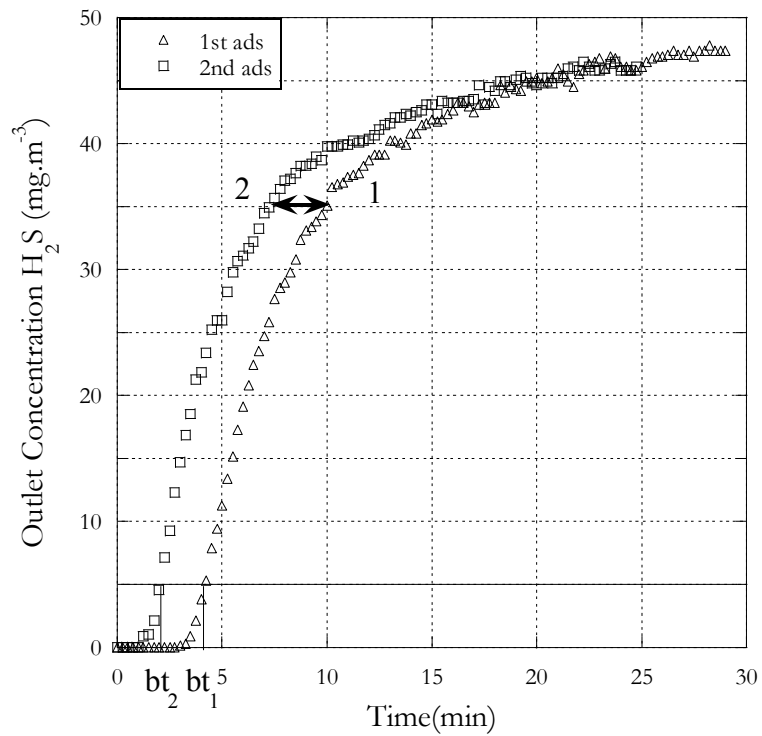


Figure 48. Courbe de percée de l' $H_2S$ , adsorption et régénération du cycle. Conditions de régénération: T: 110 °C; P: 1 bar

### 3.3.2 Effet de la pression

Le deuxième paramètre étudié est la pression au cours de la régénération, pour cela la pompe à vide est utilisée dans le système et la pression est réduite à 0,7 bar. Ici, le but est d'éliminer les composés par une force différente de l'effet thermique. La diminution de la pression permet de désorber les molécules. Dans la figure 49 le profil de concentration est présenté. On remarque que l'écart entre les deux courbes est plus petit que dans les conditions ambiantes. Ce résultat montre qu'il y a une partie de l' $H_2S$  qui est enlevée physiquement grâce à la réduction de la pression. D'un autre côté, nous confirmons que la condition de vide seule n'est pas suffisante pour désorber complètement le matériau.

En conséquence, nous avons combiné les deux conditions : avec la température de  $110^{\circ}C$  et la pression sous vide comme indiqué sur la figure 50. Ces conditions montrent un très bon profil après la régénération. L'écart entre la première et la seconde courbe est beaucoup plus petit. Les composés sont désorbés par la température appliquée au charbon actif en même temps que par le vide appliqué dans le filtre. Ainsi la désorption du matériau est atteinte, en évitant la fixation des produits sur la surface. Nous pouvons supposer qu'en plus de la désorption de l' $H_2S$  physisorbé, les composés soufrés formés en soufre élémentaire sont également désorbés. En effet, sous vide la température de sublimation des composés du soufre est plus faible. À 700 mbar, elle est d'environ  $90^{\circ}C$ . Ces résultats montrent que le couplage de régénération thermique et l'effet du vide donne une bonne régénération.

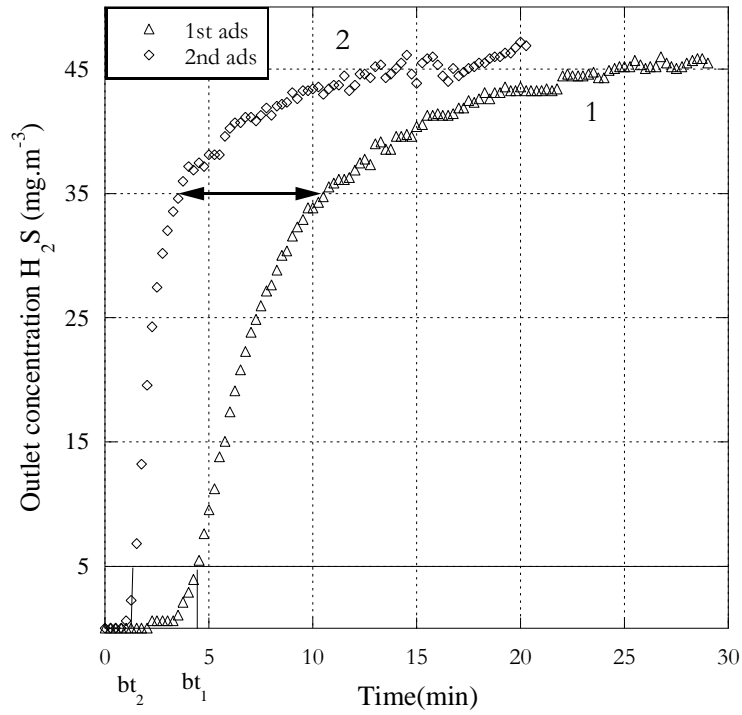


Figure 49. Courbe de percée de l'H<sub>2</sub>S, adsorption et régénération du cycle. Conditions de régénération: T: 20 °C, P: 700 mbar

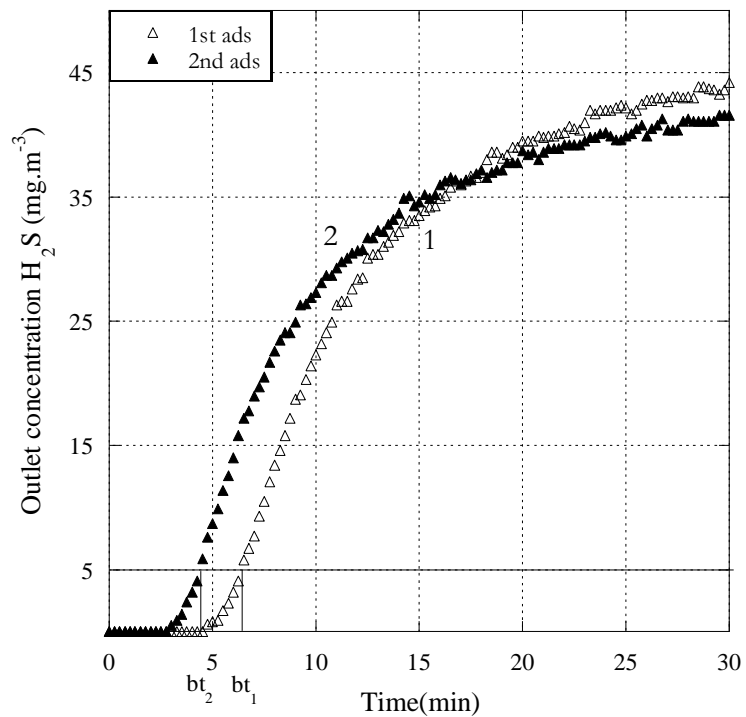


Figure 50. Courbe de percée de l'H<sub>2</sub>S, adsorption et régénération du cycle. Conditions de régénération: T: 110 °C, P: 700 mbar

Le rendement de la capacité d'adsorption (capacité d'adsorption de la deuxième adsorption/capacité d'adsorption de la première adsorption) est montré dans la figure 49. Ici, on peut observer plus clairement quelle est la meilleure combinaison des paramètres opérationnels pour régénérer la matière. De la moins efficace à la plus efficace, nous observons d'abord que la capacité d'adsorption dans les conditions ambiantes diminue rapidement pour atteindre un taux d'adsorption après la régénération d'environ 35%. Suivent ensuite les conditions à 20 °C et le système de vide avec des taux d'adsorption à la saturation de 50%. Ensuite, nous observons les deux courbes à 110 °C et à pression atmosphérique, on obtient 75% et enfin avec le couplage de la température 110 °C et de la pression à vide, on obtient 85%. Les conditions opératoires qui permettent une meilleure régénération du matériau correspondent donc aux paramètres à 110 °C et 700 mbar. En comparant avec d'autres auteurs, la température de régénération est beaucoup plus faible.

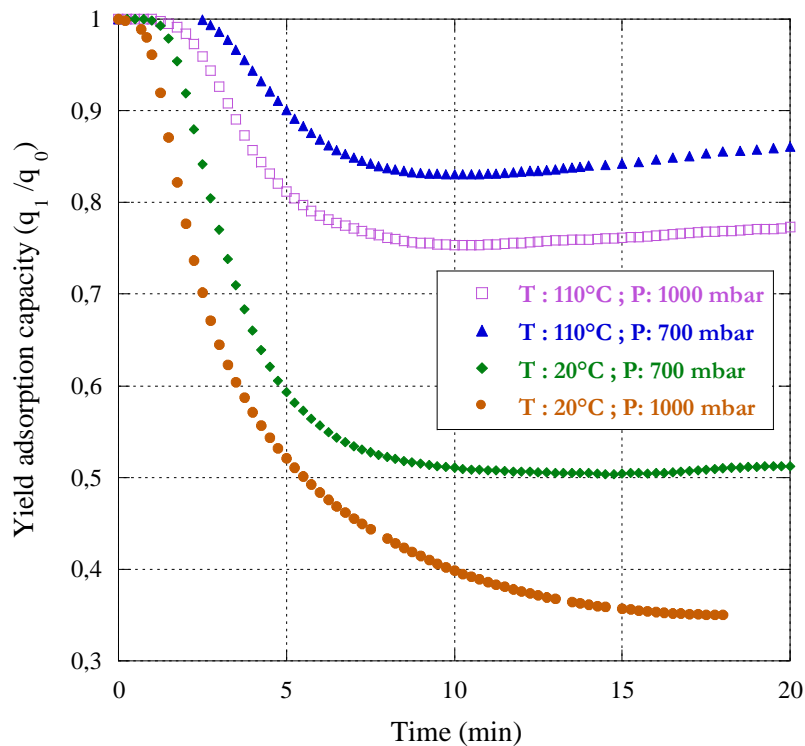


Figure 51. Rapport de la capacité d'adsorption,  $q_2/q_1$  en fonction du temps pour le charbon actif ACF 6.

### 3.3.3 Influence du temps entre les cycles et de la durée des cycles

L'influence d'autres paramètres sont également pris en compte. Le temps de régénération est étudié sur trois périodes différentes: 30, 60 et 180 minutes. La capacité d'adsorption à la saturation et au point de percée sont présentées dans le tableau 39. Comme nous pouvons le constater, la capacité d'adsorption à 30 minutes est inférieure à celle à 60 minutes. Ensuite, nous avons augmenté à 180 minutes. Cependant, dans ce cas, il n'est pas observé de meilleures performances. Cela confirme que 60 minutes est un temps approprié.

Un autre aspect pris en compte dans les cycles d'adsorption-régénération est le temps de repos ou temps de retard entre les cycles d'adsorption-désorption. Ce scénario peut être rencontré lors d'un traitement industriel du biogaz, par exemple lorsque la ligne de production est à l'arrêt pendant un certain temps. Nous considérons donc 4 h, comme un arrêt ponctuel pendant la journée, et 24 h qui pourrait être le cas d'un dimanche. Ici, nous observons une diminution du taux de capacité d'adsorption après 4 h entre les cycles. Cette diminution est plus importante après 24 h. Ce phénomène peut être expliqué par la voie d'oxydation de l' $H_2S$  et en conséquence la formation d'oxydes de soufre qui sont plus difficiles à désorber. Pour éviter cette perte d'efficacité de la régénération, celle-ci doit être effectuée dès que le matériau est épuisé. Un filtre parallèle est donc recommandé pour optimiser l'adsorption-régénération.

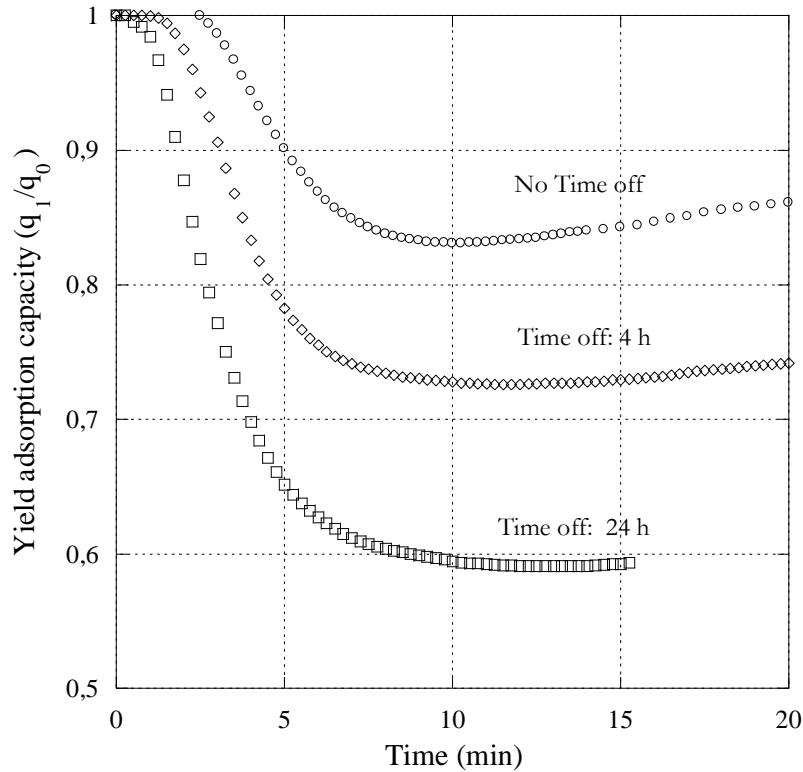


Figure 52. Cycles d'adsorption désorption: 0 h, 4 h, 24 h.

### 3.3.4 Pérennité de cycles adsorption/désorption

Pour analyser la viabilité du procédé, les cycles d'adsorption/désorption à la saturation ont été effectués comme indiqué dans la figure 53. Ce graphique montre les changements après chaque régénération d'adsorption de manière significative. Même si au début la capacité d'adsorption après la régénération est d'environ 90%, après une séquence d'adsorption-régénération le matériau adsorbant n'est plus régénéré. Ceci peut être expliqué par la formation de composés plus forts dans l'adsorbant. En conséquence, le charbon actif est épuisé. Comme la capacité d'adsorption diminue considérablement après le quatrième cycle, le processus a été arrêté à ce stade. Ainsi, le charbon actif est saturé et le matériel n'était plus utile comme adsorbant de sulfure d'hydrogène.

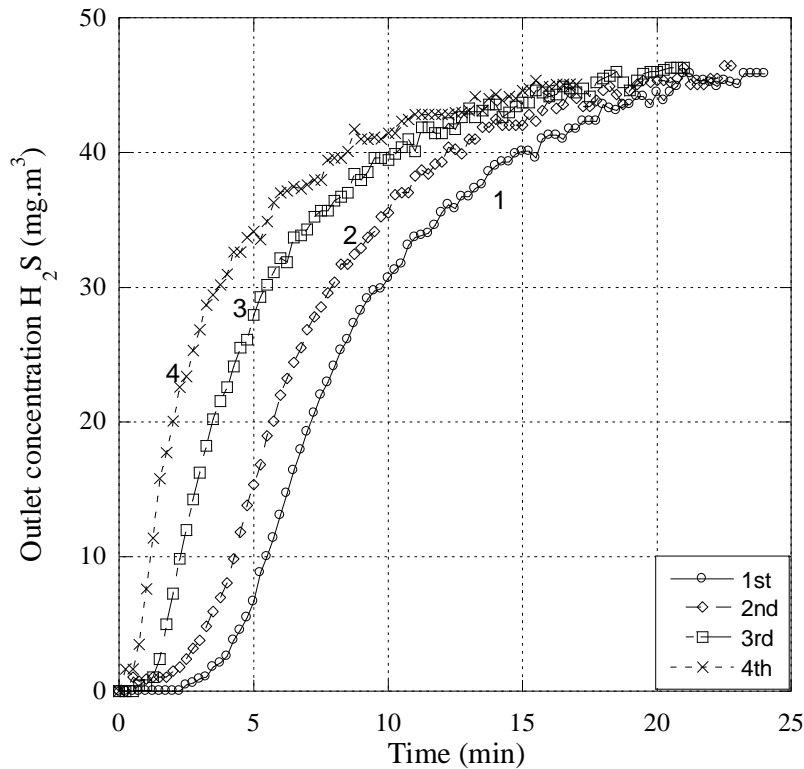


Figure 53. Cycles d'adsorption/désorption. Conditions de fonctionnement 110 °C et 700 mbar.

### 3.3.5 Conclusion générale sur le système de régénération dans des conditions sèches

Les résultats présentés dans cette étude montrent que l'utilisation d'une température de 110 °C et sous vide, permettent une bonne régénération du tissu de charbon actif. En effet, l'utilisation d'une faible température défavorise le développement d'autres réactions et la dégradation du matériau. Ces résultats ouvrent la possibilité de régénération des charbons actifs non modifiés par un moyen efficace et économique, ce qui augmente la durée de vie des matériaux. Cependant, les cycles d'adsorption/désorption ont montré que la capacité d'adsorption diminue après les régénérations, montrant que même si dans le premier cycle la régénération est atteinte, le procédé n'est pas durable. Ceci peut s'expliquer étant donné que lors de la régénération, la formation de composés de soufre se développe, et par conséquent, le matériau n'est plus régénérable. Pour améliorer la régénération, nous avons considéré la protection de la surface par un système de pré-humidification, où l'adsorption de H<sub>2</sub>S va être développée dans le film d'eau. Ces conditions vont a priori permettre la désorption des composés pendant la régénération en évitant les réactions à la surface du matériau.

### 3.3.6 Effet de l'humidité sur l'adsorption-régénération

Les mécanismes d'adsorption dans une atmosphère sèche et humide ont montré une voie différente. Ainsi, nous nous concentrons dans cette partie sur l'étude de l'influence de l'humidité dans la phase d'adsorption mais aussi lors du processus de régénération. Le rôle de l'humidité dans le gaz et la quantité adsorbée par le charbon actif est essentiel (Bagreev, Bandosz 2001, Huang, Chen Chu & 2006) ont montré l'amélioration de la capacité d'adsorption par la présence d'eau.

En conséquence 0% ; 20% et 44% en masse d'eau est adsorbée dans le matériau. La pré-humidification est effectuée avant l'adsorption de la façon suivante: un débit d'air saturé d'eau à 20 °C passe à travers le filtre pour créer une atmosphère humide.

Deux méthodes ont été utilisées pour établir la teneur en eau dans le filtre. Après le processus d'humidification, un échantillon est analysé par un analyseur Thermogravimétrique ATG SETSYS Evolution. En parallèle, un échantillon pré-humidifié a été pesé et séché dans une étuve pendant 48 h. Ensuite, la quantité d'eau adsorbée est obtenue par la différence entre les deux masses. Les deux méthodes ont montré des valeurs similaires.

Dans la figure 57 la comparaison de la capacité d'adsorption dans trois conditions opératoires différentes est présentée. Le profil de concentration correspondant est représenté sur la figure 56. Le taux a été calculé au point de saturation. Dans des conditions sèches, la capacité d'adsorption diminue rapidement et atteint 60% de la capacité d'adsorption. A 20% en masse d'eau adsorbée, la capacité d'adsorption diminue également, mais cette valeur est d'environ 80% du taux initial d'adsorption. Enfin, pour 44% en masse d'eau adsorbée, la capacité d'adsorption est maintenue à la même capacité d'adsorption après la régénération. Dans des conditions humides, le couplage de la pression et de la température sous vide permet de désorber très efficacement le H<sub>2</sub>S.



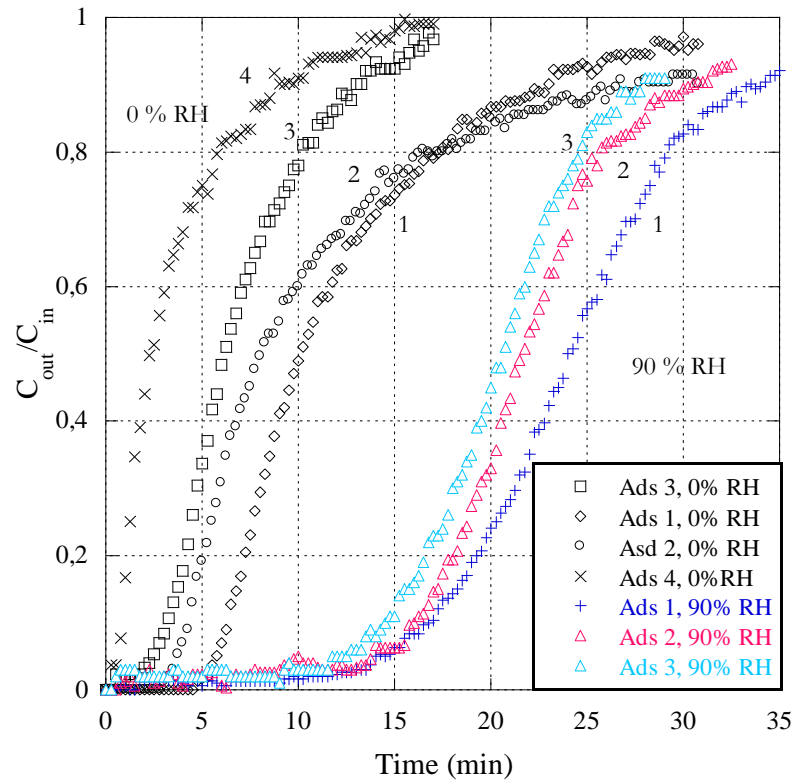


Figure 56. Courbe de percée de l'H<sub>2</sub>S Adsorption/ regeneration. Comparaison entre 0 et 90% HR. Conditions de régénération : T:110°C ; P:0.7 bar.

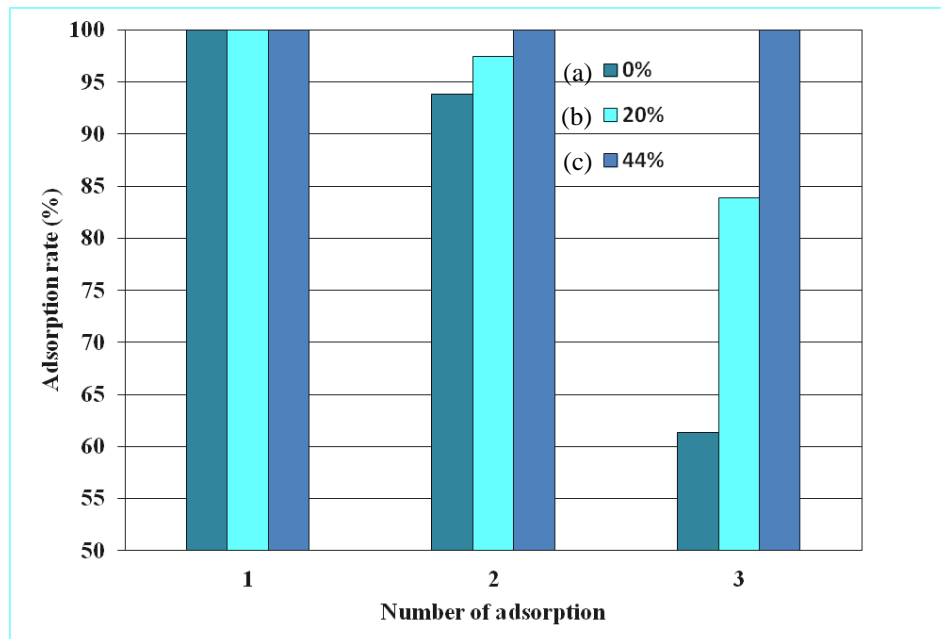


Figure 57. Les trois premières capacités d'adsorption à saturation du taux d'humidité différents.

### 3.3.7 Pérennité des cycles d'adsorption/désorption dans les conditions humides

Suite aux meilleurs résultats obtenus, la condition de régénération a été fixée à une pression de 700mbar, à la température 110 °C et avec pré-humidification avec 40% en masse d'eau. L'adsorption a été stoppée à 15 ppmv. Dans ces conditions d'opération, dix cycles de d'adsorption/régénération ont été réalisées. Sur la figure 58 des courbes de percée pour les différents cycles sont présentées.

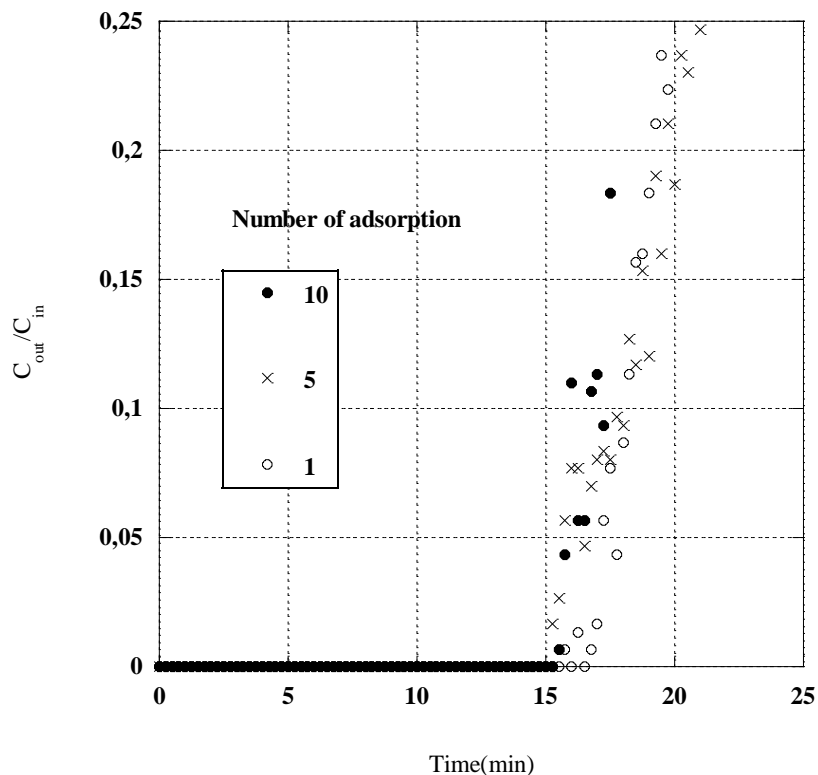


Figure 58. Courbes de percée pour différents nombres de cycles

La capacité d'adsorption obtenue à partir des courbes précédentes est présentée dans la figure 59. Nous observons que la capacité d'adsorption maintient une valeur comprise entre 3,0 et 3,2  $\text{mg.g}^{-1}$  cycle après cycle. En conséquence, les conditions de fonctionnement ainsi que la pré-humidification du matériau utilisé, nous permettent de régénérer le charbon actif améliorant ainsi nettement son cycle de vie.

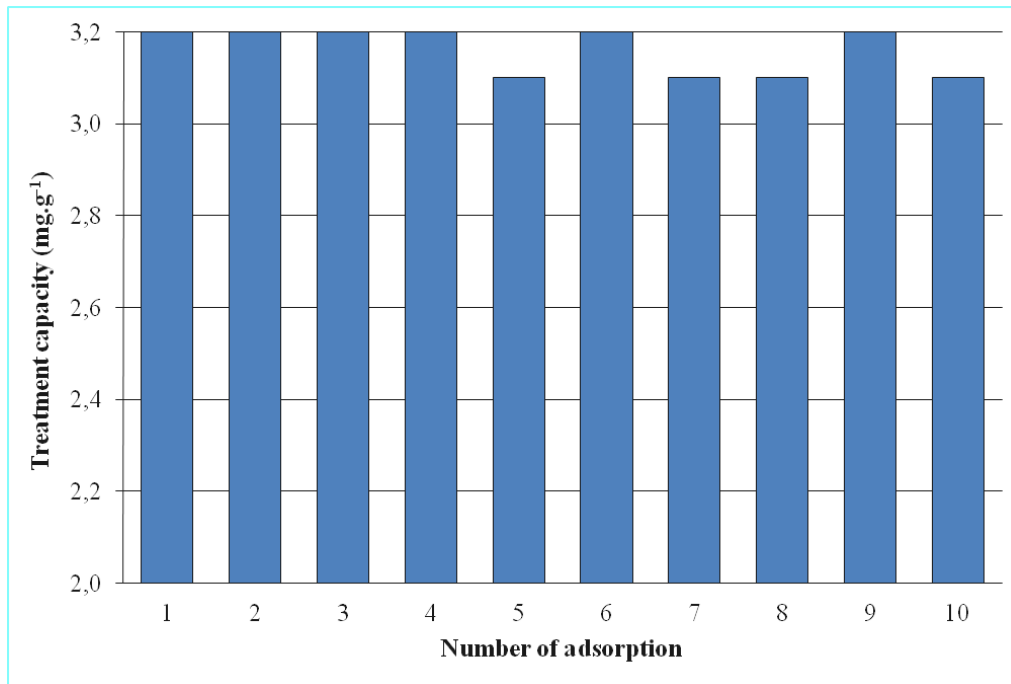


Figure 59. Capacité d'adsorption du H<sub>2</sub>S pour les dix premiers cycles

### 3.4 Conclusions

La méthode de régénération proposée ici est basée sur la théorie selon laquelle l'adsorption à faible concentration est régie par les phénomènes de physisorption plutôt que chimisorption / oxydation, ce que confirme la bonne performance après régénération à basse température. La régénération proposée est basée sur deux principes : un effet thermique et la régénération sous vide. Ainsi, la désorption du matériau est atteinte, en évitant la fixation des produits à la surface. L'utilisation de basses températures défavorisent le développement d'autres réactions et la dégradation des matériaux. Ces résultats suggèrent la possibilité de régénérer des charbons actifs non modifiés. Cependant, d'après l'étude de la pérennité des cycles dans des conditions d'atmosphère sèche il a été observé que les performances diminuent cycle après cycle. En réponse, il a été envisagé l'utilisation d'un film d'eau pour protéger le matériau en évitant la fixation par des liaisons fortes dans le charbon actif. En conséquence, on observe un système de régénération plus efficace par rapport au matériau non pré-humidifié. Au cours des expériences de pérennité, ce taux d'adsorption est maintenu après 10 cycles. En conséquence, la régénération du matériau est réalisée à faible température (110 °C) et sous vide. En outre, la capacité d'adsorption est augmentée de 30% par rapport au matériau sans pré-humidification. Ces résultats montrent l'importance du rôle de l'eau au

cours du traitement de l' $\text{H}_2\text{S}$ , ce qui permet l'amélioration du cycle de vie du matériau par un facteur 10 au moins.

## 4 Conclusions et perspectives

### 4.1 Conclusions

Le biogaz est une source importante d'énergie alternative. Cependant, la présence de plusieurs composants diminue son potentiel et limite ses applications supplémentaires. Parmi eux, cette thèse a été concentrée sur deux composés de nature différente, les siloxanes et le sulfure d'hydrogène. Dans le premier cas, les siloxanes sont caractérisés par leur faible solubilité dans l'eau, et une grande pression de vapeur. En outre, leur contenu dans le biogaz est faible. D'un autre côté, le sulfure d'hydrogène est très soluble dans l'eau et se trouve en concentration plus élevée dans le biogaz. Pour cela, dans le premier chapitre, les sources de biogaz et sa composition ont été analysées en mettant un accent sur les technologies de séparation des siloxanes et du sulfure d'hydrogène. En conséquence, différentes technologies de séparation ont été sélectionnées : dans le cas des siloxanes, l'absorption a été étudiée dans le deuxième chapitre. Dans le cas du sulfure d'hydrogène, l'adsorption sur charbon actif a été privilégiée. Les dispositifs expérimentaux mis en place au laboratoire ont été conçus dans le but d'effectuer les expériences dans des conditions en dynamique.

Concernant les siloxanes, les résultats montrent que l'huile de moteur a une meilleure capacité d'absorption que l'huile de coupe et que le mélange eau-huile de coupe pour les siloxanes L2 et D4. Ainsi le rendement de l'huile de moteur en termes d'élimination du D4 était de 80% alors que pour le L2, elle était de 60%. Dans le cas du mélange eau-huile de coupe, on a observé une amélioration du transfert de masse de la phase gazeuse à la phase liquide par rapport à l'eau seule. Une efficacité d'élimination de 70% pour le D4 a été observée. Les résultats montrent que l'absorption des VMS dans des huiles est une voie prometteuse pour permettre leur traitement. Différents paramètres ont été étudiés: matériau absorbant, temps de séjour, température et concentration en siloxane, le processus d'absorption dépend fortement de la nature de l'absorbant et des conditions de fonctionnement. Les expériences réalisées au cours de cette étude ont montré que le niveau de concentration peut être réduit par l'absorption des siloxanes dans des huiles avec un abattement partiel la pertinence des paramètres de l'étude tels que la surface interfaciale et le temps de séjour. Néanmoins, la concentration de sortie est supérieure à la limite requise pour

la production d'énergie, d'où l'importance de l'utilisation d'un autre procédé après l'absorption. Cela peut être pris en considération par un procédé d'adsorption. Le charbon actif a montré de bons résultats.

Concernant le H<sub>2</sub>S, L'utilisation de l'adsorption par charbon actif a été étudiée comme un procédé de finition. Cette partie du procédé a fait l'objet du troisième chapitre. La méthodologie a été divisée en différents aspects. Dans un premier temps, l'évaluation des différents charbons actifs a été réalisée, d'où le choix du tissu de charbon actif, ACF6, qui correspond à FM30K, selon des critères établis pour favoriser les mécanismes en atmosphère humide ainsi que la physisorption. Il a été confirmé que, durant la phase d'adsorption, l'atmosphère humide favorise l'élimination de l'H<sub>2</sub>S. Une fois que le matériel a été sélectionné, la conception d'un procédé en dynamique a été réalisée pour étudier les conditions expérimentales in-situ. Différentes conditions ont été testées au cours de l'adsorption-régénération avec les conclusions suivantes:

En atmosphère sèche: les résultats présentés dans cette étude montrent que l'utilisation d'une température d'environ 110 °C et de la pression à vide donne une bonne régénération des tissus de charbon actif. Cette température est bien inférieure à la température rapportée dans les études précédentes. En effet, l'utilisation de basse température défavorise le développement d'autres réactions et la dégradation du matériau. Ces résultats ouvrent la possibilité de régénération des charbons actifs non modifiés par un moyen efficace et économique, ce qui augmente la durée de vie des matériaux. Cependant, les cycles d'adsorption/désorption ont montré que la capacité d'adsorption diminue au fil des régénérations, montrant que même si dans le premier cycle la régénération est atteinte, le processus n'est pas durable. Ceci peut s'expliquer étant donné que lors de la régénération, la formation de composés de soufre est développée et par conséquent le matériau est difficile à régénérer.

En atmosphère humide: La régénération est réalisée à une température d'environ 110 °C, sous la pression du vide et avec une pré-humidification du filtre. En conséquence, il a été observé une efficacité du système de régénération plus élevée par rapport au matériau non pré-humidifié. En outre, la capacité d'adsorption est augmentée à 30% par rapport au matériau sans pré-humidification. Ces résultats montrent l'importance du rôle de l'eau au cours du traitement de l'H<sub>2</sub>S, non seulement dans l'amélioration de la capacité d'adsorption, mais aussi son rôle au cours de la phase de désorption. Ce procédé a montré une amélioration de la durée de vie du matériau d'au moins 10 fois.

## 4.2 Perspectives

Différents aspects ont été étudiés dans cette thèse. L'objectif principal étant le traitement du biogaz en vue de son utilisation pour la production d'énergies nouvelles, une méthodologie exploratoire a permis la conception et l'évaluation des différents composants. Après cela, l'utilisation de l'adsorption comme un processus de finition afin d'atteindre les concentrations spécifiées a été identifiée comme une solution. Par la suite, deux siloxanes, un linéaire (L2) et un cyclique (D4) ont été étudiés. Toutefois, dans le biogaz, il y a beaucoup d'autres siloxanes qui pourraient être pris en considération dans des études ultérieures. Ces composés diffèrent par leurs caractéristiques physico-chimiques d'où l'importance de leur prise en compte dans les études futures.

Concernant la séparation des siloxanes par absorption, la possibilité de diminuer la concentration dans la phase gazeuse a été observé. L'utilisation de différents absorbants tels que l'huile de moteur, l'huile de coupe et le mélange eau-huile de coupe donne la possibilité de traiter les siloxanes. Cependant, afin d'augmenter le taux de transfert de masse, des études supplémentaires sont nécessaires. Certaines études futures pourraient être intéressantes pour l'amélioration des taux d'absorption compte tenu des effets de paramètres tels que l'agitation, la pression et le régime d'écoulement. En outre, l'étude d'un procédé d'absorption dans des colonnes avec garnissage peut être considérée. Egalement, l'étude d'autres solvants ainsi que la régénération de l'absorbant sont des aspects qui restent à approfondir.

En ce qui concerne le traitement des siloxanes sur charbons actifs, il a été observé que ce processus est très efficace, donc le couplage des technologies peut être une alternative afin d'optimiser la durée de vie des matériaux.

Enfin, concernant l'adsorption/désorption du sulfure d'hydrogène, d'autres études prenant en compte de plus fortes concentrations que celles testées dans cette thèse pourraient être intéressantes, en ce qui concerne l'adsorption/régénération non seulement comme un processus de finition mais aussi en tant qu'unité opération de grande envergure pour séparer le sulfure d'hydrogène. Egalement, l'étude paramétrique des conditions de régénération, en partant des résultats déjà obtenus, tels que le temps de régénération, la pression, la température, et la pérennité des cycles est de grande importance pour de futures recherches dans le domaine, afin d'optimiser ce procédé. De la même manière, il est important de tester le procédé avec un biogaz réel, en observant les possibles interactions, par exemple, à la surface du matériau.

# References

- Accettola, F., Guebitz, G. & Schoeftner, R. 2008, "Siloxane removal from biogas by biofiltration: biodegradation studies", *Clean Technologies and Environmental Policy*, vol. 10, no. 2, pp. 211-218.
- Adib, F., Bagreev, A. & Bandosz, T.J. 2000, " Analysis of the relationship between H<sub>2</sub>S removal capacity and surface properties of unimpregnated activated carbons ", *Environmental science & technology*, vol. 34, pp. 686-692.
- Adib, F., Bagreev, A. & Bandosz, T.J. 1999, "Effect of Surface Characteristics of Wood-Based Activated Carbons on Adsorption of Hydrogen Sulfide", *Journal of colloid and interface science*, vol. 214, no. 2, pp. 407-415.
- Allen, R.B., Annelin, R.B., Atkinson, R., Carpenter, J.C., Carter, W.L.P., Chandra, G.F.,N.J., Gerdhnard, R., Grigoras, S., Hatcher, J.A., Hobson, J.F., Kochs, P., Lehmann, R.G., Maxim, L.D., Mazzoni, S.M., Mihaich, E.M., Mitakawa, Y., Pohl, E.R., Powell, D.E., Roy, S., Sawano, T., Slater, G.S., Spivack, J.L., Stevens, C. & Wisner, D. 1997, "Volume 3 Anthropogenic Compounds Part H" in *The Handbook of Environmental Chemistry.*, ed. A. Chandra, Springer, Germany, pp. 1-321.
- Bagreev, A. & Bandosz, T.J. 2001, "H<sub>2</sub>S adsorption/oxidation on unmodified activated carbons: importance of prehumidification", *Carbon*, vol. 39, no. 15, pp. 2303-2311.
- Bagreev, A., Rahman, H. & Bandosz, T.J. 2001, "Thermal regeneration of a spent activated carbon previously used as hydrogen sulfide adsorbent", *Carbon*, vol 39, pp 1319-1326.
- Bagreev, A., Rahman, H. & Bandosz, T.J. 2002, "Study of regeneration of activated carbons used as H<sub>2</sub>S adsorbents in water treatment plants", *Advances in Environmental Research*, vol. 6, no. 3, pp. 303-311.
- Bandosz, T.J. 1999, "Effect of pore structure and surface chemistry of virgin activated carbons on removal of hydrogen sulfide", *Carbon*, vol. 37, no. 3, pp. 483-491.
- Boulinguez, B. & Le Cloirec, P. 2010, "Chemical transformations of sulfur compounds adsorbed onto activated carbon materials during thermal desorption", *Carbon*, vol. 48, no. 5, pp. 1558-1569.
- Cal, M.P., Strickler, B.W., Lizzio, A.A. & Gangwal, S.K. 2000, "High temperature hydrogen sulfide adsorption on activated carbon: II. Effects of gas temperature, gas pressure and sorbent regeneration", *Carbon*, vol. 38, no. 13, pp. 1767-1774.
- Cariaso, O.C. & Walker Jr., P.L. 1975, "Oxidation of hydrogen sulfide over microporous carbons", *Carbon*, vol. 13, no. 3, pp. 233-239.

- Cloirec, P.L. & Faur, C. "Chapter 8 Adsorption of organic compounds onto activated carbon — applications in water and air treatments" in *Interface Science and Technology* Elsevier, , pp. 375-419.
- Chiriac, R., De Araujos Morais, J., Carre, J., Bayard, R., Chovelon, J.M. & Gourdon, R. 2011, "Study of the VOC emissions from a municipal solid waste storage pilot-scale cell: Comparison with biogases from municipal waste landfill site", *Waste Management*, vol. 31, no. 11, pp. 2294-2301.
- Deublein, D. & Steinhauser, A. 2008, *Biogas from Waste and Renewable Resources*, Wiley-VCH Verlag GmbH & Co. KGaA.
- Dewil, R., Appels, L. & Baeyens, J. 2006, "Energy use of biogas hampered by the presence of siloxanes", *Energy Conversion and Management*, vol. 47, no. 13-14, pp. 1711-1722.
- Dumont, E. & Delmas, H. 2003, "Mass transfer enhancement of gas absorption in oil-in-water systems: a review", *Chemical Engineering and Processing*, vol. 42, no. 6, pp. 419-438.
- Elsayed, Y., Seredych, M., Dallas, A. & Bandosz, T.J. 2009, "Desulfurization of air at high and low H<sub>2</sub>S concentrations", *Chemical Engineering Journal*, vol. 155, no. 3, pp. 594-602.
- Furimsky, E. 1997, "Activity of spent hydroprocessing catalysts and carbon supported catalysts for conversion of hydrogen sulphide", *Applied catalysis. A, General*, vol. 156, no. 2, pp. 207-218.
- Heymes, F., Manno-Demoustier, P., Charbit, F., Fanlo, J.L. & Moulin, P. 2006, "A new efficient absorption liquid to treat exhaust air loaded with toluene", *Chemical Engineering Journal*, vol. 115, no. 3, pp. 225-231.
- Huang, C., Chen, C. & Chu, S. 2006, "Effect of moisture on H<sub>2</sub>S adsorption by copper impregnated activated carbon", *Journal of hazardous materials*, vol. 136, no. 3, pp. 866-873.
- Lalanne, F., Malhautier, L., Roux, J. & Fanlo, J. 2008, "Absorption of a mixture of volatile organic compounds (VOCs) in aqueous solutions of soluble cutting oil", *Bioresource technology*, vol. 99, no. 6, pp. 1699-1707.
- Le Leuch, L.M., Subrenat, A. & Le Cloirec, P. 2005, "Hydrogen Sulfide and Ammonia Removal on Activated Carbon Fiber Cloth-Supported Metal Oxides", *Environmental technology*, vol. 26, no. 11, pp. 1243-1254.
- Le Leuch, L.M., Subrenat, A. & Le Cloirec, P. 2003, "Hydrogen sulfide adsorption and oxidation onto activated carbon cloths: Applications to odorous gaseous emission treatments", *Langmuir*, vol. 19, no. 26, pp. 10869-10877.
- Kapdi, S.S., Vijay, V.K., Rajesh, S.K. & Prasad, R. 2005, "Biogas scrubbing, compression and storage: perspective and prospectus in Indian context", *Renewable Energy*, vol. 30, no. 8, pp. 1195-1202.
- Matsui, T. & Imamura, S. 2010, "Removal of siloxane from digestion gas of sewage sludge", *Bioresource technology*, vol. 101, no. 1, Supplement 1, pp. S29-S32.



- Monteleone, G., De Francesco, M., Galli, S., Marchetti, M. & Naticchioni, V. 2011, "Deep H<sub>2</sub>S removal from biogas for molten carbonate fuel cell (MCFC) systems", *Chemical Engineering Journal*, vol. 173, no. 2, pp. 407-414.
- Nishimura, S. & Yoda, M. 1997, "Removal of hydrogen sulfide from an anaerobic biogas using a bio-scrubber", *Water Science and Technology*, vol. 36, no. 6–7, pp. 349-356.
- Ortega, D.R. & Subrenat, A. 2009, "Siloxane treatment by adsorption into porous materials", *Environmental technology*, vol. 30, no. 10, pp. 1073-1083.
- Ortega, D. & Subrenat, A. 2009, *Étude du traitement des siloxanes par adsorption sur matériaux poreux : Application au traitement des biogaz*, Thèse, Université de Nantes.
- Ozturk, B. & Yilmaz, D. 2006, "Absorptive Removal of Volatile Organic Compounds from Flue Gas Streams", *Process Safety and Environmental Protection*, vol. 84, no. 5, pp. 391-398.
- Piechota, G., Haggmann, M. & Buczkowski, R. 2012, "Removal and determination of trimethylsilanol from the landfill gas", *Bioresource technology*, vol. 103, no. 1, pp. 16-20.
- Popat, S.C. & Deshusses, M.A. 2008, "Biological Removal of Siloxanes from Landfill and Digester Gases: Opportunities and Challenges", *Environmental science & technology*, vol. 42, no. 22, pp. 8510-8515.
- Rodríguez-Reinoso, F. 2001, "Activated Carbon and Adsorption" in *Encyclopedia of Materials: Science and Technology (Second Edition)*, eds. Editors-in-Chief: K. H. Jürgen Buschow A2Robert W. Cahn A2Merton C. Flemings A2Bernard Ilshner (print) A2Edward J. Kramer A2Subhash Mahajan & Patrick Veysière (updates), Elsevier, Oxford, pp. 22-34.
- Ryckebosch, E., Drouillon, M. & Vervaeren, H. 2011, "Techniques for transformation of biogas to biomethane", *Biomass and Bioenergy*, vol. 35, no. 5, pp. 1633-1645.
- Schweigkofler, M. & Niessner, R. 1999, *Determination of siloxanes and VOC in landfill gas and sewage gas by canister sampling and GC-MS/AES analysis*.
- Schweigkofler, M. & Niessner, R. 2001, "Removal of siloxanes in biogases", *Journal of hazardous materials*, vol. 83, no. 3, pp. 183-196.
- Soreanu, G., Beland, M., Falletta, P., Edmonson, K., Svoboda, L., Al-Jamal, M. & Seto, P. 2011, "Approaches concerning siloxane removal from biogas -A review", *Canadian Biosystems Engineering*, vol. 53, no. 8, pp. 8.1-8.18.
- Soreanu, G., Falletta, P., Béland, M., Edmonson, K., Ventresca, B. & Seto, P. 2010, "Empirical modelling and dual-performance optimisation of a hydrogen sulphide removal process for biogas treatment", *Bioresource technology*, vol. 101, no. 23, pp. 9387-9390.
- Steinhart, J.S. & Hart, S.R. 1968, "Calibration curves for thermistors", *Deep Sea Research and Oceanographic Abstracts*, vol. 15, no. 4, pp. 497-503.

- Stoddart, J., Zhu, M., Staines, J., Rothery, E. & Lewicki, R. 1999, " Experience with halogenated hydrocarbons removal from landfill gas", , pp. 489.
- Syed, M., Soreanu, G., Falletta, P. & Béland, M. 2006, "Removal of hydrogen sulfide from gas streams using biological processes - A review", *Canadian Biosystems Engineering Journal*, vol. 48, pp. 2.1-2.14.
- Subrenat, A. & Le Cloirec, P. 2004, "Adsorption onto activated carbon cloths and electrothermal regeneration: Its potential industrial applications", *Journal of environmental engineering*, vol. 130, no. 3, pp. 249-257.
- Subrenat, A., Baléo, J.N., Le Cloirec, P. & Blanc, P.E. 2001, "Electrical behaviour of activated carbon cloth heated by the joule effect: desorption application", *Carbon*, vol. 39, no. 5, pp. 707-716.
- Treybal, R.E. 1980, *Mass-Transfer Operations*, Third edn, McGraw-Hill, New York.
- Wheless, E. & Pierce, J. 2004, "Siloxanes in landfill and digester gas update".
- Yang, Q.H., Zheng, J.T., Li, Y., Wang, M.Z. & Zhang, B.J. 1999, "Adsorption and conversion of hydrogen sulfide over PAN-based ACF", *Carbon*, vol. 37, no. 12, pp. 2078-2080.
- Yusuf, M.O.L. & Ify, N.L. 2011, "The effect of waste paper on the kinetics of biogas yield from the co-digestion of cow dung and water hyacinth", *Biomass and Bioenergy*, vol. 35, no. 3, pp. 1345-1351.
- "Cahier des charges fonctionnel du contrôle des caractéristiques du biogaz injecté (éléments génériques", 2010, *GrDF*, .
- "Anthropogenic Compounds Part H *Organosilicon Materials. The Handbook of Environmental Chemistry*" 1997, in, ed. A. Chandra, Springer, Germany.

## Carolina Rojas Devia

Biogaz en vue de son utilisation en production d'énergie : séparation des siloxanes et du sulfure d'hydrogène.

Biogas as a renewable energy source: Hydrogen sulfide and siloxanes separation

### Résumé

Ce travail présente une étude de procédé de traitement des siloxanes et de l'H<sub>2</sub>S appliqué à la purification des biogaz. Une approche bibliographique montre l'intérêt de développer de nouveaux procédés de traitement à faible coût pouvant s'intégrer facilement dans une filière complète de purification des biogaz.

Une partie de l'étude est consacrée aux possibilités de traitement par transfert gaz-liquide dans des huiles. Cette technique est comparée à un procédé plus classique de traitement par adsorption sur charbon actif. Les résultats ont montré que ces 2 techniques étaient complémentaires, l'absorption dans une huile utilisée pour le traitement de fortes concentrations et l'adsorption sur charbon actif en traitement de finition.

Une autre partie de l'étude a été consacrée au traitement de l'H<sub>2</sub>S. Les niveaux d'abattement requis étant de plus en plus bas, l'approche choisie est celle d'un traitement de finition en complément des traitements principaux classiques. Le procédé étudié est celui d'un système par physi-adsorption sur charbon actif en tissu pré-humidifié. Celui-ci est régénéré in situ par chauffage électrique direct et mise en dépression du réacteur. L'étude des conditions opératoires a permis d'établir des paramètres de régénération et des conditions de traitement permettant de réaliser des cycles pérenne. L'intérêt réside ici dans les conditions douces de température et de pression utilisées pour la régénération.

#### Mots clés

**Biogaz, absorption, adsorption, sulfure d'hydrogène, siloxanes.**

### Abstract

This work presents a study of the siloxanes and hydrogen sulfide separation process applied to the biogas treatment. A bibliography review shows the interest in the development of new technologies of low cost, to integrate them into an overall process of biogas up-grading.

One part of this study is focused on the possible separation process by gas-liquid transfer into oils. This technology is compared with a more classical treatment process by adsorption into activated carbons. The results showed that both technologies are complementary, the absorption into oils used primarily to the abatement of high concentrations and the adsorption into the activated carbon as a finishing process.

A second part of this study is focused on the hydrogen sulfide treatment. The requirements of abatement are very low, thus the approach is focused on a finishing process to complement the more classical methods. Thus a system by physic-adsorption into pre-humidified activated carbon cloth was studied. The filter was regenerated in situ by direct electric heating under vacuum pressure. The study of the operating conditions allowed establishing the regeneration parameters and the process sustainability. The interest here is focused on the soft conditions of temperature and vacuum used to achieve the regeneration.

#### Key-words

**Biogas, absorption, adsorption, hydrogen sulfide, siloxanes.**